

Design and synthesis of small molecule BET inhibitors

CONFIDENTIAL – DO NOT COPY

A thesis submitted for a Degree of Doctor of Philosophy

2020

Hripsimée Kessedjian

University of Strathclyde
Department of Pure and Applied Chemistry

This thesis is the result of the author's original research. It has been composed by the author and has not been previously submitted for examination which has led to the award of a degree.

The copyright of this thesis belongs to the author under the terms of the United Kingdom Copyright Acts as qualified by University of Strathclyde Regulation 3.50. Due acknowledgement must always be made of the use of any material contained in, or derived from, this thesis.

Signed: Hripsimee Kessedjian

Date: 12th February 2020

Biological samples and animal studies

The human biological samples were sourced ethically and their research use was in accord with the terms of the informed consents under an IRB/EC approved protocol. All animal studies were ethically reviewed and carried out in accordance with Animals (Scientific Procedures) Act 1986 and the GSK Policy on the Care, Welfare and Treatment of Animals. All studies were conducted in accordance with the GSK Policy on the Care, Welfare and Treatment of Laboratory Animals and were reviewed the Institutional Animal Care and Use Committee either at GSK or by the ethical review process at the institution where the work was performed.

Copyright details

Figure 2 was reprinted from Keating, S. T.; Plutzky, J.; El-Osta, A. Epigenetic Changes in Diabetes and Cardiovascular Risk, *Circulation Research*, Volume 118, issue number 11, 1706–1722. Copyright 2016 with permission from Wolters Kluwer Health, Inc. <https://www.ahajournals.org/doi/10.1161/CIRCRESAHA.116.306819>

Acknowledgements

I would like to thank my supervisors Dr Katherine Jones and Dr Craig Jamieson for their precious advice, support and enthusiasm for the science during this incredible journey. I have learnt a lot (and still do) and I really appreciate the time you have dedicated to me over the last three years. I would like to thank Professor Harry Kelly and Professor William Kerr for the opportunity to join the PhD scheme. I would also like to thank for their help all the chemists that have happily (hopefully) spent some time discussing synthetic chemistry with me, in particular Bob, Rino and Lisa. Special thanks to Thibault and Lisa for being my mentors, I have learnt so much by discussing and being challenged by you two. I would also like to thank my former placement students: Eva, Carlos and Katherine (Mini-K). I really enjoyed working with you and hopefully managed to teach you a thing or two along the way.

Thanks to all my colleagues from the chiral separation team and from other scientific areas that have supported me during this work by providing and discussing the crystallography, computational chemistry, biological, physico-chemical and DMPK data. I would also like to thank Washio and Lisa for giving me some training on MOE and Spotfire.

Finally, I'd like to thank my family and more particularly my parents and sisters who are always here to support me. I could not have done this without you. I would also like to thank Amandine (Binome), Alicia and Thibault for their friendship and support throughout the years.

Abstract

Small molecule *Bromodomain and Extra-Terminal* (BET) inhibitors have shown promising therapeutic interest in oncology and immuno-inflammation. However, clinical studies have shown limited therapeutic window for pan-BET inhibitors, restricting their use to aggressive oncology indications. A macrophage-targeted approach, using the *Esterase Sensitive Motif* (ESM) technology, is being investigated in our laboratories. The first ESM-BET inhibitor is currently progressing through clinical studies for the treatment of rheumatoid arthritis. This cell-targeted approach has so far demonstrated reduced toxicity in preclinical animal studies. Due to the attrition rate during drug development, a second ESM-BET inhibitor is desired.

In this thesis, a novel series of ESM-BET inhibitors is investigated. The initial molecules demonstrated high *in vitro* clearance in human and monkey species. This was rationalised as due to a lack of carboxyl esterase (CES) selectivity, in particular between CES-1 (desired) and CES-2 (undesired). The current study describes how CES-1 vs. CES-2 selectivity was achieved. Further optimisation efforts led to the discovery of two advanced molecules with suitable profiles for progression into *in vivo* PK studies. In parallel to the medicinal chemistry optimisation, the synthetic route towards the key benzazepinone motif was improved in terms of yields, step count and robustness, enabling scale up to support investigation of multiple BET inhibitor series within our laboratories. Finally, partial racemisation of two chiral centres was identified during lead optimisation. A stereoselective route was established to address this issue, providing crystalline material in excellent e.e. and good yields throughout the synthetic route to support the progression of the molecules in *in vivo* studies.

Table of contents

Abstract	4
Abbreviations	7
Introduction	11
1. BET proteins and epigenetic modifications	12
2. Therapeutic value of small molecule BET inhibitors	18
3. Targeted small molecule BET inhibitors for rheumatoid arthritis treatment ..	20
4. From a pan-BET inhibitor series to an ESM-BET inhibitor series	24
4.1. Binding mode of a benzazepinone fragment into the bromodomain of BET proteins.....	26
4.2. Aims of this work.....	28
4.3. Initial compounds.....	38
4.4. Research objectives.....	40
Results and discussion	41
5. Increasing CES-2 half-life.....	41
5.1. Evaluation of <i>in silico</i> ChromlogD _{7.4} model	41
5.2. Working hypothesis to reach the desired <i>in vitro</i> profile	43
5.3. Understanding CES hydrolysis rate	44
5.4. Design hypothesis to increase the CES-2 half-life.....	47
5.5. Design of new linkers	48
5.6. Benzazepinone building block retrosynthetic analysis	52
5.7. Synthesis of the benzazepinone building block	53
5.8. Initial set of compounds – Synthesis and impact on CES activity.....	67
6. Increasing CES-1 turnover – Optimisation of molecule 5.06	79
6.1. Design hypothesis to increase CES-1 esterase turnover	81
6.2. Optimisation of the synthetic route for SAR exploration	84
6.3. Synthesis and impact of the ZA channel substituent on the CES-1 turnover.....	85
6.4. Synthesis and impact of the ESM on the CES-1 turnover	90

7.	Reaching the desired profile – Optimisation of molecule 6.26	95
7.1.	Initial pyrazole analogues (1 st generation analogues)	96
7.2.	Second generation molecules – balancing <i>in vitro</i> clearance and potency	110
7.3.	Assessment of the pharmacological profile of the lead molecules	139
8.	Synthetic chemistry route optimisation of molecules 7.38 and 7.44	143
8.1.	Partial racemisation mitigation strategy	145
8.2.	Optimisation of the reductive amination step	149
8.3.	Final steps towards the synthesis of the lead compounds 7.38 and 7.44	157
8.4.	Summary and scope of the new synthetic route.....	163
8.5.	Conclusions.....	166
	Conclusions	168
	Future work	174
	Experimental	176
	References	314

Abbreviations

Ac	Acetyl
AMP	Artificial membrane permeability
Asn	Asparagine
AUC	Area under the curve
BD	Bromodomain
BET	Bromodomain and extra-terminal domain
Brd	Bromodomain-containing protein
CES	Carboxylesterase
cChromlogD_{7.4}	Calculated chromatographic distribution coefficient at pH 7.4
ChromlogD_{7.4}	Measured chromatographic distribution coefficient at pH 7.4
CTBP	Cyanomethylenetriethylphosphorane
Cyno	Cynomolgus monkey
CYP	Cytochrome P450
DCM	Dichloromethane
d.e.	Diastereomeric excess
DEAD	Diethyl azodicarboxylate
DIBAL	Di- <i>isobutyl</i> aluminium hydride
DIPEA	<i>N,N</i> -Diisopropylamine
DMF	<i>N,N</i> -Dimethylformamide
DMP	Dess-Martin periodinane
DNA	Deoxyribonucleic acid
dppf	1,1'-Bis(diphenylphosphino)ferrocene

e.e.	Enantiomeric excess
ESI	Electrospray ionisation
ESM	Esterase sensitive motif
ET	Extra-terminal
Et	Ethyl
F	Bioavailability
h	Hour
HAC	Heavy atom count
HATU	<i>N</i> -[(Dimethylamino)-1 <i>H</i> -1,2,3-triazolo-[4,5- <i>b</i>]pyridin-1-ylmethylene]- <i>N</i> -methylmethanaminium hexafluorophosphate <i>N</i> -oxide
Heps	Hepatocytes
HLM	Human liver microsome
HPLC	High performance liquid chromatography
HRMS	High resolution mass spectrometry
Hu	Human
hWB	Human whole blood
hWB Δ<i>t</i>Bu	Difference between the hWB potencies of a compound and its <i>t</i> Bu ester direct analogue.
IC₅₀	Concentration of the substance that exhibits 50% inhibition
<i>i</i>Pr	<i>iso</i> -Propyl
IR	Infrared spectroscopy
IVC	<i>In vitro</i> clearance
LCMS	Liquid chromatography – mass spectrometry

LDA	Lithium di- <i>isopropyl</i> amide
LE	Ligand efficiency
LLE_{AT}	Lipophilic ligand efficiency (as defined by Astex)
LBF	Liver blood flow
MDAP	Mass-directed auto-preparative chromatography
Me	Methyl
min	Minute
m.p.	Melting point
MW	Molecular weight
NaHMDS	Sodium <i>bis</i> -(trimethylsilyl)amide
NMR	Nuclear magnetic resonance
PDB	Protein data bank
Ph	Phenyl
Phe	Phenylalanine
pin	Pinacolato
Piv	Pivalic
PK	Pharmacokinetics
ppm	Parts per million
Pro	Proline
PPTS	Pyridinium <i>para</i> -toluenesulfonate
PTSA	<i>Para</i> -toluenesulfonic acid
PTT	Phenyltrimethylammonium tribromide
rt	Room temperature
SAR	Structure-activity relationship

SEM	2-(Trimethylsilyl)-ethoxymethyl
S_NAr	Nucleophilic aromatic substitution
t_{1/2}	Half-life
T3P	Propylphosphonic anhydride solution, 50% in EtOAc
<i>t</i>Bu	<i>tert</i> -butyl
Tf	Triflyl
TFA	Trifluoroacetic acid
THF	Tetrahydrofuran
Thr	Threonine
tPSA	Topological polar surface area
t_R	Retention time
Trp	Tryptophan
Ts	Tosyl
Tyr	Tyrosine
WPF	Tryptophan-Proline-Phenylalanine

Introduction

Rheumatoid arthritis is an auto-immune disease affecting around 1% of the world's population.¹ The disease is caused by the over-stimulation of the immune response in the joints, leading to stiffness, pain and progressive loss of the joint function.² The symptoms are due to the accumulation of immune cells, such as macrophages, in the joint synovium, thickening the synovial liquid and preventing normal mobility of the joint. The disease further progresses by attacking the bones and cartilages within the joint, causing pain and weakening the joint.^{2,3} Studies have shown a correlation between a reduction of the number of macrophages in affected joints and an improvement over rheumatoid arthritis clinical symptoms.⁴

Macrophages are immune cells recruited by pro-inflammatory cytokines produced in response to an inflammatory stimulus (Figure 1).⁵

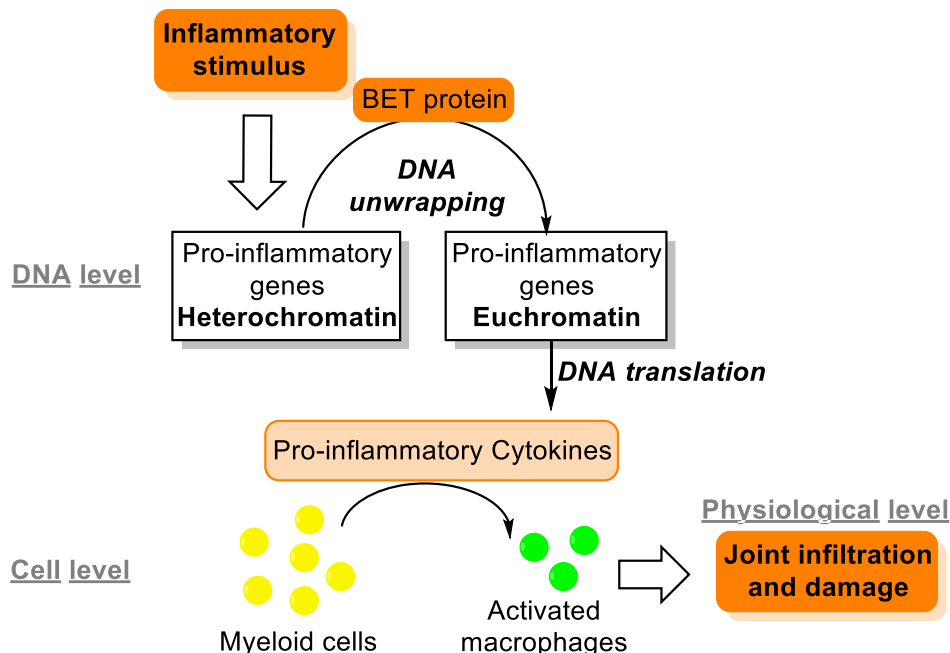


Figure 1: In rheumatoid arthritis patients, joint damage is caused by over expression of the inflammatory response. In vitro inhibition of BET proteins has been shown to reduce the production of several pro-inflammatory cytokines involved in macrophage recruitment. Limiting the macrophage activation should limit joint damages.^{6,7,8}

Inhibition of bromodomain and extra-terminal (BET) proteins has been shown to have an impact on the production of pro-inflammatory cytokines by partially blocking the corresponding gene transcription.^{6,7} Thus, BET inhibition has the potential to reduce the cytokine-induced inflammatory response by reducing the production of pro-inflammatory cytokines.^{6,8} This could limit the recruitment of macrophages involved in the inflammatory response, demonstrating the potential application of BET inhibitors for the treatment of rheumatoid arthritis.

1. BET proteins and epigenetic modifications

The BET proteins are bromodomain-containing proteins, involved in the regulation of gene expression at the deoxyribonucleic acid (DNA) level. In a cell, the DNA double helix is wrapped around histone proteins to form a nucleosome (Figure 2).⁹ Nucleosomes can themselves be tightly packed to form a chromatin fibre that is condensed in cells to form chromosomes. The nucleosome unit is formed of eight histone proteins, a repetition of two H2A, H2B, H3 and H4 units, forming a cluster around which approximately 146 base pairs of DNA are wrapped.^{9,10} A histone protein is formed of a core and two histone tails, the *C*-terminal and the *N*-terminal histone tails.

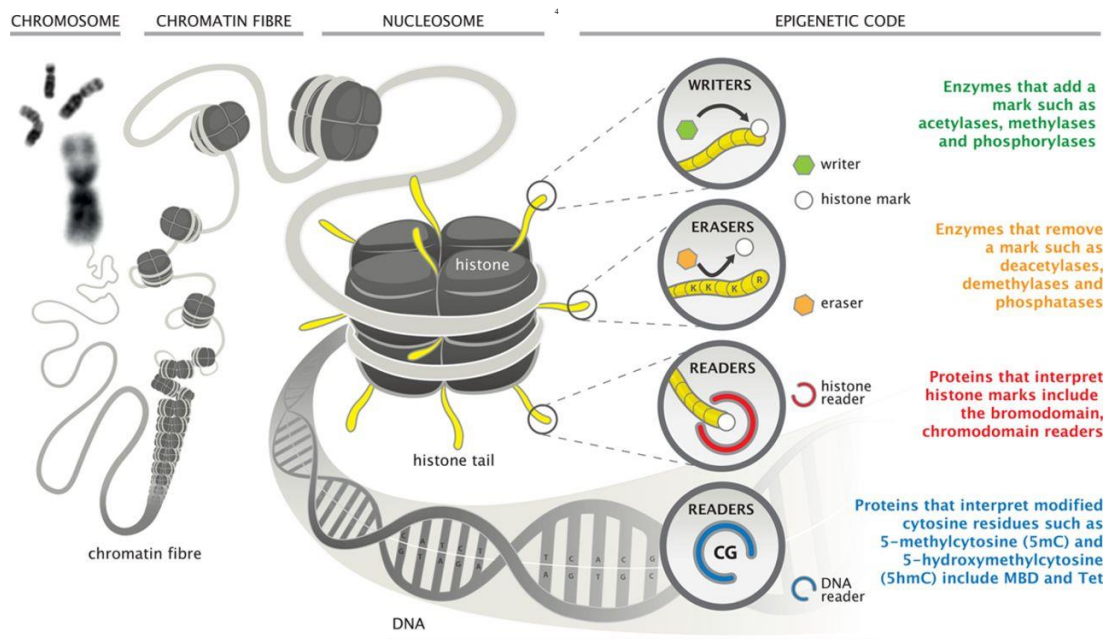


Figure 2: In cells, the DNA double helix is wrapped around histone proteins to form a nucleosome. Histone tails can interact with epigenetic proteins (writers, readers or erasers) to regulate gene expression.⁹

Proteins interacting with histone tails are referred to as epigenetic proteins. Interaction of these proteins with histone tails can trigger a variety of biological events and regulate gene expression. This regulation through histone tail modifications is called epigenetic regulation. Gene expression is governed by inherited and adaptive mechanisms to enable the organism to react to environmental and lifestyle stimuli.⁸ Epigenetic regulation is part of the adaptive mechanism and it includes, but is not restricted to, DNA methylation and covalent modifications of histone tails.⁸ Different families of epigenetic proteins are able to interact with histone tails in the following manner:

- Writers, able to add modifications onto histone tails such as acetyl, methyl and phosphate groups;
- Readers, able to recognise histone tail modifications;
- Erasers, able to remove histone tail modifications.^{8,9}

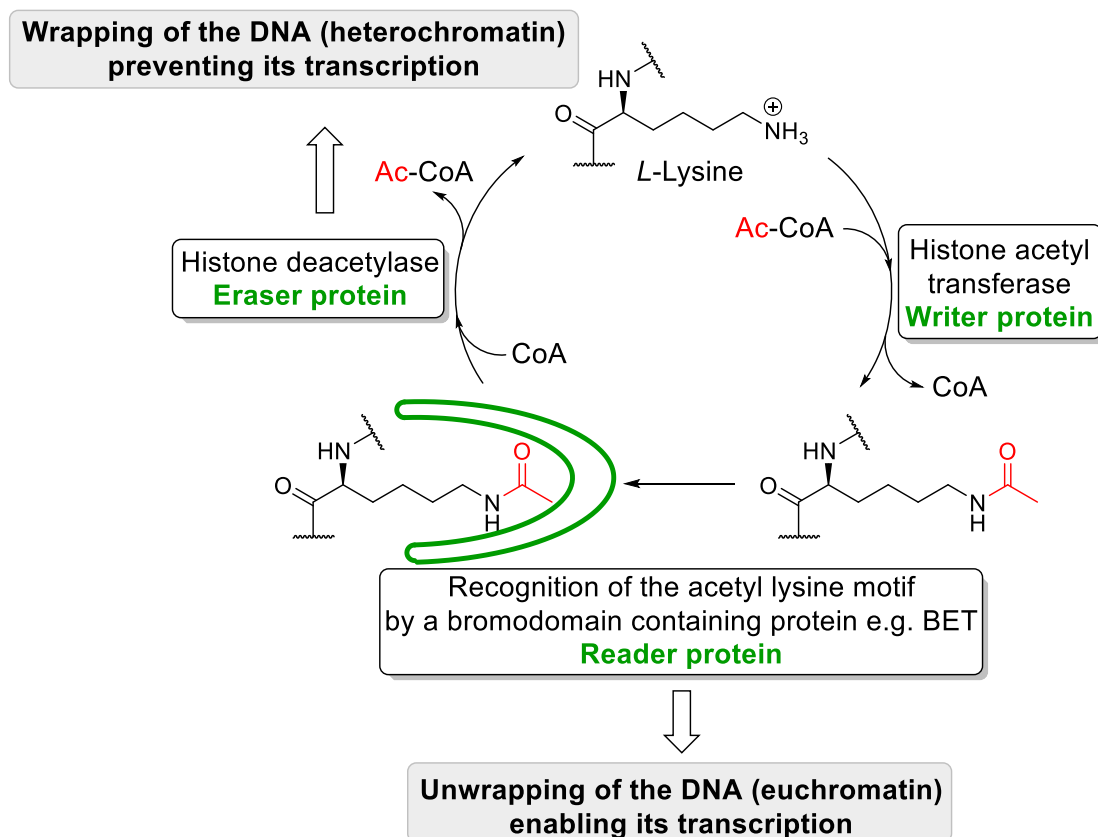


Figure 3: After acetylation of a histone tail by a writer protein, a reader protein, e.g. a BET protein (in green), can trigger the unwrapping of the DNA allowing gene expression.

For instance, histone acetyl transferase proteins are a family of writer proteins able to introduce an acetyl group onto a lysine residue of a histone tail (Figure 3).¹¹ The acetylated lysine motif can then be recognised by a family of bromodomain-containing proteins (reader proteins), including BET proteins. A bromodomain is a sequence of approximately 110 amino acids able to recognise acetylated lysine motifs on histone tails.¹² The recognition of an acetylated lysine modification on histone tails triggers the recruitment of chromatin-regulating proteins, leading to the unwrapping of the corresponding genes. Finally, after transcription, eraser proteins, such as histone deacetylases, can remove histone tail markers (in this case the acetyl group). As a consequence of this de-acetylation, the DNA will return to its tightly packed form, called heterochromatin.

BET proteins, by recognising the acetylated lysine epigenetic modification, take part in the cellular process of unwrapping DNA to its euchromatin state, the first step towards the expression of the associated genetic information.¹² Therefore, interactions of epigenetic proteins with histone tails can regulate the transcription of the DNA, by controlling its packing state in either euchromatin or heterochromatin.

There are four members of the human BET protein family: bromodomain-containing protein 2 (Brd2), Brd3, Brd4 and BrdT (Figure 4).

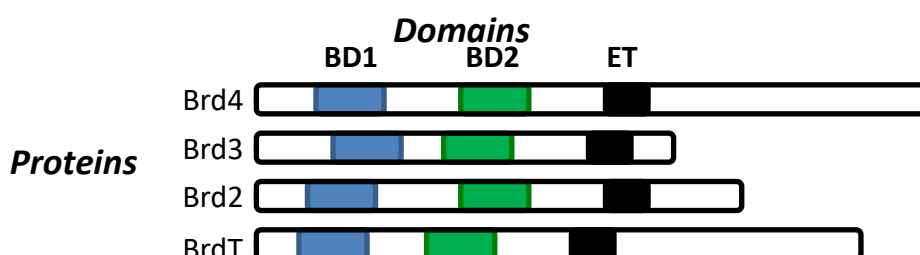


Figure 4: Proteins of the BET family showing BD1, BD2 and extra-terminal (ET) domains.

The acetylated lysine moiety is recognised by the bromodomains. Each of these BET proteins contains two bromodomains (BD), BD1 and BD2, and an extra-terminal domain (Figure 4). The two bromodomains BD1 and BD2 are both able to interact with an acetylated lysine motif. The acetylated lysine binding site of the BET bromodomains is shaped by four α -helices (α Z, α A, α B, α C) and two loops (ZA and BC) (Figure 5).^{10,13}

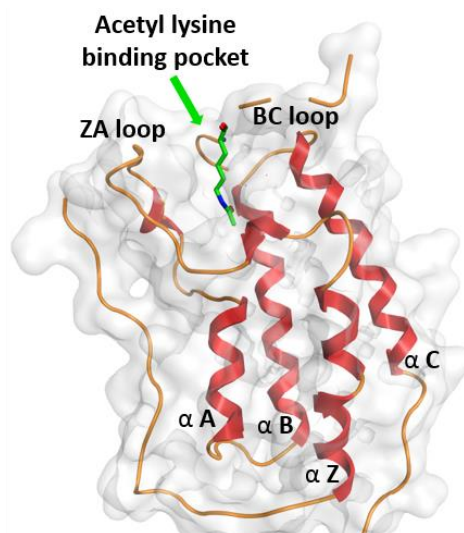


Figure 5: X-ray crystal structure of an acetylated lysine peptide (green) in the first bromodomain (BD1) of BET protein 4 (Brd4) showing the four α -helices (in red) and the ZA and BC loops shaping the binding site (PDB file **gsk3uvw**).¹⁴

The acetylated lysine (green) interacts with the bromodomain *via* a direct hydrogen bond between the oxygen of the acetyl group and one of the hydrogens of the side-chain amide of Asn140 (yellow, Figure 6). In addition, there is a water-mediated hydrogen bond between the acetyl oxygen atom and the hydroxyl group of Tyr97 (orange).ⁱ

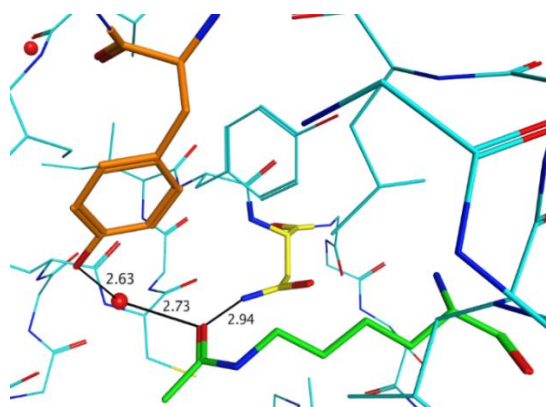


Figure 6: X-ray crystal structure of an acetylated lysine (green) in Brd4 BD1 (blue) showing a hydrogen bond between the acetylated lysine and Asn140 (yellow) and a water-mediated hydrogen bond with Tyr97 (orange). Hydrogen bonds are drawn in black and distances are measured in Å (PDB file **gsk3uvw**).¹⁴

ⁱ The position of these amino acids in the protein sequence is given for Brd4 BD1. However, these two residues are conserved within BD1 and BD2 of the four proteins Brd2, Brd3, Brd4 and BrdT.

Another key feature of the BET bromodomains is the presence of three conserved residues (tryptophan Trp81, proline Pro82 and phenylalanine Phe83) delimiting a lipophilic space, described in the literature as the WPF shelf (Figure 7).^{12,13,35}

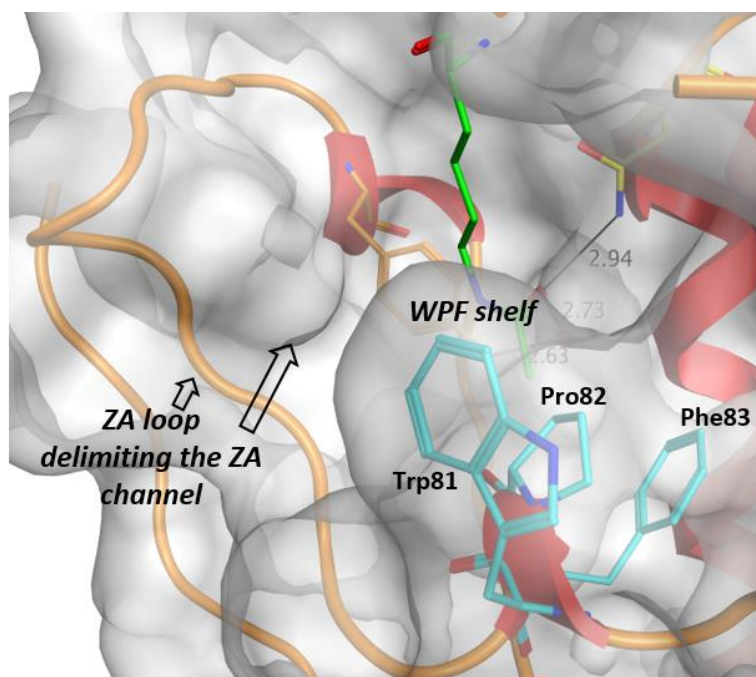


Figure 7: X-ray crystal structure of an acetylated lysine (green) in Brd4 BD1 (blue) showing the WPF shelf and ZA channel (PDB file [gsk3uvw](#)).¹⁴

Interactions with these residues are known to be beneficial to BET potency, and due to some variations of these residues in non-BET bromodomains, interactions with the WPF shelf can be used to achieve selectivity against non-BET bromodomain-containing proteins.^{13,35} Finally, the ZA loop forms a region, referred to as the ZA channel.^{12,13,35} The ZA and BC loops are the main points of diversity, in terms of amino acid sequences, between all the bromodomain-containing proteins. The width of the ZA channel can vary substantially between BET and non-BET bromodomains. As a consequence, the ZA channel equally can be used to achieve selectivity against non-BET bromodomains.^{12,13}

2. Therapeutic value of small molecule BET inhibitors

Due to their ability to regulate gene expression and the cell cycle, BET proteins are of tremendous interest for pharmaceutical research.¹⁵ BET proteins have been shown to play a role in several disease indications within oncology and immuno-inflammation therapeutic areas.¹² In particular, studies have shown that disruption of the epigenetic regulation, such as increased levels of acetylated histone tails, has an impact on the production of pro-inflammatory cytokines in rheumatoid arthritis patients.³ This finding demonstrates the relevance of targeting proteins involved in the epigenetic regulation of the DNA transcription for rheumatoid arthritis indications.

Several BET inhibitors have already progressed to clinical trials in recent years for a number of disease indications, in particular RVX208, molecule **2.1**, for cardiovascular diseases (Phase III) and I-BET762, molecule **2.2**, for oncology therapy (Phase II) (Figure 8).^{16,17,18}

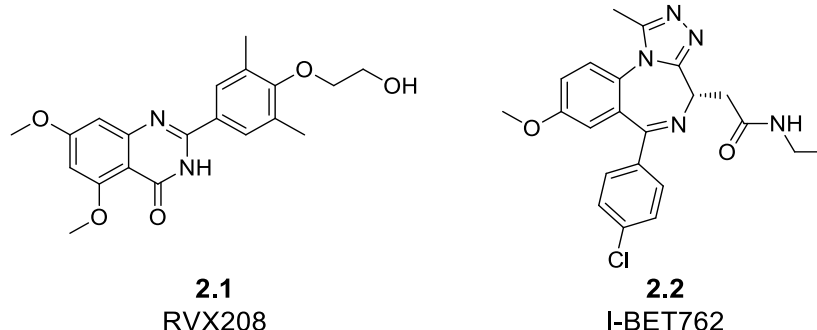
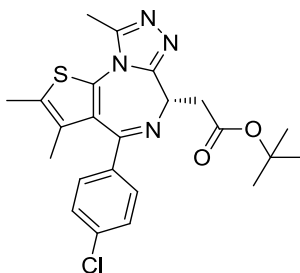


Figure 8: Structures of two small molecule pan-BET inhibitors currently in clinical trials.

RVX208 preferentially binds to the BD2 domain across the BET family (Brd2, Brd3, Brd4 and BrdT), whereas I-BET762 is a pan-BET inhibitor, which is equipotent across the BET family and the two bromodomains (BD1 and BD2).¹⁶ The early development of these molecules has demonstrated attractive preclinical pharmacological profiles for these indications. However, they were also associated with target-mediated toxicity

such as a high level of hepatic transaminases during clinical trials for RVX208, which were found to be reversible upon discontinuing the treatment administration.¹⁹ Mice studies on JQ1, one of the early BET inhibitors closely structurally related to I-BET762 (Figure 9), have shown to cause body weight loss, hematology changes and testicular changes.¹⁷ Clinical trials of other BET inhibitors for oncology indications have also reported severe thrombocytopenia, fatigue, nausea and gastro-intestinal side-effects.¹⁵



2.3
JQ1

Figure 9: Structure of JQ1, one of the first reported BET inhibitors.

Based on all of the above, the therapeutic window for these early molecules was found to be incompatible with non-oncologic indications,¹⁶ and in particular with diseases such as rheumatoid arthritis, where a chronic treatment is necessary. Therefore, developing a BET inhibitor with a higher therapeutic index than these predecessors is highly desirable in order to treat chronic diseases such as rheumatoid arthritis.

A strategy to increase the therapeutic index could be to deliver the BET-inhibitor molecule to the cell type of interest, such as macrophages for rheumatoid arthritis patients. This would limit the exposure of the BET-inhibitor in other cell types and, therefore, should decrease the target-mediated toxicity usually observed with systemic BET inhibition.

3. Targeted small molecule BET inhibitors for rheumatoid arthritis treatment

A technology that targets cells from the monocyte-macrophage lineage has been developed by Chroma Therapeutics.²⁰ Targeting a drug molecule to the relevant cells has the potential to reduce the levels of target-mediated toxicity, by limiting the drug's systemic exposure. A cell targeted approach has, therefore, the potential to improve the therapeutic window of a drug. The technology developed by Chroma Therapeutics has demonstrated an increased therapeutic window in *in vivo* studies on transgenic mice, for a histone deacetylase inhibitor (an epigenetic protein inhibitor).²⁰ This targeting technology is based on the introduction of an esterase sensitive motif (ESM) onto a drug molecule (Figure 10).

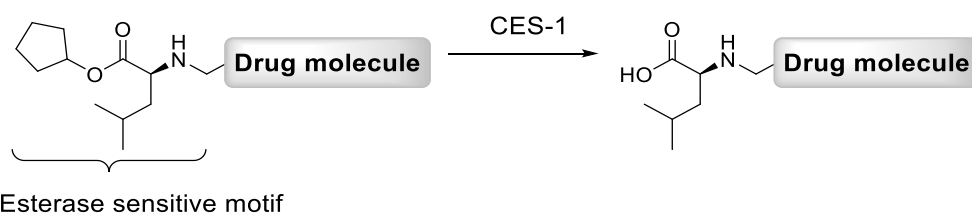


Figure 10: The esterase sensitive motif (ESM) is specifically hydrolysed by CES-1 to give the corresponding acid.

The ESM, derived from natural amino acids, can be specifically hydrolysed by carboxylesterase 1 (CES-1) to give the corresponding acid.²⁰ In human, CES-1 is predominantly expressed in cells from the monocyte-macrophage lineage and in hepatocytes. In CES-1 negative cells, the ESM targeted histone deacetylase inhibitor has demonstrated similar activity level to the non-targeted inhibitor.²⁰ In CES-1 positive cells, a 10-30 fold increase in inhibitory activity was reported.²⁰ This study also showed significant production of the corresponding acid specifically in cells containing CES-1. The acid, due to its intrinsic polarity at physiological pH (7.4), has limited cell membrane permeability, in contrast to the corresponding ester which is

neutral at this pH (measured pK_a amino ester $\sim 5-6$), and therefore has higher membrane permeability (Figure 11). These principles govern the ESM targeting mechanism, and combined with a drug molecule, the ESM technology can target the drug molecule to CES-1 positive cells as a result of the hydrolysis which occurs specifically in those cells.

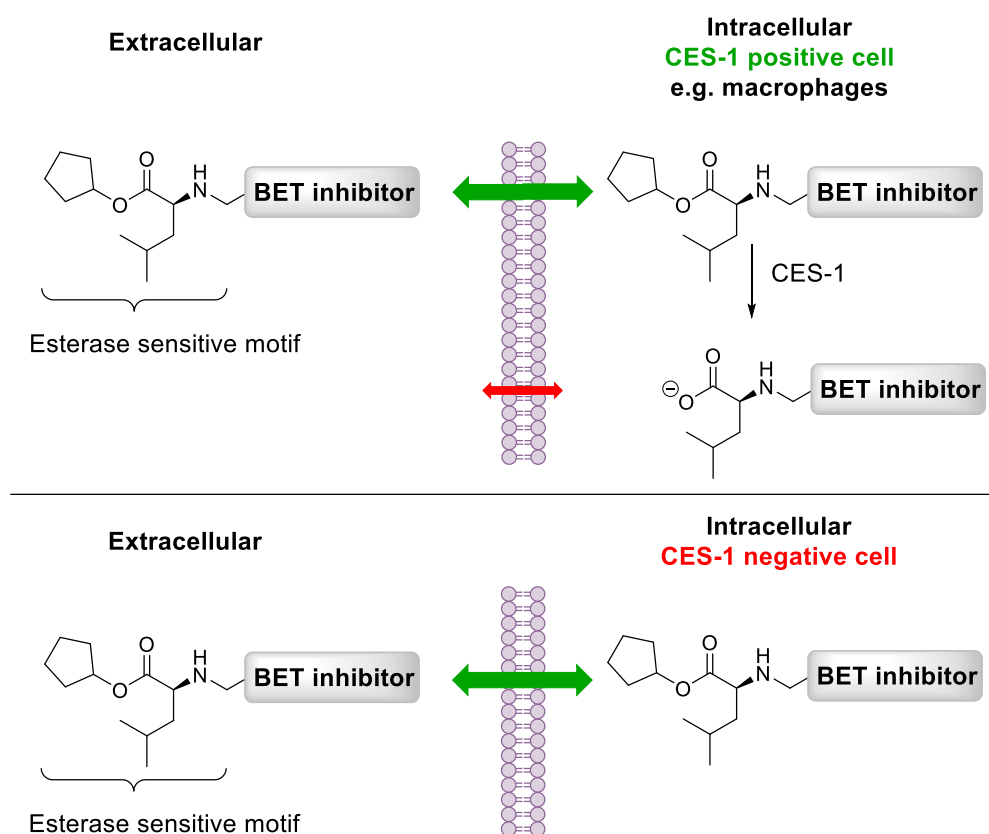


Figure 11: The principle of the ESM targeting mechanism. In CES-1 positive cells, the ester is hydrolysed to its corresponding acid. Due to its polarity, the acid is retained longer in the targeted cells. In CES-1 negative cells, the acid is not generated.

A drug molecule bearing an ESM group can permeate into cells as the ester and only in CES-1 positive cells is the acid generated. Due to its limited permeability, the acid bearing the drug molecule is retained in the cells for an extended time. This creates a high local concentration of the drug in CES-1 positive cells. In CES-1 negative cells, due to the lack of the specific esterase, the acid is not generated and the drug remains

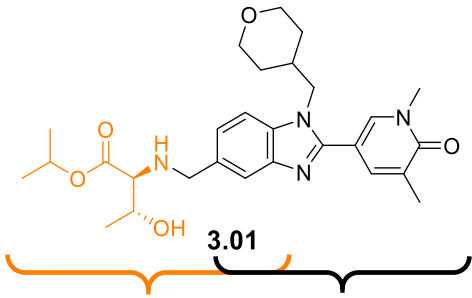
in equilibrium with the systemic circulation, and is therefore rapidly cleared by esterase metabolic enzymes in the liver.

In human, CES-1 is mainly present in cells from the monocyte-macrophage lineage and in the liver.²⁰ The distribution of CES-1 in human has two consequences: the generation of the acid, and subsequent retention of the drug, in the cells from the monocyte-macrophage lineage;²¹ and, the rapid systemic clearance of the ester due to the presence of CES-1 in hepatocytes.

Due to the crucial role of macrophages in the inflammation of joints of rheumatoid arthritis patients and the role of BET proteins in inflammatory mechanisms,^{4,6,8} a BET inhibitor associated with the ESM technology is of interest for rheumatoid arthritis treatment and is currently under investigation in our laboratories.

Profile of the first ESM-BET inhibitor suitable for in vivo studies

The structure and the profile of the first ESM-BET inhibitor progressed into pre-clinical studies is shown in Table 1.



	3.01
	CES-1 pharmacophore BET pharmacophore
hWB pIC ₅₀	7.6
hWB Δ <i>t</i> Bu ⁱⁱ	+ 0.9
Brd4 BD1 pIC ₅₀	7.3
ChromlogD _{7.4}	3.0
AMP (nm/s) / tPSA (Å ²)	73 / 108
HLM IVC (-/+ benzil) (mL/min/g)	1.5 / 0.9
Heps IVC Hu / Cyno (LBF)	73% / 41%

Table 1: Structure and profile of the first ESM-BET inhibitor suitable for *in vivo* studies.

Molecule **3.01** has the ESM (drawn in orange) branched on the BET inhibitor (drawn in black). The pyridone is the acetyl mimetic motif and the ESM is branched on the benzimidazole core, residing in the ZA channel (*cf.* section 4.1). The profile of the molecule, shown in Table 1,ⁱⁱⁱ has proven to be suitable for *in vivo* studies in cynomolgus monkey and the molecule has shown promising *in vitro* and *in vivo* results.²¹ Initial studies show a decrease in pro-inflammatory activity in cells from the monocyte-macrophage lineage and reduced pre-clinical toxicity when compared to the pan-BET molecules currently in clinical trials.²¹ Indeed, the rapid hepatic metabolic

ⁱⁱ hWB Δ*t*Bu is the difference between the human whole blood potencies of the compound and its *t*Bu ester direct analogue (non-hydrolysed by CES). It is used in this thesis to estimate the CES turnover.

ⁱⁱⁱ The assays will be discussed in section 4.2.

clearance, due to the presence of the ESM group, helps to moderate the target-mediated adverse effects usually observed with pan-BET inhibitors. This is achieved by limiting the duration of systemic exposure and retaining the active metabolite (the acid) only in the targeted cells, thereby increasing the therapeutic window when compared to a non-targeted pan-BET inhibitor.²¹

Due to the high attrition rate between the pre-clinical stage and the launch of a drug on the market,²² it is of interest to discover and progress a second ESM-BET inhibitor with a similar profile to molecule **3.01** but with some structural diversity to mitigate any unexpected structurally-related toxicity. The investigation of a new ESM-BET inhibitor series will be described herein, aiming to identify a molecule with the potential to be assessed in pre-clinical safety studies, and potentially beyond.

4. From a pan-BET inhibitor series to an ESM-BET inhibitor series

Historically, several pan-BET series have been developed in our laboratories.^{23,24,25} Amongst them, one of the most recently identified series has a benzazepinone acetylated lysine mimetic, as exemplified in molecule **4.01** and molecule **4.02** (Figure 12).²⁶

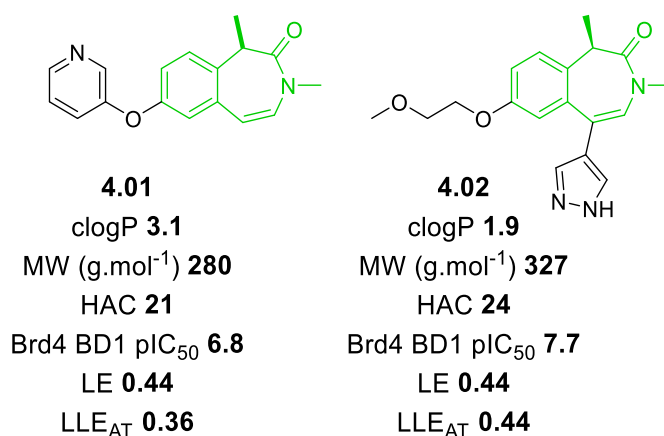


Figure 12: Structure and selected properties of molecules **4.01** and **4.02**, highlighted in green is the structure of the benzazepinone motif.

A number of studies over the last two decades have shown the importance of physico-chemical properties of hit and lead molecules in medicinal chemistry.^{22,27,28,29} From these observations, based on the study of molecular properties of past clinical successes and failures, a set of drug-like parameters for good oral absorption was defined, guiding scientists during the design and synthesis of oral drug candidate molecules.^{27,28,30} To assist with the comparison of activities and some key physico-chemical parameters of fragments or more advanced molecules, several tools such as the ligand efficiency index (**LE**, Equation 1)^{31,32} or the lipophilic ligand efficiency metric developed by Astex Ltd (**LLE_{AT}**, Equation 2),³³ have been reported in the literature. A threshold value of 0.30 kcal.mol⁻¹ (1.3 kJ.mol⁻¹) per heavy atom count (HAC), calculated based on a pIC₅₀ of 8 and a HAC of 36, is commonly used to define a good starting point for lead optimisation.³³

$$(1) \text{LE} = \Delta G^0 / \text{HAC} = - RT \text{Ln}(\text{K}_i) / \text{HAC} \approx 1.37 \times \text{pIC}_{50} / \text{HAC}$$

Equation 1: Ligand Efficiency (LE) is defined as the Gibbs free energy of binding per HAC.³²

$$(2) \text{LLE}_{\text{AT}} = 0.111 + [1.37 \times (\text{pIC}_{50} - \text{clogP})] / \text{HAC}$$

Equation 2: Lipophilic ligand efficiency developed by Astex Ltd, LLE_{AT}, takes into consideration the lipophilicity of the molecule in addition to the potency and HAC.³³

Whilst LE only considers the binding energy and the HAC, the LLE_{AT} offers a more advanced and interesting comparison of two molecules or fragments. Specifically, the LLE_{AT}, in addition to the binding energy and HAC, takes into consideration the lipophilicity of the molecule. This is particularly interesting as high lipophilicity has been correlated with lack of success in clinical studies of a candidate drug.³⁰ Therefore, a tool enabling the comparison of two fragments in terms of potency and lipophilicity

together is very valuable. In order to maintain the same threshold value of 0.30 to compare fragments between the two tools, the scales of LLE_{AT} and LE have been harmonised by adding 0.111 to the calculated LLE_{AT}.

Molecule **4.02** (Figure 12) is significantly more potent in the Brd4 BD1 assay, however molecule **4.01** is smaller. Interestingly, both fragments exhibit a similar LE value, well above the 0.30 conventional threshold. The different profiles of molecule **4.01** (small and more lipophilic) and molecule **4.02** (more potent, more polar but with a higher molecular weight) are more easily compared using the LLE_{AT}. Molecule **4.02**, despite a larger molecular weight, showed a clear advantage in terms of potency and polarity, translating into a high LLE_{AT} value.

Despite these differences in LLE_{AT}, these two fragments show excellent LE and LLE_{AT} making them good starting points to develop an ESM-BET inhibitor series.

4.1. Binding mode of a benzazepinone fragment into the bromodomain of BET proteins

As explained in section 1, the two bromodomains BD1 and BD2 of the four BET proteins (Brd2, Brd3, Brd4 and BrdT) can bind an acetylated lysine motif. Figure 13 shows the X-ray crystal structure of a benzazepinone fragment, molecule **4.01**, in the Brd2 BD2 binding site.³⁴

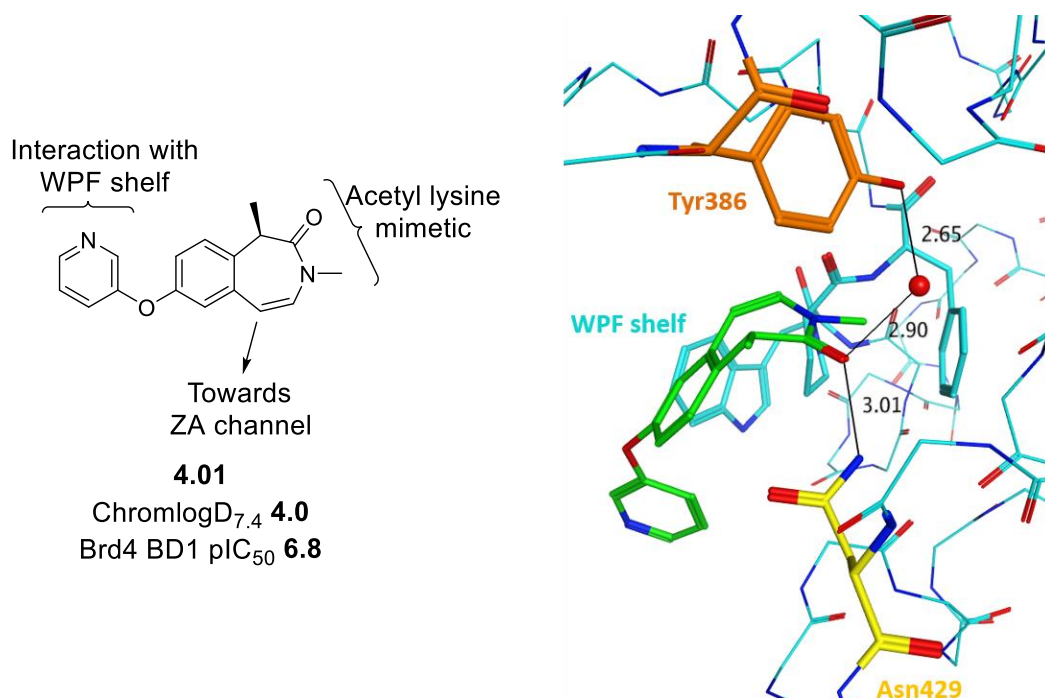


Figure 13: X-ray crystal structure of molecule **4.01** (green) in Brd2 BD2, showing direct and indirect hydrogen bonds (black) between Asn429 (yellow), Tyr386 (orange) and the amide carbonyl of the benzazepinone motif. Distances are measured in Å (PDB file *gsk7toac*).³⁴

The amide of the benzazepinone motif interacts with the bromodomain binding site *via* a hydrogen bond between the carbonyl oxygen and the amide functionality of Asn429 (yellow). There is also an indirect hydrogen bond, mediated by a water molecule, between the oxygen of the benzazepinone amide and the hydroxyl group of Tyr386 (orange).³⁵ These interactions of the benzazepinone group with the Asn and the Tyr residues are similar to the interactions of the bromodomain with the acetylated lysine fragment (Figure 6, p.16). These two interactions have proven to be important for small molecule BET inhibitors and are conserved in most fragments demonstrating activity against the BET family.¹³

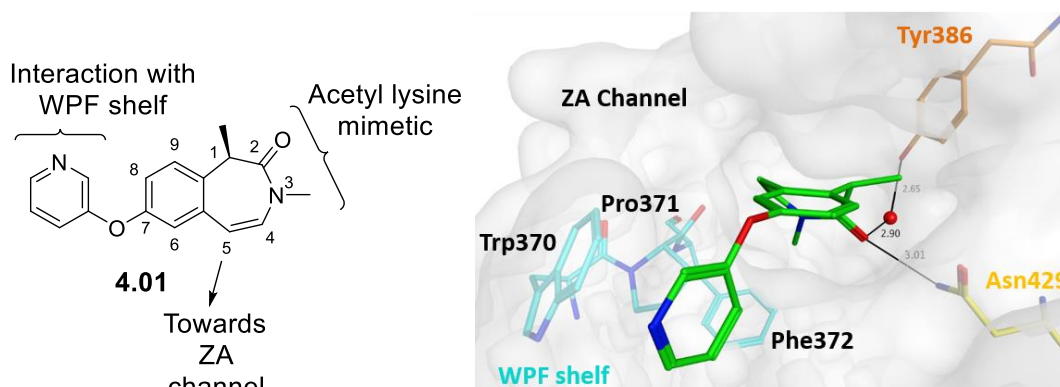


Figure 14: Structure of molecule **4.01** and X-ray crystal structure of molecule **4.01** (green) in Brd2 BD2 showing the ZA channel and the WPF residues (blue). (PDB file *gsk7toac*).³⁴

This X-ray crystal structure (Figure 14) also shows that the pyridine ring of molecule **4.01** interacts with the WPF shelf lipophilic region *via* edge-to-face interactions with the tryptophan Trp370 and there is no interaction of this fragment with the ZA channel. Initial X-ray crystallography of molecule **4.01** has demonstrated that interactions with each of these three regions of the BET bromodomains are feasible using the benzazepinone motif: the amide bond of the benzazepinone motif maintains the crucial interactions with Asn and Tyr residues and acts as an acetyl mimetic, interaction with the WPF shelf is possible from position 7 of molecule **4.01** and the ZA channel is accessible from position 5 of molecule **4.01** (Figure 14).

4.2. Aims of this work

Previous work within our laboratories has shown that the ESM group can be incorporated directly onto the WPF shelf group (discussed in section 4.3),³⁶ with the ESM group positioned outside of the bromodomain towards the solvent. The primary goal of the work described in this thesis is to understand if an ESM-BET inhibitor, with a good BET inhibitory activity and a low *in vitro* clearance profile (desired profile discussed later in this section), can be obtained by branching the ESM onto the WPF

shelf of the benzazepinone series (Figure 15). Subsequent efforts will then focus on identifying a molecule suitable for progression into *in vivo* pharmacokinetic (PK) studies with balanced properties between the BET pharmacophore and the targeting mechanism, driven by the CES-1 metabolic preference.

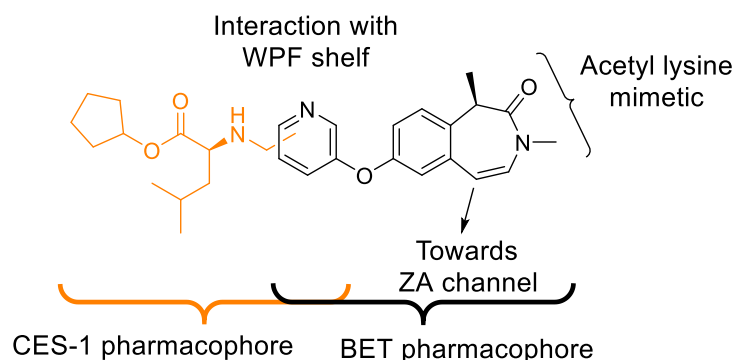


Figure 15: Representation of a hybrid ESM-BET inhibitor, highlighting the BET pharmacophore (in black) and the CES-1 pharmacophore (in orange).

The desired profile of an ESM-BET inhibitor suitable for progression to *in vivo* PK studies is described in Table 2.

Desired profile of an ESM-BET inhibitor	
hWB pIC ₅₀	≥ 7.6
hWB Δ <i>t</i> Bu ^{iv}	~ 1.0
Brd4 BD1 pIC ₅₀ ^{iv}	≥ 7.0
ChromlogD _{7.4}	≤ 3.3
AMP (nm/s) / tPSA (Å ²)	> 50 / ≤ 125
HLM IVC (- / + benzil) (mL/min/g)	≤ 3.0 / ≤ 2.0
Heps IVC Hu / Cyno (LBF)	≤ 75% / ≤ 75%

Table 2: Desired profile for an ESM-BET inhibitor in the benzazepinone series for progression to *in vivo* PK studies.

^{iv} hWB Δ*t*Bu is the difference between the human whole blood potencies of the compound and its *t*Bu direct analogue (non-hydrolysed by CES). It is used in this thesis to estimate the CES turnover. The Brd4 BD1 assay is a biochemical assay where the BD2 bromodomain is unable to bind an acetyl-lysine mimetic due to a mutation. The *in vitro* clearance (IVC) was routinely measured using human liver microsomes (HLM) and hepatocytes (heps) in human and monkeys to understand the metabolic rate of our molecules.

The required physico-chemical properties, potency and impact of the ESM mechanism on the desired profile required to progress a molecule into PK studies will be discussed in the subsequent sections.

4.2.1. Required human whole blood potency

The optimization efforts of the first ESM-BET inhibitor in our laboratories have demonstrated that a human whole blood (hWB) potency of 7.6, associated with low *in vitro* clearance (discussed in section 4.2.3.3), is required to progress a molecule to *in vivo* PK studies.

Previous studies on an ESM epigenetic protein inhibitor (histone deacetylase) have demonstrated that in CES-1 positive cells, there is a significant amount of the corresponding acid generated and that the potency is enhanced compared to CES-1 negative cells.²⁰ This is due to the generation, in the CES-1 positive cells, of the pharmacologically active acid. The acid, due to its limited permeability, is retained in the targeted cells and, due to its inhibitory activity, it contributes to the enhanced potency observed compared to CES-1 negative cells.^v Therefore, the human whole blood potency measured after 24 h incubation in our assay is a result of the BET inhibition of both the ester and the active acid metabolite. Both the ester and the acid demonstrate BET inhibitory activity due to the fact that the ESM moiety is directed towards the solvent and is not directly interacting with the BET protein.

^v Indeed, in a *in vitro* assay where an ESM-BET inhibitor is incubated in presence of CES-1 positive cells, the presence of acid can be measured in the cytosol of the CES-1 positive cells. However, in the same assay, no trace of acid can be detected in the buffer solution. This demonstrates the lack of permeability of the acid. In addition, this assay also demonstrated the *t*Bu-ESM analogues are not hydrolysed in CES-1 positive cells.

4.2.2. Impact of the ESM targeting mechanism on the desired profile

In addition to the BET bromodomain potency, the hydrolysis of the ester by CES-1 is an important component of the targeting mechanism, and also impacts the clearance of the molecule. Indeed, CES-1 is present in macrophages but also in hepatocytes, hence the CES-1 turnover is an important consideration in relation to the bioavailability of an ESM-BET inhibitor.

Studies have shown the *t*Bu ester analogue of an ESM-drug is not hydrolysed to the corresponding acid by CES-1.^{20,21} The *t*Bu ESM-BET molecules were therefore used as negative controls to monitor CES-1 activity, by measuring the difference in human whole blood activity between an hydrolysable ESM-BET inhibitor and the corresponding non-hydrolysable *t*Bu-ESM-BET inhibitor (formally expressed as hWB Δt Bu). During the optimisation of the first series of ESM-BET inhibitors, it was demonstrated that a difference of approximately one unit between the human whole blood potency of the hydrolysable versus the non-hydrolysable ESM was optimal to reach the correct balance between the targeting mechanism (generation of the acid in the targeted cells) and the first pass metabolism of the compound (Figure 16).²¹

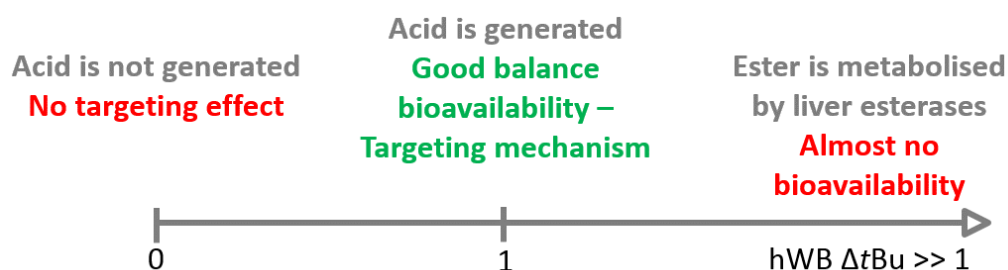


Figure 16: Representation of the balance between targeting effect and bioavailability of an ESM-targeted drug molecule. The two opposite factors can be balanced by measuring the difference in human whole blood potency of the ESM-BET inhibitor and the corresponding non-hydrolysable *t*Bu control.

Indeed, when hWB Δt Bu \sim 0, there is no targeting effect as the ester is not hydrolysed to its corresponding acid. When hWB Δt Bu \gg 1, the CES-1 turnover is extremely

rapid and therefore the drug is almost totally cleared during first pass hepatic metabolism. Therefore, efforts were focused on reaching a hWB Δt_{Bu} value of one log unit.

4.2.3. Physico-chemical properties

In recent years, studies into the attrition rate during drug development have highlighted the importance of controlling the physico-chemical properties of a drug candidate to minimize the risk of failure.²² Thus, tuning parameters such as lipophilicity, topological polar surface area (tPSA), molecular size and permeability have proven to improve the likelihood of success during the development of oral drugs.³⁷ Given the importance of physico-chemical properties for the development of an oral drug, and with the objective of designing an ESM-BET inhibitor within a good physico-chemical space, an analysis of several key parameters was conducted on the previous series of ESM-BET inhibitors at the outset of the work described in this thesis. Lipophilicity is a particularly important parameter to balance in a molecule. Indeed, a molecule with low lipophilicity is likely to have poor membrane permeability which is likely to cause poor oral absorption and low bioavailability.³⁷ Conversely, a lipophilic molecule is likely to have a high metabolic clearance and therefore poor bioavailability.³⁷ Therefore, relationships between ChromlogD_{7.4}, the chromatographically measured distribution coefficient at pH 7.4, and artificial membrane permeability (AMP) on one hand, and between ChromlogD_{7.4} with human hepatocyte *in vitro* clearance (IVC) on the other were established by the author. This analysis enabled the design of the desired physico-chemical profile for a second small molecule ESM-BET inhibitor (Table 2).

4.2.3.1. Relationship between ChromlogD_{7.4} and AMP

Measured AMP and ChromlogD_{7.4} data of the first ESM-BET series generated previously in our laboratories were obtained and analysed by the author. The experimental data was plotted on the graph shown in Figure 17.

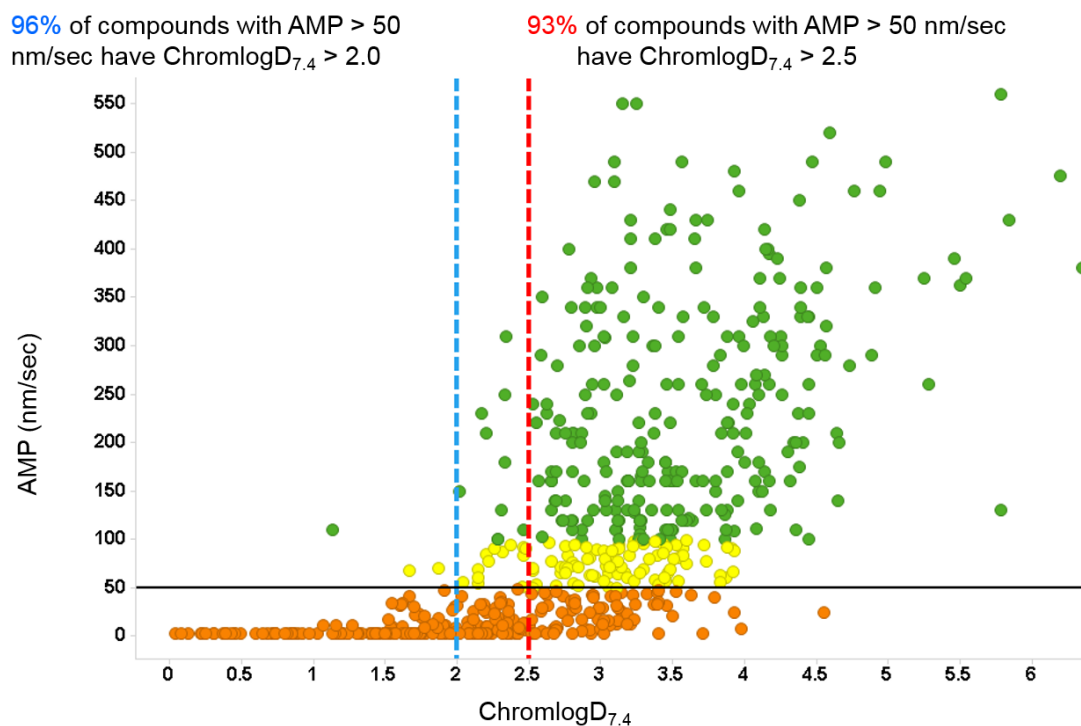


Figure 17: AMP vs. ChromlogD_{7.4} showing a large majority of the compounds from the first ESM-BET inhibitor series with a good AMP have a ChromlogD_{7.4} above 2.5. Colouring: green: AMP > 100 nm/sec; yellow: 50 < AMP < 100 nm/sec; orange: AMP < 50 nm/sec.

This analysis shows that:

- 93% of the compounds with an AMP > 50 nm/sec have a ChromlogD_{7.4} > 2.5, and
- 96% of the compounds with an AMP > 50 nm/sec have a ChromlogD_{7.4} > 2.0.

The analysis demonstrates that compounds with low ChromlogD_{7.4} are predicted to have poor cell membrane permeability, in accordance with the literature.²⁷ This analysis also shows that only 3% of compounds with a good predicted permeability (> 50 nm/s) have a ChromlogD_{7.4} value between 2.0 and 2.5. As a consequence of this

analysis, the synthesis of ESM-BET inhibitors in the benzazepinone series was focused mainly on compounds with calculated $\text{ChromlogD}_{7.4} > 2.5$ in order to enhance the probability of good cell permeability.

4.2.3.2. Polar surface area (PSA)

Egan *et al.* have shown that lipophilicity and polar surface area (PSA) can help to guide the design of small molecules for an oral drug profile by targeting molecular properties associated with well-absorbed compounds.^{27,37,38} This analysis concluded that most compounds within a clogP range of 2.5-3.3 and with good oral absorption have a tPSA $\leq 120\text{-}125 \text{ \AA}^2$. These criteria were therefore used as the upper limit to guide the design of compounds for the ESM-BET benzazepinone series (Table 2, p.29).

4.2.3.3. Relationship between $\text{ChromlogD}_{7.4}$ and human hepatocyte *in vitro* clearance

The human hepatocyte *in vitro* clearance assay is the gold standard used in pharmaceutical research to evaluate the phase I and phase II metabolism of a drug molecule. Hepatocyte *in vitro* clearance data is used to predict the *in vivo* PK of the compounds,³⁹ and thus it is commonly used early in a structure-activity relationship (SAR) analysis to identify compounds suitable for progression into more expensive and time consuming *in vivo* PK experiments.

In addition to examining the correlation between the lipophilicity of the compounds and the membrane permeability, an analysis of the relationship between human hepatocyte *in vitro* clearance and $\text{ChromlogD}_{7.4}$ for the previous series of ESM-BET inhibitors was conducted by the author (Figure 18).

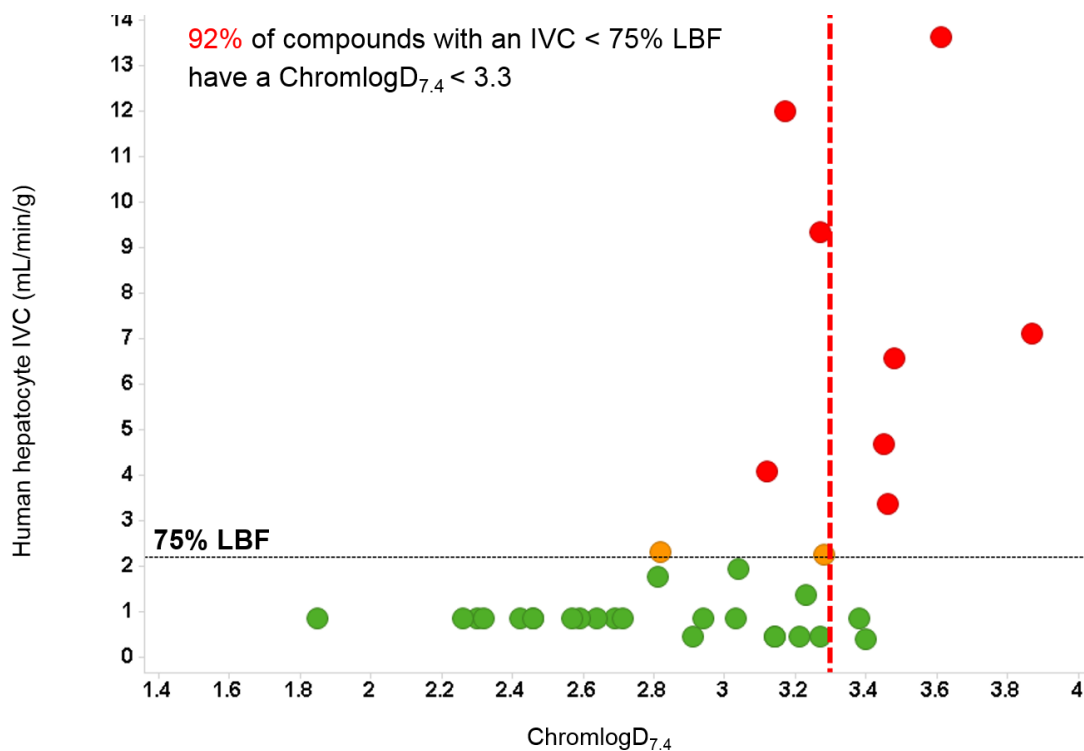


Figure 18: Human hepatocyte *in vitro* clearance data and ChromlogD_{7.4} for previous ESM-BET inhibitors series. This representation shows that most compounds with a good human hepatocyte *in vitro* clearance have a ChromlogD_{7.4} under 3.3.

It is worth noting the available data set for this analysis is much smaller than for the analysis of the relationship between AMP and ChromlogD_{7.4}. Nevertheless, this small data set can be used to understand the trend between human hepatocyte *in vitro* clearance and ChromlogD_{7.4}. Figure 18 shows that all compounds with a ChromlogD_{7.4} > 3.4 have a high human hepatocyte *in vitro* clearance (> 75% liver blood flow (LBF)). This analysis also shows that 92% of the compounds with good human hepatocyte *in vitro* clearance (< 75% liver blood flow), have a ChromlogD_{7.4} < 3.3. This result, that lipophilic molecules tend to have higher intrinsic clearance than more polar compounds, is again supported by the literature.²⁷ Based on the analysis of the relationship between the ChromlogD_{7.4} and the human hepatocyte *in vitro* clearance data of previous ESM-BET inhibitor series, the synthesis of compounds was focused

on molecules with an *in silico* ChromlogD_{7.4} < 3.3, as shown in the desired profile criteria in Table 2 (p.29).

The screening cascade (Figure 19), used to drive our optimisation trajectory, was therefore designed to reflect the emphasis on populating good physico-chemical property space as established from the analysis presented above.

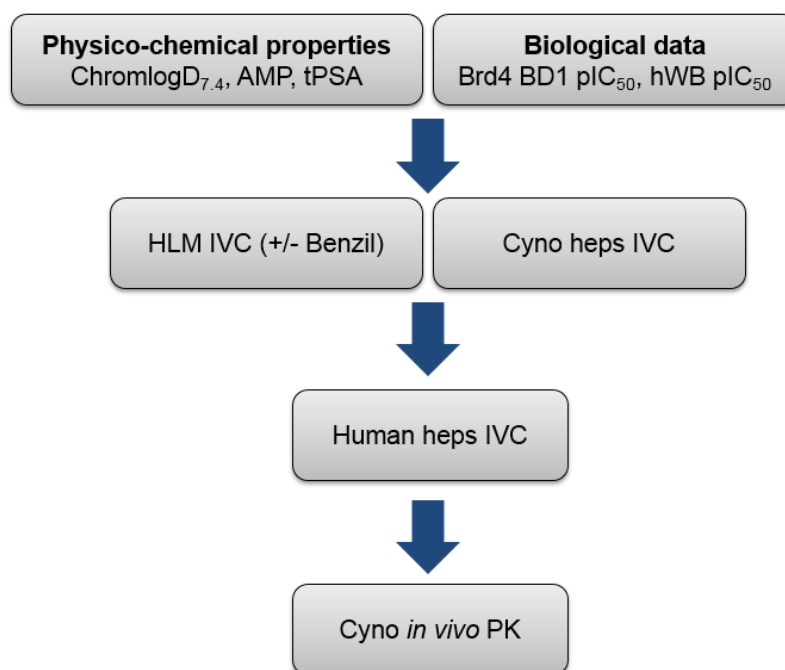


Figure 19: Screening cascade used for progression of the benzazepinone series of ESM-BET inhibitors.⁴⁰

Molecules with the desired human whole blood potency, a positive hWB Δ /Bu and within the desired physico-chemical space were progressed for human liver microsome *in vitro* clearance (HLM IVC) assays. Although the hepatocyte *in vitro* clearance assay is the gold standard for prediction of *in vivo* clearance from *in vitro* clearance data, the cheaper and higher throughput human liver microsome *in vitro* clearance assay is often used to triage compounds to send for hepatocyte *in vitro* clearance. Microsomes are vesicles formed from lysate of hepatocyte cells and are often used to predict phase I metabolism. As the phase II metabolism is not

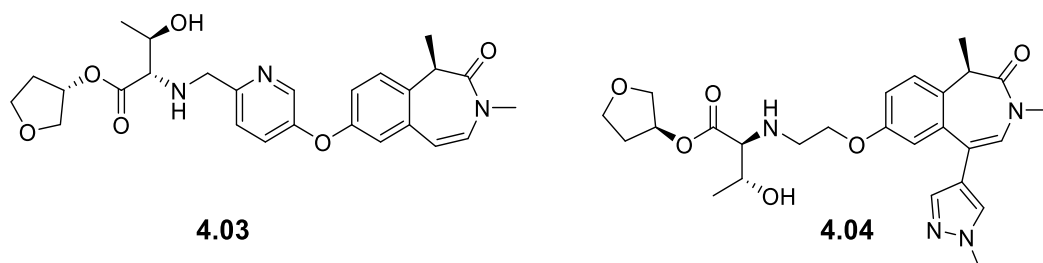
represented, it is often an under-prediction of the actual clearance of the molecule.³⁹ Molecules with high human liver microsome *in vitro* clearance (> 3.0 mL/min/g) were therefore not submitted for human hepatocyte *in vitro* clearance assays.

The human liver microsome *in vitro* clearance assays were performed twice for each new compound. The second human liver microsome *in vitro* clearance assay was run in presence of benzil, a diketone derivative used as a human CES inhibitor, suppressing the CES component of the phase I metabolic activities.^{41,42,43} These two assays were routinely used to dissociate the underlying metabolism of the molecule (human liver microsome *in vitro* clearance + benzil) from the overall metabolic activity including the specific metabolic esterase activity (human liver microsome *in vitro* clearance - benzil). Compounds with an overall human liver microsome *in vitro* clearance (- benzil) < 3.0 mL/min/g, corresponding to an 80% liver blood flow threshold, were then progressed to human hepatocyte *in vitro* clearance to understand phase I and phase II metabolism of the compounds. In parallel to the human liver microsome *in vitro* clearance assays, the cynomolgus monkey hepatocytes *in vitro* clearance data was generated in preparation for *in vivo* PK studies.

To conclude, analysis of the progenitor ESM-BET inhibitor series and literature guidelines of the desired physico-chemical space for oral drug molecules have been used to inform the desired profile for a successor series of ESM-BET inhibitors (Table 2, p.29). Reaching this desired profile with an ESM-benzazepinone compound, should enable the progression of the selected molecule to *in vivo* PK studies, the first step towards the development of an oral ESM-BET inhibitor drug candidate, as a potential alternative to our existing asset.

4.3. Initial compounds

Prior to the work described in this thesis, the first ESM-BET inhibitors from the benzazepinone series were designed based on molecules **4.01** and **4.02**.³⁶ The data associated with these compounds (molecules **4.03** and **4.04**) is shown in Table 3.



	Molecule 4.03	Molecule 4.04	Desired profile
hWB pIC ₅₀	7.4	8.1	≥ 7.6
hWB Δ <i>t</i> Bu ^{vi}	+ 1.5	+ 0.9	~ + 1.0
Brd4 BD1 pIC ₅₀	7.0	7.6	≥ 7.0
ChromlogD _{7.4}	3.9	3.0	≤ 3.3
AMP (nm/s) / tPSA (Å ²)	270 / 110	235 / 115	≥ 50 / ≤ 125
HLM IVC (-/+ benzil) (mL/min/g)	7.7 / 3.0	5.7 / 1.6	≤ 3.0 / ≤ 2.0
Heps IVC Hu / Cyno (LBF)	- / > 99%	- / 95%	≤ 75% / ≤ 75%
CES-2 t _{1/2} (min)	-	3	> 139

Table 3: Chemical structures and physico-chemical and biological data for molecule **4.03** and **4.04**.

The data on these initial compounds showed a hWB Δ*t*Bu > 0, demonstrating the ESM group is hydrolysed by CES-1, one of the crucial requirements for the targeting mechanism. Molecule **4.03** also shows a comparatively high ChromlogD_{7.4}, which is associated with elevated human liver microsome *in vitro* clearance and cynomolgus

^{vi} hWB Δ*t*Bu is the difference between the human whole blood potencies of the compound and its *t*Bu direct analogue (non-hydrolysed by CES). It is used in this thesis to estimate the CES turnover.

monkey (cyno) hepatocyte *in vitro* clearance. Molecule **4.04** overall showed good potency and an acceptable physico-chemical profile. However, the human liver microsome *in vitro* clearance assay showed a high overall value (HLM-benzil), despite the low underlying clearance of the molecule (HLM+benzil).^{vii} This deconvolution of the human liver microsome *in vitro* clearance data demonstrates that the apparent high clearance of the compound is due to an excessive esterase turnover. This is in apparent contradiction with the hWB Δt Bu value, showing an ester hydrolysis rate in the desired range (~1).

The human liver microsome *in vitro* clearance additive, benzil, can inhibit both CES-1 and CES-2 esterases,⁴⁴ and CES-2 is not present in myeloid cells. Therefore, it was proposed by the research team that molecule **4.04** might be hydrolysed by both esterases CES-1 and CES-2,⁴⁵ as this would be consistent with the human liver microsome *in vitro* clearance profile and the hWB Δt Bu value observed. To confirm this hypothesis, the half-life ($t_{1/2}$) of molecule **4.04** in the presence of human CES-2 was measured. The extremely short CES-2 half-life measured for molecule **4.04** (3 min) demonstrates the lack of esterase selectivity of our molecule, at least in the human CES family of esterases, and therefore highlighted one of the first issues to be addressed in this chemical series.

^{vii} Benzil is a CES inhibitor able to inhibit the esterase component of the human liver phase I metabolism.

4.4. Research objectives

4.4.1. Synthetic chemistry

At the beginning of this work, the synthesis of the benzazepinone motif was low yielding and was rapidly identified as a priority in order to facilitate the efficient establishment of the SAR within the ESM-benzazepinone series. One of the first research objectives was therefore to identify key intermediates for the ESM-benzazepinone series and to improve the synthesis of the benzazepinone motif in order to support the development of the SAR in this series.

4.4.2. Medicinal chemistry

From the initial data on molecules **4.03** and **4.04**, the medicinal chemistry objectives for the work described in this thesis were to:

- Understand the CES hydrolytic activity and design molecules with an increased CES-2 $t_{1/2}$ whilst maintaining an appropriate level of CES-1 turnover. This was anticipated to be instrumental in decreasing the high *in vitro* clearance observed in the initial lead molecules.
- Designing molecules with controlled lipophilicity, i.e. $2.5 \leq \text{ChromlogD}_{7.4} \leq 3.3$, equally should be instrumental in the reduction of the *in vitro* clearance as demonstrated in Figure 18 (p.35).
- Maintain the human whole blood potency above a pIC_{50} of 7.6 and meeting the desired overall profile (Table 2, p.29) in order to identify one or several molecules suitable for progression into monkey *in vivo* PK and safety studies.

Results and discussion

5. Increasing CES-2 half-life

This chapter describes the substrate requirements to reach the catalytic triad in CES-1 and CES-2 and the strategy implemented to increase the CES-2 half-life in our series.

5.1. Evaluation of *in silico* ChromlogD_{7.4} model

As demonstrated in section 4.2.3, the ChromlogD_{7.4} values can be optimised for ESM-drug molecules to balance metabolic clearance and permeability. Therefore, molecules proposed for synthesis were submitted to the model for ChromlogD_{7.4} calculation available in our laboratories. However, the first few compounds synthesised within the ESM- benzazepinone series showed a significant discrepancy between the *in silico* ChromlogD_{7.4} model and the ChromlogD_{7.4} values determined experimentally, as exemplified in Table 4.

	Molecule 4.03	Molecule 4.04
Calculated ChromlogD _{7.4} (global model)	2.9	2.1
Measured ChromlogD _{7.4}	3.9	3.0

Table 4: Comparison of calculated (global model) and measured ChromlogD_{7.4}.

The lack of accuracy associated with the global ChromlogD_{7.4} model for the ESM-benzazepinone molecules ultimately led to the synthesis of several molecules which were more lipophilic than desired. After identification of this issue, an analysis of the first set of ESM-benzazepinone molecules was conducted by the author at the outset of this work, in order to establish the relationship between the calculated and measured values. This difference between the model and the experimental values is illustrated in Figure 20.

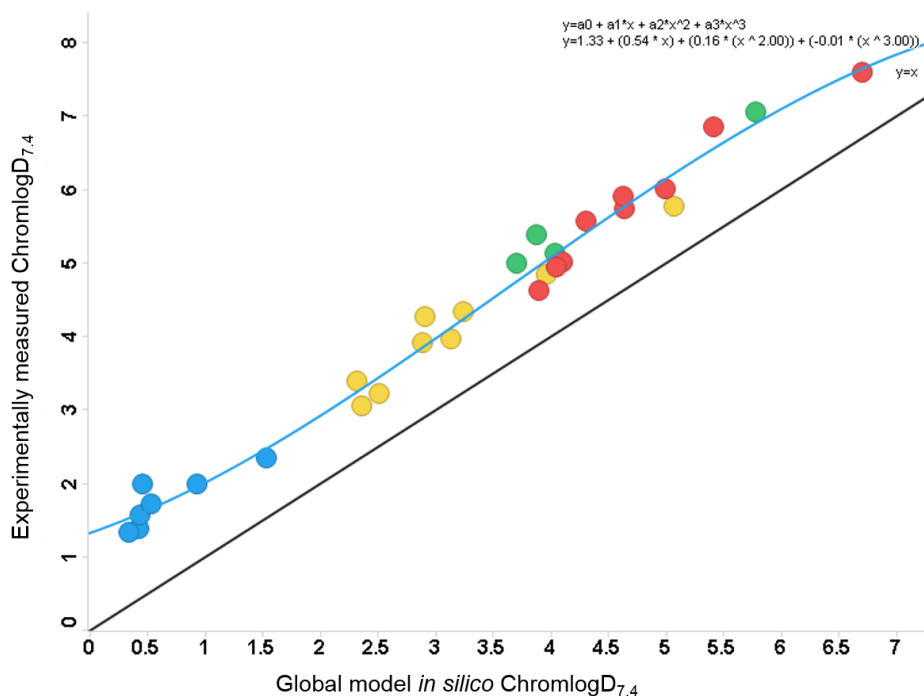


Figure 20: Measured $\text{ChromlogD}_{7.4}$ vs. the calculated value. The black line is the unity line ($y = x$) and the blue curve is the third-degree polynomial curve fitting the experimental data. From the equation of the blue fitting curve, more accurate *in silico* $\text{ChromlogD}_{7.4}$ values were generated. Colouring per the ESM pharmacophore used: red *tBu-Thr*, green *iPr-Thr*, yellow (*S*)-*THF-Thr*, blue acid.

This plot shows in black the unity line ($y = x$) and the calculated and measured $\text{ChromlogD}_{7.4}$ values for ESM-benzazepinone compounds. The difference between calculated and measured values is often substantial, resulting in an under-estimation of the lipophilicity of the compounds by approximately one log unit. A third-degree polynomial curve, fitting the experimental data, was generated from this plot; the equation associated to the curve is:

$$Y = 1.33 + 0.54 X + 0.16 X^2 - 0.01 X^3$$

Y = corrected calculated
 $\text{ChromlogD}_{7.4}$
 X = global model for
 $\text{ChromlogD}_{7.4}$

Equation 3: Corrected calculated $\text{ChromlogD}_{7.4}$ equation for ESM-benzazepinone molecules

This equation was used to generate more accurate calculated ChromlogD_{7.4} values and was used by the team for subsequent work carried out in this series. Hereafter, it will be referred to as cChromlogD_{7.4}.

5.2. Working hypothesis to reach the desired *in vitro* profile

As stated above, one of the key challenges to reach the desired profile is to understand how to modulate the CES activity. Indeed, controlling both CES activity and the lipophilicity, will be instrumental in reaching the desired *in vitro* clearance properties. The human CES-1 active site is described in the literature as a lipophilic pocket with a narrow channel.⁴⁶ By incorporating steric bulk in the ZA channel and thereby reducing the linearity of the molecule, the affinity of the compound for the CES-1 active site should decrease, potentially slowing the esterase turnover to reach the desired value of hWB ΔtBu ~ 1. Introducing an appropriate substituent in the ZA channel should also help to increase the human whole blood potency of molecule **4.03**, by increasing the BET activity, and also help to reduce the lipophilicity as exemplified in Table 5.

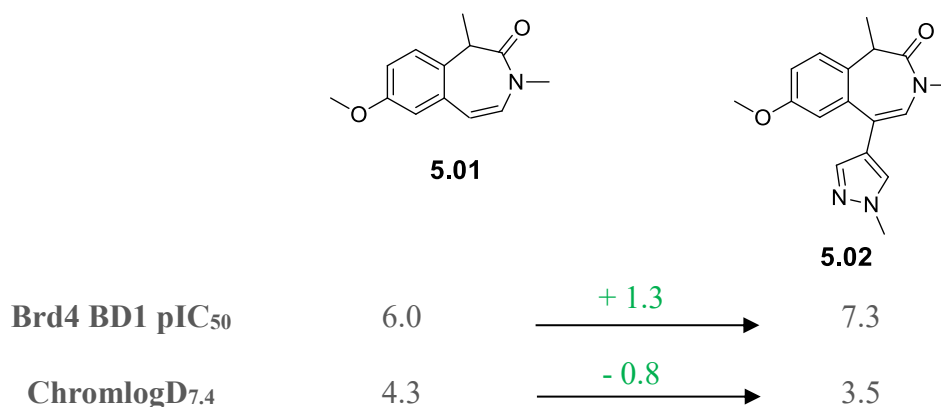


Table 5: Effect of the addition of a substituent in the ZA channel on the Brd4 Bdl potency and lipophilicity.

In addition to the relatively high CES-1 turnover, molecule **4.04** (Table 3, p.38) showed a very short CES-2 $t_{1/2}$. CES-2 is a metabolic esterase mainly present in the human intestinal membrane,⁴⁷ therefore a high turnover by this CES isoform would negatively impact oral bioavailability, and is thus undesirable for the development of an oral ESM-BET inhibitor. In addition to the CES-2 instability, the *in vitro* clearance of molecule **4.04** in cynomolgus monkey hepatocytes proved to be very high. Similarities between human and cynomolgus monkey CES families have been established and the relevance of the use of monkey as a large animal species for PK and toxicity studies for CES-based mechanism drugs has been acknowledged.⁴⁸ However, it is worth highlighting that depending on the substrate, the ester hydrolysis rate by cynomolgus monkey CES may be substantially higher than the human CES hydrolysis rate of the same substrate.⁴⁸ It was proposed by the author that the high cynomolgus monkey hepatocytes *in vitro* clearance, the high apparent human liver microsome *in vitro* clearance (-benzil) and the short CES-2 $t_{1/2}$ of molecule **4.04** were resulting from a single issue: a lack of esterase selectivity.

5.3. Understanding CES hydrolysis rate

The CES family is divided into five subfamilies: CES-1, CES-2, CES-3, CES-4 and CES-5, according to their amino acid sequences.⁴⁹ Each CES-X subfamily is further subdivided according to species differences e.g. CES-1A for human, monkey and rabbits, CES-1B for rat, mouse and hamster and CES-1C for dog, cat, and pig.

In human, the distribution and level of expression of the CES-X subfamilies can substantially vary.⁴⁹ CES-1 is mainly expressed in the liver and in myeloid cells.^{46,49} CES-2 is mainly located in intestinal cells.⁴⁶ CES-3 can be found in the liver and

gastrointestinal tract but is expressed at very low levels compared to CES-1 and CES-2.⁴⁹ CES-4 does not appear to play a role in the human metabolic system.⁴⁹ Finally, CES-5 has a different structure compared to the other CES-X families,⁴⁹ and this should prevent any selectivity issues using the ESM technology. Therefore, CES-2 appears to be the only member of the CES family able to potentially cause an issue during the development of an oral drug using the ESM technology. Consequently, the research efforts presented in this thesis were focussed on increasing the CES-2 stability of the compounds whilst maintaining some degree of CES-1 turnover, necessary for the targeting mechanism.

In several reports, it has been suggested that the steric bulk of the ester could have a significant importance on the hydrolysis rate by and within the CES family.^{47,48,49} In particular, an ester substrate leading to a sterically hindered acid and a small alcohol would favour CES-1 hydrolysis over CES-2 (Figure 21).^{47,49} Conversely, a more narrow and flexible acid and a bulky alcohol would favour rapid hydrolysis by CES-2.

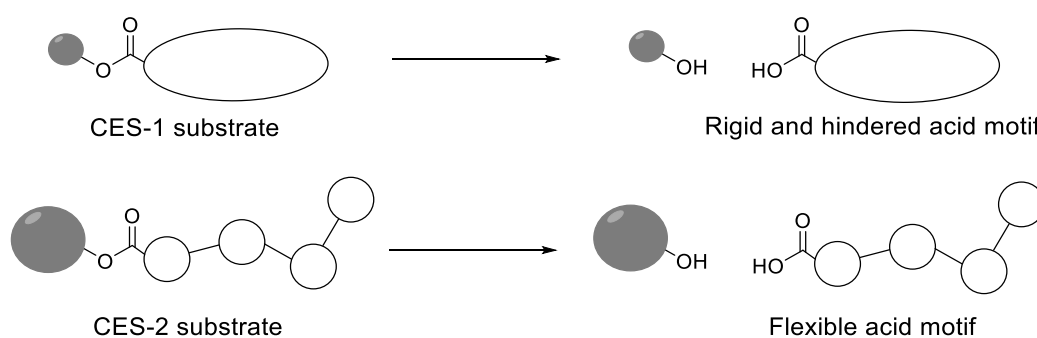


Figure 21: Mnemonic for substrate specificity for CES-1 and CES-2 hydrolysis.

The hydrolysis of a substrate by CES-1 or CES-2 occurs by the nucleophilic attack of a serine residue onto the ester functionality.⁴⁶ The reaction progresses due to the stabilization of the ionic species generated during the ester cleavage by adjacent hydrogen bond donors on amino acid residues in the hydrolytic cavity.⁴⁶ This set of amino acids responsible for the ester hydrolysis in the CES family, are known as the

CES catalytic triad (hydrolytic serine and two adjacent stabilising amino acid residues, histidine and glutamate).⁴⁶

Crystallographic data for CES-1 is available in the public domain, however, no crystal structure of human CES-2 protein has yet been reported.⁴⁹ A homology model of CES-2 compared to CES-1 suggested that the entrance to the binding site of the two esterases is different.⁴⁶ In CES-1, the ester substrate can access the catalytic triad through a deep pocket with a narrow gorge at the entrance (Figure 22). In CES-2, due to the replacement of a valine residue in CES-1 by a larger phenylalanine residue, the access of the substrate to the hydrolytic site is forbidden at this position. However, a loop present in CES-1 is missing in CES-2 and this creates a new possible entrance for an ester substrate to access the catalytic triad. This new access point requires a flexible and slightly narrower linker to the amino ester motif, which are able to bend and match the shape of this new access to reach the catalytic domain.

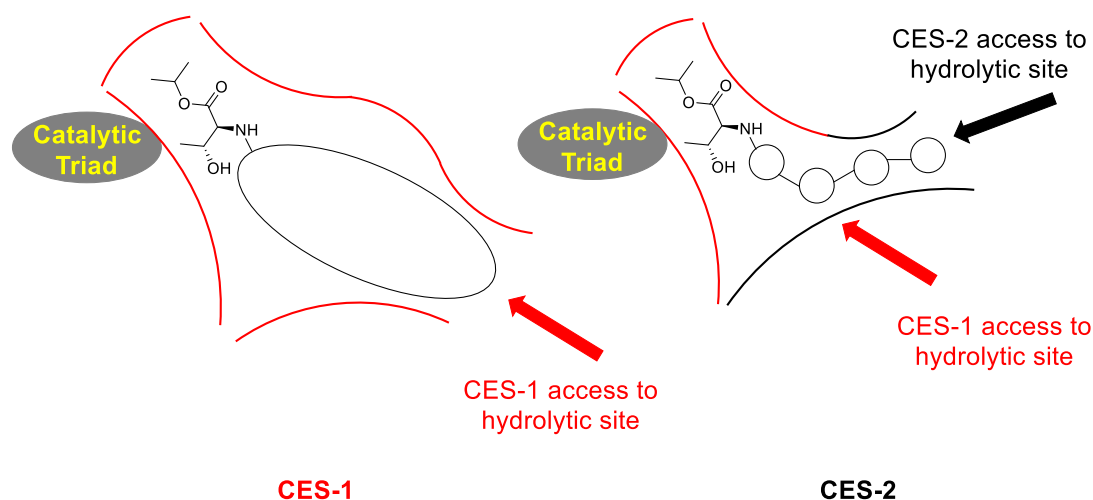


Figure 22: Schematic representation of the access to CES-1 and CES-2 hydrolytic sites.

These differences in size and angle to access the catalytic triad in CES-1 and CES-2 explain the differences in substrate preference, shown qualitatively in Figure 21 (p.45).

5.4. Design hypothesis to increase the CES-2 half-life

Based on the differences between the CES-1 and CES-2 active sites presented above, the strategy developed by the author to increase the CES-2 $t_{1/2}$ whilst maintaining the CES-1 turnover was based on increasing the steric hindrance of the linker to the ESM (Figure 23).

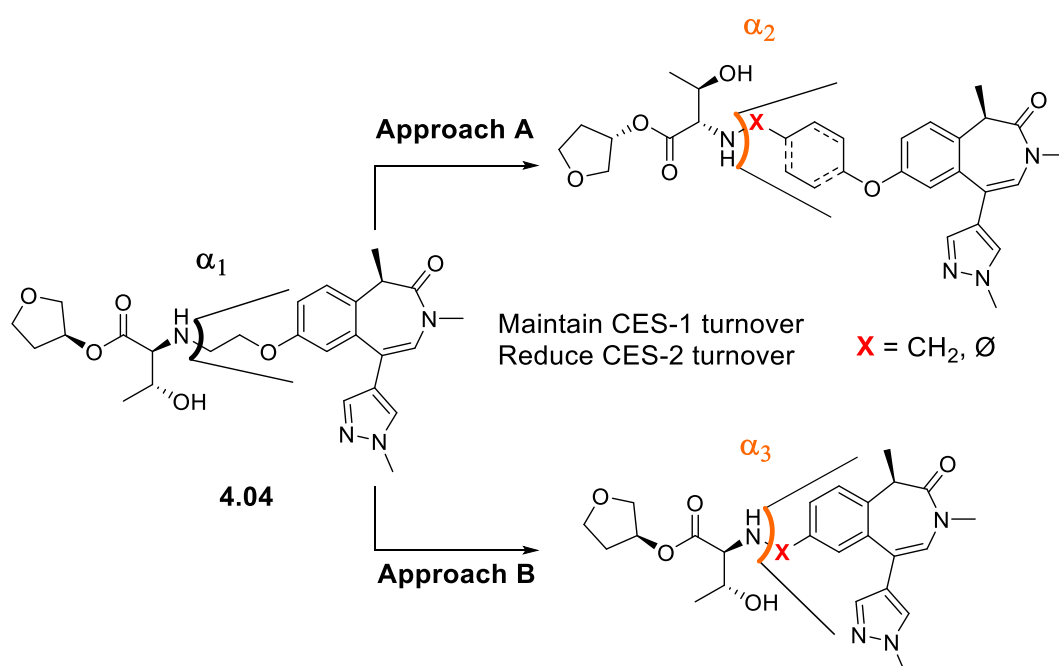


Figure 23: Strategy to increase the CES-2 half-life based on increasing the steric hindrance of the linker.

Two approaches to increase the steric hindrance of the linker were investigated:

- Physically increasing the steric hindrance of the linker by replacing the ethyl linker with a saturated or unsaturated ring (**approach A**).
- Increasing the steric hindrance of the linker by reducing the linker length and thus bringing the bulky BET inhibitor closer to the ESM (**approach B**).

These two approaches both aimed at accessing a linker angle α_2 or $\alpha_3 > \alpha_1$ (Figure 23). With a more rigid and sterically hindered linker to the ESM, the new molecules should be preferred substrates for CES-1 compared to CES-2. Indeed, to reach the

catalytic triad, the molecule needs some level of flexibility to reach the CES-2 hydrolytic site due to the non-linear shape of the active site. In CES-1, the pocket is able to accommodate larger and more rigid linkers to the ESM due to the comparatively linear shape of the active site, thus these new molecules should retain some level of CES-1 hydrolysis. This set of molecules should therefore demonstrate a longer CES-2 $t_{1/2}$ and retain some level of CES-1 hydrolysis compared to molecule **4.04**.

5.5. Design of new linkers

5.5.1. Approach A

As shown in molecule **4.03**, an aromatic ring can be used as the linker to the ESM whilst demonstrating good Brd4 BD1 potency (Table 3, p.38). Therefore, the aliphatic linker of molecule **4.04** was replaced by an aromatic ring to provide molecule **5.03** (Figure 24). The aryl ring will increase the steric hindrance of the linker and decrease its flexibility, and accordingly decrease the affinity of the molecule for the CES-2 active site. This new molecule was designed with a pyrazine ring to help balance the ChromlogD_{7.4} of the molecule. Molecule **5.03** has a cChromlogD_{7.4} within the desired range and the new linker is the single point change compared to molecule **4.04** (both the ESM and ZA channel groups are retained).

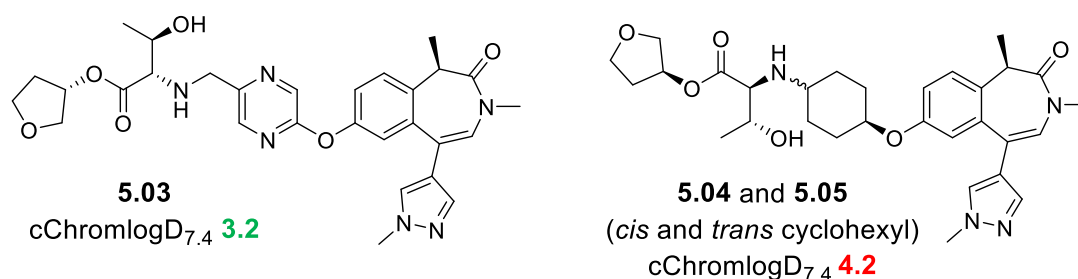


Figure 24: Structure of molecule **5.03-5.05** to investigate the impact of the linker on the CES-2 stability.

In parallel, cyclohexanol linkers in molecules **5.04** and **5.05** were also designed by the author to increase the steric hindrance of the linker. In particular, introducing sp³ character in the linker *via* the use of a saturated ring was thought to be an alternative solution to increase further the CES-2 half-life. Molecules **5.04** and **5.05** unfortunately showed a high cChromlogD_{7.4}, above the desired range [2.5-3.3]. However, to compare the sole impact of the linker on the CES-2 turnover, the decision was made not to make any additional change to molecules **5.04** and **5.05**. This would enable a direct comparison of the CES-2 stability for the different linkers. However, the difference in lipophilicity of the molecule was expected to have an impact on the wider profile of the molecule, in particular on the *in vitro* clearance data.

5.5.2. Approach B

The second approach investigated was to shorten the linker to its minimum length. This was thought to potentially bring two positive considerations. Firstly, this approach should increase the CES-2 half-life by bringing the ESM closer to the benzazepinone core and therefore decreasing the affinity for CES-2, by reducing the flexibility and the linearity of the molecule. This would also significantly decrease the molecular weight of the compounds to a 400-475 g/mol range, which is an under-investigated space in the ESM-BET series of interest to our laboratories (delimited by the dotted lines in Figure 25). Indeed, as shown on the box plot, most ESM series investigated so far have a median molecular weight in the 478-514 g/mol range.

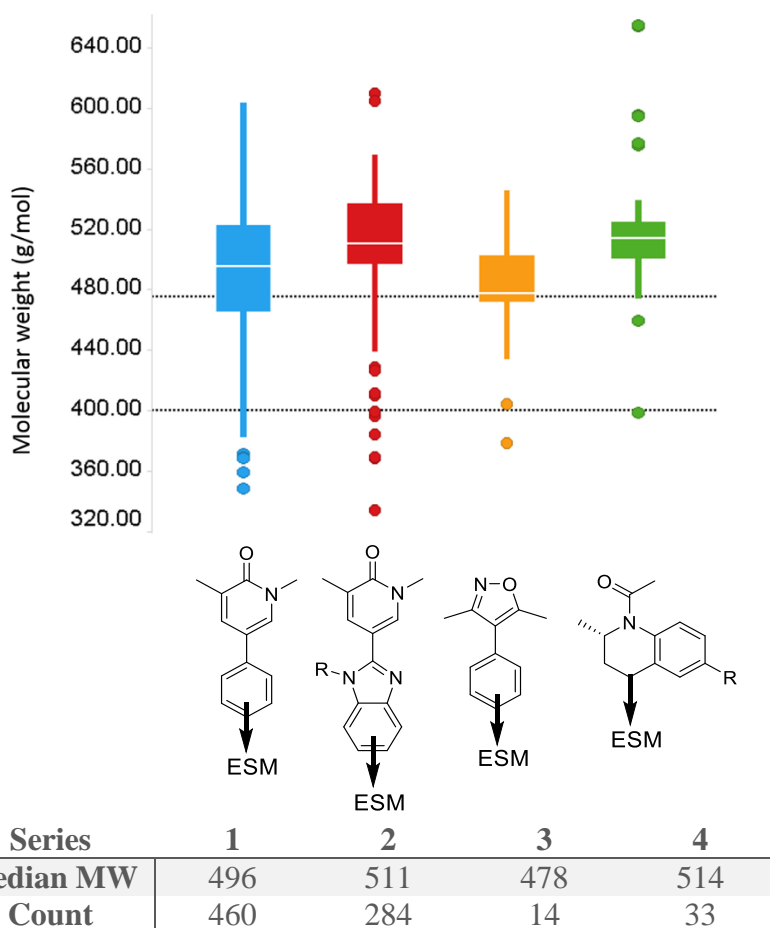


Figure 25: Box plot for the historical series of ESM-BET inhibitors (unpublished data) showing the series median molecular weight is above 475 g/mol.

Two compounds, molecules **5.06** and **5.07**, were therefore designed to understand the effect of short linkers on the CES-2 half-life. Molecule **5.06** (Figure 26) has a benzylic linker which is the original linker used with the ESM technology as developed by Chroma Therapeutics for their histone deacetylase inhibitor molecules.²⁰ It is worth noting that the pyrazine linker of molecule **5.03** was also designed with this methylene to the ESM, to retain the original design.

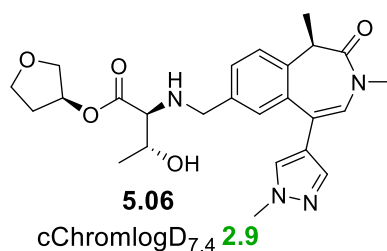


Figure 26: ESM-BET inhibitor with the original benzylic linker to the ESM as described by Chroma Therapeutics.

Finally, an ESM directly attached to the core of the BET inhibitor, molecule **5.07** (Figure 27), was designed to understand if this minimal design was compatible with the CES-1 targeting mechanism, and if it would increase the CES-2 half-life (Figure 27).

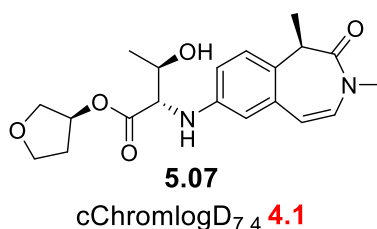


Figure 27: Directly attached ESM-BET inhibitor.

In this compound, the absence of a methylene linker between the ESM and the acetyl-lysine mimetic significantly reduces the flexibility, and thus the ability of this compound to fit in the CES-X pocket. Due to the relative lack of flexibility of this molecule compared to progenitor **4.04**, this molecule was designed to have an increased CES-2 stability. The absence of the pyrazole ring, by making the molecule more linear was thought to be a good starting point to understand if this molecule still demonstrates some level of CES-1 hydrolysis. If CES-1 and CES-2 turnovers were to be in the optimal range, the properties of this molecule, in particular the ChromlogD_{7.4} and potency, could be refined for example by subsequently introducing a ZA channel substituent.

5.6. Benzazepinone building block retrosynthetic analysis

To achieve the synthesis of molecules **5.03-5.07**, the core template **5.08** was identified as a possible common building block (Figure 28).

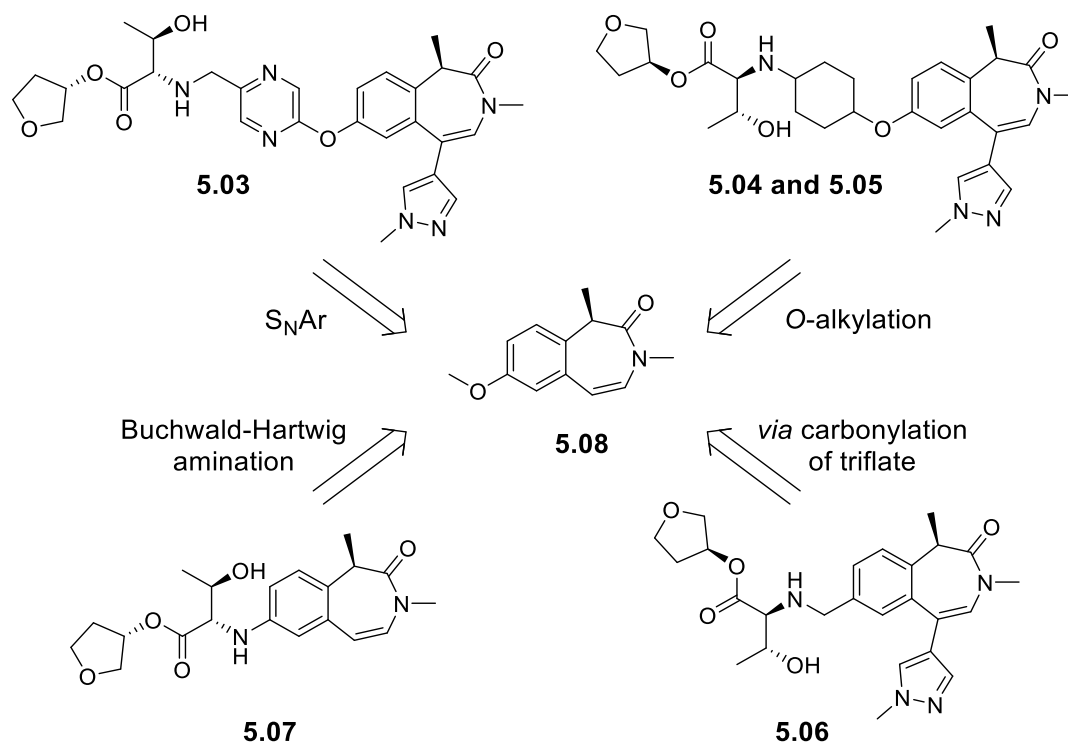
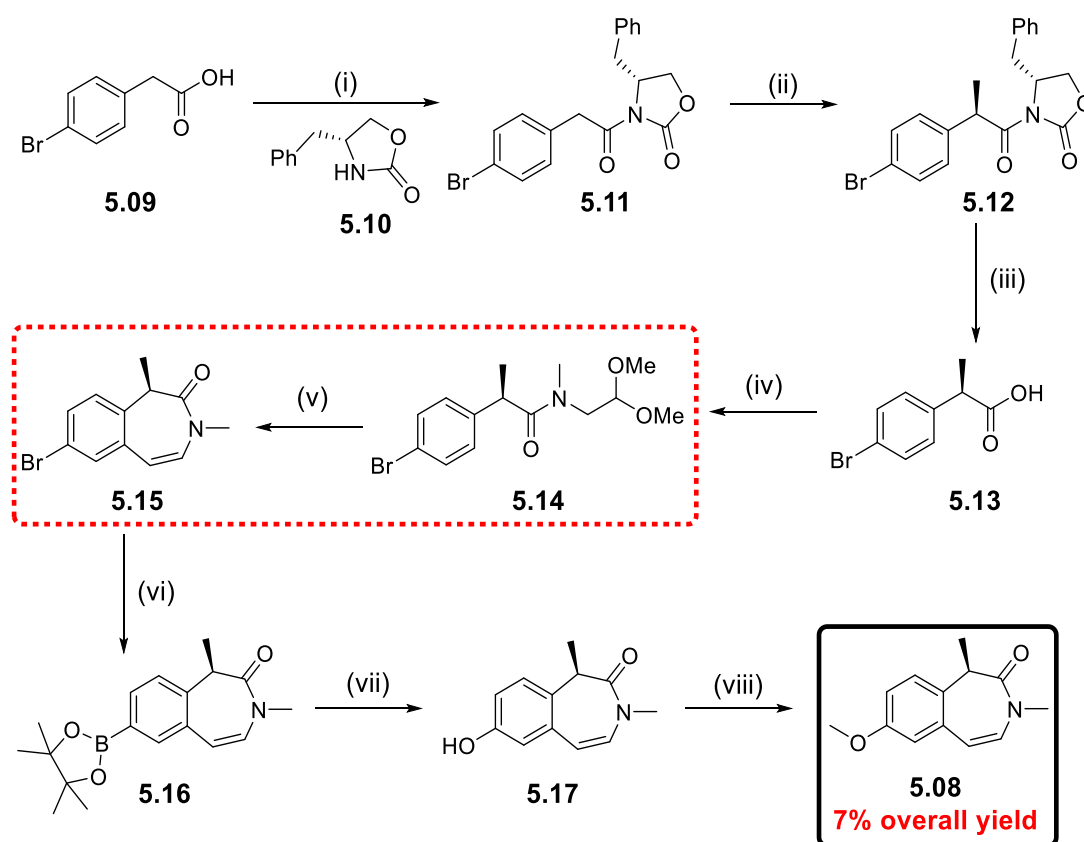


Figure 28: Synthetic strategy for investigating an *ESM-BET* inhibitor series containing the benzazepinone motif as the acetylated-lysine mimetic.

Molecule **5.08** was thought to be a very versatile intermediate enabling synthetic chemistry using S_NAr , *O*-alkylation, or cross-coupling chemistry *via* the corresponding triflate. Optimisation of the synthetic route towards this building block was needed to facilitate its synthesis on a scale of several hundred grams to support this and any future SAR investigations on this series.

5.7. Synthesis of the benzazepinone building block

Prior to the work described in this thesis, the route used to access intermediate **5.08** had eight steps with an overall maximum yield of 7%^{viii} as shown in Scheme 1.⁵⁰



(i) PivCl, NEt₃, toluene, 80 °C - 100 °C, 16 h, 60%, (ii) NaHMDS, MeI, THF, -78 °C to rt, 8 h, 79%, 99% d.e. (iii) LiOH, H₂O₂, THF : water, 0 °C to rt, 1 h, 88% (iv) 2,2-dimethoxy-*N*-methylethan-1-amine, T3P, DIPEA, THF, 80 °C, 2 h, 80% (v) AlCl₃, DCM, 0 °C to rt, 16 h, 5-32% (vi) KOAc, B₂pin₂, PdCl₂(dppf).DCM, 1,4-dioxane, 80 °C, 16 h, 97% (vii) H₂O₂, NaOH, THF, water, 0 °C, 2 h, 76% (viii) MeI, Cs₂CO₃, DMF, rt, 8 h, 90%.

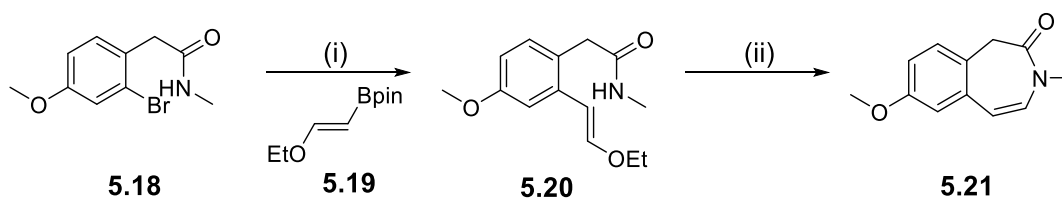
*Scheme 1: First generation synthetic route to access key building block molecule 5.08.*²⁶

In this route, the commercial carboxylic acid **5.09** is coupled with the Evans auxiliary **5.10** via a mixed anhydride to give building block **5.11**.⁵¹ The methyl group is then introduced with an excellent diastereomeric excess (d.e.). The chiral auxiliary is then

^{viii} The overall yield was calculated using the highest yields obtained for each step using this route.

cleaved to afford the carboxylic acid **5.13**. This acid is then used in a T3P-mediated amide coupling to afford amide **5.14**.⁵² The seven-membered ring is then closed by a low yielding intramolecular Friedel-Crafts acylation.²⁶ The halide **5.15** is then converted to the methoxy **5.08** in a three-step sequence *via* oxidation of the boronic ester **5.16**, followed by the protection of the phenol **5.17**.²⁶ Two main issues were identified with this route: the high number of steps and the inconsistency in yields (5-32%) during the Friedel-Crafts intramolecular acylation to close the seven-membered ring (step 5).

In order to improve and shorten the synthesis of this common building block, a new ring closing reaction was investigated. An alternative ring closing sequence was known for the des-methyl benzazepinone intermediate **5.21** (Scheme 2).²⁶

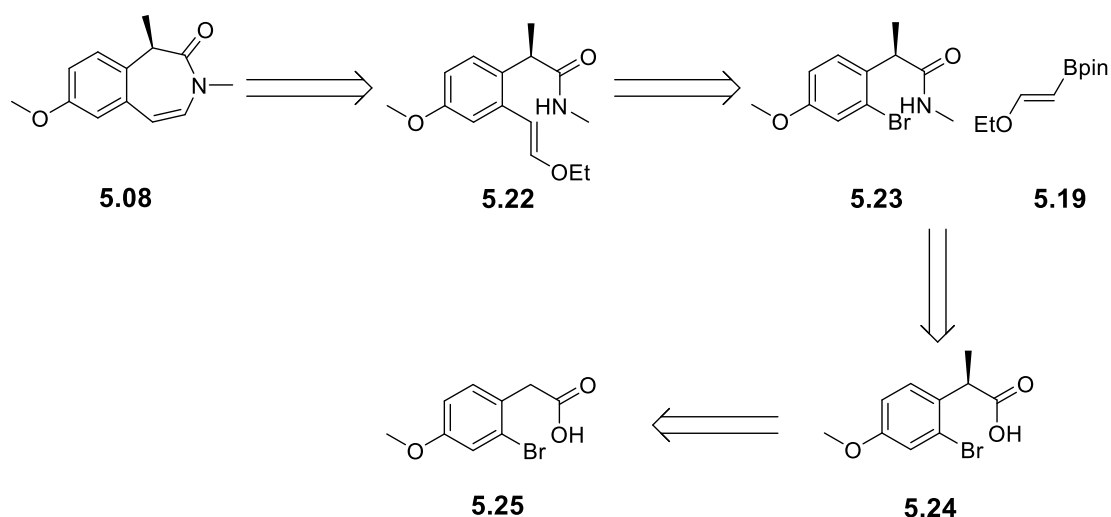


(i) K_2CO_3 , $Pd(PPh_3)_4$, 1,4-dioxane, water, 120 °C, 3.5 h, 82%.

(ii) 4 M HCl in 1,4-dioxane, 70 °C, 1 h, 75%.

*Scheme 2: Ring closing conditions known for des-methyl benzazepinone intermediate 5.21.*²⁶

In this sequence, a vinyl ether **5.20** is formed by a Suzuki cross-coupling of molecule **5.18**. The lactam is then closed by an intramolecular reaction of the amide nitrogen with the aldehyde deprotected *in situ* from the vinyl ether **5.20**. These cyclisation conditions had the advantage of being robust on scale-up for the des-methyl intermediate **5.21**. Based on the identification of this disconnection, the scope of these ring closing conditions was investigated for the synthesis of molecule **5.08**, as shown in the new retrosynthetic analysis (Scheme 3).



Scheme 3: Retrosynthetic analysis for molecule 5.08.

In this new retrosynthetic route, the cyclisation is obtained by intramolecular reaction between the amide nitrogen and the aldehyde generated *in situ* from the vinyl ether **5.22**. The enol ether **5.22** could be accessed through a cross-coupling between the aryl bromide **5.23** and the boronic ester **5.19**. Aryl bromide **5.23** could be obtained by an amide coupling using acid **5.24**. Finally, the α -methyl carboxylic acid **5.24** could be synthesized from the carboxylic acid **5.25**, a relatively inexpensive building block (£165 for 25 g)^{ix}, by enantioselective alkylation at the α -position of the carbonyl functionality.

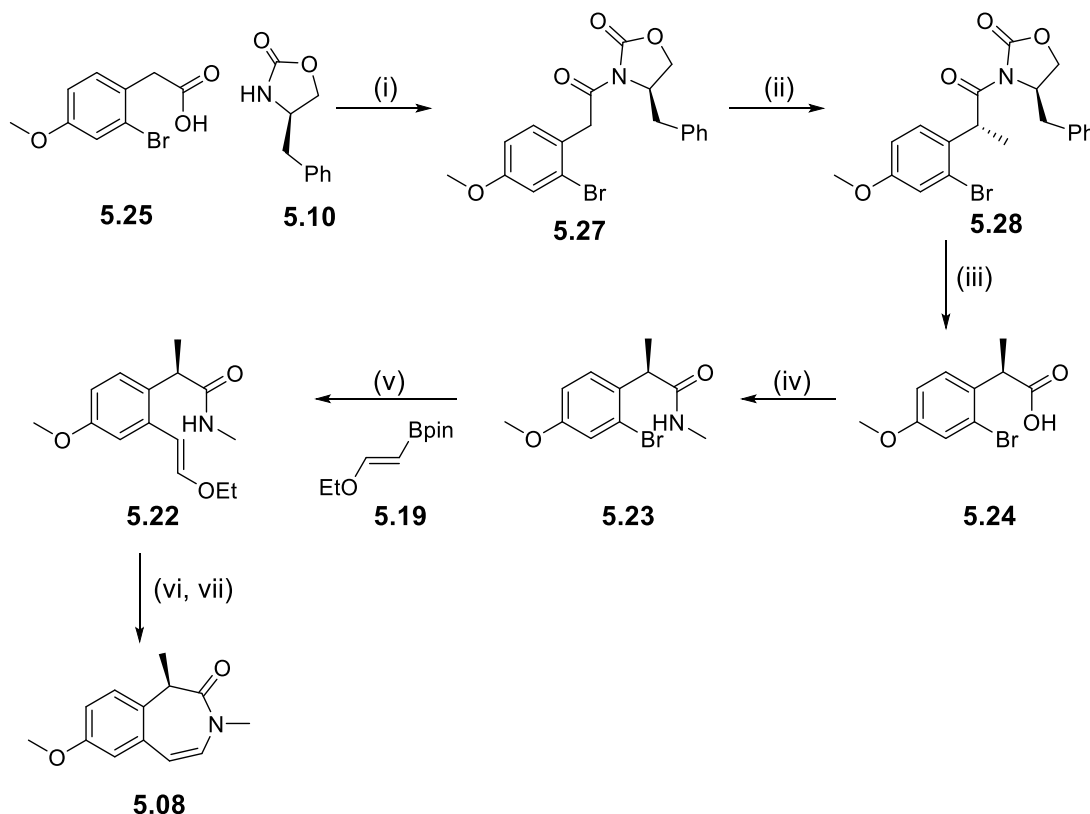
The main advantages of this new route to access molecule **5.08** are that it avoided the problematic ring closing reaction, whilst reducing the number of steps and used robust transformations throughout the entire route.

^{ix} Sigma-Aldrich, March 2017.

5.7.1. Synthesis of molecule 5.08 using the new disconnections

5.7.1.1. Step 1: Coupling of the chiral auxiliary

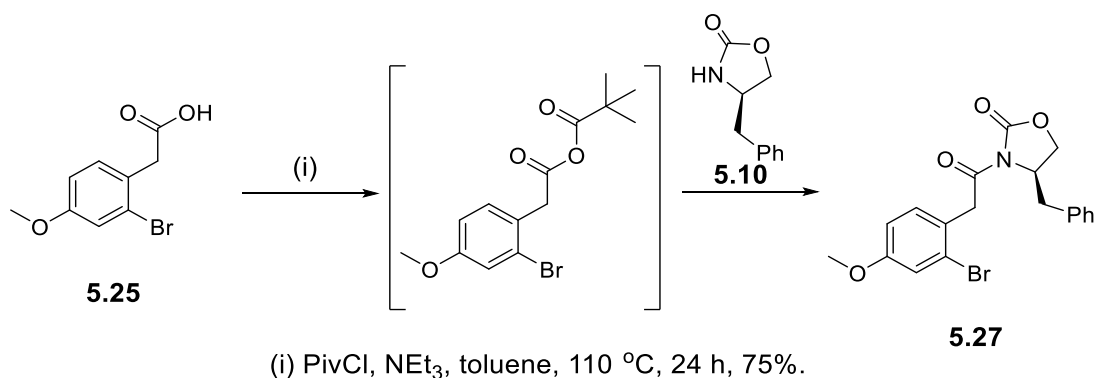
The new route used to synthesize molecule **5.08** from the commercially available carboxylic acid **5.25** is shown in Scheme 4.



(i) PivCl, NEt₃, toluene, 110 °C, 24 h, 75% (ii) NaHMDS, MeI, THF, -78 °C to rt, 24 h, 81% (iii) LiOH, H₂O₂, THF, water, 0 °C to rt, 25 h, 92% (iv) MeNH₂ in THF, HATU, DIPEA, DMF, rt, 50 min, 80% in two batches (v) K₂CO₃, Pd(PPh₃)₄, 1,4-dioxane, water, 120 °C, 2 h, 81% (vi) 4 M HCl in 1,4-dioxane, 70 °C, 1 h, 82%, e.e. 83% (vii) Recrystallisation in MeCN 71%, e.e. 99%.

Scheme 4: New synthetic route for molecule 5.08.

To introduce the methyl in a stereoselective fashion, the phenylalanine-derived oxazolidinone developed by Evans was initially chosen as chiral auxiliary.⁵³ The stoichiometric auxiliary was introduced by amide coupling *via* the pivalic anhydride formed *in situ* (Scheme 5).



Scheme 5: Step 1, introduction of the chiral auxiliary.

Amide couplings using the mixed anhydride generated *in situ* are reported to give variable yields, depending on the acid starting material, the temperature and the stoichiometry of the acid starting material.⁵¹ Therefore, several reaction conditions were examined to optimise the process for the substrate molecule **5.25** (Table 6).

Entry	Acid equivalents	Temperature (°C)	Reaction time (h)	Yield (%)
1	1.5	110	4	39
2	1.5	110	24	75
3	1.5	80 (1 h), 100 (18 h)	19	44
4	2.0	110	4	58
5	2.0	110	20	64

Table 6: Conditions used for coupling of the Evans auxiliary to molecule 5.25. The chiral auxiliary was used as the limiting reagent.

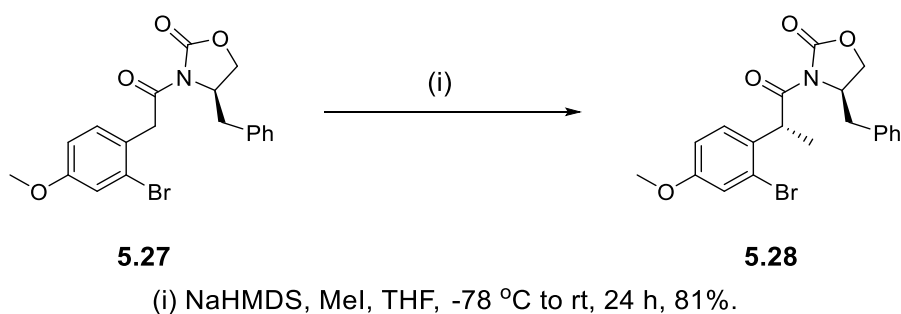
Initially, the reaction was performed with 1.5 equivalents of acid (with respect to the Evans auxiliary) at 110 °C for 4 hours and provided the desired product in 39% yield (entry 1). Increasing the reaction time from 4 hours (entry 1) to 24 hours (entry 2) significantly increased the reaction yield (+36%). By contrast, increasing the reaction time whilst reducing the temperature of the reaction (entry 3) resulted in only a small increase in yield when compared to entry 1 (+5%). When the stoichiometry of acid was increased to two equivalents and the reaction mixture heated to 110 °C for 4 hours (entry 4), the yield was increased by 19% compared to entry 1. Finally, when the

reaction time was increased to 20 hours with two equivalents of acid, the reaction only gave a 6% increase in product yield compared to the 4 hours reaction time (entry 4).

In conclusion, the yield was successfully increased from 39% to 75% by varying three reaction parameters. The conditions shown in entry 2 have shown the best results overall in terms of yield and economy of acid starting material and were therefore subsequently used.

5.7.1.2. Step 2: Stereoselective alkylation

The methyl substituent was then introduced through the generation of the enolate with NaHMDS and alkylating the methylene in the α -position of the carbonyl functionality with methyl iodide (Scheme 6).



Scheme 6: Stereoselective alkylation.

The diastereomeric excess obtained using this Evans auxiliary is attributable to the chelation of the metallic cation with the two carbonyl groups, locking the conformation of the molecule. Due to the steric hindrance on the upper face, created by the benzyl group, the enolate attacks the alkyl halide preferentially from the face opposite to the benzyl group, providing the d.e.

5.7.1.2.1 Impact of the aryl ring substitution pattern on the d.e.

a- Calculations of the enolates' relative energy

The d.e. obtained in the original route (Scheme 1, p.53) was 99% with the phenylalanine-derived chiral auxiliary. Computational calculations,^x carried out by another member of our laboratory, of the relative stabilities of the *Z* and *E* enolates have indicated that the *E*-enolate (undesired) is significantly less favoured than the *Z*-enolate with a 43.5 kJ/mol energy difference (Figure 29).^{54,55,56} The *E*-enolate exhibits a steric strain between the aryl ring and the oxazolidinone substituent (as shown in red in Figure 29). The *Z*-enolate does not exhibit this steric strain. Moreover, the desired *Z*-enolate has some additional stabilisation from one of the protons of the aryl ring (as shown in green in Figure 29).

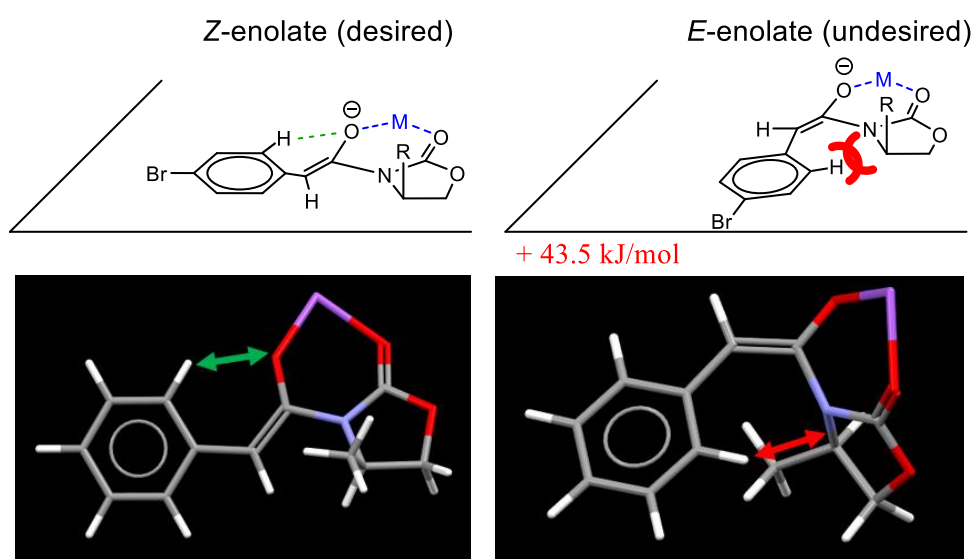


Figure 29: The *E*-enolate was calculated as being 43.5 kJ/mol higher in energy than the *Z*-enolate. These calculations highlighted a possible steric hindrance between the aryl ring and the oxazolidinone (red arrow). In addition, there is a possible beneficial intramolecular interaction in the *Z*-enolate between one of the protons of the aryl ring and the negative charge of the enolate oxygen atom (green arrow).^x

^x All calculations were performed at the B3LYP/6-31+G** level of theory using Gaussian 16. Post-optimisation frequency calculations confirmed that all structures were genuine local minima and transition states on the energy hypersurface. The calculations were performed in the gas phase at 0 °K, in infinite dilution.

The energy difference between the *Z* and *E* enolates can explain the d.e. observed experimentally for substrate **5.11**. Unfortunately, when using the substrate **5.27**, the d.e. obtained using the same reaction conditions, was only 86% (as determined by ¹H NMR). The relative energy between the two enolates was calculated for the two substrates **5.11** and **5.27** (Table 7).⁵⁴⁻⁵⁶

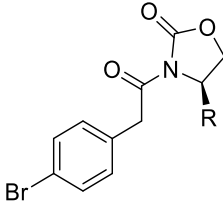
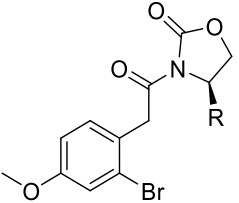
Oxazolidinone R group		Aryl ring	
			
Bn		+ 43.5 (molecule 5.11)	+ 52.3 (molecule 5.27)

Table 7: Relative energy difference (in kJ/mol) between the *Z* and the *E* enolate intermediates for different aryl rings. The *E*-enolate is always calculated to be higher in energy.^x

In all cases, the *E*-enolate was always calculated to be higher in energy. The energy difference between the *Z* and the *E* enolates for molecule **5.27** is calculated to be slightly larger than for molecule **5.11**. From these computational results, the same d.e. or even a higher d.e. for molecule **5.27** would be expected. However, experimentally we observe an erosion of the d.e. for substrate **5.27**. Therefore, the energy difference between the two enolate intermediates cannot explain the d.e. erosion between substrate **5.11** and substrate **5.27**.

b- Calculations of the transition states' relative energy

The difference in d.e. between the two substrates could be explained by the energy difference between the pro-*E* and pro-*Z* transition states during the formation of the two enolates. Computational calculations of the pro-*Z* and pro-*E* transition states have provided the structures shown in Figure 30.⁵⁴ To simplify the computational calculations, in the first instance, the substituents of the oxazolidinone and of the aryl ring are not shown.

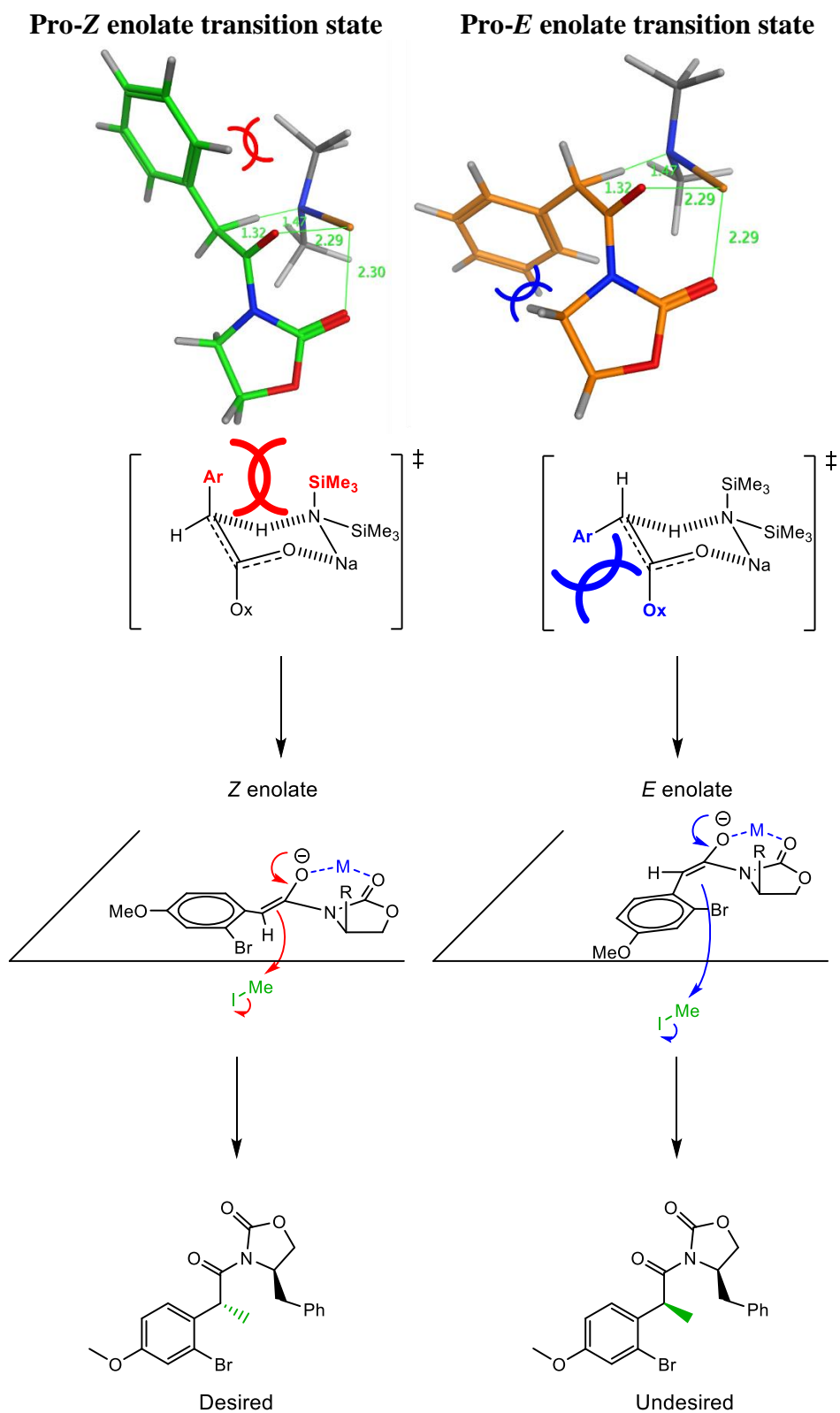


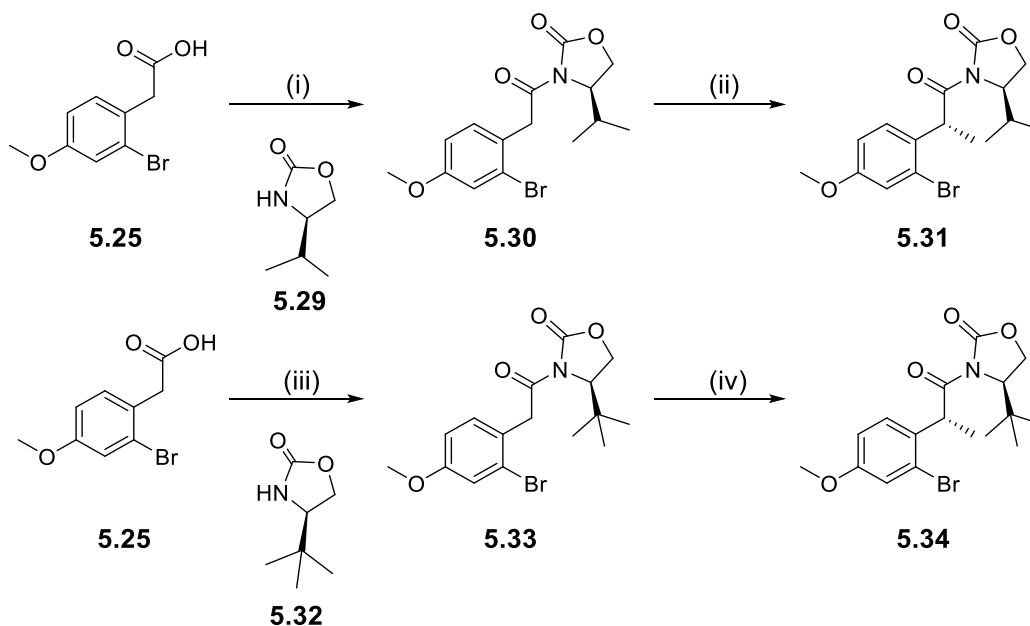
Figure 30: Transition states for the formation of the Z or E enolates of substrate 5.27 showing unfavourable interactions that govern the stereochemistry of the enolate. Attack of the enolate is preferred on the face opposite to the bulky group. The Z or E enolates give rise to different diastereomers.

When the *Z*-enolate is formed, there is an unfavourable 1,3-diaxial strain (red) between the aromatic ring (Ar) and the SiMe₃ group in the axial position. During the formation of the *E*-enolate, there is an unfavoured interaction (blue) between the aromatic ring (Ar) and the oxazolidinone ring (Ox). Computational modelling of the transition states has shown the energy difference between the pro-*E* and pro-*Z* transition states for the two different aryl rings **5.11** and **5.27** is identical.⁵⁴ The pro-*E* transition state was found to be 3.3 kJ/mol higher in energy than the pro-*Z* transition state for both aryl rings. This is in contradiction with the experimental results where a lower d.e. was obtained for substrate **5.27** compared to substrate **5.11**. This highlights some of the limitations of the model used. A calculation at a higher level of theory might be in more agreement with the experimental data and provide an understanding of the impact of the aryl ring substitution pattern on the d.e. Alternatively, the lack of correlation with the experimental data might be due to the fact that the simple isolated gas phase model used here does not account for more complex interactions that might be seen in condensed phases, such as solvent system.

5.7.1.2.2. Impact of the oxazolidinone substituent on the d.e.

In parallel to the impact of the aryl ring substituents on the d.e., different Evans auxiliaries were investigated with the hypothesis that increasing the steric bulk of the oxazolidinone substituent could favour a greater d.e. by favouring the formation of the *Z*-enolate over the *E*-enolate. To test this hypothesis, the valine-derived oxazolidinone adduct (molecule **5.30**, Scheme 7) and the *tert*-leucine-derived oxazolidinone adduct (molecule **5.33**) were examined in the same synthetic sequences as the phenylalanine-derived oxazolidinone. Alkylated products **5.31** and **5.34** were again synthesised *via*

the pivalic mixed anhydride using the same reaction conditions as previously described in Scheme 5 (p.57).



(i) PivCl, NEt₃, toluene, 110 °C, 24 h, 30%.

(ii) NaHMDS, MeI, THF, -78 °C to rt, 2.5 h, 39%, 80% d.e. by NMR.

(iii) PivCl, NEt₃, toluene, 110 °C, 24 h, 17%.

(iv) NaHMDS, MeI, THF, -78 °C to rt, 2.5 h, 55%, > 95% d.e. by NMR.

Scheme 7: Alkylation using different chiral auxiliaries.

The alkylation of the valine-derived oxazolidinone adduct **5.30** provided intermediate **5.31** with an 80% d.e. (as determined by ¹H NMR), thus providing a similar result to the phenylalanine-derived oxazolidinone. In contrast, when using the *tert*-leucine-derived oxazolidinone analogue **5.33**, the undesired enantiomer was not observed. This can be explained by the increase of the steric bulk at the oxazolidinone chiral centre. When the substituent of the oxazolidinone is a *t*Bu group, one of the methyl substituents is projecting towards the methylene being deprotonated (Transition state C, Figure 31).⁵⁷ In contrast, when the oxazolidinone systems derived from phenylalanine (Transition state A) and from valine (Transition state B) are used on the substrate of interest, a hydrogen atom is directed towards the methylene group

being deprotonated, reducing the steric strain between the aryl ring (in blue, Figure 31) and the oxazolidinone. By increasing the steric strain between the aryl ring and the oxazolidinone, the *E*-enolate formation becomes less favourable and it experimentally results in a higher d.e. for **5.34** compared to products **5.28** and **5.31**.

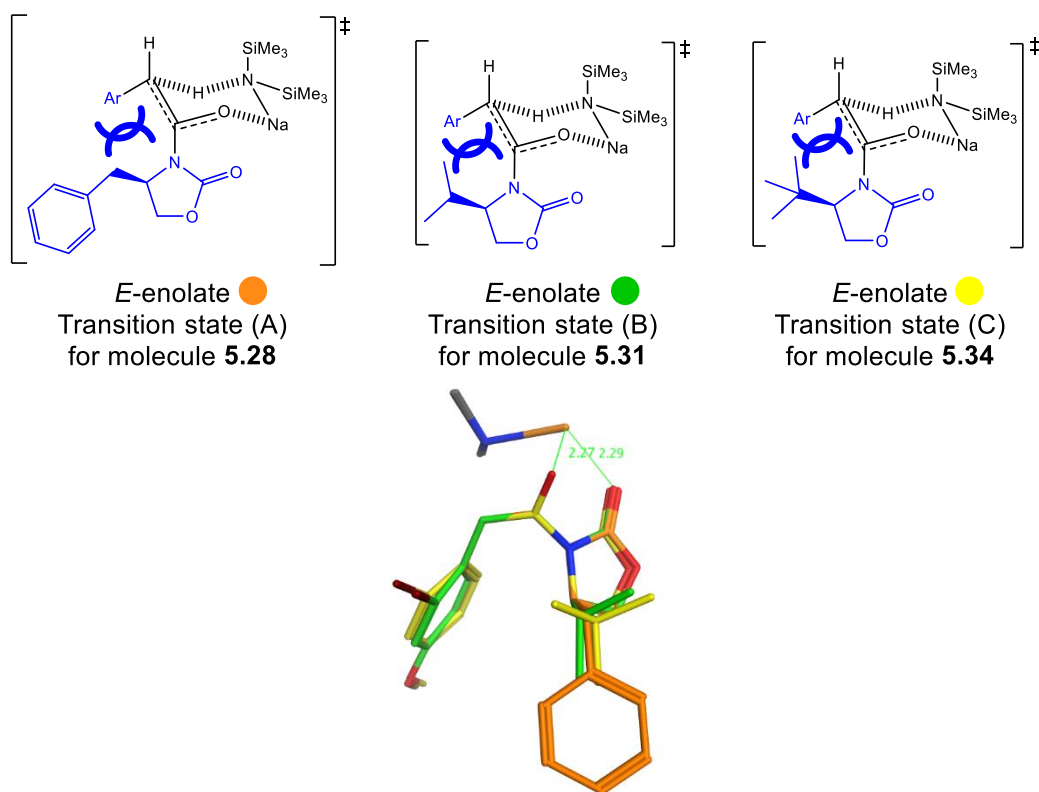


Figure 31: Transition states with the three different oxazolidinones. The high steric hindrance of the *tert*-leucine-derived oxazolidinone favoured the formation of the desired *Z*-enolate only, yielding to a higher d.e. than the valine or phenylalanine-derived oxazolidinones.⁵⁴

Computational calculations, carried out by another member of our laboratory, of the relative transition state energies for these three oxazolidinones have confirmed that the energy difference for the transition states of the *tert*-leucine-derived oxazolidinone is larger than for the valine or phenylalanine substrates (Table 8).⁵⁴ However, as mentioned earlier, the computational method does not enable one to discriminate between the two substrates **5.11** and **5.27**.

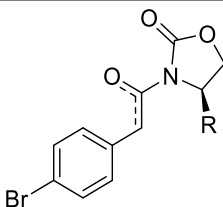
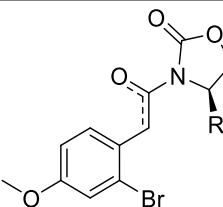
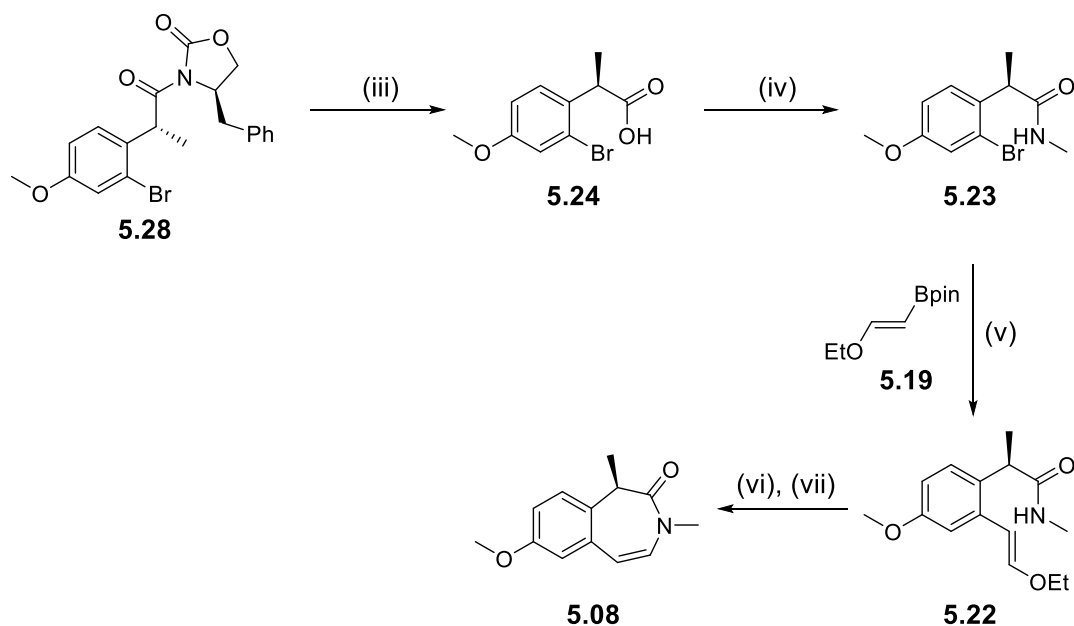
Aryl ring Oxazolidinone R group		
Bn	+ 3.3	+ 3.3
<i>i</i> Pr	-	+ 5.0
<i>t</i> Bu	-	+ 6.3

Table 8: Relative energy difference (in kJ/mol) between the *E* and the *Z* enolate transition states for different aryl rings and different Evans oxazolidinone.⁵⁴

To conclude, the *tert*-leucine-derived oxazolidinone provided the desired d.e. for the substrate of interest. In parallel to this work on using alternative oxazolidinone motifs, separation of the two diastereomers of material **5.28** (86% d.e.) by column chromatography or recrystallisation were unsuccessful. The material was carried through the synthetic route with this d.e., aiming to establish suitable recrystallisation conditions to reach the desired e.e. for molecule **5.08**.

5.7.1.3. Final steps of the synthesis

The final steps of the synthesis were completed as described in Scheme 8. After the introduction of the methyl, the chiral auxiliary was hydrolysed using hydroperoxide anion generated *in situ* using lithium hydroxide and hydrogen peroxide. A HATU mediated coupling afforded the amide **5.23** in good yield. This material was then used in a Suzuki cross-coupling with the vinyl ether boronic ester **5.19** to afford molecule **5.22** in good yield.



(iii) LiOH, H₂O₂, Water : THF, 0 °C, 25 h, 92%. (iv) MeNH₂ in THF, HATU, DIPEA, DMF, rt, 45 min, 80% in two batches (v) K₂CO₃, Pd(PPh₃)₄, 1,4-dioxane, water, 120 °C, 2 h, 81% (vi) 4 M HCl in 1,4-dioxane, 70 °C, 1 h, 82%, e.e. 83% (vii) Recrystallisation in MeCN 71%, e.e. 99%.

Scheme 8: Final steps of the synthesis of intermediate 5.08.

Finally, precursor **5.22** was used in a one-pot deprotection and cyclisation of the aldehyde under acidic conditions to afford the desired building block **5.08** in good yield. The stereochemistry of the chiral centre observed during step 2 (86% d.e.)^{xi} was retained during the following synthetic steps and translated into an 83% e.e.^{xii} for molecule **5.08**. The material was recrystallized from MeCN in 71% yield to afford the desired product with an excellent e.e. of 99%.^{xii}

In conclusion, the retrosynthetic analysis conducted on the key benzazepinone building block has allowed the replacement of the capricious ring closing step with a very robust cyclisation. Overall, the development of this new synthetic route, using robust transformations, has enabled the removal of two reaction steps and increased

^{xi} Measured by NMR

^{xii} Measured by chiral HPLC

the overall yield from 7% to 20%. This new route has successfully been used on hundreds of grams scale to supply this key building block to the research team to develop new SAR knowledge on several series containing this benzazepinone motif.

5.8. Initial set of compounds – Synthesis and impact on CES activity

With the key building block **5.08** in hand, the five molecules shown in Figure 32 were synthesized to investigate their CES-2 stability as explained in section 5.5. Firstly, the direct analogues of molecule **4.04** with an aromatic linker (molecule **5.03**) and a saturated cyclohexyl linker (molecules **5.04** and **5.05**) were synthesized (approach A). Secondly, shorter linkers such as benzylic linker (molecule **5.06**) and the directly linked ESM (molecule **5.07**) were synthesized to investigate approach B.

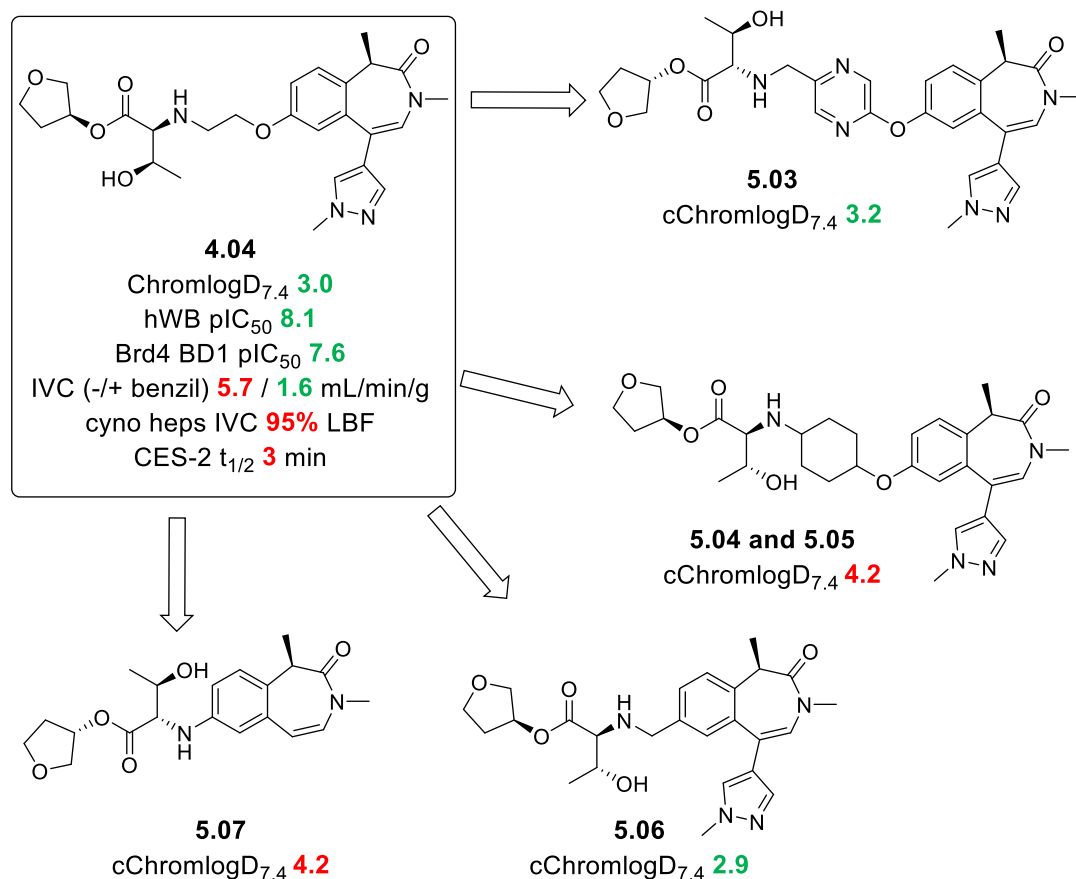
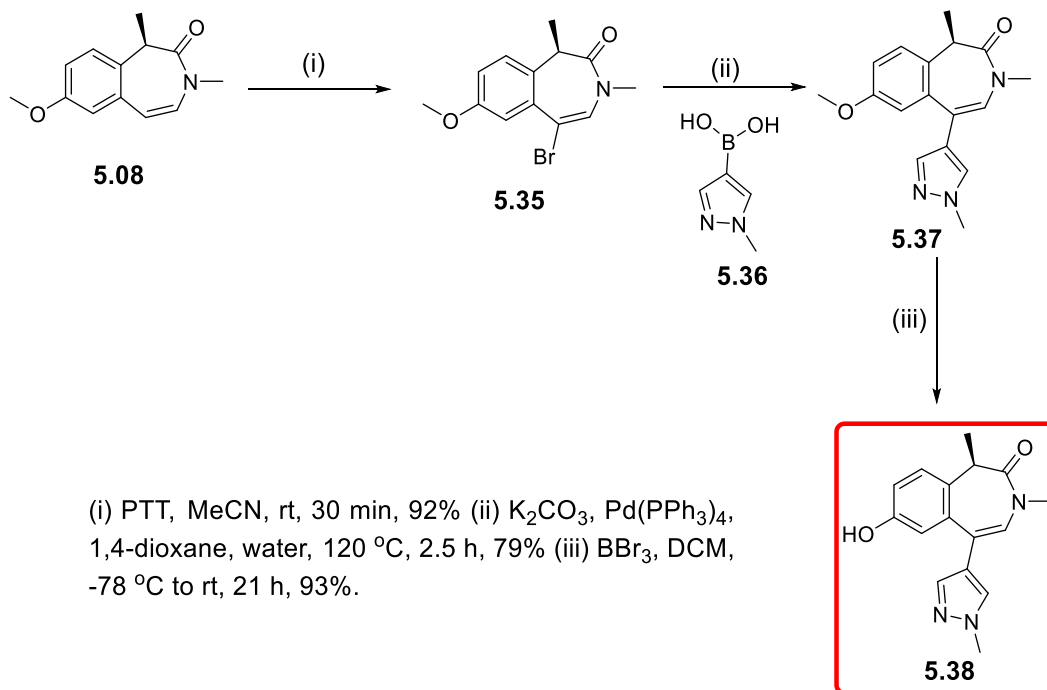


Figure 32: Single point changes around molecule **4.04** to understand the impact of the linker on the CES-2 turnover.

5.8.1. Synthesis of the common intermediate 5.38

All molecules prioritised for synthesis shared a unique synthetic intermediate **5.38**, which was prepared in three steps from the benzazepinone intermediate **5.08** (Scheme 9).



Scheme 9: Synthesis of molecule 5.38.

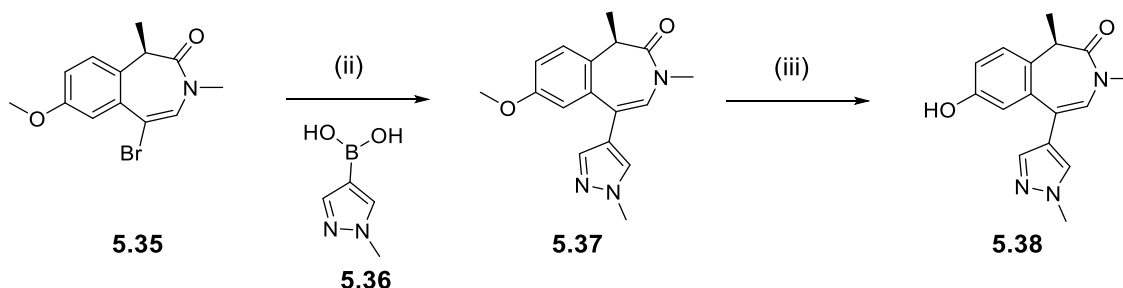
The synthesis of this key building block will be described hereafter.

5.8.1.1. Bromination of the core molecule

Molecule **5.08** was brominated selectively at the desired position using phenyltrimethylammonium tribromide (PTT). PTT is a mild brominating agent able to generate small amounts of Br_2 *in situ*. It is typically used to selectively introduce a bromine atom at the α -position of ketones or alkenes.^{58,59,60,61,62} It is known for its interesting selectivity, especially with respect to aromatic rings, and for its ease of handling, as a shelf-stable solid.^{59,63} For our substrate **5.08**, the bromination with PTT was complete in 30 min at room temperature, and in excellent yield.

5.8.1.2. Suzuki cross coupling and demethylation

Vinyl bromide **5.35** was then used in a Suzuki cross-coupling with the commercially available boronic acid **5.36** to give intermediate **5.37** (Scheme 10).



(ii) K_2CO_3 , $\text{Pd}(\text{PPh}_3)_4$, 1,4-dioxane, water, 120 °C, 2.5 h, 79%.

(iii) BBr_3 , DCM, -78 °C to rt, 21 h, 93%.

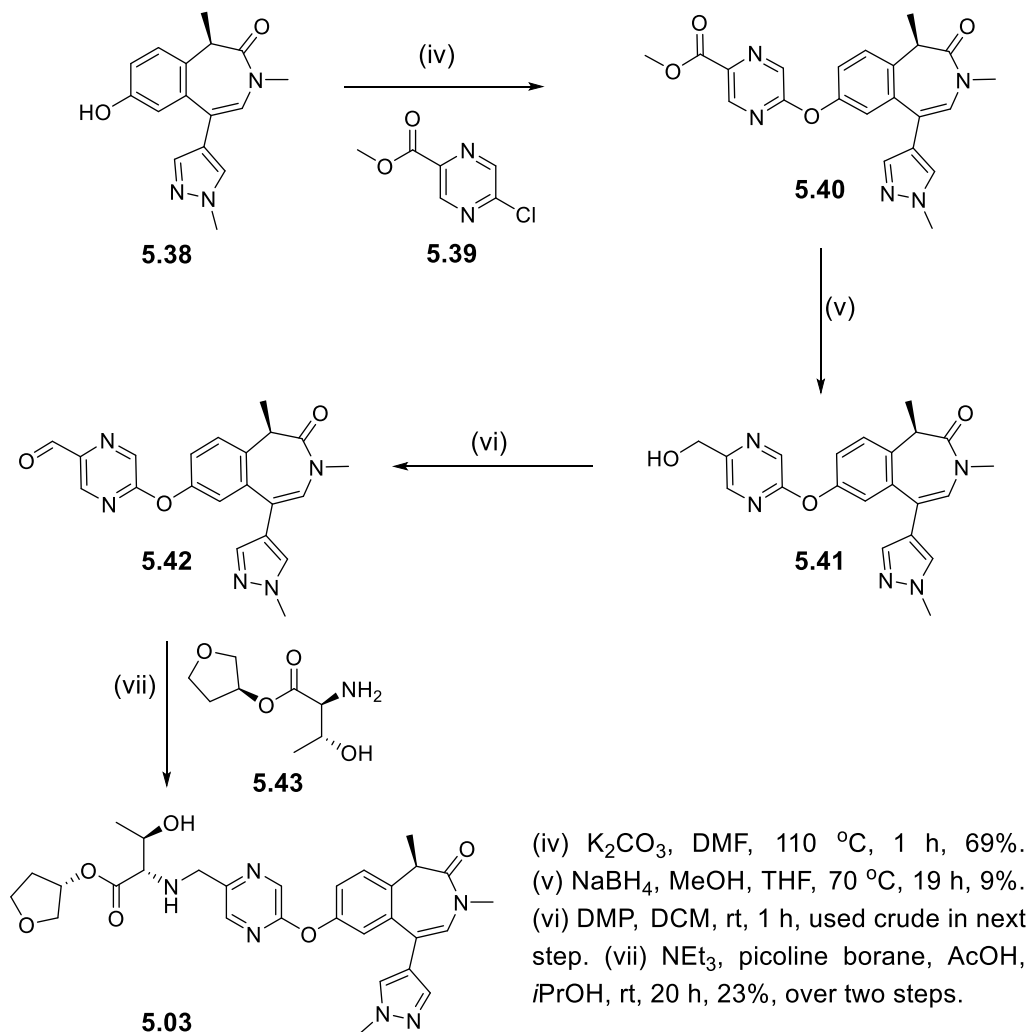
Scheme 10: Cross-coupling conditions to introduce the ZA channel substituent and deprotection of the methoxy group.

Suzuki-Miyaura cross couplings are amongst the five most commonly used reactions in medicinal chemistry, demonstrating the importance and robustness of this transformation.⁶⁴ The coupling occurs between a boronic acid and an aryl halide. First reported in 1979, several variations have been established enabling the use of a diversity of coupling partners, extending the scope of the initial reaction with a range of boron-based coupling partners.^{65,66,67,68} In the current study, molecule **5.37** was obtained by coupling the bromo-alkene **5.35** with the boronic acid **5.36** with a good yield of 79%. Phenol **5.38** was subsequently obtained in excellent yield by deprotection of the methoxy group using boron tribromide.^{69,70}

This synthesis of the key phenol intermediate **5.38**, for the investigation of the CES-2 stability of a small set of molecules, proved to be very robust, and enabled the rapid preparation of molecules **5.03-5.07**.

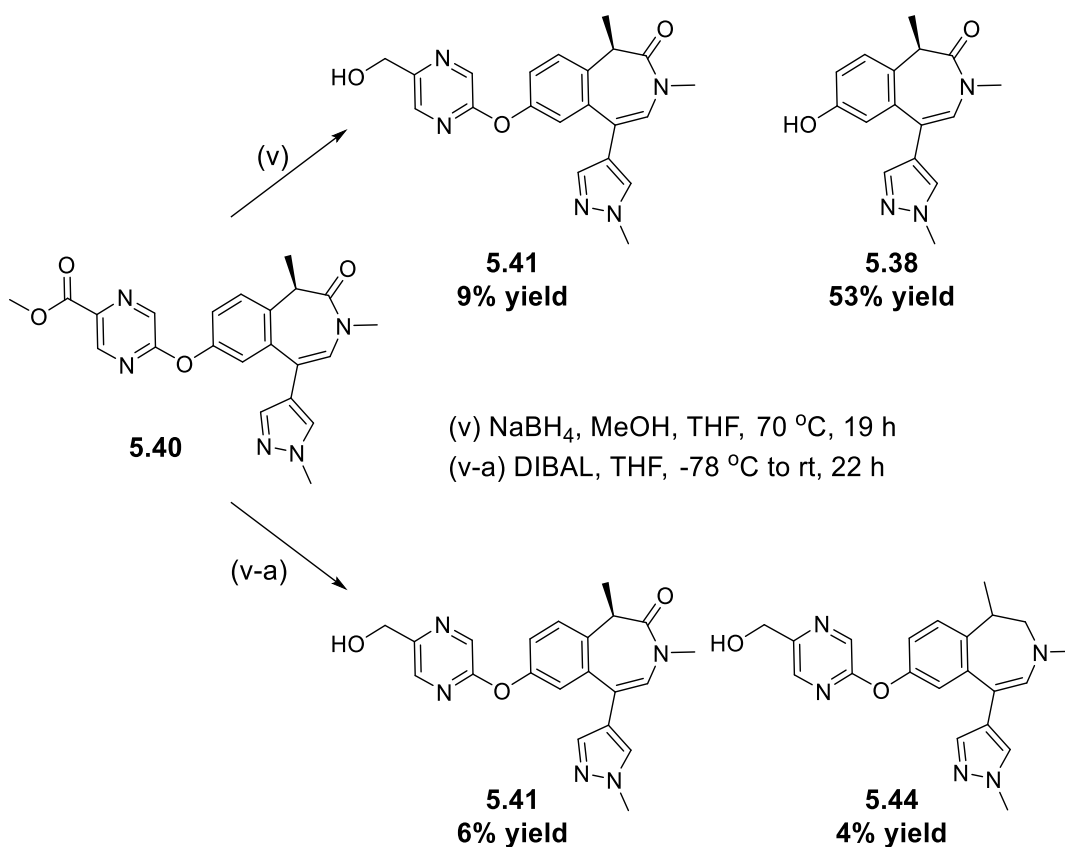
5.8.2. Synthesis of an aryl linker – molecule 5.03

Molecule **5.03** was synthesized in a four-step sequence from the common phenol intermediate **5.38** as shown in Scheme 11.



Scheme 11: Synthetic route for molecule **5.03**.

The phenol **5.38** was functionalised *via* a nucleophilic aromatic substitution ($\text{S}_{\text{N}}\text{Ar}$) to introduce the pyrazine ring and give molecule **5.40**.^{71,72,73} The ester functionality of molecule **5.40** was then reduced to afford alcohol **5.41** (Scheme 12).



Scheme 12: Reduction of the ester **5.40** to alcohol **5.41**.

The reduction was first attempted with sodium borohydride in a mixture of MeOH-THF. These reduction conditions, which usually provide high yields, gave a surprisingly low yield for our substrate (9%).⁷⁴ In this case, a substantial amount of molecule **5.38** was isolated (53% yield) explaining the apparent low yield for the ester reduction. A test reaction using DIBAL as the reducing agent was performed in parallel. The reaction appeared to give a number of products as evidenced by LCMS and upon purification, afforded the desired intermediate **5.41** (6% yield) and a new product **5.44** (4% yield) with a reduced amide. Due to a cleaner reaction profile and the possibility of recovering the previous intermediate **5.38**, the reduction of the ester was conducted with sodium borohydride in MeOH-THF.

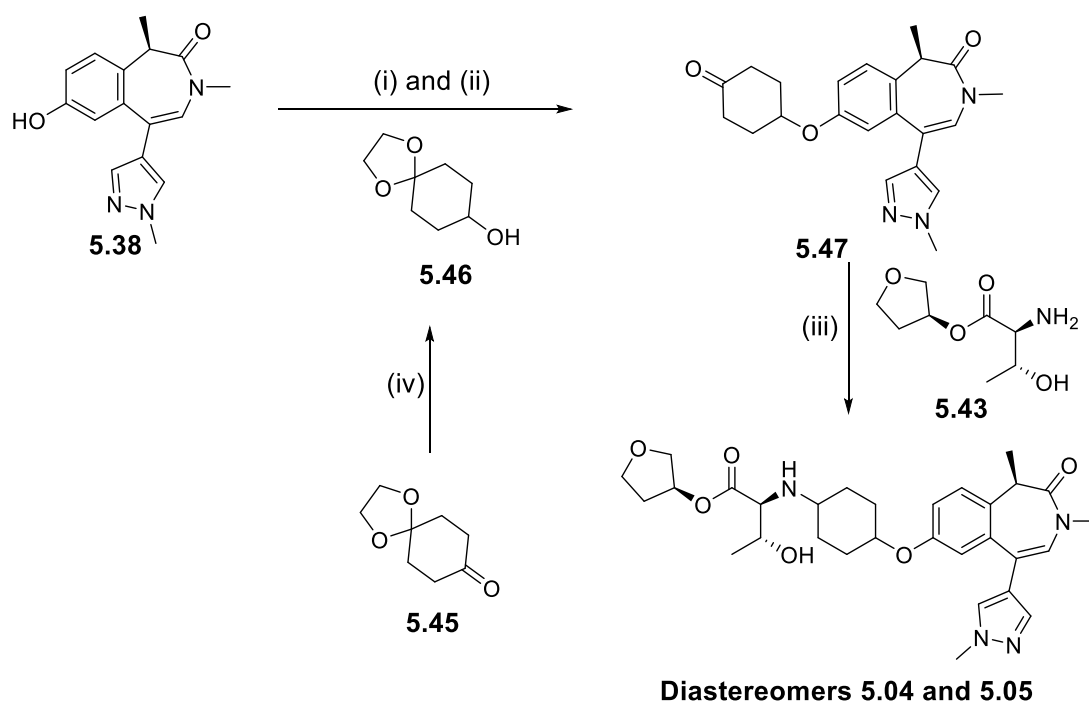
The formation of the phenol **5.38** could be attributable to an $\text{S}_{\text{N}}\text{Ar}$ reaction on the starting material **5.40** by the methoxide ion present in the reaction mixture. This would

be favoured by the presence of the ester in the *para* position and the stability of the benzazepinone phenol **5.38** generated. A possible improvement of the reaction conditions would be to use a different additive to enhance the reactivity of NaBH₄, such as ZnCl₂,⁷⁵ or to use a stronger reducing agent such as LiBH₄.

Alcohol **5.41** was then oxidized using Dess-Martin periodinane (DMP) to give the corresponding aldehyde **5.42** (Scheme 11), used crude in a reductive amination with the amino ester **5.43**, available in our laboratory,⁷⁶ to afford the desired molecule **5.03**.

5.8.3. Synthesis of a saturated cyclic linker – molecules **5.04** and **5.05**

The synthetic route used to obtain molecules **5.04** and **5.05** from phenol intermediate **5.38** is shown in Scheme 13.



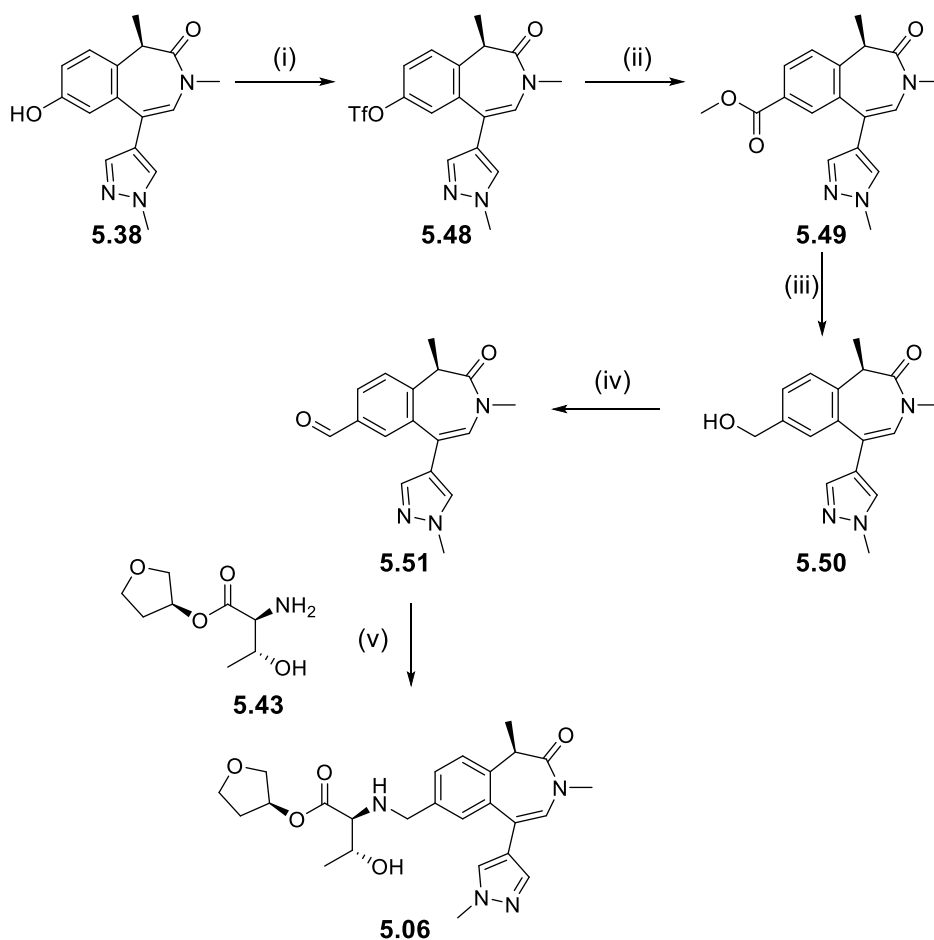
(i) CTBP, toluene, 100 °C to 120 °C, 75 min. (ii) 2 M aqueous HCl, rt to 60 °C, 25 h, 31% over two steps. (iii) NEt₃, picoline borane, AcOH, *i*PrOH, rt, 51 h, **5.04** (8% yield, d.e. 80%) and **5.05** (7% yield, d.e. 80%). (iv) NaBH₄, MeOH, 0 °C, 2 h, 84%.

*Scheme 13: Synthetic route to molecules **5.04** and **5.05** from the common phenol intermediate **5.38**.*

The intermediate ether **5.47** was synthesized by a Mitsunobu reaction^{77,78,79} between the phenol **5.38** and alcohol **5.46**, itself obtained by reduction of the commercially available ketone **5.45**.⁸⁰ The Mitsunobu reaction was carried out with cyanomethylenetriethylphosphorane (CTBP) at 120 °C.^{81,82} This reagent is described in the literature as stable at high temperature and very efficient for Mitsunobu reactions with secondary alcohols compared to the traditional conditions using diethyl azodicarboxylate (DEAD) and PPh₃. The use of CTBP was crucial for the success of this challenging Mitsunobu reaction; indeed, no product was formed at 100 °C, but complete conversion (observed by HPLC) to the desired product was rapidly achieved at 120 °C. The crude acetal was then deprotected under acidic conditions to afford the desired ketone **5.47** with a 31% isolated yield over the two transformations. The desired target molecules **5.04** and **5.05** were obtained by reductive amination on the ketone **5.47** with the amino ester **5.43**. Due to technical issues with the automated purification system, the amounts of products recovered were low and the two unattributed diastereomers *cis* and *trans* were both obtained with a d.e. of 80% (by ¹H NMR). Due to the very low amounts recovered, further separation and characterisation of the diastereomers was precluded. However, the quantity synthesized was sufficient for generating the required biological data.

5.8.4. Synthesis of a benzylic methylene linker – molecule 5.06

The reaction sequence to synthesize molecule **5.06** from the common intermediate **5.38** is shown in Scheme 14.



(i) $\text{PhN}(\text{SO}_2\text{CF}_3)_2$, NEt_3 , DCM, 0 °C to rt, 2.5 h, 62% (ii) $\text{Pd}(\text{OAc})_2$, Xantphos, NEt_3 , CO gas, MeOH, DMF, rt to 60 °C, 28 h, 52% (+ 14% of recovered triflate starting material in two batches) (iii) LiBH_4 , THF, 55 °C, 18 h, 94% (iv) DMP, DCM, rt, 15 min, 54% (v) Picoline borane, AcOH, iPrOH, rt, 2.5 h, 46%.

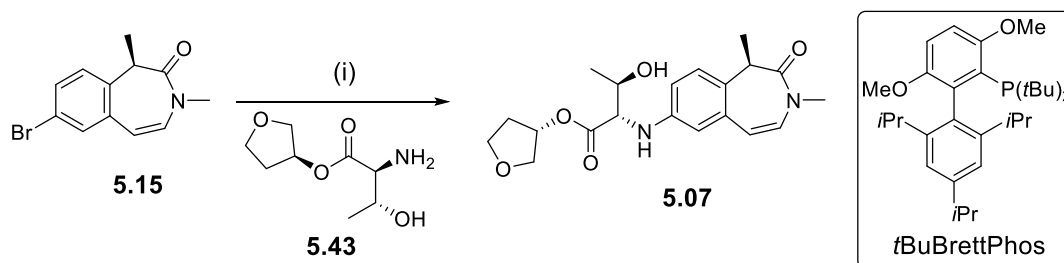
Scheme 14: Synthesis of molecule 5.06.

The phenol **5.38** was converted to the triflate **5.48** using *N*-phenyl-*bis*-(trifluoromethanesulfonimide), $\text{PhN}(\text{Tf})_2$. This bench stable solid triflating agent affords an ease of use, especially upon scale up, and avoids the use of the more hazardous liquid triflic anhydride. Aryl triflate **5.48**, which was sufficiently stable to be purified by column chromatography, was obtained in a 62% yield. The triflate molecule **5.48** was then used in a palladium-mediated carbonylation reaction to give the ester **5.49**. This transformation gave a moderate 52% yield due to the partial

conversion of the triflate. Indeed, a substantial amount (14%) of the starting material **5.48** was recovered during purification. The ester derivative **5.49** was reduced to the alcohol **5.50**, which was subsequently oxidized with DMP to give the corresponding aldehyde **5.51**. Molecule **5.06** was ultimately obtained by reductive amination in a 45% yield.

5.8.5. Synthesis of a directly attached ESM – molecule **5.07**

The directly attached ESM molecule **5.07** was synthesized from the bromo intermediate **5.15** available in the laboratory (Scheme 15).^{xiii}



Scheme 15: Synthesis of molecule **5.07**.

The aryl halide **5.15** was used in a Buchwald-Hartwig coupling^{83,84} with the amino ester **5.43**. The catalyst and solvent, identified elsewhere in our laboratories in a screen of reaction conditions as the best yielding conditions for the coupling of the ESM amine with a different aryl bromide starting material,^{85,86} provided a low yield for the substrate **5.15**. This is likely to be due to the limited solubility of the amino ester in the reaction mixture. To improve this, NEt_3 was added during the reaction, to help the dissolution of the amino ester salt. Only partial conversion to the desired product was

^{xiii} From the initial route to access the benzazepinone molecule **5.08**

achieved, however, a sufficient amount was isolated to profile this molecule and some of the starting material **5.15** was also recovered (32% isolated yield).

In previous examples in our laboratories with a different aryl-bromide substrate, the reaction showed better yields with more lipophilic amino esters such as *t*Bu-*L*-threonine and *i*Pr-*L*-threonine.⁸⁵ This is thought to be due to the increased solubility of the ESM in toluene. The use of a stronger base such as *t*BuOK,⁸⁷ for the amination of substrate **5.15**, was not attempted due to the known racemisation of the chiral centre in the α -position to the amide carbonyl functionality in presence of a strong inorganic base in moderate to high temperature, as observed previously in our laboratories.⁸⁸

5.8.6. Results and discussion on initial set of compounds

After the successful synthesis of the five molecules **5.03-5.07** with alternative linkers to explore the CES-2 SAR, the key biological and physico-chemical data were measured. This data is shown in Table 9, along with the desired profile of an ESM-BET inhibitor.

								Desired profile
		4.04	5.03	5.04	5.05	5.06	5.07	
R group								-
hWB pIC ₅₀	8.1	7.5	8.0	8.1	7.3	6.0	≥ 7.6	
Brd4 BD1 pIC ₅₀	7.6	7.7	8.0	7.8	7.3	7.4	≥ 7.0	
ChromlogD _{7.4}	3.0	3.2	3.7	3.8	2.7	2.9	≤ 3.3	
AMP (nm/s) / tPSA	235 / 115	78 / 141	36 / 115	92 / 115	205 / 106	140 / 88	≥ 50 / ≤ 125	
MW (g/mol)	499	563	553	553	468	374	-	
CES-2 t _{1/2} (min)	3	17	> 139	71	> 139	-	≥ 139	
HLM IVC (-/+ benzil) (mL/min/g)	5.7 / 1.6	6.6 / 4.1	9.2 / 6.5	8.3 / 6.3	1.2 / 0.7	-	≤ 3.0 / ≤ 2.0	
Heps IVC Cyno (LBF)	95%	93%	-	-	74%	-	≤ 75%	

Table 9: Impact of the nature of the linker onto the CES-2 half-life and in vitro profile of the molecules.

Most of the compounds showed good to excellent human whole blood potency, except for molecule **5.07**. This directly attached ESM compound showed a ten-fold drop between the biochemical assay (Brd4 BD1 pIC₅₀) and the human whole blood pIC₅₀. As molecule **5.07** demonstrates good permeability (AMP of 140 nm/s), the drop in potency is thought to be due to a small or absent turnover of the ESM by CES-1 in the targeted cells. This is also supported by comparison of the profiles of molecules **5.06** and **5.07**. Indeed, both compounds showed similar physicochemical properties (AMP, ChromlogD_{7.4}) and the same Brd4 BD1 pIC₅₀, within the margin of the assay error, but their human whole blood potency is significantly different.

The CES-2 t_{1/2} of the remaining four compounds **5.03-5.06** were measured and pleasingly they showed a significantly improved CES-2 t_{1/2} compared to the original lead compound **4.04**, with molecules **5.04** and **5.06** being at the upper limit of the assay with a half-life above 139 min. Interestingly the *cis* and *trans* cyclohexanol linkers showed a significant difference in CES-2 affinity, likely to be due to their different shape complementarity between the molecule and the CES-2 hydrolytic cavity.

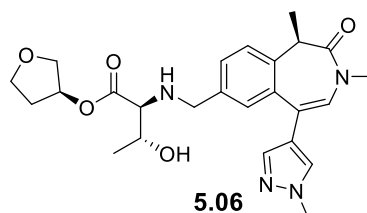
Molecule **5.06** exhibits the most promising profile with an excellent human liver microsome *in vitro* clearance demonstrating some level of CES-1 hydrolysis through the -/+ benzil difference and a slow or absent CES-2 hydrolysis. In addition, this compound has one of the lowest calculated tPSA values amongst this set of molecules, and is one of the lowest molecular weight compounds in the ESM-BET inhibitor series known so far, making it a particularly interesting lead molecule in an excellent physico-chemical space.

From this analysis of the linker changes, the decision was made by the author to further optimise the methylene linked compound **5.06**.

6. Increasing CES-1 turnover – Optimisation of molecule 5.06

This chapter describes the optimisation of the lead molecule **5.06**, in particular in terms of CES-1 turnover and *in vitro* clearance.

The extended profile of molecule **5.06** is shown in Table 10, along with the target property space.



	Molecule 5.06	Desired profile
hWB pIC ₅₀	7.3	≥ 7.6
hWB Δ <i>t</i> Bu	+ 0.2	~ + 1.0
Brd4 BD1 pIC ₅₀	7.3	≥ 7.0
ChromlogD _{7.4}	2.7	≤ 3.3
AMP (nm/s) / tPSA (Å ²)	205 / 106	≥ 50 / ≤ 125
CES-2 t _{1/2} (min)	> 139	> 139
HLM IVC (-/+ benzil) (mL/min/g)	1.2 / 0.7	≤ 3.0 / ≤ 2.0
Heps IVC Hu / Cyno (LBF)	85% / 74%	< 75% / < 75%

Table 10: Chemical structure, physico-chemical and biological data for molecule **5.06**.

As discussed in the previous section, molecule **5.06** exhibited a significantly improved CES-2 half-life, compared to the hit molecule **4.04**, due to the replacement of the ethanolamine linker (molecule **4.04**) by the benzylic system of molecule **5.06**. Pleasingly, molecule **5.06** demonstrated a good Brd4 BD1 potency, however the hWB pIC₅₀ was slightly lower than desired. This was likely to be due to a moderate CES-1 turnover, as demonstrated by the low hWB Δ*t*Bu. This parameter is used as an

indication of the ESM targeting effect by demonstrating the acid is generated in the targeted cell and is providing an enhanced human whole blood potency compared to a non-hydrolysable ESM (*t*Bu analogue). From these two observations, one of the key questions with such a profile remained: *can the hWB Δt Bu, indicative of the ESM targeting effect, be increased to the desired level whilst maintaining a long CES-2 half-life?*

In addition to the CES-X activities, the molecule demonstrated a very interesting *in vitro* clearance profile. Indeed, this compound was the first molecule from the benzazepinone series with the ESM group towards the WPF residues to demonstrate a cynomolgus monkey hepatocytes *in vitro* clearance predicted below 75% liver blood flow. This was thought to be due to a decrease in esterase promiscuity for this compound, through replacement of the flexible linker in molecule **4.04** by a more rigid and shorter linker in molecule **5.06**, which is less compatible with the hydrolytic active site of non-ESM-targeted cynomolgus monkey esterases.

In human, although the liver microsome *in vitro* clearance was encouraging, the hepatocyte *in vitro* clearance remained too high. This indicated that despite only modest phase I metabolism, including a controlled esterase turnover, the phase II metabolism was too high and needed to be addressed.

At the time of this analysis, new *in vivo* cynomolgus monkey PK data^{xiv} generated in our laboratory suggested that the cynomolgus monkey hepatocytes *in vitro* clearance should be lower than 60% liver blood flow in order to achieve an acceptable *in vivo* monkey PK profile.⁸⁹ As a consequence of this experimental PK result, and of the

^{xiv} On a lead molecule on a related series not described in this thesis.

author's analysis of the profile of molecule **5.06**, new analogues were designed, with the following aims:

- Firstly, increase the hWB Δt_{Bu} to ~ 1 , which should be instrumental in increasing the human whole blood potency of the molecule to the desired level. This would also help us to understand if the CES-2 hydrolysis rate can be independently lowered without reducing the CES-1 turnover and therefore without reducing the ESM-targeting effect.
- Secondly, decrease the cynomolgus monkey hepatocytes *in vitro* clearance to under 60% liver blood flow and reach the desired human hepatocyte *in vitro* clearance value ($< 75\%$ liver blood flow), whilst maintaining an optimal physico-chemical profile as previously established (ChromlogD_{7.4} $\sim [2.5-3.3]$; tPSA $\leq 120 \text{ \AA}^2$ and AMP $\geq 50 \text{ nm/sec}$).

6.1. Design hypothesis to increase CES-1 esterase turnover

To increase the hWB Δt_{Bu} , several modifications around molecule **5.06** were designed as shown in Figure 34. In this thesis, modifications will focus on the ESM and the ZA channel substituent.

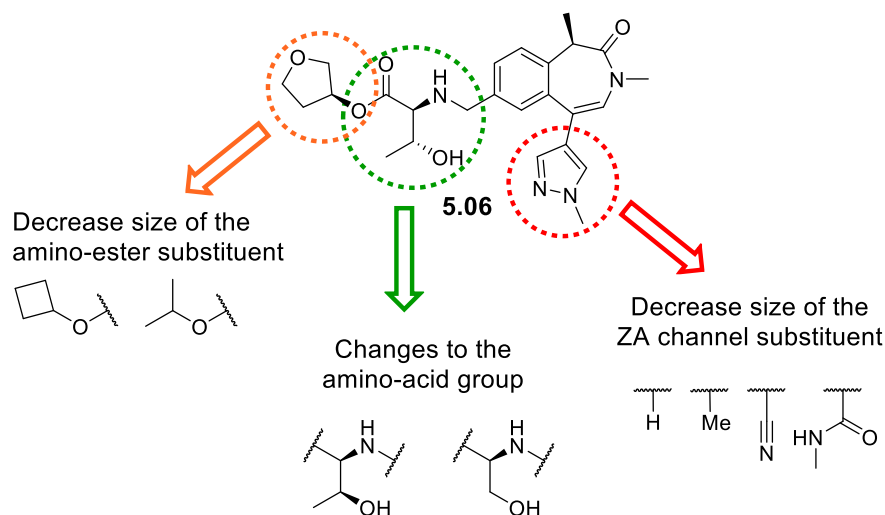


Figure 34: Strategies to increase the hWB Δt_{Bu} of molecule **5.06**.

Firstly, the size of the ZA channel group is likely to impact the CES-1 turnover. Indeed, a more linear molecule should have a greater affinity for the CES-1 hydrolytic active site as explained in section 5.2. Therefore, small ZA channel groups, such as hydrogen, methyl, nitrile and methyl carboxamide, were designed to understand if the CES-1 turnover, through the comparison of the hWB Δt_{Bu} parameter, could be improved by decreasing the size of the ZA channel substituent.

Secondly, reducing the size of the amino ester could increase the CES-1 turnover by enhancing the ability of the molecule to be accommodated in the esterase active site. Therefore, molecules with an ESM derived from the *L*-serine amino acid were designed to understand their impact on the turnover compared to molecule **5.06**, based on the *L*-threonine. In addition, as enzymes are stereospecific, using the *L*-allo-threonine (epimer of the *L*-threonine at the β -position to the carbonyl) as the amino acid motif should have an impact on the esterase turnover. The *L*-allo-threonine has been used previously within our laboratory and has proven to be successful in reducing the cynomolgus monkey hepatocytes *in vitro* clearance.⁹⁰ Consequently, ESMs based

on this non-natural amino acid were also included in the set of compounds used to investigate the impact of the ESM on the CES-1 turnover.

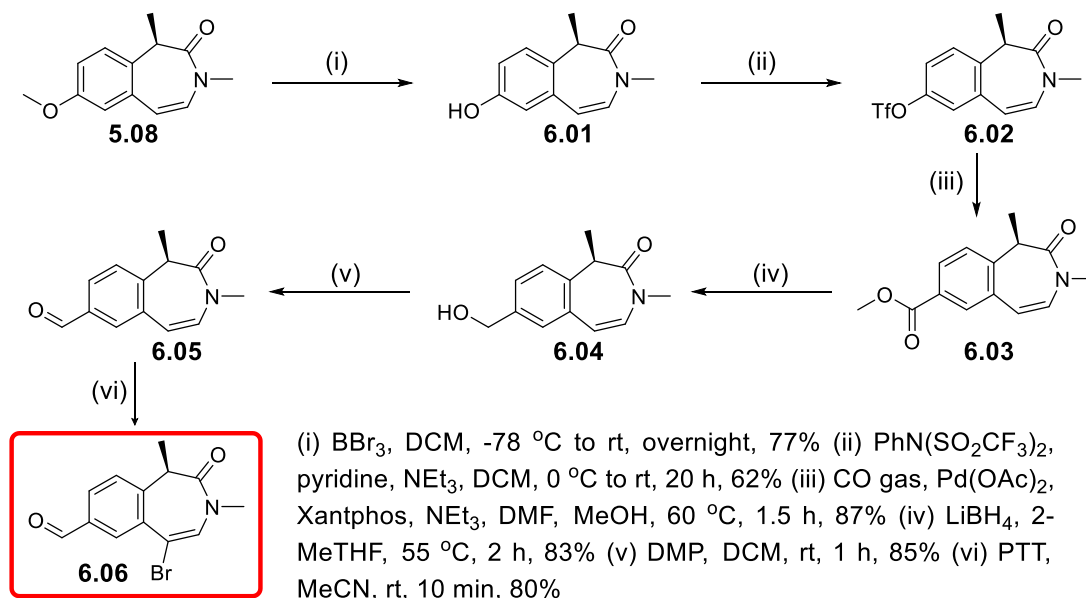
Thirdly, the nature of the ester group itself is expected to impact the ester hydrolysis rate through steric and electronic effects.⁹¹ Indeed, when the ester motif is being hydrolysed by CES-1, the ester is occupying a small, rigid and lipophilic pocket.^{46,47,49} Therefore, hindered ester motifs or polar ester motifs (e.g. a THF-ester) will have a disfavoured conformation in the catalytic pocket, slowing down the hydrolysis rate. Conversely, a smaller and more lipophilic ester (e.g. cyclobutyl-ester) should have a higher CES-1 catalytic rate due to a better ability to fit in the catalytic pocket. This is confirmed by historical data, the ESM-BET series have shown that cyclobutyl and *isopropyl* ESM esters are hydrolysed more rapidly than the corresponding (*S*)-THF ESM ester. Therefore, these two esters were used in combination with the different amino acids selected above.

As described in section 4.2.3, the physico-chemical space thought to be required to develop a balanced ESM-BET inhibitor is well defined. Therefore, all molecules synthesized to tune the CES-1 turnover SAR around molecule **5.06** were carefully designed to comply with these guidelines.

This work to understand the impact of each vector on the CES-1 turnover was divided into two independent parts: the impact of the ZA channel substituent and the impact of the ESM group itself. To help to investigate these two points of diversification, the synthetic route was optimised to enable late stage functionalisation of these two vectors.

6.2. Optimisation of the synthetic route for SAR exploration

To rapidly establish SAR around molecule **5.06**, the late stage intermediate **6.06** was synthesized enabling a two-step derivatization to the final molecules. The synthetic route to synthesize this key intermediate, which is related to the route developed for the initial analogues, is shown in Scheme 16.



Scheme 16: Synthetic route to key intermediate **6.06** for SAR establishment on the two vectors of interest.

The synthesis was initiated by the demethylation of the ether derivative **5.08** to give the free hydroxy analogue **6.01**. The methoxy group was deprotected using boron tribromide at $-78\text{ }^\circ\text{C}$ in a good yield of 77%. Subsequently, the phenol was then reacted with $\text{PhN}(\text{Tf})_2$ in good yield to afford the triflate **6.02**. Molecule **6.02** proved to be stable enough to be purified by silica column chromatography. The triflate **6.02** was then used in a carbonylation reaction, using CO gas and a Pd catalyst, to afford the corresponding methyl ester **6.03** in a very good yield. The ester functionality was reduced to the corresponding alcohol **6.04** using LiBH_4 at $55\text{ }^\circ\text{C}$, before reoxidation to give the corresponding aldehyde **6.05**. This aldehyde was finally reacted with PTT to

give the key bromo-aldehyde intermediate **6.06**. Molecule **6.06** was used to generate most analogues around molecule **5.06**.

6.3. Synthesis and impact of the ZA channel substituent on the CES-1 turnover

As discussed in section 6.1, to understand the impact of the ZA channel substituent on potency, but more importantly on the CES-1 turnover, different substituents with a range of steric bulk were introduced. All analogues were designed with the (*S*)-THF threonine ESM, sharing the substructure shown in Figure 35. The direct *t*Bu-*L*-threonine analogues were also synthesized to enable the determination of the hWB Δt_{Bu} parameter.

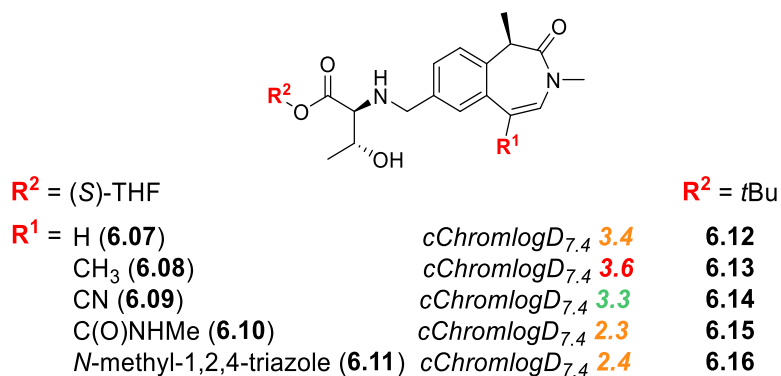


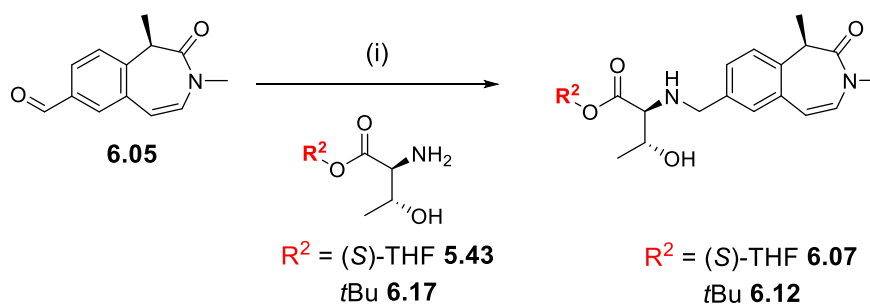
Figure 35: Common substructure to investigate impact of ZA channel substituents.

The direct analogue of compound **5.06** without a substituent in the ZA channel, molecule **6.07**, was synthesized as a single point comparison to understand the maximum turnover achievable with the (*S*)-THF-*L*-threonine amino ester. Deletion of the ZA channel group increases the linearity of the molecule and this should favour its affinity for the CES-1 hydrolytic cavity, therefore should favour the hydrolysis of this ester compared to molecules with a substituent in the ZA channel.

A range of small substituents such as methyl **6.08**, nitrile **6.09** and secondary amide **6.10** were also designed to investigate how the size and shape of the ZA channel

substituent can impact both Brd4 BD1 and human whole blood potencies.^{xv} Finally, molecule **6.11** was designed incorporating the *N*-methyl-1,2,4-triazole as this group has shown to have a good balance between Brd4 BD1 potency and reducing the lipophilicity of the molecule in the pan-BET benzazepinone series.²⁶ The synthesis and data generated for these analogues will be presented hereafter.

6.3.1. Synthesis of molecules **6.07** and **6.12** – $R^1 = H$



(i) DIPEA, AcOH, NaBH(OAc)₃, 40 °C to rt, 25-56%.

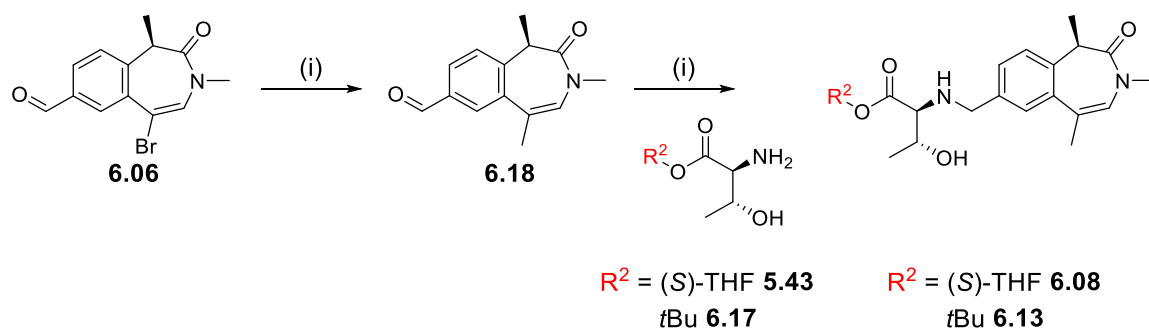
*Scheme 17: Synthesis of molecules **6.07** and **6.12** from the common intermediate **6.05**.*

The aldehyde **6.05**, an intermediate for the synthesis of the bromo-aldehyde **6.06** (Scheme 16, p.84), was used in two reductive amination reactions to give the desired products **6.07** and **6.12**, respectively with 25% and 56% yield (Scheme 17).

6.3.2. Synthesis of molecules **6.08** and **6.13** – $R^1 = methyl$

The two steps to synthesize molecule **6.08** from the common intermediate **6.06** are shown in Scheme 18.

^{xv} Nitrile analogues were designed by the author but synthesized by another member of our laboratory from intermediate **6.06** supplied by the author.

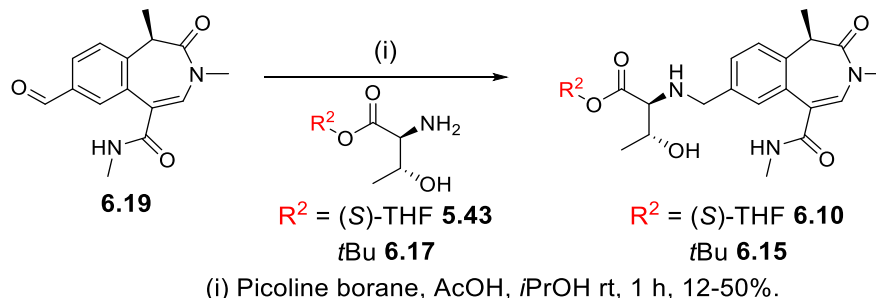


- (i) $\text{B}_3\text{O}_3\text{Me}_3$, $\text{Pd}(\text{PPh}_3)_4$, K_3PO_4 , 1,4-dioxane, water, 80 °C to 110 °C, 4 h, 38%.
(ii) DIPEA, AcOH, $\text{NaBH}(\text{OAc})_3$, 40 °C to rt, 4.5 h, 29-43%.

Scheme 18: Synthetic route to molecules **6.08** and **6.13** from the common intermediate **6.06**.

The bromo-aldehyde **6.06** was used in a Suzuki cross coupling to afford intermediate **6.18**. This aldehyde was used in a reductive amination with an amino ester and sodium triacetoxyborohydride as the reducing agent to give the desired products **6.08** and **6.13**, respectively in 29% and 43% yield.

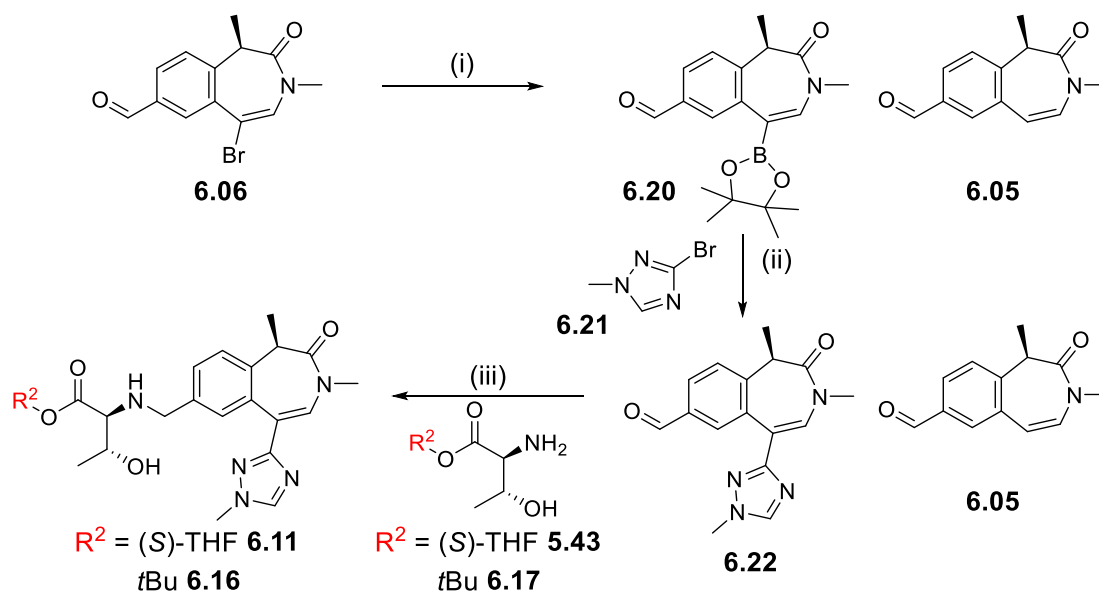
6.3.3. Synthesis of molecules **6.10** and **6.15** – $R^1 = \text{secondary amide}$



Scheme 19: Synthesis of molecules **6.10** and **6.15**.

Intermediate **6.19** was used in two reductive amination reactions to give molecules **6.10** and **6.15** with 50% and 12% yield, respectively (Scheme 19). Molecule **6.19** was available elsewhere in the laboratory as an intermediate.⁹² It can be synthesized in a one-step carbonylation reaction in the presence of CO gas and methylamine from the vinyl bromide building block **6.06**.

6.3.4. Synthesis of molecules 6.11 and 6.16 – $R^1 = N$ -methyl-1,2,4-triazole



(i) B_2pin_2 , $PdCl_2(dppf)$.DCM, KOAc, 1,4-dioxane, 95 °C, 2 h, 67% of product **6.20**, 32% of molecule **6.05** recovered. (ii) K_2CO_3 , $PdCl_2(dppf)$.DCM, *i*PrOH, water, 120 °C, 30 min, 57% yield of product **6.22**, 31% yield of product **6.05** (iii) DIPEA, AcOH, $NaBH(OAc)_3$, THF, 40 °C, 4 h, 17-45%.

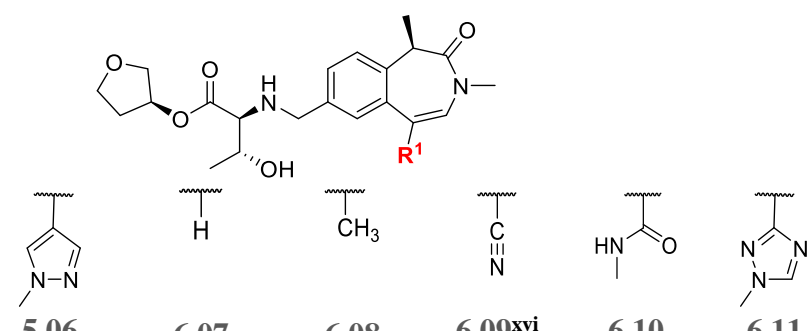
Scheme 20: Synthetic route for molecules 6.11 and 6.16 from the common intermediate 6.06.

The bromo-aldehyde **6.06** was used in a Miyaura borylation reaction (Scheme 20).^{93,94}

The resulting pinacol borane intermediate **6.20** was used in a Suzuki cross coupling to afford aldehyde **6.22** in 67% yield. This somewhat moderate yield can be explained by the partial deborylation of molecule **6.20**, to give the side-product **6.05** in 32% isolated yield.⁹⁵ Aldehyde **6.22** was then used in reductive amination reactions to afford molecules **6.11** and **6.16** in 17% and 45% yield, respectively.

6.3.5. Results and discussion of the impact of the ZA channel substituent

The data associated with the analogues with varied ZA channel substituents is summarized in Table 11.



	5.06	6.07	6.08	6.09^{xvi}	6.10	6.11
hWB pIC ₅₀	7.3	7.7	7.8	6.8	5.6	6.3
hWB ΔtBu	+ 0.2	+ 1.5	+ 1.3	+ 0.7	- 0.2	0.0
Brd4 BD1 pIC ₅₀	7.3	5.7	6.6	6.2	5.2	6.1
ChromlogD _{7.4}	2.7	3.0	3.5	3.2	1.7	2.0
AMP (nm/s) / tPSA	205 / 106	370 / 88	420 / 88	340 / 112	20 / 117	50 / 119
HLM IVC (-/+ benzil) (mL/min/g)	1.2 / 0.7	4.5 / 1.1	4.5 / 2.1	-	-	-

Table 11: Impact of ZA channel substituent investigation on molecules' profiles.

Comparison of molecule **5.06** and **6.07** shows the ZA channel substituent plays a critical role in the rate of esterase turnover as shown by the difference in hWB ΔtBu values and the difference between the human liver microsome *in vitro* clearance -/+ benzil. When no ZA channel substituent is present, the turnover is high with a hWB ΔtBu of + 1.5. When the size of the ZA channel substituent is increased (H < Me < CN < amide or 5-membered rings), the turnover progressively decreases. This set also highlights the important role played by the ZA channel substituent in modulating the lipophilicity of the molecules. Indeed, a fairly large range of ChromlogD_{7.4} can be achieved [1.7-3.5] by modification of this group. These two

^{xvi} This nitrile analogue was designed by the author but synthesized by another member of our laboratory from intermediate **6.06** supplied by the author.

factors: turnover of the ester and lipophilicity of the molecule, both directly impacted by the choice of the ZA channel substituent, are likely to be instrumental in controlling the *in vitro* clearance of future compounds.

It is also worth noting that the Brd4 BD1 potency is strongly impacted by the choice of the ZA channel substituent. When the ZA channel group is a secondary amide **6.10**, or a hydrogen atom **6.07**, the Brd4 BD1 potency is the lowest in this series of molecules. Interestingly, molecule **6.11** shows the 1,2,4-triazole is 10-fold less potent in the Brd4 BD1 assay than the pyrazole **5.06**, but both demonstrate a very slow or absent esterase turnover [hWB $\Delta t_{Bu} \sim 0$], when used in combination with the (*S*)-THF-*L*-threonine.

Overall, these results confirm the design hypothesis outlined in section 6.1. This small set of compounds demonstrates that the ZA channel substituent has a very strong impact on the hWB Δt_{Bu} , which is used as an early indicator of the esterase turnover. Moreover, this set demonstrated that the ZA channel group is also a key component of the Brd4 BD1 potency of the molecule, and thus is very likely to play a crucial role in the design of the next molecules. Therefore, careful choice of the ZA channel group will be instrumental in reaching the desired profile of an ESM-BET inhibitor, especially in terms of potency, CES-1 turnover and very likely in terms of *in vitro* clearance.

6.4. Synthesis and impact of the ESM on the CES-1 turnover

The second hypothesis developed in section 6.1 was that the ESM itself could be used to regulate the CES-1 turnover, by varying the ester group and/or by varying the amino acid group. To understand the impact of the ESM itself on the CES-1 turnover, a series

of close analogues were designed. In order to accommodate smaller and more lipophilic esters such as *isopropyl* and *cyclobutyl* esters whilst remaining within the desired ChromlogD_{7.4} range, the targets were designed with *N*-methyl-1,2,4-triazole. These molecules would therefore be within the targeted ChromlogD_{7.4} range, whilst enabling a direct comparison with the (*S*)-THF-*L*-threonine analogue **6.11**. The target compounds were synthesized using the same synthetic route as for molecule **6.11** (*cf.* Scheme 20, p.88) using aldehyde **6.22** as starting material. The reductive amination yields are shown in Table 12.

	6.23	6.24	6.25	
Yield	48%	24%	16%	R ² = <i>i</i> Pr (6.26) 42% R ² = <i>t</i> Bu (6.27) 34%

Table 12: Yield for reductive amination final step.

The structures and associated data for these compounds are shown in Table 13.

	6.11	6.23	6.24	6.25	6.26
hWB pIC ₅₀	6.3	7.1	7.2	7.3	7.3
hWB Δ <i>t</i> Bu	0.0	+ 0.8	-	+ 1.0	+ 1.3
Brd4 BD1 pIC ₅₀	6.1	6.4	6.4	6.4	6.5
ChromlogD _{7,4}	2.0	3.1	2.9	3.4	2.4
AMP (nm/s) / tPSA	50 119	260 110	290 110	310 110	136 110
HLM IVC (-/+ benzil) (mL/min/g)	-	1.1 / 0.8	1.2 / 0.7	1.9 / 1.3	1.2 / 0.6
Heps IVC Cyno (LBF)	-	71%	64%	80%	55%
CES-2 <i>t</i> _{1/2} (min)	-	> 139	> 139	-	> 139

Table 13: Impact of ester and amino acid groups on the molecules' profiles.

Compounds **6.23** and **6.25** represented a single point change at the ester position compared to molecule **6.11**. Both analogues exhibited a hWB Δ*t*Bu within the desired range and significantly higher than molecule **6.11**. This indicated that the *i*Pr and the cyclobutyl ester are hydrolysed more rapidly than the (*S*)-THF analogue, and was thought to be due to the smaller steric hindrance of these two groups, compared to the THF ester, which should facilitate the attack on the acyl functionality. In addition, the hydrolytic triad of CES-1 is accessed through a hydrophobic gorge, delimited by aromatic amino acids.⁹⁶ The gradient of lipophilicity increases from the entrance to the

catalytic triad. All things being equal, this should favour access to the catalytic triad by more lipophilic substrates such as molecules **6.23** and **6.25** compared to more polar compounds such as molecule **6.11**.

This focused set of molecules also showed the amino acid motif itself has an impact on the hydrolysis rate. Indeed, the serine ESM **6.26** has a higher esterase turnover than its direct threonine analogue **6.23**,^{xvii} confirming the design hypothesis for this molecule. Moreover, using serine decreased the ChromlogD_{7.4} (~ 0.5) which can be used to modulate the physico-chemical profile of the molecule.

As well as contributing to the regulation of the turnover, the choice of the amino acid motif can have an impact on the *in vitro* clearance as demonstrated by comparison of the *L*-threonine **6.23**, *L-allo*-threonine **6.24** and the *L*-serine **6.26**. These three molecules demonstrate a low human liver microsome *in vitro* clearance profile, but interestingly, the *L-allo*-threonine analogue **6.24** demonstrated a significantly lower cynomolgus monkey hepatocytes *in vitro* clearance than the corresponding natural amino acid **6.23**. The serine analogue **6.26** displayed an even lower cynomolgus monkey hepatocytes *in vitro* clearance, likely to be due to its lower lipophilicity.

This small set of molecules showed that the choice of the amino acid and of the ester motif has a significant impact on the esterase turnover, as well as balancing the physico-chemical profile of the molecule. This, in conjunction with the choice of the ZA channel group, should therefore be crucial to reach the desired profile.

Furthermore, to understand further the CES-1 vs. CES-2 stability and as molecules **6.23** and **6.26** exhibited good hWB $\Delta t_{Bu} \sim 1$, the CES-2 half-life of these molecules

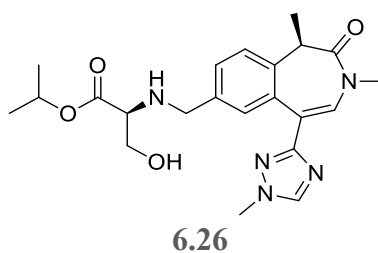
^{xvii} By comparison of the hWB Δt_{Bu} and the -/+benzil differences for compounds **6.23** and **6.25**.

was measured. Pleasingly, both molecules as well as molecule **6.24** showed a half-life above 139 min in presence of CES-2. This demonstrated that CES-1 hydrolysis can successfully be increased whilst keeping a low or absent CES-2 turnover. All of the above led to the identification of a new lead molecule **6.26**, demonstrating a profile very close to the target profile defined at the outset of the current study. Whilst additional studies were undertaken to evaluate the wider pharmacological profile of molecule **6.26**, further investigations were conducted by the author to identify molecules with higher whole blood potency, whilst still fulfilling the desired profile.

7. Reaching the desired profile – Optimisation of molecule 6.26

This chapter describes the optimisation of the new lead molecule **6.26** in terms of potency. The knowledge around CES-1 and CES-2 turnover and *in vitro* clearance established for this series are also applied to design and identify new compounds with a suitable profile for *in vivo* studies.

After identification of molecule **6.26** as an emerging lead candidate, further optimisation around this compound was conducted in order to meet the desired profile. The profile of molecule **6.26** is shown in Table 14, along with the desired profile defined at the outset of this work. The lead molecule **6.26** exhibited a marginally lower Brd4 BD1 potency than desired and, as a consequence, a lower human whole blood potency than was considered optimal. However, compound **6.26** had good physico-chemical properties and exhibited a good *in vitro* clearance profile, unlike previous exemplars. As the esterase turnover, monitored by the hWB Δt_{Bu} parameter, was in the desired range, the Brd4 BD1 potency needed to be increased in order to increase the human whole blood potency.



Desired profile

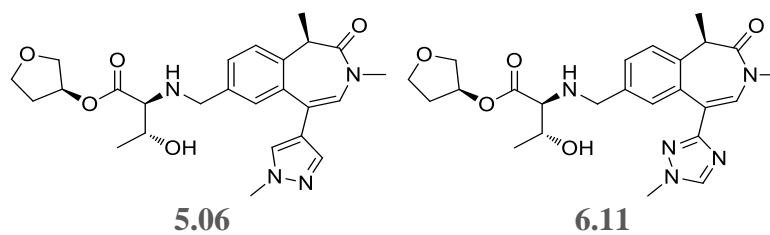
hWB pIC ₅₀	7.3	≥ 7.6
hWB ΔtBu	+ 1.3	~ + 1.0
Brd4 BD1 pIC ₅₀	6.5	≥ 7.0
ChromlogD _{7.4}	2.4	≤ 3.3
AMP (nm/s) / tPSA	136 / 110	≥ 50 / ≤ 125
HLM IVC (mL/min/g)	1.2	≤ 3
Heps IVC Cyno (LBF)	55%	≤ 60%
Heps IVC human (LBF)	60%	≤ 60%
CES-2 t _{1/2} (min)	> 139	> 139

Table 14: Comparison of the profiles of the new lead molecule **6.26** and the desired profile.

7.1. Initial pyrazole analogues (1st generation analogues)

7.1.1. Design rationale

In order to increase the Brd4 BD1 potency, an analysis of the compounds already synthesized in this series was performed. This study highlighted that the pyrazole substituent in molecule **5.06** had a higher Brd4 BD1 potency than the 1,2,4-triazole in molecule **6.11**, as shown in Table 15. Accordingly, this high Brd4 BD1 potency translated into a higher human whole blood potency than for molecule **5.06**.



	5.06	6.11
hWB pIC ₅₀	7.3	6.3
hWB Δ <i>t</i> Bu	+ 0.2	0.0
Brd4 BD1 pIC ₅₀	7.3	6.1
ChromlogD _{7,4}	2.7	2.0

Table 15: Comparison of the profiles of the matched pair **5.06** and **6.11** according to their ZA channel substituents.

Molecule **5.06** exhibited the desired Brd4 BD1 potency, nevertheless its hWB Δ*t*Bu (+ 0.2) needed to be increased. Therefore, a new set of targets were designed (Figure 36). As demonstrated in section 6.4, the use of smaller ester groups such as *i*Pr or cyclobutyl esters, the use of the serine derived amino ester, or a combination of both strategies would be anticipated to reach the desired CES-1 turnover with a hWB Δ*t*Bu ~ 1. The *L*-allo-threonine moiety had also been shown to decrease the cynomolgus monkey hepatocytes *in vitro* clearance compared to the *L*-threonine as shown in Table 13 (p.92), therefore this non-natural amino acid motif was also incorporated in the new set of target molecules. When applying these more lipophilic amino esters and in order to design compounds in the correct physico-chemical space, the unsubstituted pyrazole derivative was used to help balance the ChromlogD_{7,4} of the molecules and thus maintain optimal physico-chemical properties as shown in Figure 36.

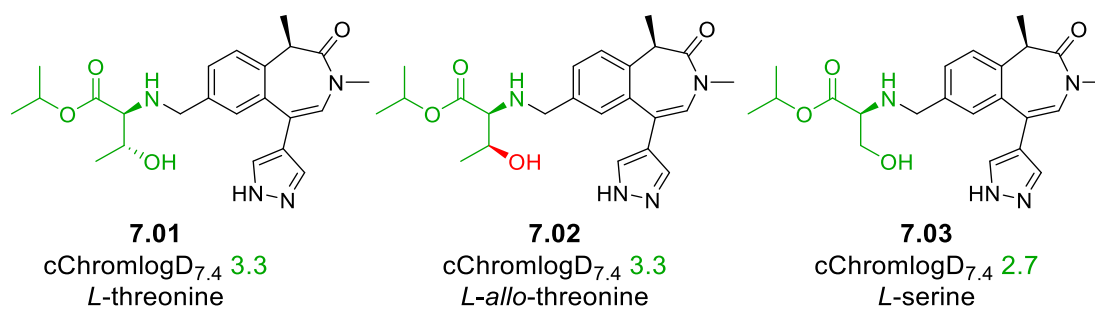
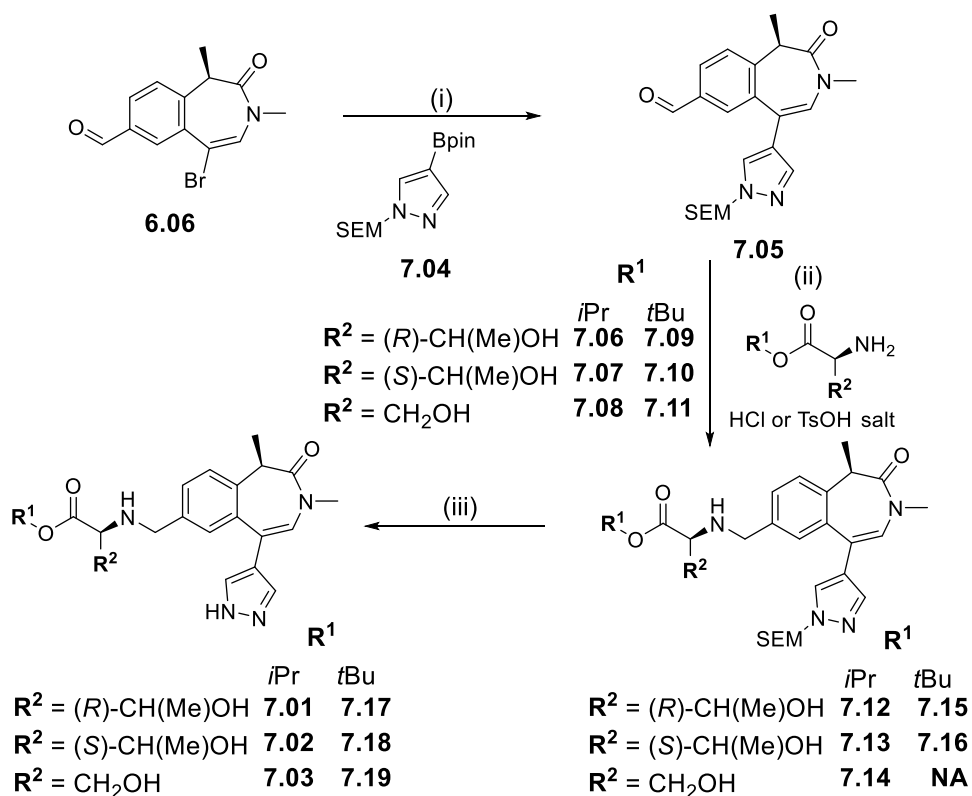


Figure 36: Targets designed within the correct lipophilicity range to provide high Brd4 BD1 potency (> 7.0).

7.1.2. Synthesis

The three target molecules **7.01-7.03**, along with the *t*Bu analogues **7.17** and **7.18**, were synthesized from the common intermediate **6.06** (Scheme 16, p.84) by Suzuki cross-coupling with the SEM-protected pyrazole boronic ester **7.04** as shown in Scheme 21.

This reaction provided an excellent isolated yield of 96%.



- (i) K₂CO₃, Pd(PPh₃)₄, 1,4-dioxane, water, 120 °C, 1 h, 96% yield.
(ii) DIPEA, AcOH, NaBH(OAc)₃, THF, 40 °C, 4 h.
(iii) 1 M solution of BBr₃ in DCM, -78 °C, 20 min.

Scheme 21: Synthesis of molecules **7.01-7.03** and **7.17-7.19**.

The product of this coupling, aldehyde **7.05**, was used in a series of reductive amination reactions with the different amino ester motifs **7.06-7.10**, to afford the desired products **7.01-7.03**, **7.17** and **7.18**, after deprotection of the SEM group.^{xviii} Deprotection of the SEM group with TBAF was found to be very slow at room temperature (more than 24 h).⁹⁷ Heating at 40 °C decreased the reaction time, however this was associated with formation of several impurities, often leading to challenging purification.⁹⁷ Therefore, alternative deprotection conditions were attempted. The deprotection of the SEM protecting group has been exemplified in the literature with several Lewis acids such as ZnCl₂ or MgBr₂.^{98,99} In our case, the use of boron tribromide at -78 °C afforded the desired deprotected molecules in a few minutes with a very clean reaction profile as determined by HPLC. The yields associated with the reductive amination and deprotection reactions are shown in Table 16.

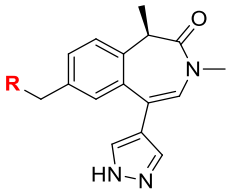
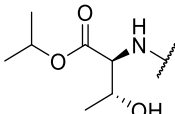
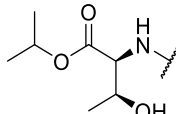
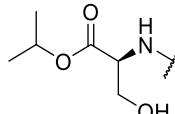
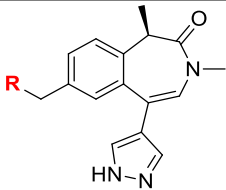
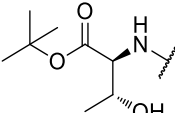
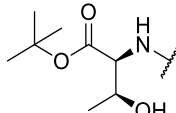
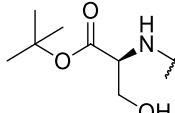
			
	7.01	7.02	7.03
Reductive amination yield	46%	67%	65%
Deprotection yield	17%	46%	19%
			
	7.17	7.18	7.19
Reductive amination yield	36%	37%	48%*
Deprotection yield	5% + 10% acid	6% + 16% acid	18%*

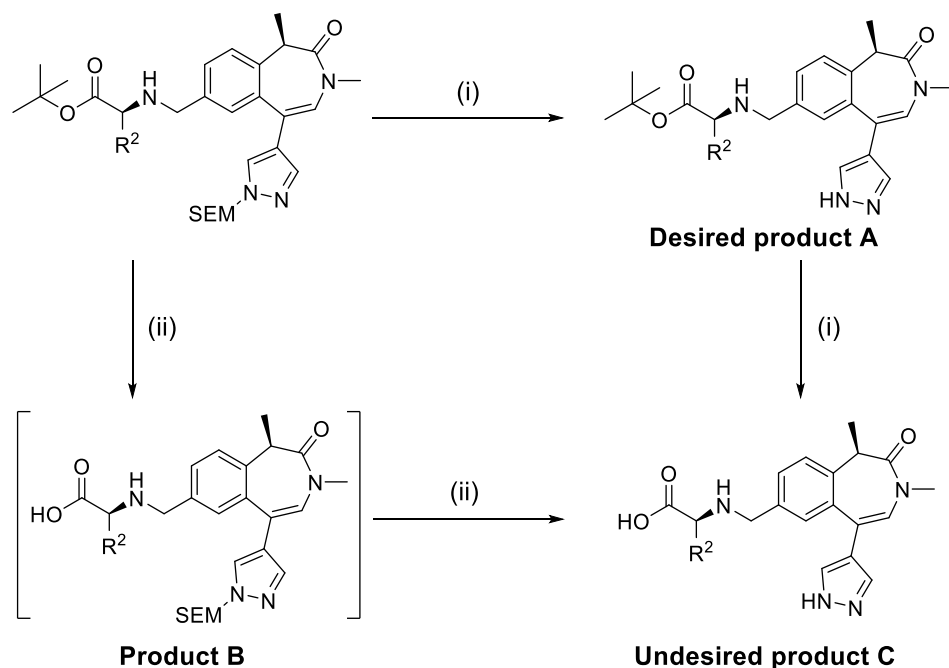
Table 16: Yields for reductive amination and deprotection steps. *For molecule **7.19**, the aldehyde **7.05** was deprotected, and then the reductive amination was carried out.

^{xviii} For molecule **7.19**, the aldehyde **7.05** was deprotected, and then the reductive amination was carried out.

The reductive amination reactions showed moderate yields between 36% and 67%. The deprotection reactions, unfortunately, had low isolated yields for molecules **7.01** and **7.03**, despite very clean reaction profiles.^{xix} This is due to the high solubility of the molecule in water, limiting recovery upon aqueous work-up. Indeed, following the deprotection with BBr₃, the reaction mixtures were quenched with a saturated aqueous solution of sodium bicarbonate. The products were then extracted with ethyl acetate, however significant amounts of products remained in the aqueous layer. This was partially overcome for substrate **7.02** by re-extracting the aqueous layer with a 10% methanol in ethyl acetate solution. Due to the affinity of the product for polar systems, the crude product **7.02** was purified by C18 reverse phase chromatography to afford the desired compound with an improved deprotection yield of 46%.

The same synthetic route was used to synthesize the corresponding *t*Bu analogues **7.17** and **7.18**. The reductive amination reactions showed similar moderate yields, however the selective deprotection reaction of the SEM group in presence of an acid labile *t*Bu ester was challenging. Deprotection of the SEM protecting group was first attempted with HCl in dioxane (Scheme 22). Unfortunately, under these Brønsted acid conditions, the *t*Bu ester was hydrolysed to the corresponding acid faster than the SEM deprotection occurred.

^{xix} Monitored by HPLC.



(i) 1 M solution of BBr₃ in DCM, -78 °C to rt.

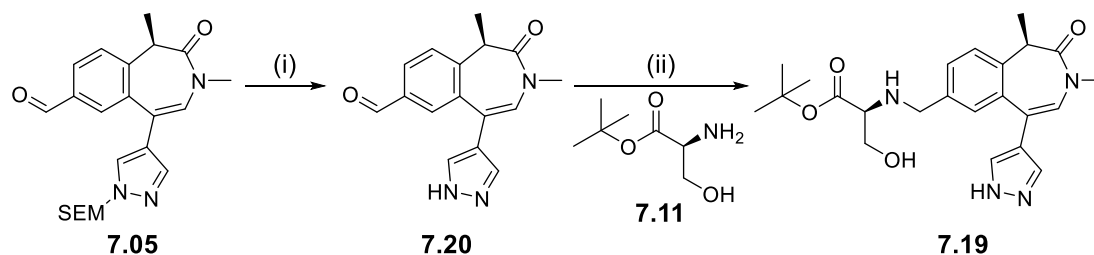
(ii) 4 M HCl in 1,4-dioxane, rt.

Scheme 22: Reaction conditions to deprotect SEM protecting group for tBu ester targets.

Selective deprotection conditions were therefore necessary to synthesize the *t*Bu ester analogues. The use of boron tribromide from -78 °C to room temperature was found to rapidly deprotect the SEM protecting group in 5-10 minutes to give the product of general structure A (Scheme 22). By leaving the reaction mixture to proceed further at room temperature, the *t*Bu ester was found to be hydrolysed to the corresponding acid C.¹⁰⁰ The *t*Bu ester molecule A and the corresponding carboxylic acid C could be isolated and purified from the crude mixture. These unoptimized conditions enabled the deprotection of the SEM group in presence of a *t*Bu ester by careful monitoring of the reaction. The desired *t*Bu ester products **7.17** and **7.18** were isolated in sufficient quantity to submit to the human whole blood assay and enabled the calculation of the hWB Δt Bu values, key parameters to understand the esterase turnover. In these cases, some carboxylic acid products were also isolated and characterised (10% and 16% isolated yield, respectively). The acid products obtained were used by another member

of our laboratory to develop analytical methods for the CES-2 hydrolysis assay to measure the half-life of the compounds for this CES isoform.⁴⁵

In parallel to the BBr₃ deprotection conditions, a route to the *t*Bu ester analogue **7.19** was examined by changing the order of the synthetic sequence, as shown in Scheme 23.



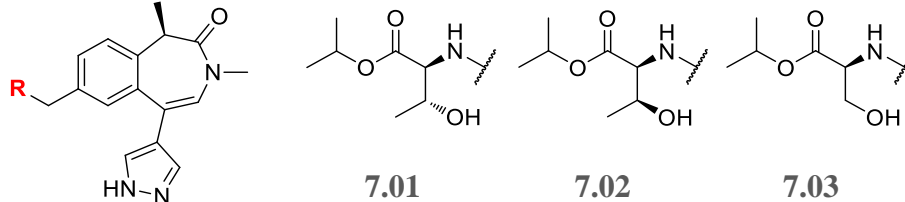
(i) 1 M solution of BBr₃ in DCM, -78 °C to rt, 45 min, 18%.
(ii) DIPEA, AcOH, NaBH(OAc)₃, THF, 40 °C to rt, 2 h, 48%.

Scheme 23: Alternative strategy to obtain the tBu ESM analogues.

The SEM-protected aldehyde **7.05** was treated with boron tribromide to provide aldehyde **7.20** in a modest 18% yield. This benzylic aldehyde could unfortunately not be extracted with methanol-ethyl acetate due to the formation of the corresponding methyl hemiacetal as inferred from LCMS analysis of the crude reaction mixture. A more sterically encumbered alcohol, like *i*PrOH could have potentially been used to quench the excess of boron tribromide and avoid the issues associated with the formation of the hemiacetal. Alternative deprotection and purification conditions using HCl in 1,4-dioxane were later optimised for a similar intermediate providing an excellent 97% isolated yield for the aldehyde deprotection step as exemplified in section 8.3.2 (*vide infra*). Aldehyde **7.20** was then successfully used in a reductive amination to provide the desired molecule **7.19** in 48% isolated yield.

7.1.3. Data for the initial pyrazoles

Following successful synthesis and purification, the target compounds were assessed in primary biological assays, as well as relevant physico-chemical tests and DMPK evaluation. The data associated with molecules **7.01-7.03** is shown in Table 17.



	7.01	7.02	7.03	Desired profile
hWB pIC ₅₀	7.8	8.3	8.1	≥ 7.6
hWB ΔtBu	+ 0.8	+ 1.4	+ 1.1	~ + 1.0
Brd4 BD1 pIC ₅₀	6.9	7.7	7.5	≥ 7.0
ChromlogD _{7.4}	3.1	3.0	2.5	≤ 3.3
AMP (nm/s) / tPSA	- / 108	205 / 108	52 / 108	≥ 50 / ≤ 125
HLM IVC (-/+ benzil) (mL/min/g)	6.8 / 4.7	3.3 / 2.2	3.5 / 1.6	≤ 3

Table 17: Data associated with analogues **7.01-7.03**.

As anticipated in the design hypothesis, the pyrazole group in the ZA channel demonstrated a high Brd4 BD1 potency and molecules **7.01-7.03** demonstrated an appropriate level of CES-1 turnover. This translated into excellent human whole blood potencies, well above the desired value of 7.6. The physico-chemical parameters for these three analogues are within the desired range, however all three molecules demonstrate elevated levels of human liver microsome *in vitro* clearance. The comparison of the human liver microsome *in vitro* clearance values with and without the esterase inhibitor benzil enabled more complete understanding of the metabolism. Indeed, molecules **7.01** and **7.02** demonstrated high underlying non-esterase phase I metabolism, with a human microsomal clearance in the presence of benzil of 4.7 and 2.2 mL/min/g, respectively. Molecule **7.03**, despite having a lower lipophilicity, also showed high human liver microsome *in vitro* clearance. The direct analogues

containing the *N*-methyl-1,2,4-triazole, molecules **6.23**, **6.24** and **6.26**, all demonstrated low human liver microsome *in vitro* clearance ≤ 1.2 mL/min/g, with comparable measured lipophilicities (Table 13, p.92). This suggests the pyrazole ring of molecules **7.01**, **7.02** and **7.03** has an inherent phase I metabolic liability.

To understand the potential sites of metabolism on these analogues, molecule **7.01** was submitted for *in silico* metabolite identification, using *MetaSite* software.^{101,102} This tool enables the identification of the most likely sites of CYP-mediated metabolism in the molecule. The results of the *in silico* metabolite identification analysis are shown in Figure 37.¹⁰³

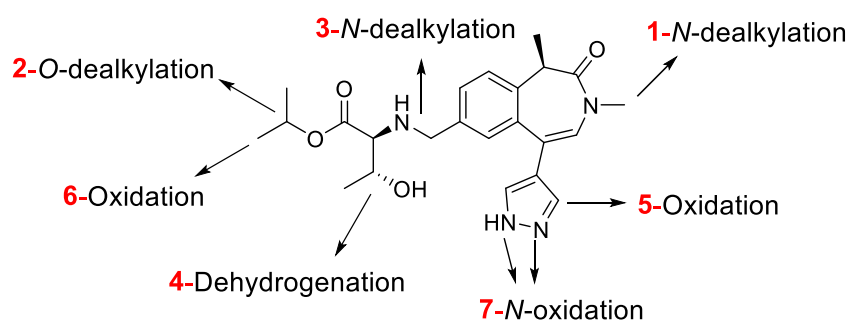


Figure 37: Potential sites of metabolism of molecule **7.01** as predicted by the *MetaSite* software. The numbers in red rank the most probable sites of metabolism.¹⁰³

This analysis predicted some potential *N*-dealkylation of the amide or amine groups and the ESM was also highlighted by the software as having potential metabolic soft spots. Interestingly, the analysis also identified the positions 3 and 5 of the pyrazole ring as potential sites for oxidation by metabolic enzymes. This could explain the difference in *in vitro* clearance observed between molecules **7.01** and **7.02** (both containing a pyrazole ring) on the one hand and molecules **6.23** and **6.24** (containing a 1,2,4-triazole) on the other (Table 18). Indeed, the *in vitro* clearance of the pyrazole is significantly higher than the triazole with comparable lipophilicity (ChromlogD_{7.4}) and ESM. The matched pair comparison of the *in vitro* clearance associated with these

two ZA channel groups seems to support the *MetaSite* predictions of one or two metabolic soft spots on the pyrazole ring of molecules **7.01** and **7.02** (Figure 37).

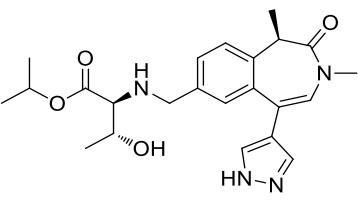
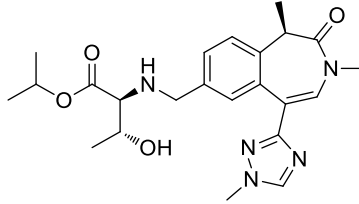
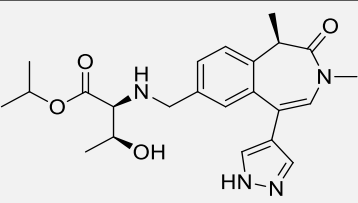
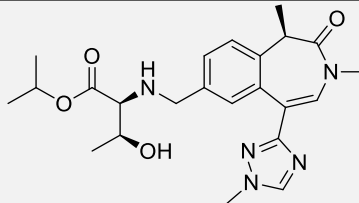
		
	7.01	6.23
ChromlogD _{7.4}	3.1	3.1
HLM IVC (-/+ benzil) (mL/min/g)	6.8 / 4.7	1.1 / 0.8
		
	7.02	6.24
ChromlogD _{7.4}	3.0	2.9
HLM IVC (-/+ benzil) (mL/min/g)	3.3 / 2.2	1.2 / 0.7

Table 18: Comparison of the lipophilicity and human liver microsome *in vitro* clearance for two pairs of molecules with a single point change at the ZA channel group.

It is understood that metabolism of five membered heteroaryl rings is governed by several factors including lipophilicity, metabolic soft spots and the electronic nature of the rings.^{104,105} *N*-oxidation and *C*-oxidation of pyrazoles have been observed in *in vivo* studies and led to conjugation of the metabolite (phase II metabolism) and excretion of the metabolites in urine.¹⁰⁵ The identification of positions 3 and 5 of the pyrazole as metabolic soft spots implies that to reduce the *in vitro* clearance, these positions should be blocked or the electron density of the ring should be further decreased. Indeed, the sole reduction of the lipophilicity in molecule **7.03** (Table 17, p.103) was insufficient to reduce the human liver microsome *in vitro* clearance to the desired level, suggesting the presence of a metabolic soft spot. Several strategies to

block these positions could be investigated. In the literature, blocking metabolically vulnerable positions with a heteroatom or a substituent (e.g. Me, CF₃, CH₂F, F, D) has been successful in several instances.^{104,106,107,108} Moreover, adding an heteroatom has proven to be successful in reducing the CYP450 mediated metabolism by decreasing further the electron density of the ring.¹⁰⁴ These strategies will be incorporated into the design of the second generation analogues.

In parallel to the investigation of the metabolism SAR of the ZA channel group, the origin of the 10-fold difference in Brd4 BD1 potencies between the pyrazole ring and the triazole ring was investigated in collaboration with our computational chemistry group. The X-ray crystal structures of molecules **6.26** and **7.03** in Brd2 BD2 are shown in Figure 38.¹⁰⁹

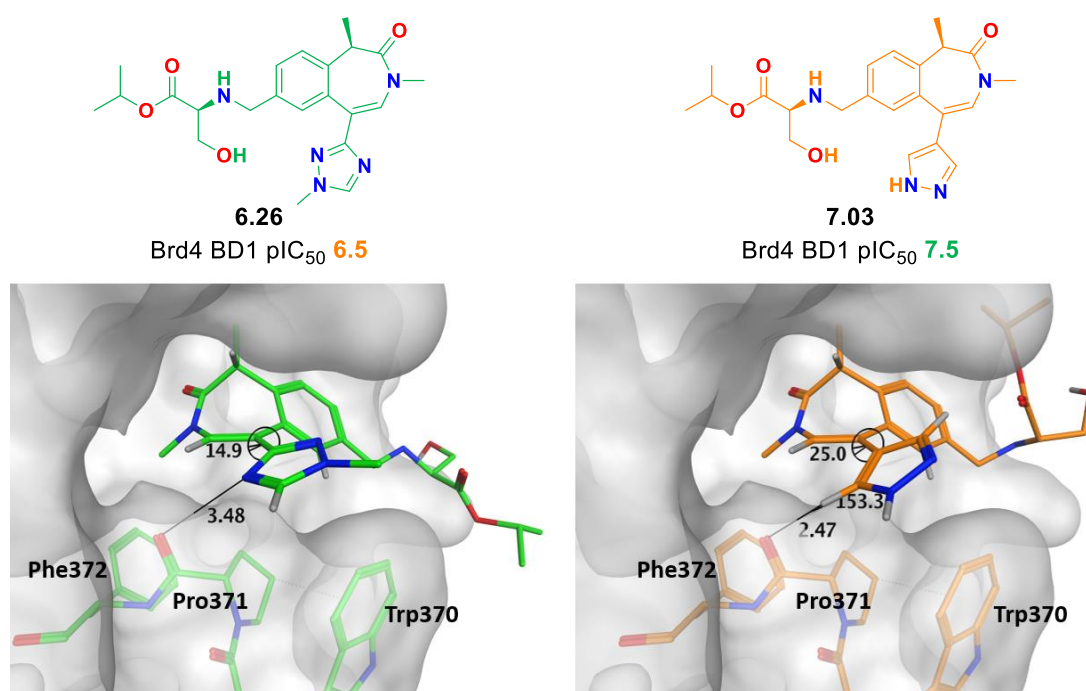


Figure 38: X-ray crystal structures of molecules **6.26** and **7.03** in Brd2 BD2 BET protein (PDB files *gsk1jmbq* and *gsk1idyr*).¹⁰⁹ The dihedral angles between the alkene and the heterocycle were measured at 14.9° and 25.0°, respectively for molecules **6.26** and **7.03**. The distance between the CH in position 3 of the pyrazole (molecule **7.03**) and the oxygen atom of Pro371 was measured at 2.47 Å and the angle between the C-H---O atoms was measured at 153.3°.

The two molecules overlaid well in these crystal structures suggesting a similar binding pose in each case. The main difference in interactions between the molecules and the protein was inferred to be attributable to two concurrent factors: a weak interaction with the carbonyl of Pro 371, and the dihedral angle between the alkene and the aryl groups.¹¹⁰ Firstly, in the binding pose of molecule **7.03** in the BET protein, the CH in position 3 or 5 of the pyrazole is directed towards the carbonyl functionality of Pro371. The partial positive charge on the hydrogen atom of this carbon in position 3 (or 5) of the pyrazole could create a positive interaction with the lone pair of the carbonyl oxygen atom. Such C-H---O interactions have been described in the literature as weak hydrogen bonds (< 8.4 kJ/mol),¹¹¹ with the caveat of sometimes being difficult to distinguish from the adirectional Van der Waals contact interactions, in particular when the angle of these weak C-H---O interactions varies from linearity.^{112,113,114} Such C-H---O interactions are too weak to direct the binding mode of the ligand but are nevertheless able to have a supportive contribution to the binding affinity governed by stronger hydrogen bonds with the protein.¹¹² The favourable geometry for these weak C-H---O interactions has been described as a C-H---O angle greater than 160° and short distances (< 2.5 Å). In our case, the C-H---O angle measured for molecule **7.03** in the X-ray crystal structure is 153° and the H---O distance was measured as 2.5 Å. This suboptimal geometry would suggest a modest contribution to the binding energy of our ligand to the BET protein, well below the proposed 8.4 kJ/mol. Conversely, the 1,2,4-triazole of molecule **6.26** has nitrogen atoms in position 2 and 4. These heteroatoms, bearing a partial negative charge, could create an unfavourable interaction with the lone pair of the oxygen atom of the carbonyl of Pro371, decreasing

the affinity of the molecule for the BET protein, hence decreasing the Brd4 BD1 potency.¹¹⁰

Secondly, the dihedral angle between the benzazepinone alkene and the heteroaryl ring is impacted by the nature of the atoms in the pseudo-*ortho* positions to the benzazepinone branching point (two CH moieties or two N atoms). Figure 39 shows the energy profile for different dihedral angles between the heteroaryl and the alkene for a 4-substituted-pyrazole or a 1,2,4-triazole benzazepinone molecule.¹¹⁰ As the benzylic linker and the ESM group are not designed to interact with the BET protein, this chain often led to several different possible poses during the computational energy calculations as no key interaction is established. To simplify the calculations and interpretation of the impact of the dihedral angle variations with the two different heterocycles, the decision was made not to include the ESM chain in the calculations in order to understand the sole impact of the nature of the heterocycle on the dihedral angle.

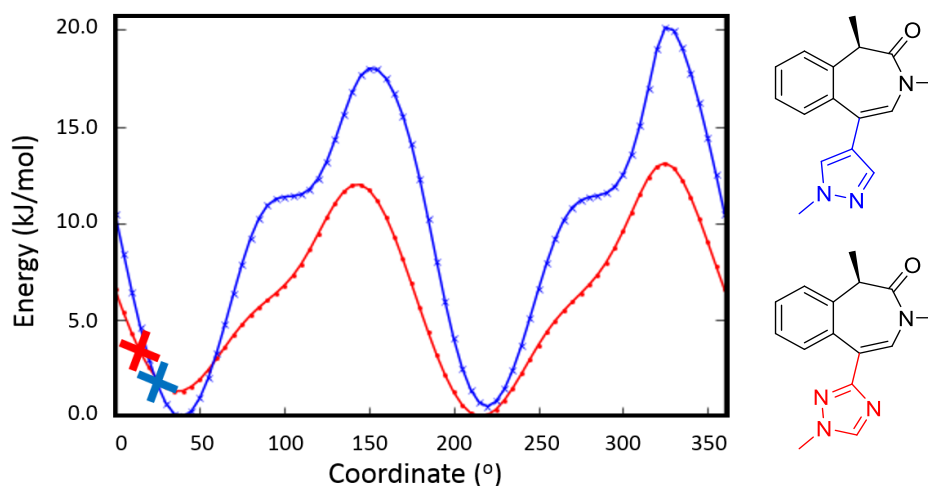


Figure 39: Diagram showing the variation of energy for different dihedral angles between the benzazepinone alkene and the heteroaryl. The energy associated with the pyrazole is shown in blue and the triazole energy profile is shown in red.¹¹⁰ The crosses mark the energy associated with these motifs at the dihedral angles measured in the BET protein.

For the two molecules, there are two minima around 40° and 220°. As shown in the X-ray crystal structures in the Brd2 BD2 domain (Figure 38), the measured dihedral angle between the alkene and the pyrazole **7.03** is 25.0° (blue cross) and is 14.9° for the triazole **6.26** (red cross). Comparison of this energy for the two rings showed a higher energy for the 1,2,4-triazole (red cross) than for the pyrazole (blue cross) of approximately 2.3 kJ/mol. A 10-fold difference in potency corresponds to a difference in Gibbs free energy of around 5.7 kJ/mol (Equation 4).¹¹⁵

$$\Delta G = -2.3 RT \log K = -5.7 \log K \quad (\text{in kJ/mol})$$

with R = 8.314 J/mol and T = 298 K.

Equation 4: Relationship between the Gibbs free energy and the binding constant.

Thus, the conformational strain depending on the nature of the heteroaryl ring is likely to be responsible for approximately half of the potency difference observed between the 1,2,4-triazole and the pyrazole. Collectively both effects, the conformation of the molecule and the weak C-H---O interaction are of a strength that is consistent with the higher potency of the pyrazole compared to the 1,2,4-triazole.

To conclude, the metabolite identification study and the X-ray crystallography in the BET protein have proven to be tremendously important in understanding the SAR of these matched pairs of pyrazole and 1,2,4-triazole analogues. The data analysis of molecules **7.01-7.03** has highlighted two crucial points for the future investigations: the methine systems in the positions 3 or 5 of the pyrazole is increasing the potency of the BET inhibitors and blocking this position could contribute to lowering the phase I metabolism of the future analogues. These two concepts will be used to guide the design of the second-generation analogues.

7.2. Second generation molecules – balancing *in vitro* clearance and potency

7.2.1. Design of the second-generation molecules

As explained in section 7.1.3, crystallographic and modelling rationalisation of the structure-activity relationship supported the hypothesis that a methine system in the pseudo-*ortho* position to the benzazepinone branching point was important to reach the desired potency level but was associated with some metabolic liability (Figure 40). Conversely, the presence of a nitrogen atom in the pseudo-*ortho* position confers metabolic stability but negatively impacts the BET potency.

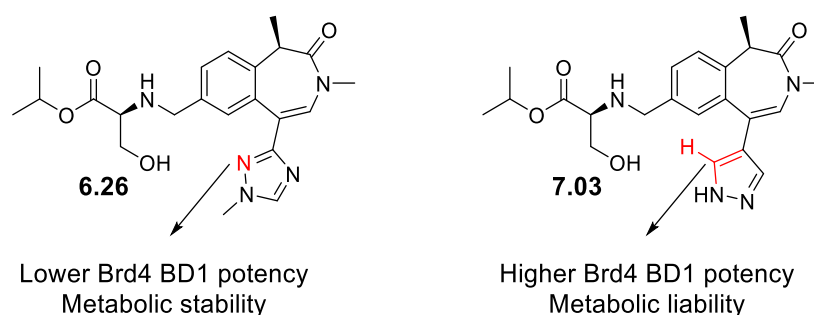


Figure 40: Summary of the emerging structure-activity relationship in the series.

In order to combine high Brd4 BD1 potency and low human microsome *in vitro* clearance, two strategies were investigated in parallel:

1st approach: Combining high potency and low metabolism by blocking only one of the two pseudo-*ortho* positions relative to the benzazepinone branching point in the 5 membered ring (Figure 41).

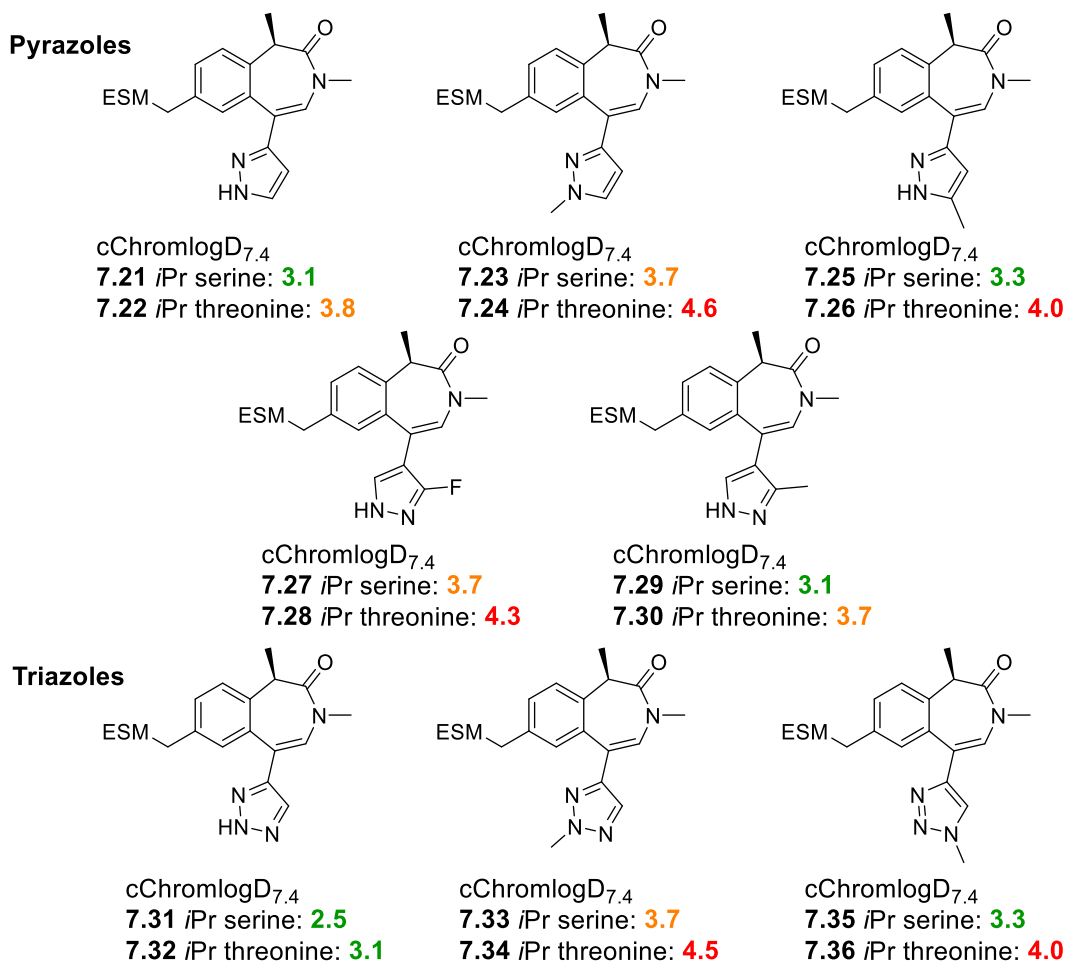


Figure 41: Calculated Chromlog_{D7.4} for a range of heteroaryl rings with one of the pseudo-ortho positions blocked, relative to the benzazepinone branching point. These targets were designed to combine high potency and reduced CYP mediated metabolism compared to molecules 7.01-7.03. The calculated values for L-threonine and L-allo-threonine are identical and are therefore designated only by threonine.

Introducing a heteroatom in one of the pseudo-ortho positions relative to the benzazepinone branching point could reduce the CYP-mediated metabolism observed in molecules 7.01-7.03. This led to the design of molecules 7.21-7.26 and 7.31-7.36. The addition of a methyl group in position 1 or 5 (molecules 7.23-7.26) increases the steric hindrance around the pyrazole system, and could further decrease the metabolic activity on the suspected soft spot by decreasing the accessibility of the labile site by the metabolic enzymes.¹⁰⁸ In addition, the position 5 of a pyrazole ring has been associated with oxidative phase I metabolism reaction, therefore substituting this

position could decrease the metabolic activity.¹⁰⁵ Direct analogues of molecule **7.03** with a fluorine atom or a methyl group to block one of the vulnerable pseudo-*ortho* positions of the pyrazole (**7.27-7.30**) have also been designed, to reduce the CYP-mediated metabolism compared to molecule **7.03**. Finally, the triazole analogues **7.31-7.36** were designed with one nitrogen atom and one free methine unit in the two pseudo-*ortho* positions relative to the benzazepinone branching point. As explained in section 7.1.3, a triazole ring, which is more electron-deficient than a pyrazole ring, could have a reduced *in vitro* clearance. These analogues should help to understand if by blocking one of the two metabolic soft spots predicted by the *MetaSite* software, the CYP-mediated metabolism could be reduced under the targeted value of 3 mL/min/g.

The serine ESM of these analogues were first synthesized for these molecules to understand the correlation between the calculated chromlogD_{7.4} (calculated as per Equation 3, p.42) and the measured chromlogD_{7.4}. After validation of the chromlogD_{7.4} model developed in this thesis, selected threonine derivatives will be synthesized if in the desired lipophilicity range.

2nd approach: *Increasing the potency of 1,2,4-triazole already exhibiting low human liver microsomal metabolism* (Figure 42).

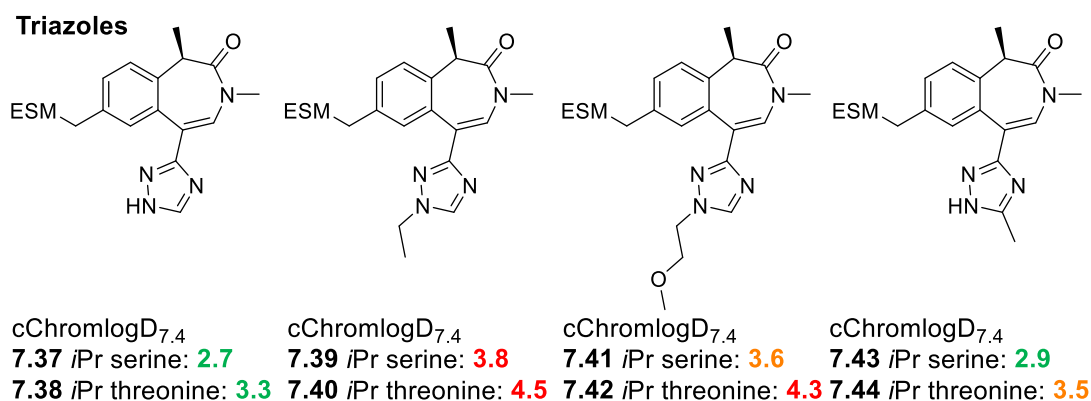
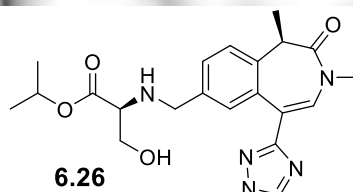
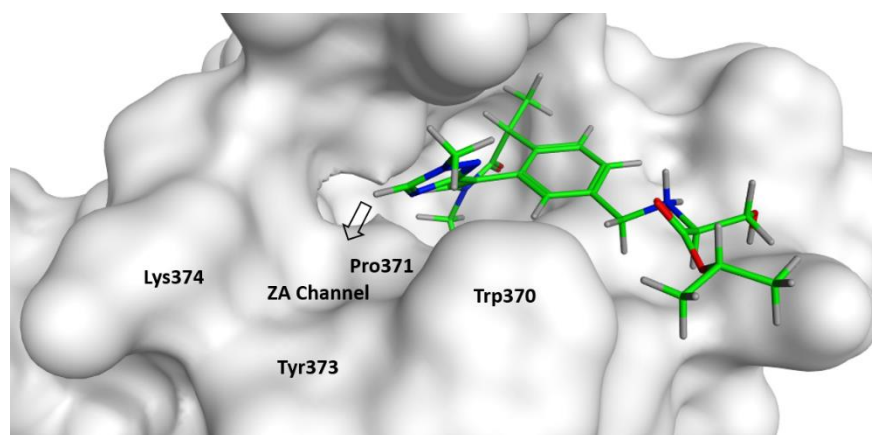


Figure 42: Proposed targets containing the 1,2,4-triazole demonstrating low human liver microsomal *in vitro* clearance, with a small single point change to increase the potency of these analogues compared to molecule **6.26**.

Molecules **7.37** and **7.38** were designed with an unsubstituted triazole to understand if a hydrogen bond donor in one of the pseudo-*ortho* positions to the benzazepinone branching point could act in a similar fashion to the methine of the pyrazole by creating a positive interaction between the NH partial positive charge and the carbonyl of Pro371.

Molecules **7.39-7.44** were designed to improve the interaction of the triazole motif with the ZA channel. Indeed, the X-ray crystal structure of molecule **6.26**¹⁰⁹ (Figure 43) indicated that the triazole was contributing to potency by an edge-to-face interaction with the Trp370, however it also suggested the possibility of interacting more optimally with the protein pocket by occupying the ZA channel, in particular the space created by three residues: Trp370, Tyr373 and Lys374.



Molecules **7.39-7.42**

Can a larger substituent in position 4 cause a conformational change of the molecule and increase the Brd4 BD1 potency?

Molecules **7.43** and **7.44**

Can a substituent in position 5 increase the occupancy of ZA channel and therefore increase the Brd4 BD1 potency?

*Figure 43: X-ray crystal structure of molecule **6.26** in Brd2 BD2 showing the potency could be improved by enhancing the interaction with the ZA channel, in particular by occupying the pocket created by Trp370, Tyr373 and Lys374 (PDB file **gsk1jmbq**).¹⁰⁹*

This new interaction could potentially be obtained by substituting the 5-position of the triazole (e.g. molecules **7.43** and **7.44**). In addition, a methyl substituent in position 5 would increase the electron density of the triazole. This could increase the edge-to-face interaction with the Trp370, and as such increase the potency of the target molecules. It worth noting, however, that increasing the electron density of the triazole could negatively impact the *in vitro* clearance.

Finally, increasing the length of the substituent in position 1 in molecules **7.39-7.42** could potentially cause a change of conformation of the molecule in order to favour the interaction of the ethyl group or the methoxyethyl chain with the channel delimited by the residues Trp370, Tyr373 and Lys374. Molecule **7.39**, although anticipated to

be too lipophilic, was synthesized to challenge the potency hypothesis with a single point change compared to molecule **6.26**.

As discussed previously, the *i*Pr-*L*-serine ESM of these analogues were first synthesized for these second-generation molecules to verify the correlation between the calculated $\text{chromlogD}_{7.4}$ (calculated as per Equation 3) and the measured $\text{chromlogD}_{7.4}$.

7.2.2. Synthesis

The synthesis of the molecules designed in section 7.2.1 was performed using the route previously described in this thesis (Scheme 20, p.88), according to the general reaction scheme shown in Figure 44. The common intermediate pinacol boronic ester **6.20** was used in a Suzuki cross coupling with aryl bromides, followed by a reductive amination onto the aldehyde functionality. Depending on the aryl bromide building-blocks used in the cross-coupling reactions, the reductive amination step was followed by a SEM deprotection if necessary.

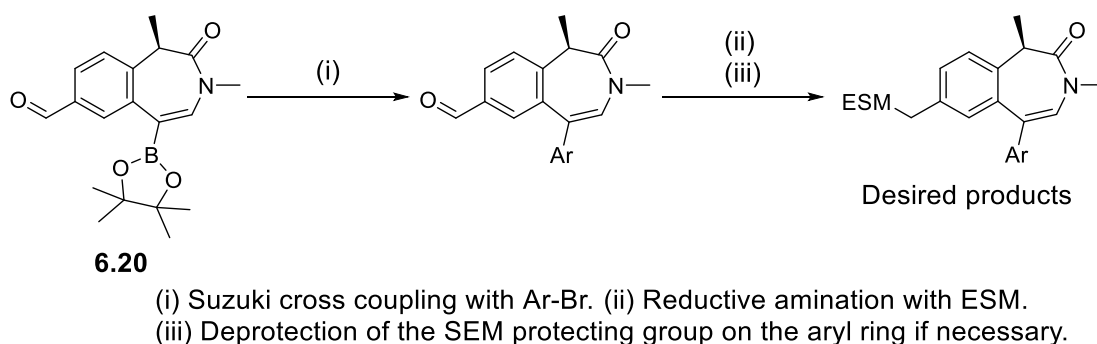
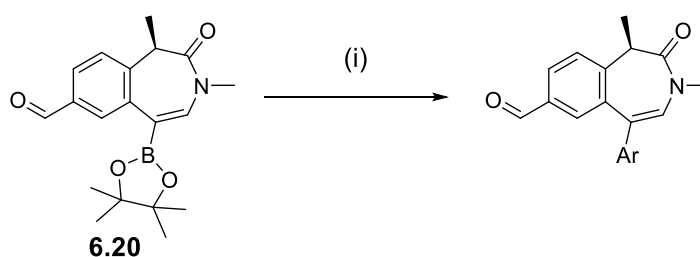


Figure 44: General reaction scheme for the synthesis of the second-generation molecules.

The *t*Bu direct analogues were also synthesized using the same synthetic route. The reaction conditions and the yields associated with these reactions will be discussed in the following sections.^{xx}

7.2.2.1. Suzuki cross coupling reactions

The conditions for the Suzuki cross coupling to introduce the ZA channel group are shown in Table 19. These conditions were found to be versatile for a range of heteroaryl bromides with yield varying from 31% to 98% and enabled the rapid development of the structure activity relationship for this series.



(i) Ar-Br, Pd XPhos G2, XPhos, K₃PO₄ (2 M aq.), *i*PrOH, 120 °C, 30 min (microwave)

Product Ar	Yield	Product Ar	Yield
<p>7.45 mixture of regioisomers [1:1 ratio]^a</p>	68%	<p>7.50</p>	98%
<p>7.46</p>	48%	<p>7.51</p>	31%

^{xx} Molecules **7.27**, **7.29**, **7.31** and **7.32** were designed by the author but synthesized by another member of our laboratory from intermediate **6.20** supplied by the author. The synthesis of these analogues will not be included in this thesis, but the physico-chemical and biological data associated with these molecules will be discussed in the following section.

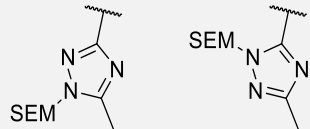
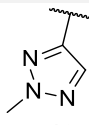
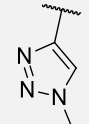
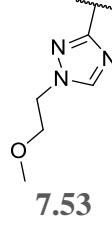
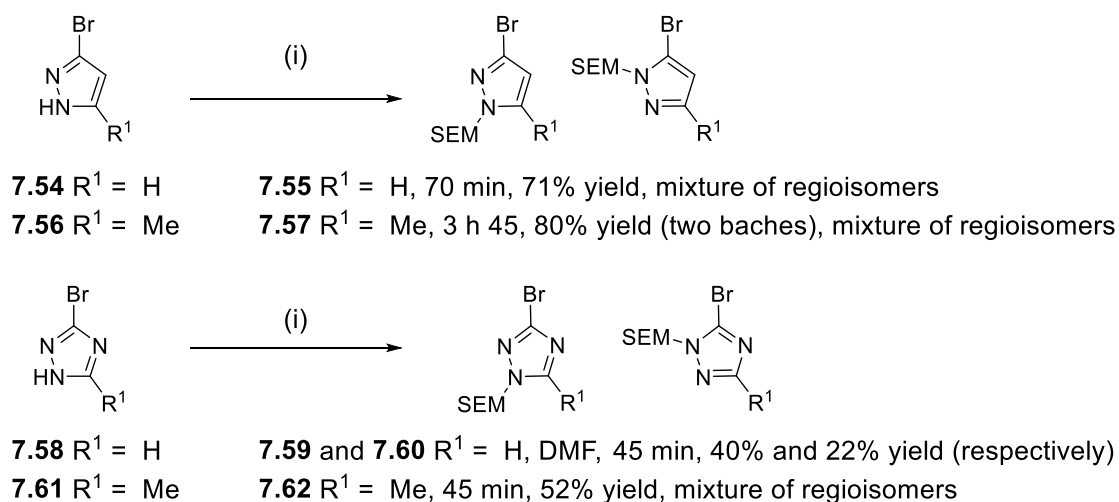
 <p>7.47 mixture of regioisomers [1:1 ratio]^a</p>	39%	 <p>7.52 mixture of regioisomers [1:0.2 ratio]^a</p>	50%	
 <p>7.48</p>	89%			
 <p>7.49</p>	56%			
			 <p>7.53</p>	50%

Table 19: Reaction conditions and yields for the Suzuki cross coupling reactions.
^a Ratio was determined by ¹H NMR.

The majority of the aryl bromide motifs used in this study were commercially available. For building blocks **7.45**, **7.47** and **7.52** the unprotected heteroaryl bromide materials were purchased and protected with SEMCl (Scheme 24).^{116,117,118,119}

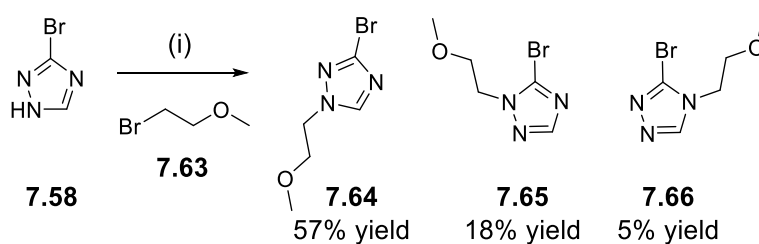


(i) NaH, SEMCl, THF, 0 °C to rt.

Scheme 24: Protection of the heteroaryls with SEMCl.^{xxi}

^{xxi} The protection of building block **7.58** was carried out by another team member and the experimental procedure will not be included in this thesis.

The protected building blocks **7.55**, **7.57** and **7.62** were obtained as mixture of regioisomers. The mixtures were not separated by column chromatography and the decision was made to use the building blocks as a mixture of regioisomers. The triazole **7.58** was protected using similar reaction conditions but the separation of the regioisomers was successful by column chromatography, delivering the two intermediates **7.59** and **7.60**. Finally, the methoxyethyl substituted triazole was synthesized from the 3-bromo-1,2,4-triazole by an S_N2 reaction on the bromoalkyl **7.63** as shown in Scheme 25.

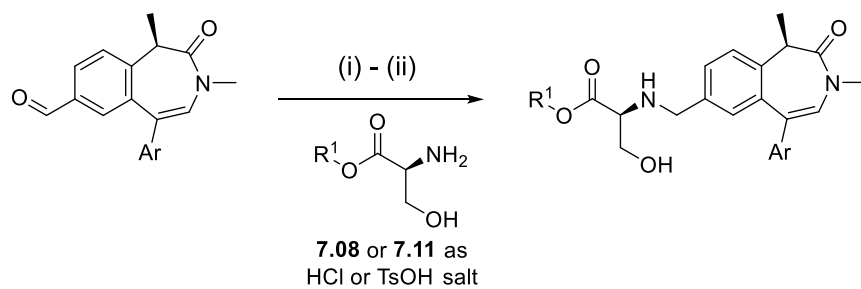


Scheme 25: Alkylation of 3-bromo-1,2,4-triazole.

A mixture of the three regioisomers was obtained. The regioisomers were analysed by ¹H NMR, ¹⁵N HMBC and LCMS. The desired regioisomer **7.64** was obtained as the main alkylation product. The other two regioisomers produced were separated by column chromatography.

7.2.2.2. Reductive amination reactions

Following the synthesis of the Suzuki cross coupling products shown in Table 19 (p.117), intermediates **7.45-7.53** were used in reductive amination transformations as shown in Scheme 26.



(i) **Conditions A:** 1) ESM (1.5 eq), DIPEA (2 eq), AcOH (2.5 eq), THF, 40 °C.
2) NaBH(OAc)₃ (2.5-3 eq), rt.

Conditions B: ESM (1.5 eq), picoline borane (1.2 eq), AcOH, *i*PrOH, rt.

(ii) Deprotection of SEM group if necessary using either

Conditions C: 1 M solution of BBr₃ in DCM or

Conditions D: 4 M HCl in 1,4-dioxane.

Scheme 26: General reaction scheme for the reductive aminations carried out on building blocks 7.45-7.53.

Two sets of reaction conditions (A or B) were used during the development of the structure activity relationship, as shown in Table 20.

Entry	Ar	R ¹	Reactions conditions	Product	Yield (%)	
					Reductive amination	Deprotection
1		<i>i</i> Pr	<i>cf.</i> section 8	7.21	-	-
2		<i>t</i> Bu	A/C	7.67	-	8 ^a
3		<i>i</i> Pr	A	7.23	72 ^b	-
4		<i>t</i> Bu	A	7.68	19 ^b	-
5		<i>i</i> Pr	A/C	7.69 (with SEM) / 7.25	23	36
6		<i>i</i> Pr	A	7.33	55	-
7		<i>i</i> Pr	A	7.35	42 ^b	-
8		<i>t</i> Bu	A	7.70	35 ^b	-
9		<i>i</i> Pr	D/B	7.71 (aldehyde) 7.37	9 ^{b,e}	97 ^c
10		<i>t</i> Bu	B/C	7.72 (with SEM) / 7.73	68	5 ^a
11		<i>i</i> Pr	B	7.39	18 ^e	-
12		<i>i</i> Pr	A/C	7.43	-	3 ^{d,e}
13		<i>t</i> Bu	D/B	7.74 (aldehyde) / 7.75	4	46 ^c
14		<i>i</i> Pr	B	7.41	7 ^f	-

^aBBr₃ deprotection of the SEM group enabled the isolation of the *t*Bu ester and the corresponding acid. ^bYield including reductive amination and chiral separation. ^cDeprotection was carried out before the reductive amination. ^dDeprotection of the product was carried out on the crude material. The yield indicated is over the reductive amination, deprotection and chiral separation. ^eIncomplete conversion of the aldehyde starting material was observed by HPLC analysis. ^fSignificant amounts of reduction of the aldehyde to the corresponding alcohol was observed in the reaction mixture.

Table 20: Yields obtained for transformations described in Scheme 26 (p.119).

Most reductive aminations were carried out under general conditions A, using sodium triacetoxyborohydride as the imine-reducing agent (entries 2-8 and 12). These conditions provided low to good yields depending on the substrate. The poor yield for entry 12 was due to poor conversion of the aldehyde to the imine. Alternative reaction conditions using picoline borane (entries 9-11, 13 and 14) were then attempted to improve the conversion of the aldehyde as these mild conditions have been successful in previous ESM-series developed in our laboratories.^{90,120} Unfortunately, reduction of the aldehyde to the alcohol was observed for most entries using general reaction conditions B and provided the desired amine in poor yields. These picoline borane conditions have shown a higher success rate with poorly water-soluble aldehyde and amine systems;¹²⁰ in our case both reactants were found to be highly water-soluble and these conditions proved not to be suitable for these substrates.

Despite the sub-optimal reductive amination conditions, methods A or B enabled the synthesis of all desired intermediates and final molecules necessary to establish the structure activity relationship in our series. Molecules bearing a SEM protecting group were deprotected using boron tribromide or HCl as previously discussed in section 7.1.2. Most final molecules obtained following this synthetic sequence showed presence of at least one diastereomeric impurity by ¹H NMR. Achiral chromatography methods to isolate the desired diastereomer were often unsuccessful, and the mixtures required chiral chromatography to efficiently separate the undesired diastereomer from the desired product. Improvement of the reductive amination conditions, and of the chiral integrity of the intermediates and products will be detailed in section 8.

7.2.2.3. ChromlogD_{7.4} correlation between the measured and calculated values and synthesis of chosen *iPr-L-allo-threonine* analogues.

With the measured chromlogD_{7.4} values in hand for these different *L*-serine analogues, the corrective model developed in this thesis (section 5.1) was evaluated. Better understanding of the model would enable the decision to synthesize more lipophilic analogues of the best molecules such as *L*-threonine or *L-allo*-threonine.

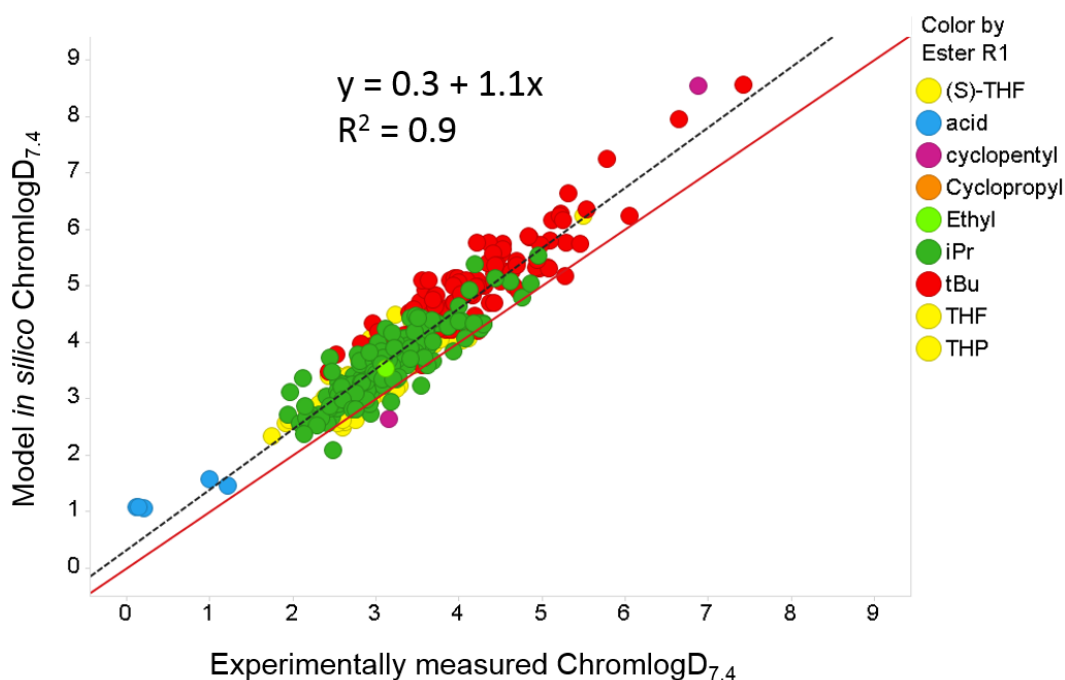
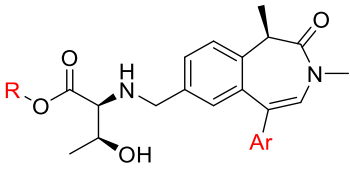
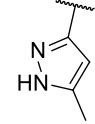
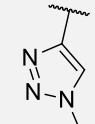
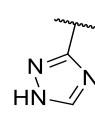
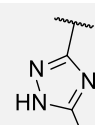
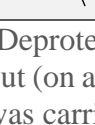
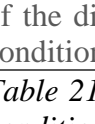


Figure 45: Comparison of the measured chromlogD_{7.4} and the *in silico* values calculated using Equation 3. The red line is the unity line. The black line is the straight line for best fit for the values shown on the graph.

The comparison of the chromlogD_{7.4} values calculated using Equation 3 and their corresponding measured values is shown in Figure 45. The calculated values are lying 0.3 log unit on average above the measured values. This small difference, inherent to every *in silico* model, is minimal and enabled the validation of the use of the chromlogD_{7.4} equation to select which molecules to synthesize next.

Based on this, several *iPr-L-allo*-threonine analogues were synthesized as they were predicted to be in the correct lipophilicity range. The aldehyde building blocks from Table 19 (p.117) were used in reductive amination reactions with *iPr-L-allo*-threonine building blocks; the yields are shown in Table 21. As the *L-allo*-threonine ESM-BET inhibitors have shown to have lower cynomolgus monkey hepatocytes *in vitro* clearance compared to the analogues containing the natural *L*-threonine amino ester, the decision was made to synthesize only the *L-allo*-threonine analogues.

	Yield		Reaction conditions	
	reductive amination	deprotection	reductive amination	deprotection
 7.26 R = <i>iPr</i>	20% yield over two steps		B	D
 7.36 R = <i>iPr</i>	64%	-	A	-
 7.38 R = <i>iPr</i>	23%	25% ^a	A	C
 7.79 R = <i>tBu</i>	10%	97% ^b	A	D
 7.44 R = <i>iPr</i>	12%	46% ^{c,d}	B	D
 7.80 R = <i>tBu</i>	5%	46% ^c	B	D

^aDeprotection yield includes chiral separation. ^bThe reductive amination was carried out (on aldehyde **7.71**) after the SEM-deprotection reaction. ^cThe reductive amination was carried out (on aldehyde **7.74**) after the SEM-deprotection reaction. ^dSeparation of the diastereomers was unsuccessful at this stage despite an extensive screen of conditions.

Table 21: Yields for reductive aminations to install the *iPr-L-allo*-threonine. Sets of conditions A-D are detailed in Scheme 26 (p.119).

The data associated with these molecules will be discussed in the next section with the *iPr-L*-serine analogues. However, the triazole derivative **7.44** showed the presence of 27% of a diastereomer. An extensive screen of purification conditions was carried out;

however, they were unsuccessful in separating the mixture. A stereoselective route, discussed in section 8, enabled the synthesis of molecule **7.44** with the required purity. The biological and physico-chemical data reported hereafter were obtained from the pure batch of molecule **7.44**.

7.2.3. Data for the second-generation molecules

7.2.3.1. Blocking position 3 of the pyrazole to decrease in vitro clearance and maintain potency.

The second-generation analogues were designed following two approaches. The first design hypothesis was aiming to understand if high potency and low metabolism can be combined by blocking one of the two pseudo-*ortho* positions of the five-membered ring, relative to the benzazepinone substitution point. Molecules **7.21-7.36** were designed to answer this question, and the data associated with these compounds is shown in Table 22.

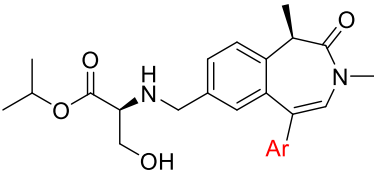
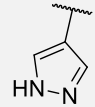
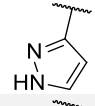
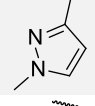
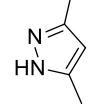
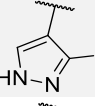
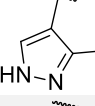
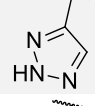
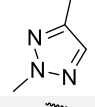
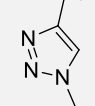
		ChromlogD _{7.4}	Brd4 BD1 pIC ₅₀	HLM IVC (-benzil) (mL/min/g)
	7.03	2.5	7.5	3.5
	7.21	2.8	6.9	3.2
	7.23	3.2	7.0	2.4
	7.25	3.2	7.4	3.0
	7.27	3.1	6.9	9.9
	7.29	2.8	5.7	-
	7.31	2.3	6.3	2.4
	7.33	3.4	7.4	3.3
	7.35	2.6	6.9	0.8

Table 22: Data associated with molecules 7.21-7.35, aiming to understand the structure activity relationship in terms of Brd4 BD1 potency and *in vitro* clearance.

The pyrazole rings used in molecules 7.21 and 7.23 showed a modest decrease in potency with respect to the reference molecule 7.03. Pleasingly, adding a methyl in position 5 (molecule 7.25) regained the potency lost by moving the nitrogen atom to the pseudo-ortho position. Molecules 7.21, 7.23 and 7.25 demonstrated, as proposed during their design, a reduced human liver microsome *in vitro* clearance despite a slight increase in lipophilicity, by blocking the potential metabolic soft spot of molecule 7.03 with a nitrogen atom. The addition of a methyl group in position 1 or 5

(molecules **7.23** and **7.25**) further decreased the metabolic activity by increasing steric hindrance near the metabolic soft spot. These potency and phase I clearance trends are also confirmed by the 1,2,3-triazole **7.31** similarly demonstrating a loss in potency and a lower human liver microsome *in vitro* clearance, likely to be due to the presence of the nitrogen atom in position 2 of the ring. The addition of a methyl group in position 2 (molecule **7.33**) increased the potency by 10-fold but also increased the lipophilicity above the desired range, driving a higher human liver microsome *in vitro* clearance. The addition of a methyl in position 1 (molecule **7.35**) was only associated with a modest increase in lipophilicity and potency but pleasingly demonstrated a lower *in vitro* clearance than the unsubstituted 1,2,3 triazole **7.31**. These analogues showed that blocking one of the two pseudo-*ortho* positions to the benzazepinone branching point with a nitrogen atom can reduce the phase I metabolism, even if this is also associated with a small loss of Brd4 BD1 potency. This compound set also showed modification of the substitution pattern of the aryl ring can be instrumental to increase the potency and further reduce the microsomal *in vitro* clearance.

When trying to block one of the two pseudo-*ortho* positions to the benzazepinone branching point with a fluorine atom (molecule **7.27**) or with a methyl group (molecule **7.29**), significant reductions in potency are observed, especially for molecule **7.29**. The loss of potency due to the addition of a methyl at this position is likely to be due to a conformational change or movement of the molecule in the bromodomain to accommodate the extra methyl. Indeed, computational calculations showed a dihedral angle of 50° or 55° (depending on the tautomeric form) is associated with the minimum conformational energy for molecule **7.29**. This angle is significantly larger than the

angles measured in the X-ray crystal structures for the pyrazole **7.03** (25.0°, Figure 38, p.106) or for the triazole **6.26** (14.9°, Figure 38, p.106), both more potent than molecule **7.29**. Thus, the methyl is having a very significant impact on the dihedral angle between the aryl ring and the benzazepinone alkene, likely causing an extra strain on the molecule to fit in the BET bromodomain site, and is therefore responsible for the decrease in potency. As a consequence of its poor potency, this molecule was not assessed in *in vitro* clearance assays.

The loss of potency and the higher phase I clearance of molecule **7.27** is perhaps more surprising as fluorine atoms have frequently been used in medicinal chemistry as hydrogen bioisosteres to decrease the phase I metabolism.¹²¹ The increase in microsomal clearance is likely to be attributable to the higher lipophilicity of molecule **7.27** compared to molecule **7.03**. Computational calculations of the dihedral angle associated with the minimum conformational energy for molecule **7.27** was found to be 40° (for both tautomers), which is identical to the calculated minimal energy for the very potent molecule **7.03**. However, as explained in section 7.1.3 (Figure 38, p.106), the partial positive charge on one of the pseudo-*ortho* positions to the benzazepinone branching point is thought to be necessary to reach the desired potency. As the halide is more electronegative than carbon atoms, replacing the hydrogen atom by the fluorine atom is causing an inversion of the polarity of the bond. This could potentially be responsible for the loss of potency observed due to the absence of the weak hydrogen bond previously proposed to exist with Pro371. Given that fluorine is slightly larger than the hydrogen,¹²¹ the loss of potency could also be due to a subtle change of conformation of the molecule to accommodate the larger fluorine atom in the bromodomain. The hypothesis of the steric hindrance of the pseudo-*ortho* position

substituent (H < F < Me) reducing the potency by causing an increasing strain of the molecule in the protein correlates with the potency trend observed **7.03** > **7.27** > **7.29**. In conclusion, in accordance with the design hypothesis, blocking the 3-position of the heteroaryl of molecule **7.03** with a nitrogen atom successfully enabled the reduction of human liver microsome *in vitro* clearance in several analogues. However, this was associated with a small to moderate loss of Brd4 BD1 potency, compared to the progenitor compound. Addition of a methyl group at selected positions led to molecules exhibiting high potency (e.g. pyrazole **7.25** or triazole **7.33**), however, introduction of substituents (F, Me) on the carbon in 3-position was not tolerated either in terms of phase I clearance or potency.

7.2.3.2. *Improving the potency of triazole analogues.*

The second approach led to the design and synthesis of molecules **7.37**, **7.39**, **7.41**, **7.43** (Table 23), aiming to understand if an alternative substitution pattern on the 1,2,4-triazole ring with compounds already exhibiting low human liver microsome metabolism could increase the Brd4 BD1 potency.

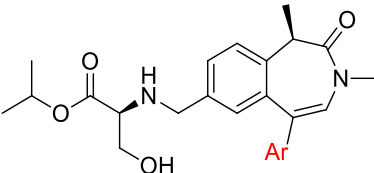
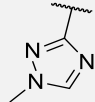
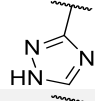
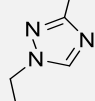
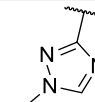
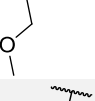
	ChromlogD _{7.4}	Brd4 BD1 pIC ₅₀	HLM IVC (-benzil) (mL/min/g)	
	6.26	2.4	6.5	1.2
	7.37	1.9	6.8	< 0.4
	7.39	2.9	6.1	1.9
	7.41	2.8	6.0	1.3
	7.43	2.2	7.2	< 0.4

Table 23: Data associated with molecules 7.37-7.43, aiming to understand if the potency of the 1,2,4-triazoles could be improved by altering the substitution of the ring, whilst maintaining the low human liver microsome in vitro clearance.

Molecule **7.37** was designed to understand if one NH in position 2 or 4 (Tautomer 2 or 3, Figure 46) could mimic the positive interaction between the CH partial positive charge and the carbonyl of Pro371, described in section 7.1.3. Unfortunately, the difference in potency between molecules **6.26** and **7.37** remains within the limit of error of the assay (± 0.3) and is significantly below the potency exhibited by the pyrazole **7.03** (Table 22). This indicated that 1,2,4-triazoles are inherently less potent than the pyrazole **7.03** or the 1,2,3-triazole **7.33**, as they prove to be unable to replicate the positive electrostatic interaction with Pro371 observed for the most potent analogues **7.03** and **7.33**. This can be explained by calculating, for each tautomeric form, the energy associated with the dihedral angle between the alkene and the heteroaryl for the three possible tautomers (Figure 46).¹¹⁰

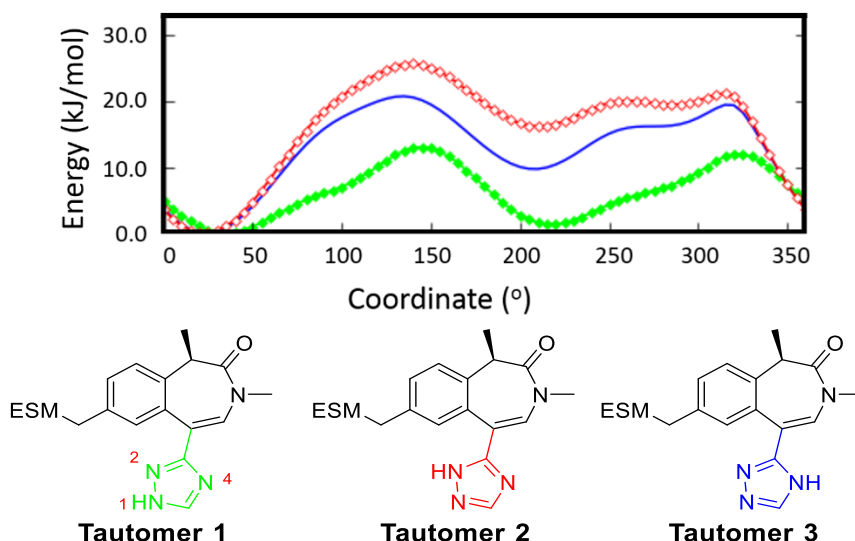


Figure 46: Energy associated with the three tautomers according to the different dihedral angles between the alkene and the 1,2,4 triazole. The energy profile for tautomer 1 is shown in green, tautomer 2 in red and tautomer 3 in blue.¹¹⁰

These calculations were performed by another member of our laboratory and showed two minima for the three tautomers. For tautomer **1**, where the NH is in position 1, there are two unprotonated nitrogen atoms in positions 2 and 4, therefore one nitrogen atom is having a disfavoured electrostatic interaction with the carbonyl of Pro371, thus decreasing the potency of the molecule. The lowest energy minima for tautomers **2** and **3** correspond to a dihedral angle around 30° and are placing the non-protonated nitrogen in the vicinity of Pro371 as drawn in Figure 47. The second conformational energy minima of tautomer 2 and 3 with a dihedral angle around 220° are placing the protonated NH in the vicinity of Pro371, however they are 10 kJ/mol higher for tautomer 3 and approximately 18 kJ/mol higher for tautomer 2 and are therefore less favoured.

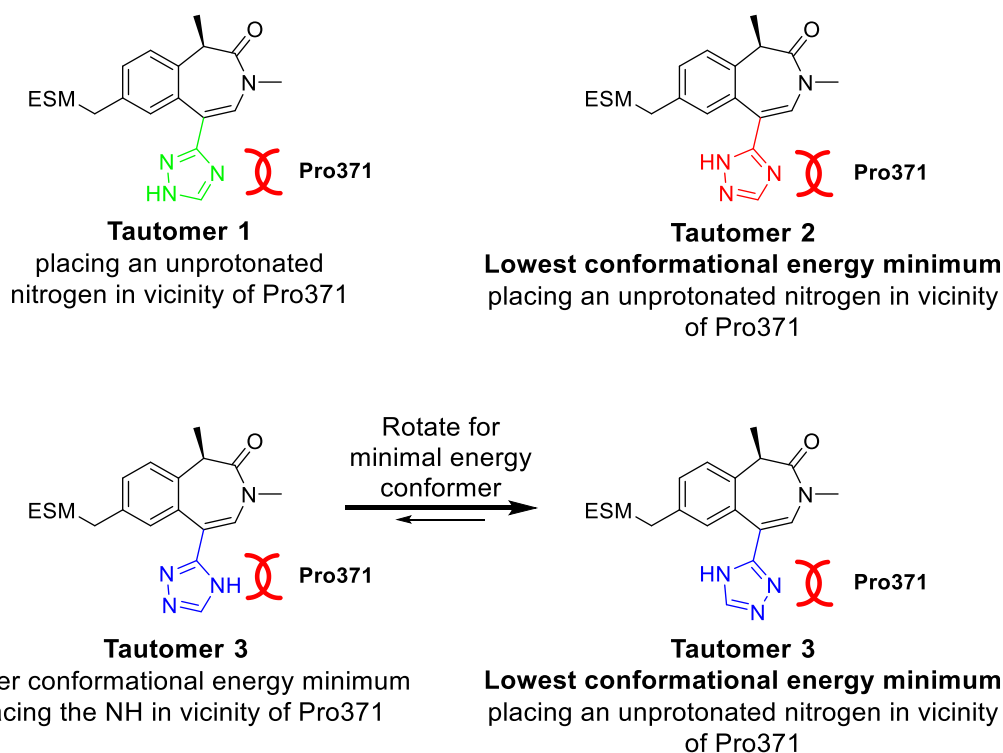
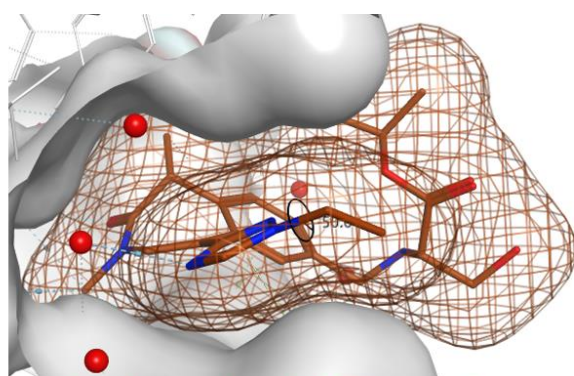
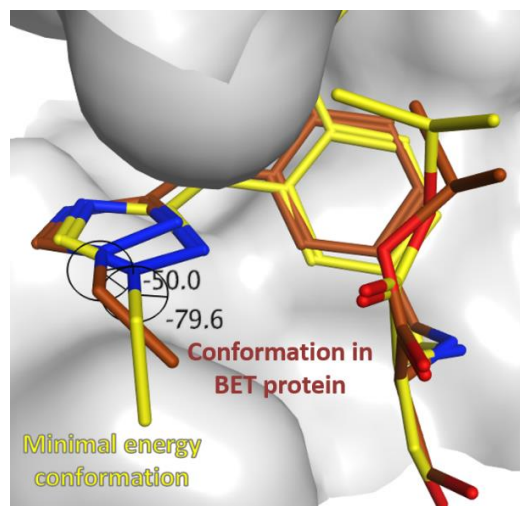
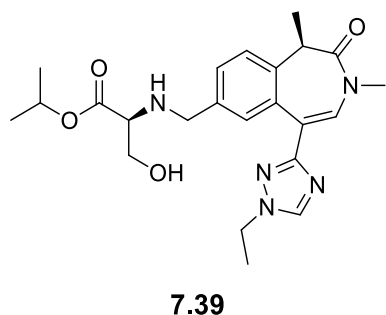


Figure 47: In the calculated minimal conformational energy, the three tautomers of the 1,2,4-triazole are placing an unprotonated nitrogen atom in the vicinity of Pro371, creating a disfavoured electrostatic interaction. This explains why the potency of this heteroaryl is lower than the pyrazole **7.03**.

This means that all three possible tautomers have a minimum conformational energy placing an unprotonated nitrogen atom in the vicinity of Pro371, therefore potentially causing a disfavoured electrostatic interaction with this amino acid residue. This perhaps accounts for why the unsubstituted 1,2,4-triazole of molecule **7.37** is unable to mimic the interaction observed with the very potent pyrazole **7.03** (Brd4 BD1 pIC₅₀ 7.5) and is thus demonstrating moderate potency in the Brd4 BD1 assay (pIC₅₀ 6.8). As a consequence, the substituents of the triazole were altered aiming to improve the potency by enhancing the interaction with the BET protein, as explained in section 7.2.1. Molecules **7.39** and **7.41** (Table 23, p.129) unfortunately showed a significantly reduced affinity for the BET bromodomains. An X-ray crystallographic study of molecule **7.39** (represented in brown) in Brd2 BD2 is shown in Figure 48.



Ligand is in shape complementarity with protein

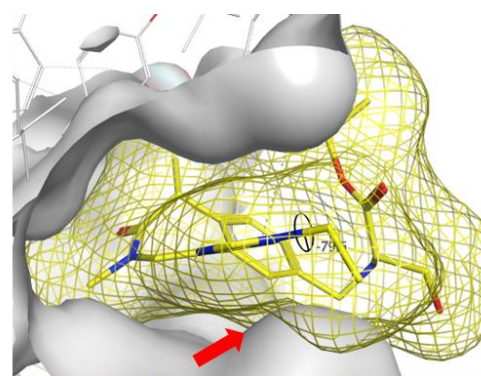
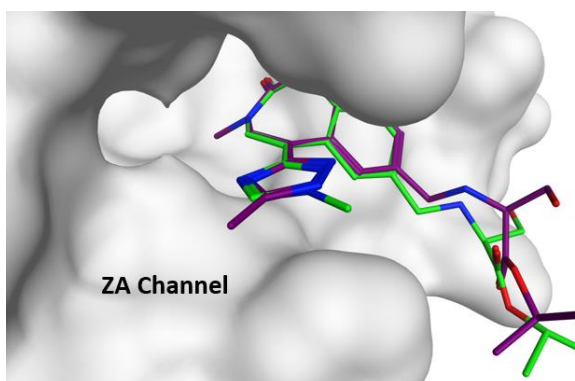


Figure 48: X-ray crystal structure of molecule **7.39** in Brd2 BD2 is shown in brown (PDB file **gsk9vcgg**)¹⁰⁹. The pale grey surface is the surface of the BET bromodomain. The molecule in yellow is the conformation with the minimum energy, calculated by MOE, overlaid with the BET Brd2 BD2 protein surface.

Molecule **7.39** is adopting the conformation shown in brown in order to fit the BET active site. Some analysis carried out by the author showed that by minimizing the energy of the molecule in absence of the BET protein and solvent using MOE software, the molecule adopts its preferred conformation shown in yellow. The overlay of the two structures in Figure 48 showed the main conformational change is the orientation of the ethyl group compared to the triazole ring. The dihedral angle for the brown conformation (i.e. in BET) is 50°, whereas for the minimum energy conformation (in yellow), the dihedral angle is almost 80°. The brown ligand surface suggested a good shape complementarity with the BET protein. Conversely, for the minimum energy

conformation in yellow, the two surfaces of the protein and the ligand are overlapping in the ethyl-triazole area (indicated by the red arrow in Figure 48). This means that to fit the BET protein, the ethyl is forced to adopt a higher energy conformation with a dihedral angle difference of 30° compared to its minimum conformation energy. This strain on the molecule is likely to be causing the loss of potency observed between molecules **6.26** and **7.39** ($\Delta pIC_{50} = 0.5$). The same phenomenon is likely to also cause the loss of potency observed for the extended chain molecule **7.41** ($\Delta pIC_{50} = 0.5$).

Finally, the crystal structure of molecule **6.26** (Figure 49) showed a substituent in position 5 of the triazole would be directed towards the ZA channel, and this observation led to the design of molecule **7.43**, aiming to increase the potency of these molecules.



*Figure 49: X-ray crystal structure of molecules **6.26** (in green) and **7.43** (in purple) in Brd2 BD2 (PDB files *gsk1jmbq* and *gsk5tien*).¹⁰⁹ The methyl substituent of molecule **7.43** is in the ZA channel unlike the methyl substituent of molecule **6.26**. This is responsible for a small increase BET potency of molecule **7.43** compared to molecule **6.26**.*

Pleasingly, molecule **7.43** demonstrated a modest increase in Brd4 BD1 potency, just above the variability of the Brd4 BD1 assay. A crystal structure of molecule **7.43** (Figure 49) showed a similar binding mode in the BET protein as molecule **6.26**, with the methyl substituent occupying the ZA channel. This increased occupancy of the ZA

channel is likely to be responsible for the small increase in potency measured for molecule **7.43**.

In summary, all the 1,2,4-triazoles synthesized pleasingly exhibited a low human liver microsome *in vitro* clearance. This validated the design hypothesis that by blocking the two metabolic soft spots in pseudo-*ortho* positions to the benzazepinone branching point, the human liver microsome *in vitro* clearance can be reduced. Molecule **7.37** showed a similar potency to molecule **6.26**, despite the loss of the methyl in the 1-position. The loss of the methyl provided a molecule with a lower lipophilicity translating into very low human liver microsomal clearance. Substitution in the 1-position of the ring system with a methyl was tolerated in molecule **6.26**, however larger sp^3 substituents were not tolerated and caused a loss in potency (molecules **7.39** and **7.41**). A sp or sp^2 substituent maintaining a flat angle with the 1,2,4-triazole could potentially be tolerated in the BET protein. The introduction of substituents in the pseudo-*ortho* position to the benzazepinone has proven to negatively impact the potency, as explained in section 7.2.3, and were not attempted within the 1,2,4-triazole series. Finally, substitution at the 5-position with a methyl, molecule **7.43**, showed a modest but significant increase in Brd4 BD1 potency compared to molecule **6.26** due to partial occupancy of the ZA channel. Pleasingly, this molecule also retained a very low human liver microsome clearance.

7.2.3.3. Data for the selected *iPr-L-allo-threonine* analogues.

The data associated with the selection of *iPr-L-allo-threonine* analogues is shown in Table 24, along with their corresponding *L-serine* analogues for comparison.

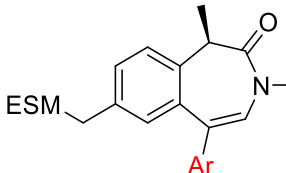
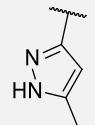
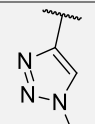
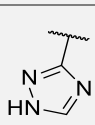
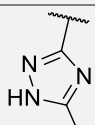
	ESM	ChromlogD _{7.4}	Brd4 BD1 pIC ₅₀ / hWB pIC ₅₀	HLM IVC (-benzil) (mL/min/g)
	<i>iPr-L-serine</i> 7.25	3.2	7.4 / 8.5	3.0
	<i>iPr-L-allo-threonine</i> 7.26	3.5	7.3 / 7.8	4.9
	<i>iPr-L-serine</i> 7.35	2.6	6.9 / 7.8	0.8
	<i>iPr-L-allo-threonine</i> 7.36	3.0	6.8 / 7.6	2.3
	<i>iPr-L-serine</i> 7.37	1.9	6.8 / 7.2	< 0.4
	<i>iPr-L-allo-threonine</i> 7.38	2.4	6.7 / 7.2	0.7
	<i>iPr-L-serine</i> 7.43	2.2	7.2 / 7.6	< 0.4
	<i>iPr-L-allo-threonine</i> 7.44	2.5	6.9 / 7.3	0.5

Table 24: Comparison of *L-serine* and *L-allo-threonine* direct analogues for a small selection of compounds. Due to a slightly higher chromlogD_{7.4}, only the molecules within the desired lipophilicity range were synthesized and profiled.

The *iPr-L-allo-threonine* analogues demonstrated similar Brd4 BD1 potency to their corresponding *iPr-L-serine* analogues, and the majority of the molecules showed a human whole blood potency above the 7.6 desired threshold. The *iPr-L-allo-threonine* molecules exhibited a slightly higher lipophilicity than the direct serine analogues as expected by the addition of a methyl substituent. This increased lipophilicity in general correlated with an increased human liver microsome *in vitro* clearance. However, with the exception of molecule **7.26**, all molecules remained under the *in vitro* clearance threshold defined at the outset of this work. As molecule **7.26** exhibited a chromlogD_{7.4} above the upper limit defined, this translated into a high human liver microsome *in vitro* clearance. Based on these initial *in vitro* clearance results, these molecules, with the exception of molecule **7.26**, were further profiled in the hepatocyte *in vitro* clearance assay.

7.2.3.4. *Extended profile of the molecules showing low in vitro clearance and good potency and selection of the molecules for in vivo studies.*

Molecules demonstrating a good Brd4 BD1 potency and a human liver microsome *in vitro* clearance < 3 mL/min/g, were further profiled in the hepatocyte *in vitro* clearance assays (human and cynomolgus monkey). The data associated with these analogues is shown in Table 25.

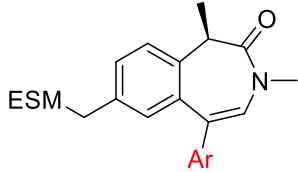
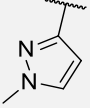
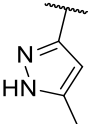
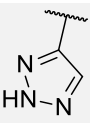
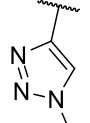
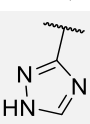
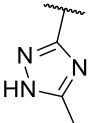
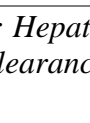
	ESM	ChromlogD _{7.4}	HLM IVC (-benzil) (mL/min/g)	hWB pIC ₅₀	Heps IVC (LBF) Cyno / Human
	<i>iPr-L-serine 7.23</i>	3.2	2.4	7.9	- / 96%
	<i>iPr-L-serine 7.25</i>	3.2	3.0	8.3	93% / 92%
	<i>iPr-L-serine 7.31</i>	2.3	2.4	7.0	87% / 84%
	<i>iPr-L-serine 7.35</i>	2.6	0.8	7.8	81% / 91%
	<i>iPr-L-allo-threonine 7.36</i>	3.0	2.3	7.6	74% / -
	<i>iPr-L-serine 7.37</i>	1.9	< 0.4	7.2	66% / 64%
	<i>iPr-L-allo-threonine 7.38</i>	2.4	0.7	7.2	38% / 49%
	<i>iPr-L-serine 7.43</i>	2.2	< 0.4	7.6	< 38% / 58%
	<i>iPr-L-allo-threonine 7.44</i>	2.5	0.5	7.3	38% / 64%

Table 25: Hepatocyte in vitro clearance data for the molecules demonstrating high potency (hWB pIC₅₀ >7.0) and human liver microsome in vitro clearance < 3.0 mL/min/g.⁴⁰

The molecules, selected based on a human liver microsome *in vitro* clearance under 3 mL/min/g, showed a broad range of values in the hepatocyte *in vitro* clearance assays (cynomolgus monkey and/or human hepatocytes). Some molecules, like the 1,2,3-triazole **7.35**, exhibited a very high human hepatocyte *in vitro* clearance which is likely to indicate a significant degree of phase II metabolism for this compound. Conversely the analogues with a 1,2,4-triazole, such as molecule **7.38**, have shown moderate to low hepatocyte *in vitro* clearance values for the two species. Two matched pairs, molecules **7.35** and **7.36** and molecules **7.37** and **7.38**, exhibited lower hepatocyte *in vitro* clearance for the *L-allo*-threonine than for the *L*-serine, despite an increase in lipophilicity ($\Delta\text{ChromlogD}_{7.4}$ 0.4 and 0.5, respectively). This suggests that increasing steric hindrance at the serine hydroxyl is decreasing metabolism. This is in accordance with the literature, where several examples of increased steric hindrance have correlated with decreased phase II metabolism, due to inhibiting glucuronide conjugation reactions.¹⁰⁸ Unfortunately, the molecules with the lowest *in vitro* hepatocyte clearance profile also showed a human whole blood potency slightly under the desired value.

In summary, the extensive investigation of potency and metabolism detailed in this chapter enabled the discovery of three new ESM-BET inhibitors, molecules **7.38**, **7.43** and **7.44**, as potential candidates for *in vivo* studies.

7.3. Assessment of the pharmacological profile of the lead molecules

The extended profile of molecules **7.38**, **7.43** and **7.44** is shown in Table 26, along with the initial lead molecule **6.26** and desired profile as determined at the outset of this work.

	6.26	7.38	7.43	7.44	Desired profile
ESM	<i>iPr-L-serine</i>	<i>iPr-L-allo-threonine</i>	<i>iPr-L-serine</i>	<i>iPr-L-allo-threonine</i>	-
hWB pIC ₅₀	7.3	7.2	7.6	7.3	≥ 7.6
hWB Δ <i>t</i> Bu	+ 1.3	+ 1.1	+ 1.5	+ 1.2	~ + 1.0
Brd4 BD1 pIC ₅₀	6.5	6.7	7.2	6.9	≥ 7.0
ChromlogD _{7.4}	2.4	2.4	2.2	2.5	≤ 3.3
AMP (nm/sec) / tPSA	136 / 110	84 / 120	42 / 120	81 / 120	≥ 50 / ≤ 125
Heps IVC Human (LBF)	60%	49%	58%	64%	≤ 60%
Heps IVC Cyno (LBF)	55%	< 38%	< 38%	38%	≤ 60%
CES-2 t _{1/2} (min)	> 139 min	> 139 min	> 139 min	> 139 min	> 139 min
Early estimated dose ¹²²	164 mg	113 mg	126 mg	130 mg	≤ 100 mg

Table 26: Profiles of the three lead molecules designed, synthesized and profiled within this project scope.

All four molecules which displayed a cynomolgus monkey hepatocytes *in vitro* clearance in the desired range contained a 1,2,4-triazole motif. This ring was

unfortunately associated with lower BET BD1 affinity as explained in section 7.1.3. This modest BD1 potency did, however, translate into an acceptable human whole blood potency, slightly under the targeted value of 7.6. Pleasingly, molecule **7.43** reached the targeted potency value, due to a marginally higher BD1 potency.

Despite the fact the three new lead molecules **7.38**, **7.43**, and **7.44** did not demonstrate significantly higher whole blood potency than the early lead molecule **6.26**, the three optimised molecules resulted into a lower human early predicted dose.^{xxii} This early dose estimation was calculated by modelling the bioavailability of each compound. The model used *in vitro* parameters such as the human whole blood potency and hepatocyte clearance. The model was built by another member of our laboratory, assuming a rapid oral absorption and an *in vivo* clearance which would mainly be liver-mediated and correlating with the *in vitro* clearance data.¹²² This evaluation of the full profile of these advanced lead molecules resulted in halting the progression of molecule **6.26**, as it was associated with a significantly higher estimated dose than for the three emerging lead molecules.

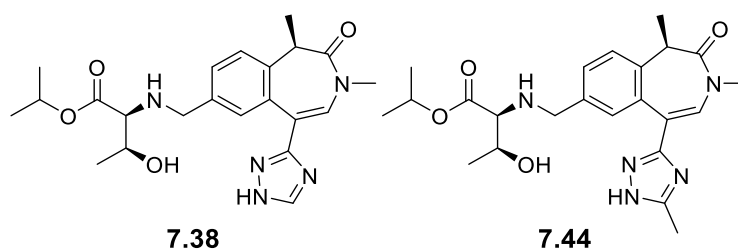
The evaluation of the broader pharmacological profile of molecules **7.38**, **7.43**, and **7.44** led to identification of a high risk of potential drug-drug interactions for molecule **7.43**, due to a significant time-dependent inhibition of cytochrome P450 3A4 at the proposed dose.¹²³ Drug-drug interactions are associated with adverse drug reactions and reduced efficacy.^{124,125} Such interactions are of particular concern in poly-therapy, which is common with elderly population, and therefore of particular relevance for the

^{xxii} Early estimated dose of active pharmaceutical ingredient for an oral administration, once daily.

development of a drug for the treatment of chronic rheumatoid arthritis. Due to this potential risk, molecule **7.43** was not selected for *in vivo* studies.

Therefore, the early estimated dose and the potential risk of drug-drug interactions stopped the progression of two of the four lead molecules, molecules **6.26** and **7.43**, discovered during the work described in this thesis. This demonstrates the importance of understanding the full pharmacological profile of potential drug candidates and the complexity of reaching the desired profile ahead of clinical studies. Molecules **7.38** and **7.44**, demonstrating the best pharmacological profiles for this series, were therefore selected for *in vivo* pharmacokinetic studies.

According to FDA regulations, a rodent and a non-rodent species must be used in pre-clinical studies so both molecules were first evaluated in rat.¹²⁶ The *in vivo* rodent pharmacokinetic results are summarized in Table 27.



Pharmacokinetic parameters	Molecule 7.38	Molecule 7.44
F (%)	69	29
<i>in vivo</i> clearance (LBF)	> 100%	> 100%
Volume (L/Kg)	9.2	9.5
t_{1/2} (h, oral)	2.8	2.2
t_{1/2} (h, i.v.)	0.2	0.2
AUC_{0-∞} (ng.h/mL, oral)	209	83
C_{max} (ng/mL, oral)	103	112
AUC_{0-∞} (ng.h/mL, i.v.)	31	31
C_{max} (ng/mL, i.v.)	40	36

Table 27: Results of the rat *in vivo* pharmacokinetic studies for molecules **7.38** and **7.44**.¹²⁷

Pleasingly, both molecules exhibited good to excellent bioavailability in rat. The modest half-life of the compounds in this species was attributed to the high number of esterases present in the blood and was expected due to the ESM-targeting mechanism.¹²⁸ In addition, significant levels of renal clearance were observed for both molecules, which contributed to the *in vivo* clearance being greater than the liver blood flow. Following on this promising initial rodent pharmacokinetic data, the molecules were scaled up in order to supply material for downstream *in vivo* evaluation in higher animal species.

8. Synthetic chemistry route optimisation of molecules 7.38 and 7.44

Due to the significant level of interest in the pharmacological profile of molecules **7.38** and **7.44** (Figure 50), their synthetic route was reinvestigated aiming to establish a stereoselective synthesis, avoiding chiral chromatography, and providing the material in sufficient quantity and purity for the future monkey PK experiments.

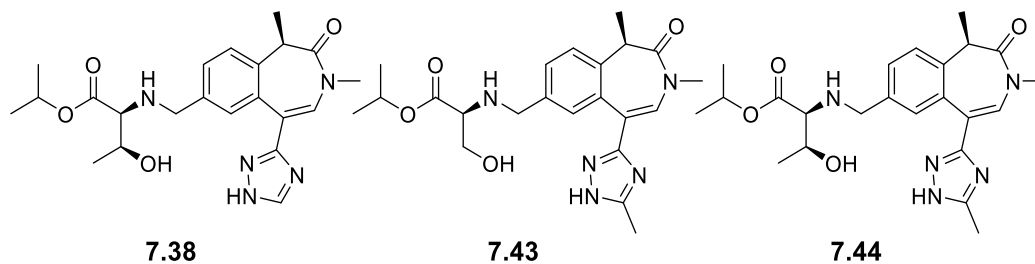
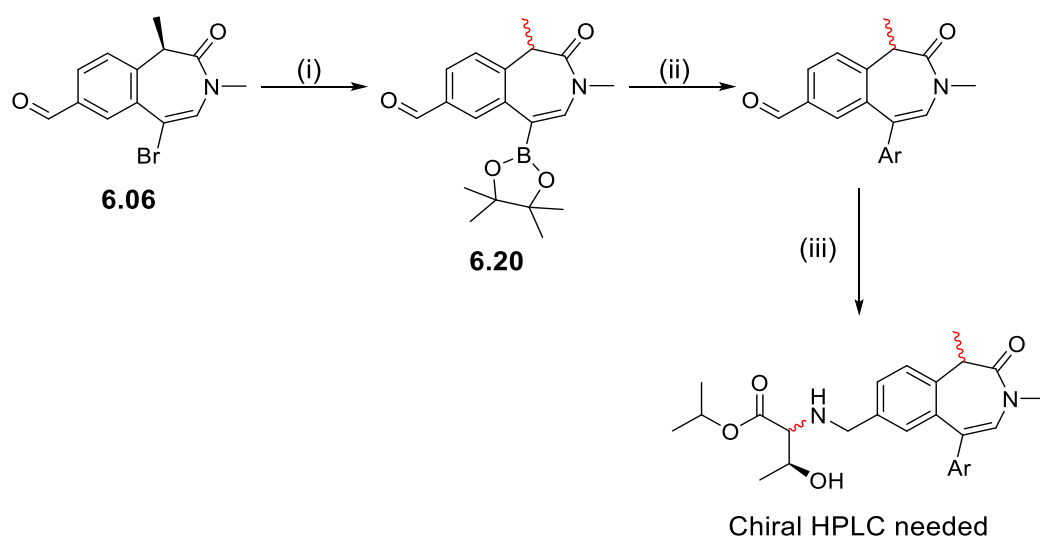


Figure 50: Structures of molecules **7.38**, **7.43** and **7.44**. The synthetic route was optimised for molecule **7.38**, and the optimised route was then applied to molecules **7.43** and **7.44**.

The majority of final molecules synthesized to understand the SAR of the series, including molecule **7.38**, had to be purified by chiral chromatography. Indeed, the presence of approximately 10% diastereomeric impurities was a recurring issue in our series. Some diastereomeric mixtures were successfully separated by normal or reverse phase achiral chromatography, however in certain cases, chiral chromatography was required to isolate the desired product. In addition, diastereomeric separation to isolate molecule **7.44** was unsuccessful despite an extensive screen of chiral chromatography conditions.¹²⁹ Therefore, a synthetic route without any racemisation was required to progress this molecule further. Investigation into the SAR synthetic route within our laboratories led to the identification of two separate issues (Scheme 27).¹³⁰ The enantiomeric excess of the aldehyde intermediate **6.06** was confirmed by chiral HPLC as greater than 99% with the racemic counterpart used as standard (Scheme 27). The same analysis was carried out on the pinacol boronic ester **6.20** and the cross-coupling

product. The chiral HPLC analysis performed showed between 5-10% of racemisation occurred during these two steps. The reductive amination conditions were investigated in the same fashion and demonstrated up to 30% racemisation at the carbon in the α -position of the amino acid moiety. The racemisation of this chiral centre was observed in our laboratories when employing either set of conditions shown below. This led to final products being complex mixtures of diastereomers requiring extensive purification to isolate the desired molecule.



- (i) B_2pin_2 , KOAc, $PdCl_2(dppf)$, 1,4-dioxane, 95 °C, 67%, **~ 5% racemisation**
(ii) Ar-Br, XPhos Pd G2, XPhos, 2 M aq. K_3PO_4 , *i*PrOH, 31-98%, **~ 5-10% racemisation**
(iii) **Conditions A:**
1) ESM (1.5 eq), DIPEA (2 eq), AcOH (2.5 eq), THF, 40 °C.
2) $NaBH(OAc)_3$ (2.5-3 eq), rt, **~5-15% racemisation**
Conditions B:
ESM (1.5 eq), picoline borane (1.2 eq), AcOH, *i*PrOH, rt, **~10-30% racemisation**

Scheme 27: Three of the reaction steps are responsible for partial racemisation of two chiral centres in the molecules.

8.1. Partial racemisation mitigation strategy

8.1.1. Hypothesis to mitigate the racemisation of the benzazepinone chiral centre

The racemisation of the benzazepinone chiral centre is due to a partial deprotonation of the CH in the α -position of the amide carbonyl of aldehyde **6.06** (shown in red in Figure 51) during the borylation and cross-coupling reactions.

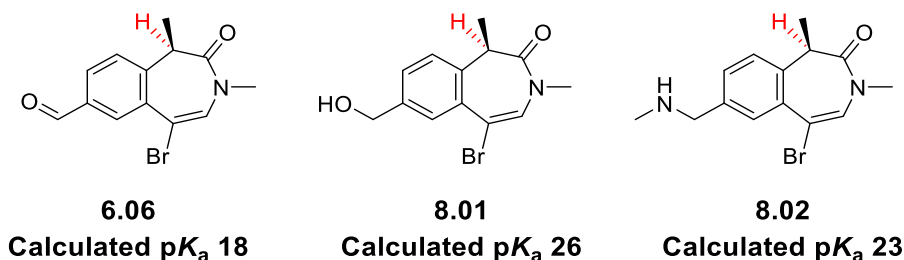
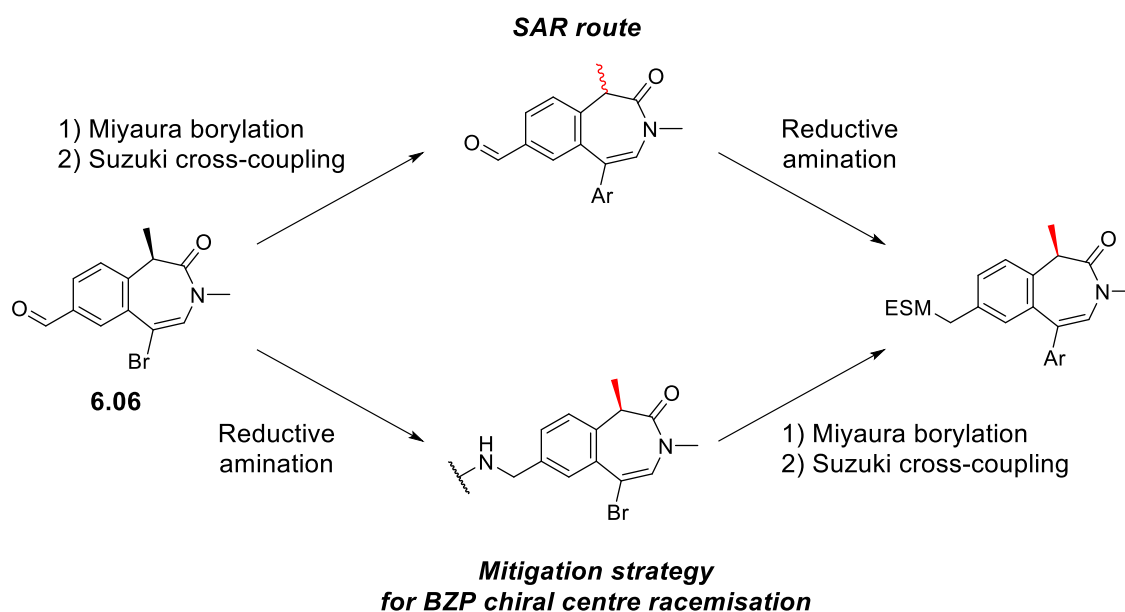


Figure 51: Calculated pK_a using the commercially available software Jaguar.^{131,132}

The acidity of this hydrogen is increased by the presence of the electron-withdrawing group in the *para* position (calculated pK_a 18).¹³¹ Therefore, it was proposed that having the corresponding benzylic alcohol in the *para* position would increase the pK_a of this CH (molecule **8.01** calculated pK_a 26).¹³¹ The higher pK_a should decrease the level of racemisation of the benzazepinone chiral centre observed during the borylation and cross-coupling. An alternative to this would be to first perform the reductive amination on the bromo-aldehyde **6.06** (Scheme 28). The aldehyde would thus be replaced by a benzylic amine, resulting in a decreased acidity of the proton in the α -position of the amide (calculated pK_a for molecule **8.02** is 23)¹³¹ compared to the aldehyde **6.06** and thus should decrease the potential for racemisation. This second hypothesis was investigated as part of this thesis.



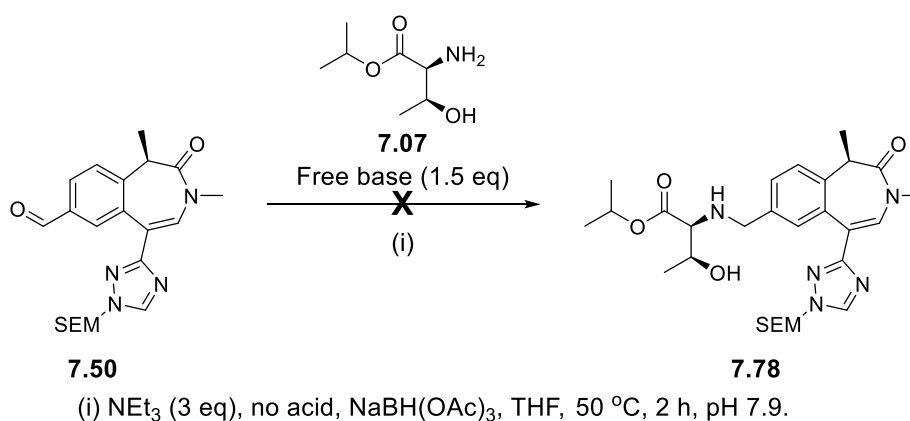
Scheme 28: Mitigation strategy for the partial racemisation of the benzazepinone chiral centre.

8.1.2. Hypothesis to mitigate the racemisation of the α -position of the amino ester

After identification of the partial racemisation during the reductive amination step, an analysis of the reaction conditions was performed. The two sets of conditions used in our laboratories were: **conditions A** [$\text{NaBH}(\text{OAc})_3$, DIPEA (2 eq.), AcOH (2.5 eq.)] and **conditions B** [picoline borane, AcOH: *i*PrOH (1:10 v/v)]. Both sets of conditions contained acetic acid, however conditions **B** had a substantially higher amount of acetic acid than conditions **A**, and conditions **B** were also associated with substantially higher level of racemisation at the amino ester. This was particularly noticeable for longer reaction times (~20 h) when the reductive amination was left overnight under conditions **B**. The key role of acetic acid in the racemisation of amino ester motif through the formation of imine intermediates is supported by literature evidence.^{133,134,135,136} However, acetic acid is still described as the additive of choice to increase the rate of the imine intermediate formation with amino acid motifs.¹³⁷ This

is associated with loss of enantiomeric excess and the need to separate the mixture of diastereomers obtained with these reaction conditions.^{137,138}

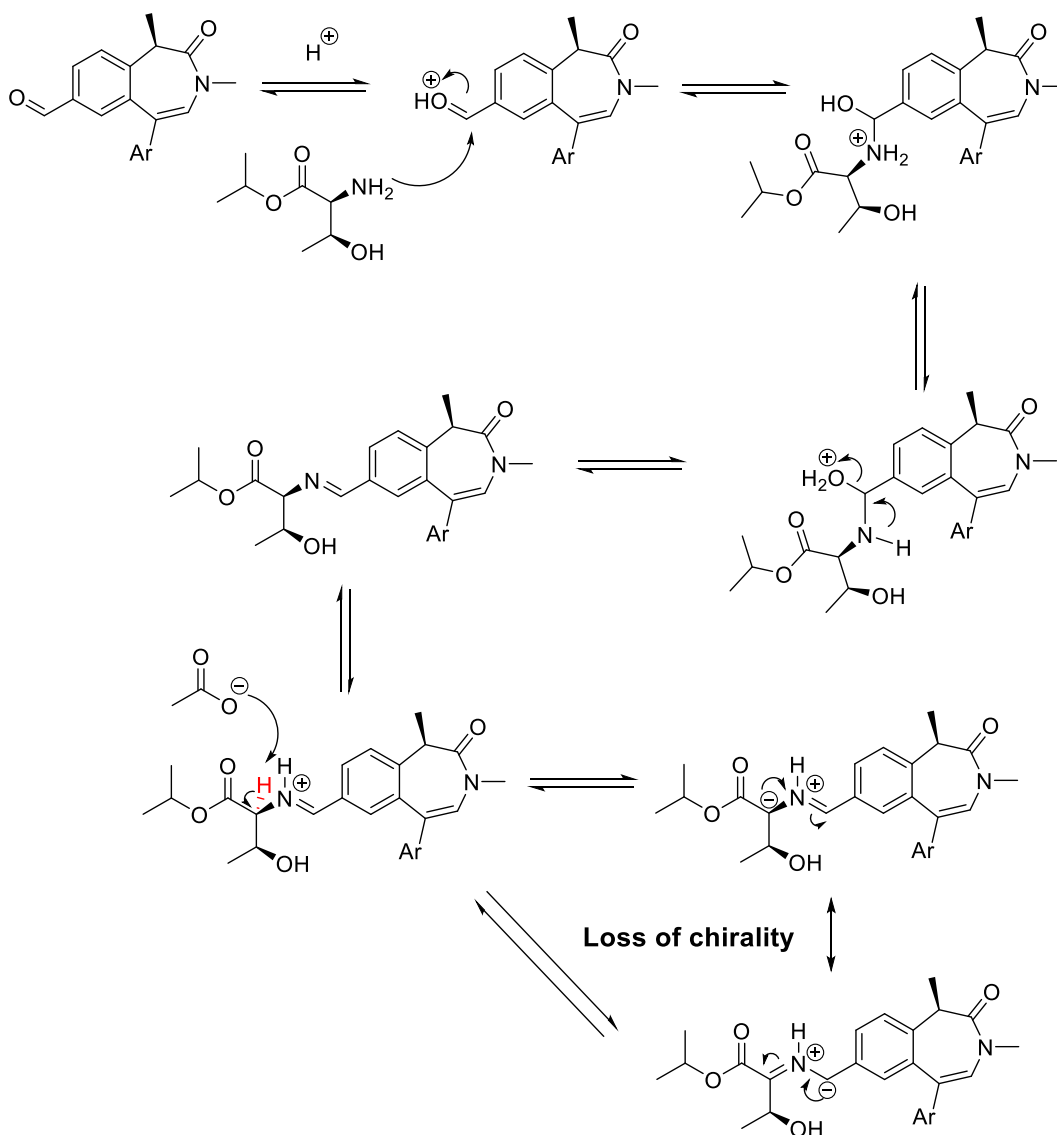
In this context, a reductive amination with the benzazepinone aldehyde of interest with triethylamine and the free base amino ester but without an acid additive was attempted (Scheme 29). After two hours, no imine formation was observed by HPLC.^{xxiii}



Scheme 29: Reductive amination attempt in absence of acid catalysis.

This confirmed the use of an additive was needed to favour the imine formation on the substrate of interest. The literature suggests racemisation in the α -position of the amino ester motif occurs after formation of the imine, by protonation of the imine followed by extraction of the proton in the α -position of the amino ester by the acetate counter anion (Scheme 30).^{133,135}

^{xxiii} The imine formation was monitored by HPLC before addition of the reducing agent.



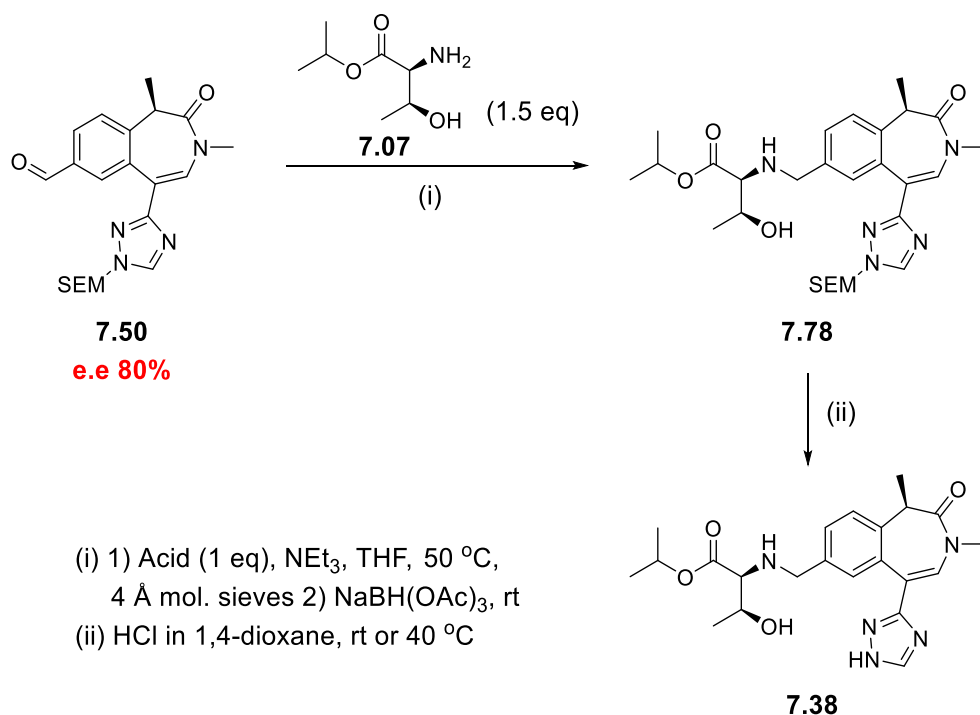
Scheme 30: Mechanism for imine formation and loss of chiral integrity of the amino ester motif.^{133,135}

Based on this mechanism, using a less basic counter-ion than acetate should minimise the racemisation, by preventing the deprotonation steps. A stronger acid should also be able to provide the required catalysis for the imine formation. For the current study, a range of less basic counter ions was therefore investigated. In addition to reducing the level of racemisation, attention will be given to increasing the reaction yield. This will be detailed in the next section.

8.2. Optimisation of the reductive amination step

8.2.1. Counter-ion investigation

To reduce the level of racemisation observed during the reductive amination in the presence of acetic acid, a range of less basic anions were selected. TFA (pK_a -0.3) and tosic acid (PTSA, pK_a -2.8) are stronger acids than acetic acid (pK_a 4.8) and therefore the corresponding weaker counter ions should be unable to deprotonate the proton in the α -position of the amino ester. This should ensure no racemisation occurs at this chiral centre during the reductive amination. In addition, pyridinium *para*-toluenesulfonic acid (PPTS, pK_a 6.0) was included in the screen to understand the effect of the pH on the reductive amination reaction outcome. Finally, hydrochloric acid (pK_a -2.2) was also investigated as the amino ester building blocks in our laboratories are often available as HCl or tosic acid salts. The reactions were performed in parallel with 1.5 equivalents of amino ester and three equivalents of triethylamine in THF at 50 °C, with activated molecular sieves and one equivalent of the acid. The pH range of the reaction mixture varied from 8.4 to 6.6 due to the addition of only one equivalent of acid for each reaction. The sodium triacetoxyborohydride was added at room temperature after the imine formation time shown in Table 28, and the results of the acid and pH screen are also shown in Table 28. At the time, the counter-ion screen was carried out on a batch of aldehyde **7.50** having an enantiomeric excess of 80% as the chiral integrity of the bromo-aldehyde **6.06** was still being confirmed at this stage.



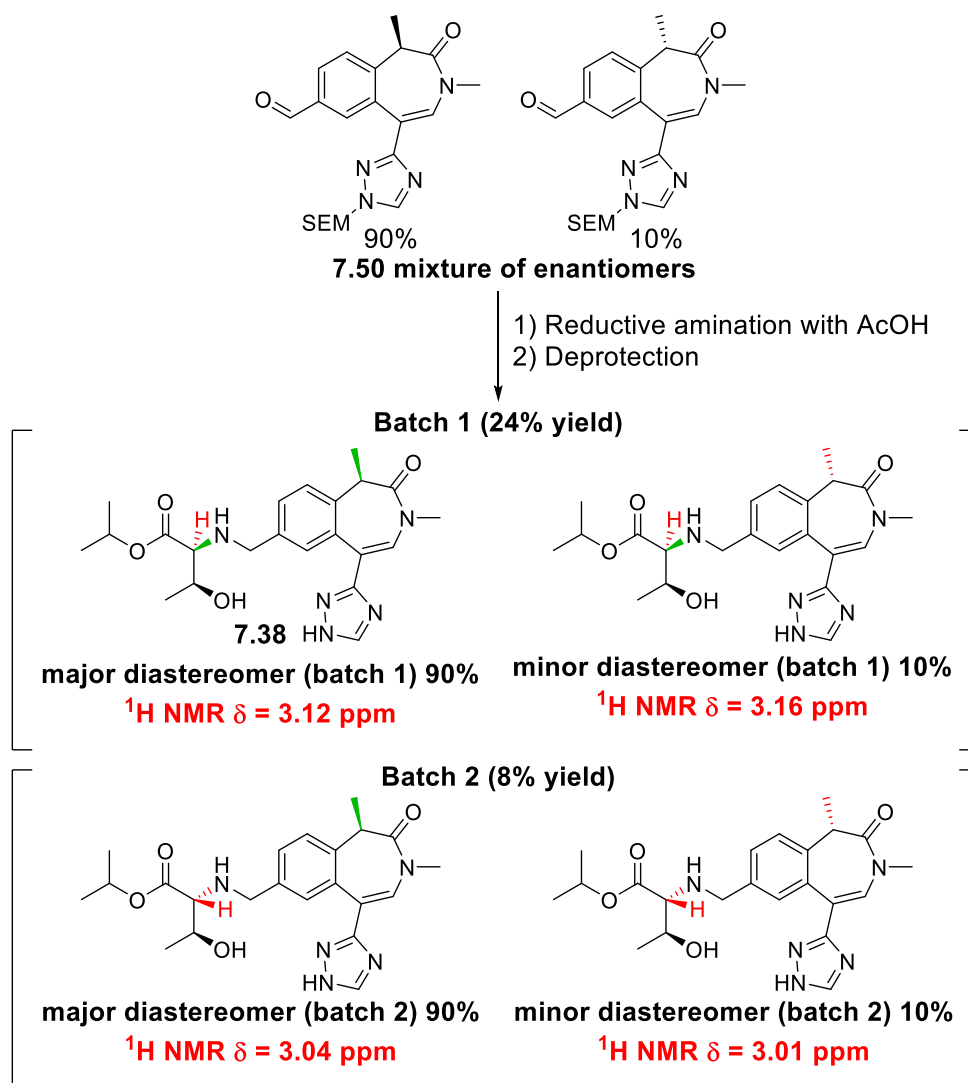
Entry	Acid	pH	Imine formation time	Yield over two steps	d.e. of molecule 7.38 (by ¹ H NMR)
1	PPTS	8.4	19 h	33%	80%
2	AcOH	7.9	19 h	24% + 8% of a different diastereomeric mixture	80%
3	HCl	7.6	24 h	15%	80%
4	PTSA	7.2	19 h	41%	80%
5	TFA	6.6	19 h	49%	80%

Table 28: Acid and pH investigations for optimisation of the reductive amination step. The d.e. was determined by ¹H NMR at the benzylic CH₂ doublet at 3.62 ppm (major diastereomer) and 3.64 ppm (minor diastereomer).

The imine was left to form between 19 h and 24 h and monitored by HPLC. After 19 h, all reactions showed presence of the imine and the reducing agent was added to the reaction mixture at room temperature. Following reduction of the imine, the triazole was deprotected using HCl in 1,4-dioxane and the diastereomeric excess was measured by ¹H NMR (Doublet at 3.62 ppm (major diastereomer) and 3.64 ppm (minor diastereomer)). At the time of the acid counter-ion screening, the batch of aldehyde

7.50 contained 10% of the undesired (*S*)-enantiomer (at the benzazepinone). The 80% e.e. of aldehyde **7.50** should therefore translate into an 80% d.e. if no racemisation occurred during the reductive amination step. If racemisation occurred in the α -position of the amino ester moiety, a mixture of four diastereomers should be obtained.

Acetic acid was used in a control experiment (entry 2). As explained in section 8.1.2, this led to some racemisation of the chiral centre in the α -position of the amino ester motif (Scheme 31). This was observed by HPLC where two close peaks ($\Delta t_R=0.01$ min on a 2 min method) were observed in the reaction mixture analysis.



Scheme 31: The use of acetic acid during the reductive amination led to partial racemisation of the chiral centre in the α -position of the amino ester (conditions entry 2, Table 28). Two mixtures of diastereomers were separated (24% and 8% yield). Both mixtures showed by NMR the presence of an another diastereomeric impurity in a 9:1 ratio. The proton in the α -position of the amino ester (shown in red) was used to determine the d.e. for the two batches. The chemical shift for this proton is indicated in red.

During the purification, four different diastereomers were obtained in two batches (24% and 8% yields), with batches consisting of a diastereomeric mixture in a 9:1 ratio as shown in Scheme 31. The four diastereomers showed a different chemical shift by $^1\text{H NMR}$ for the proton in the α -position of the amino ester (indicated in red in Scheme 31). This demonstrated that, as expected, acetic acid was not suitable to maintain the chiral integrity of the amino ester motif during the reductive amination.

Pleasingly, for entries 1 and 3-5 (Table 28) using weakly basic counter-ions, no other diastereomers were observed by HPLC or isolated during the purification, and the 80% e.e. starting material translated into an 80% d.e. product as expected. The use of both TFA and PTSA provided better yields after purification, due to a cleaner reaction profile. Finally, it is worth noting that the imine formation was significantly faster for entry 5,^{xxiv} this is likely to be due to the slightly acidic pH which favoured the imine formation.¹³⁹

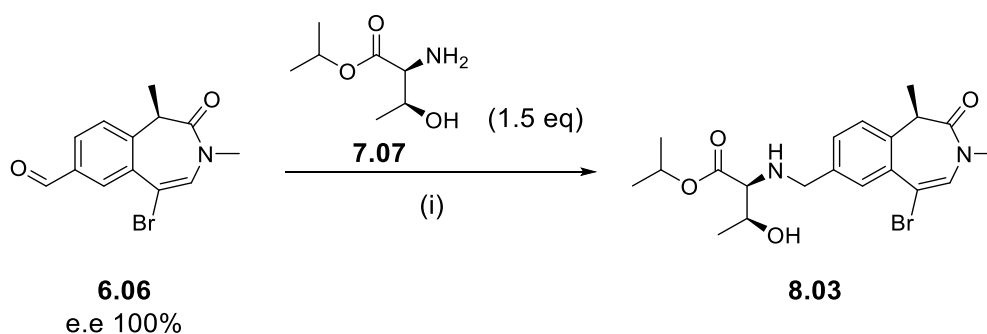
These preliminary results confirmed the key role of acetic acid in the racemisation of the chiral centre in the α -position of the amino ester moiety. This small screening set has also identified several alternative acid additives for reductive aminations which are able to prevent the racemisation of the chiral centre in the α -position of an amine. Amongst these promising acid additives, TFA and PTSA were chosen for further investigation due to their cleaner reaction profile observed by HPLC during this preliminary screen.

8.2.2. Optimisation of the reductive amination conditions

Following from the initial investigations of the counter-ion, the reductive amination with TFA as additive was attempted on aldehyde **6.06** with the *L-allo*-threonine amino ester, according to the mitigation strategy outlined in section 8.1. The optimised reaction conditions are shown in Scheme 32. Compared to entry 5 in Table 28, the

^{xxiv} Monitored by HPLC. Complete conversion was obtained in two hours, but the imine was left to stir at 50 °C overnight for comparison with the other entries and to determine if any racemisation was occurring.

amount of TFA was successfully reduced from one equivalent to a catalytic amount (0.1 eq., 25 μ L of TFA was used for 1 g of aldehyde **6.06**). Reducing the stoichiometric amount of TFA to a catalytic quantity was particularly important for the future scale-up of the target molecule as it reduces the quantities of both additives (acid and base) used to establish the pH of the reaction. The triethylamine was added dropwise until reaching a slightly acidic pH (here pH 5.8), where the reaction was left to proceed at 50 $^{\circ}$ C for 18 h.^{xxv} After formation of the imine, the reducing agent was added to the reaction mixture at room temperature and stirred until the reduction was complete.



(i) 1) TFA (0.1 eq), NEt_3 (added to set pH at 5.8), 4 \AA mol. sieves, THF, 50 $^{\circ}$ C, 18 h. 2) $\text{NaBH}(\text{OAc})_3$, rt, 4 h. 85% yield, 100% d.e.

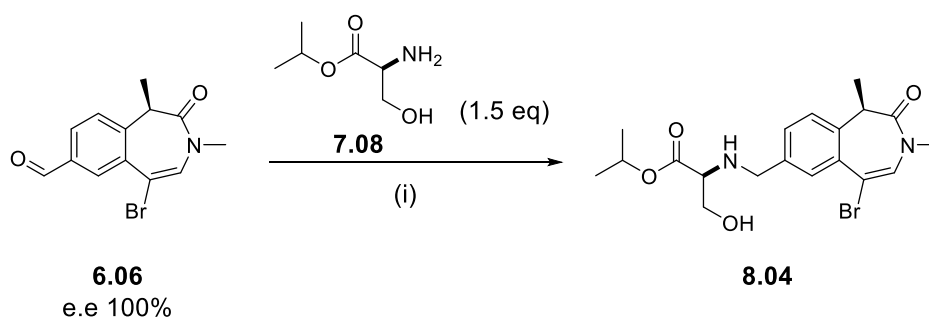
Scheme 32: Optimised reaction conditions with an amino ester and an aldehyde to avoid partial racemisation of the chiral centre in the α -position of the amino ester.

These conditions gave an excellent yield of 85% on a 1 g scale, with a 100% e.e. determined by chiral HPLC. Pleasingly, leaving the imine formation with the new TFA- NEt_3 system gave no racemisation at all, even after 18 h at 50 $^{\circ}$ C, compared to significant levels of racemisation with the AcOH- NEt_3 system. In addition, the imine formation was complete in less than two hours and these new reaction conditions gave

^{xxv} A repeat of this reaction showed the imine formation was complete in 90 min.

significant and reliably higher yields than the previous reaction conditions used to establish the SAR (section 7.1.2).

To understand the versatility of these conditions, and as molecule **7.43** contains a *L*-serine moiety, these conditions were tested with this amino ester, which was found to racemise more rapidly than the *L*-threonine or *L*-allo-threonine when using acetic acid during the imine formation. The results of these trial reactions are shown in Table 29.



(i) 1) TFA, NEt₃ (added to set pH), 4 Å mol. sieves, THF
2) NaBH(OAc)₃, rt

Entry	Amino ester	pH	Imine formation time	TFA (eq.)	T (°C)	Yield	d.e.
1	<i>L</i> -serine	5.9	17 h	1	50	66%	58% ^a
2	<i>D</i> -serine	6.1	2.5 h	1	50	57%	82% ^a
3	<i>L</i> -serine TsOH salt	6.5	20 h	0.05	rt	51%	98% ^a
4	<i>L</i> -serine TsOH salt	5.9	24 h	-	rt	72%	> 90% ^b

^a d.e. was measured by chiral HPLC. ^b d.e. was measured by ¹H NMR, none of the epimeric impurity was observed.

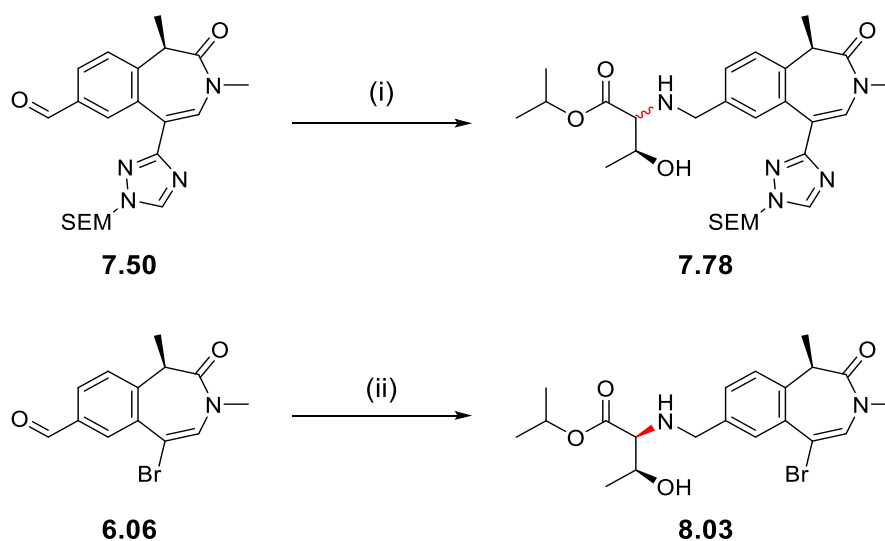
Table 29: Optimisation of the reductive amination with *L*-serine.

The first two reactions were attempted at 50 °C with the TFA-NEt₃ system at a pH around 6.0 (entries 1 and 2). Unfortunately, chiral HPLC analysis confirmed significant racemisation had occurred under these conditions. The diastereomeric excess for entry 1 was significantly lower than for entry 2 where the imine was left to

form for only 2.5 h (compared to 17 h for entry 1). These two examples were thought to be promising as they showed that shorter reaction times for the imine formation or potentially milder reaction conditions could lead to a better d.e. Therefore, a reductive amination at room temperature using the *L*-serine amino ester tosic salt and a catalytic amount of TFA to set the pH was attempted (entry 3). Pleasingly, these milder reaction conditions provided the desired reductive amination product with an excellent d.e. Finally, a reductive amination using the *L*-serine tosic salt was performed in absence of TFA (entry 4). The pH was set within the desired range by dropwise addition of NEt₃ and pleasingly no racemisation was detected by ¹H NMR, confirming PTSA is a suitable alternative additive to TFA for reductive aminations.

To conclude, an acid additive proved to be necessary to react the amino ester motif with our benzazepinone aldehyde. Acetic acid, one of the most commonly used acid catalysts for reductive amination successfully catalysed our imine formation. Unfortunately, it was also associated with partial racemisation of the chiral centre in the α -position of the amino ester moiety. A proposed mechanism from the literature suggested the racemisation was due to the ability of acetate anions to extract the proton in the α -position to the amino ester.^{133,135} A range of less basic counter-ions was investigated and TFA and PTSA were identified as suitable alternatives. These provided stereoselective conditions for reductive amination with the *L*-*allo*-threonine amino ester at 50 °C in presence of a catalytic amount of acid. However, the TFA-NEt₃ system at 50 °C still led to partial racemisation of the less hindered *L*-serine amino ester. This was overcome by decreasing the reaction temperature of the imine formation to room temperature. Finally, these new reaction conditions successfully

provided better yields and shorter reaction times compared to the reductive amination conditions previously used within our laboratory (Scheme 33).



(i) 1) ESM (1.5 eq), DIPEA (2 eq), AcOH (2.5 eq), THF, 40 °C, 1 h.
2) NaBH(OAc)₃, rt, 5 h. **23% yield, 74% d.e.**

(ii) 1) TFA (0.1 eq), NEt₃ (added to set pH at 5.8), 4 Å mol. sieves, THF, 50 °C, 18 h.
2) NaBH(OAc)₃, rt, 4 h. **85% yield, 100% d.e.**

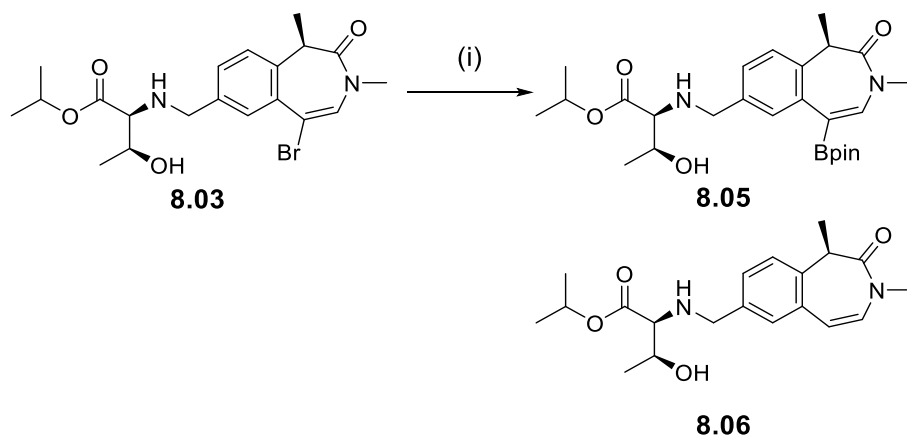
Scheme 33: Comparison of the SAR reductive amination conditions and the optimised reaction conditions, providing better yields and no racemisation

Following these successful results, the bromo-benzazepinone intermediate **8.03** was used in a borylation and Suzuki cross-coupling to install the ZA channel group.

8.3. Final steps towards the synthesis of the lead compounds **7.38** and **7.44**

8.3.1. Borylation and Suzuki cross coupling

With vinyl bromide **8.03** in hand, the borylation was attempted using the previous conditions. Some de-brominated by-product **8.06** was consistently observed during this step, however, drying the KOAc in the *vacuum* oven at 40 °C for 24 h prior to its use decreased the amount of by-product **8.06**.

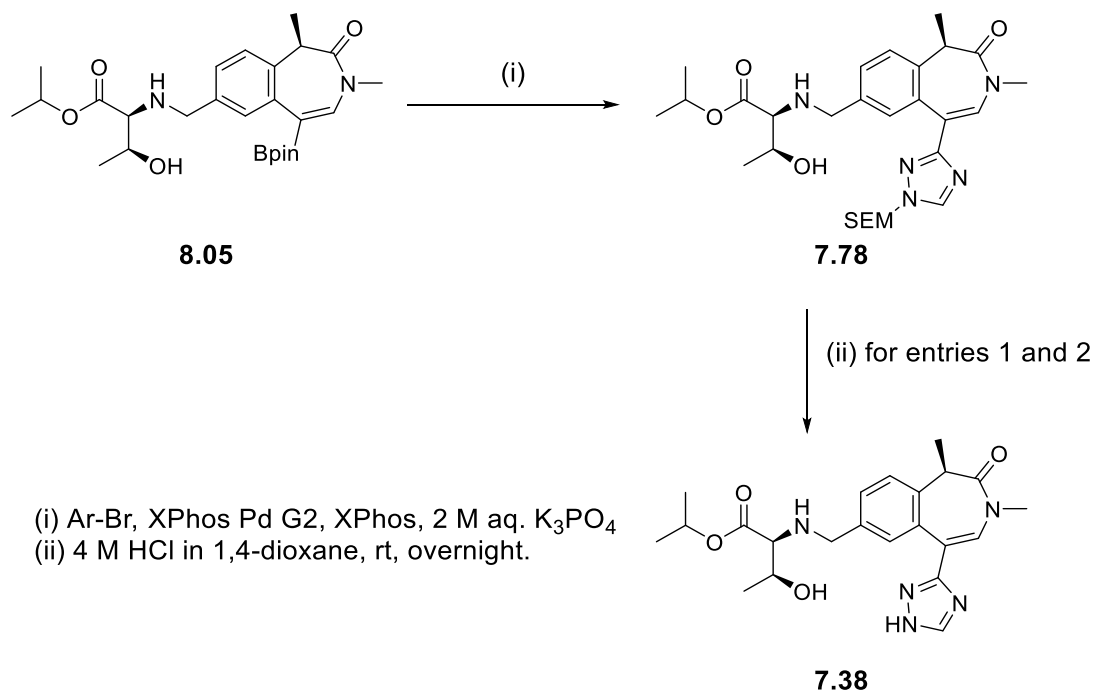


(i) B_2pin_2 , dry KOAc, $PdCl_2(dppf)$.DCM, 1,4-dioxane, 80 °C, 2 h.

Scheme 34: Borylation conditions for the synthesis of intermediate 8.05.

The isolation of the boronic ester **8.05** failed due to its partial degradation during the aqueous work-up. In subsequent reactions, the reaction mixture was filtered through a celite pad, concentrated under reduced pressure and used crude in the Suzuki cross-coupling step. The yields were therefore calculated over these two steps.

The Suzuki cross-coupling conditions used for the SAR route were already showing excellent conversion as determined by HPLC, therefore these conditions were used on the crude boronic ester **8.05** (Scheme 35). 1,4-Dioxane, the solvent used in the borylation step and *i*PrOH, the solvent used previously with the SAR route, were tested for their suitability in the cross-coupling reaction. The reaction was attempted at room temperature, at 70 °C and finally at 120 °C to understand how this parameter could influence the reaction time, and if it could impact the level of racemisation. The results are shown in Table 30.



Scheme 35: Suzuki cross-coupling conditions.

Entry	Solvent	T	Reaction time (h)	Purification	Yield 7.78
1	1,4-dioxane	rt	30 h	MDAP	30%
2	1,4-dioxane	70 °C	24 h	MDAP	35%
3	1,4-dioxane	120 °C	3.5 h	Not recovered from normal phase chromatography eluted with EtOAc in cyclohexane, EtOH in EtOAc	-
4	iPrOH	90 °C	1 h	Two normal phase chromatographies eluted with EtOAc in cyclohexane (+3% NEt ₃)	55%

Table 30: Trial Suzuki cross-coupling conditions.

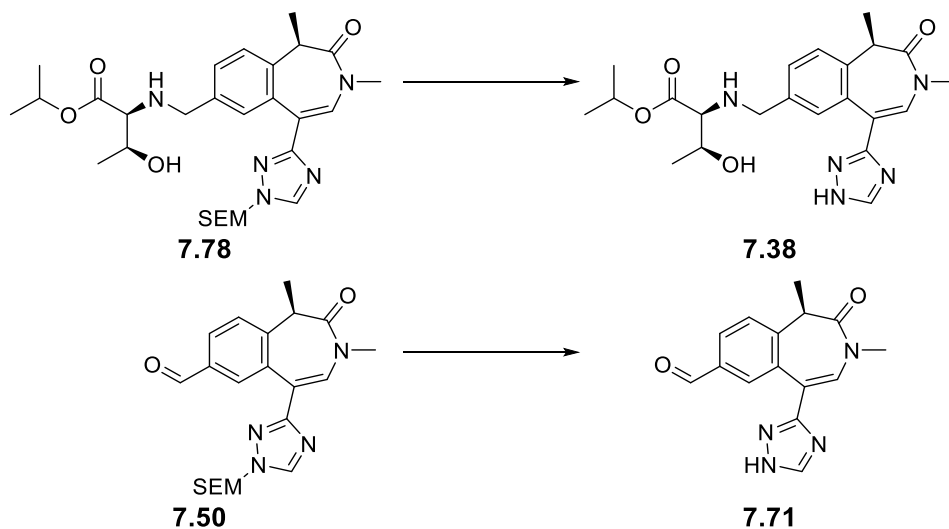
Entries 1 in Table 30 showed the cross-coupling proceeded at room temperature, however a longer reaction time was necessary to reach full conversion of the boronic ester compared to entry 3. The cross-coupling product **7.78** obtained from entries 1 and 2 were deprotected using HCl in 1,4-dioxane to afford molecule **7.38**. Pleasingly,

the e.e. associated with these batches of molecule **7.38** were 99.0% and 99.4%, respectively. This indicated that, as proposed in section 8.1.1, performing the borylation and cross-coupling on substrate **7.78**, bearing a benzylic amino ester instead of an aldehyde (molecule **6.06**), retained the chiral integrity of the molecule. In parallel to the promising enantiomeric excess observed, purification by normal phase chromatography was attempted in entry 3, to replace the MDAP approach which is not a method of choice for multi-gram scale synthesis. Unfortunately, the product was not recovered after the column chromatography. This was overcome by adding 3% of NEt_3 to the cyclohexane to equilibrate the column in entry 4. This prevented the retention of molecule **7.78**, which is basic in nature, on the acidic silica media. The SEM-protected product **7.78** was obtained in 1 h at 90 °C and purified using the normal phase system with NEt_3 additive in 55% yield over two steps.

To summarize, the pinacol boronic ester was found to be unstable to a simple aqueous work up and was therefore used crude in the cross-coupling reaction. Replacing solvent between the borylation step and the Suzuki coupling resulted in a cleaner reaction profile for the cross-coupling product. The Suzuki coupling occurred at room temperature, however, protracted reaction times were required, whereas at 90 °C the reaction was complete in an hour. These two steps were successfully performed on several grams, and provided the desired intermediate with an excellent enantiomeric excess. The SEM-deprotection step will be discussed in the following section.

8.3.2. Deprotection of the 1,2,4-triazole

Throughout the development of this series, several methods have been used to deprotect the 1,2,4-triazole as summarized in Table 31.



Entry	Substrate	Reaction conditions	Purification	Yield
1	7.78	BBr ₃ , 1 M in DCM, -78 °C to rt	<i>MDAP</i>	77% ^a
2	7.78	HCl 4 M in 1,4-dioxane, 40 °C	<i>Reverse phase chromatography and MDAP</i>	57% ^a
3	7.50	HCl 4 M in 1,4-dioxane, 40 °C	<i>Reverse phase chromatography</i>	97% ^a
4	7.78 .HCl	HCl in Et ₂ O and acetone	<i>Filtration</i>	79%

^aThis batch was synthesized following the SAR route and therefore contained 5% of a diastereomeric impurity by ¹H NMR.

Table 31: Deprotection reaction conditions and associated yields.

The deprotection with boron tribromide was very rapid and provided the desired product in 77% yield (entry 1). The protecting group was also very efficiently removed by HCl in 1,4-dioxane at 40 °C either on the amino ester substrate **7.78** (entry 2) or the

aldehyde substrate **7.50** (entry 3). Several attempts to crystallise the material **7.38** obtained using this reaction solvent failed. Finally, as the final product **7.38** is significantly more polar than the SEM-protected triazole **7.78**, a deprotection reaction using HCl in Et₂O was carried out to attempt to precipitate the desired product as the HCl salt upon its formation (entry 4). The material **7.78** (an oil) was dissolved in the minimum amount of acetone and HCl in Et₂O was added. The deprotection reaction was left overnight and a white solid precipitated. After filtration, this provided the desired material **7.38** as the HCl salt in a very good yield of 79%. This material was analysed by microscope¹⁴⁰ and by X-ray powder diffraction.¹⁴¹ When striking a crystalline material, the X-ray beam is diffracted according to a regular pattern based on the crystal lattice structure. When the diffracted beam satisfies Bragg's law (Equation 5), the intensity on the X-ray diffractogram increases for the specific angles 2θ . If the material is amorphous, all intensities are within the same count range.

$$n\lambda = 2d \sin (\theta)$$

Equation 5: Bragg's equation for X-ray diffraction, where λ is the wavelength of the incident X-ray beam, d is the distance between atomic layers in the crystal, θ is the diffracted angle.

Pleasingly, the microscopy and X-ray diffractogram confirmed the HCl salt of molecule **7.38** obtained in these conditions was crystalline (Figure 52).

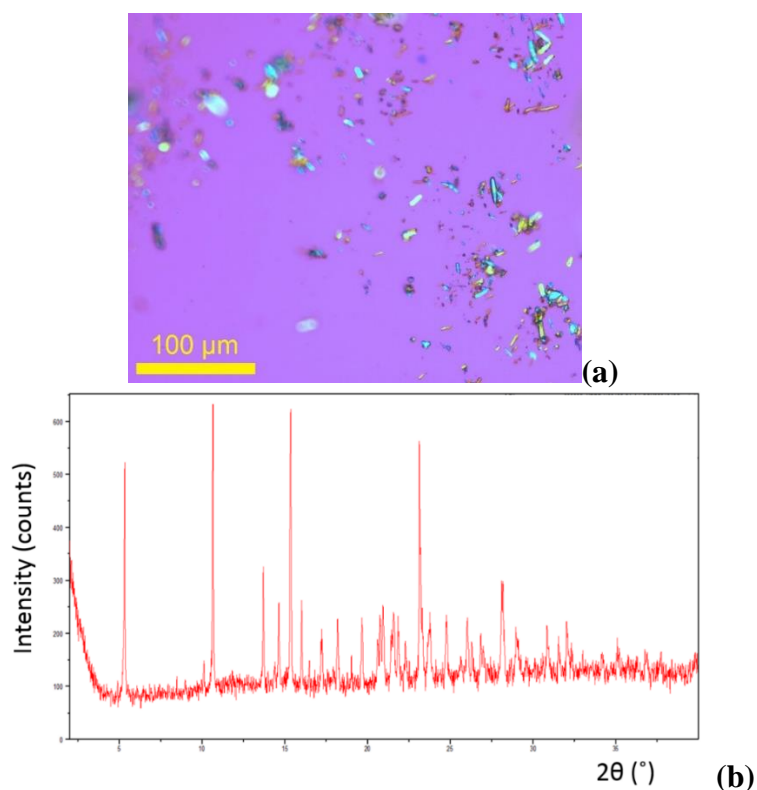
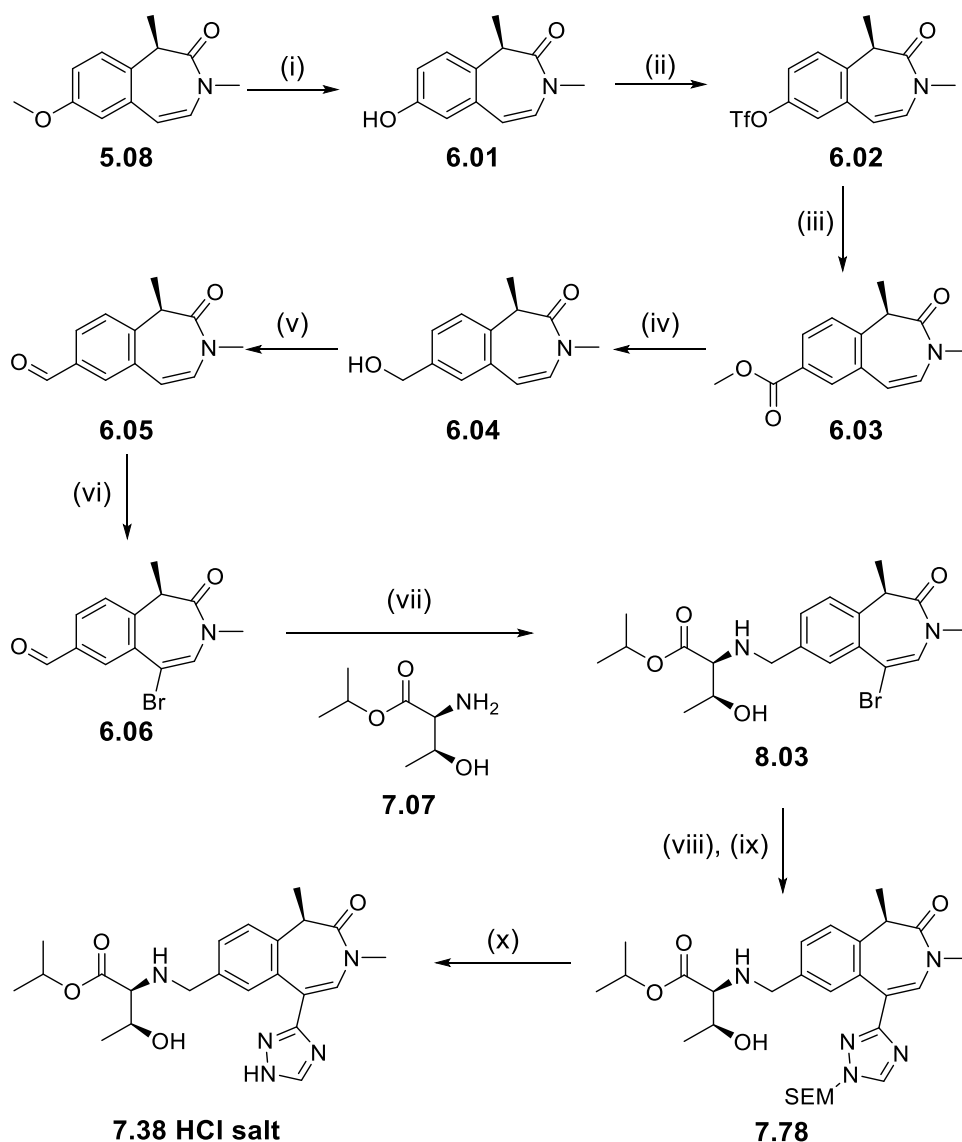


Figure 52: (a)-Microscope image (x20). (b)-X-ray powder diffraction diffractogram of molecule **7.38** as the HCl salt as obtained using the conditions in entry 4, Table 31.

8.4. Summary and scope of the new synthetic route

The stereoselective synthetic route from intermediate **5.08** to the final product **7.38** is summarized in Scheme 36. The optimised synthesis of intermediate **5.08** from commercial building blocks has previously been established in Scheme 4 in this study (page 56).



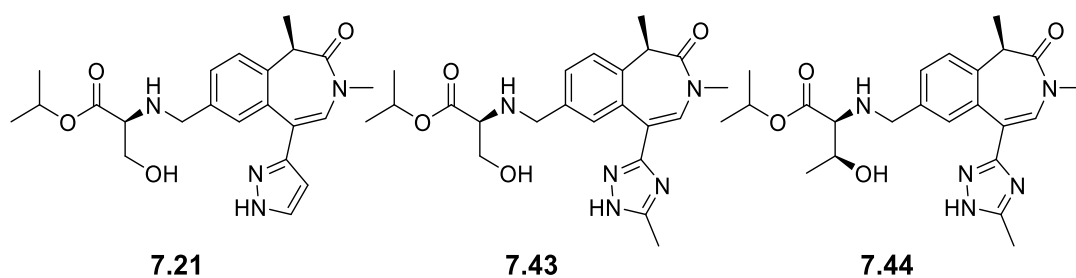
(i) BBr_3 , DCM, $-78\text{ }^\circ\text{C}$ to rt, overnight, 77% (ii) $\text{PhN}(\text{SO}_2\text{CF}_3)_2$, pyridine, NEt_3 , DCM, $0\text{ }^\circ\text{C}$ to rt, 20 h, 62% (iii) CO gas, $\text{Pd}(\text{OAc})_2$, Xantphos, NEt_3 , DMF, MeOH, $60\text{ }^\circ\text{C}$, 1.5 h, 87% (iv) LiBH_4 , 2-MeTHF, $55\text{ }^\circ\text{C}$, 2 h, 83% (v) DMP, DCM, rt, 1 h, 85% (vi) PTT, MeCN, rt, 10 min, 80% (vii) TFA (0.1 eq), NEt_3 (added to set pH at 5.8), 4 Å mol. sieves, THF, $50\text{ }^\circ\text{C}$, 18 h, then $\text{NaBH}(\text{OAc})_3$, rt, 4 h. 85% yield, 100% d.e. (viii) B_2pin_2 , dry KOAc, $\text{PdCl}_2(\text{dppf})$.DCM, 1,4-dioxane, $80\text{ }^\circ\text{C}$, 2h (ix) Ar-Br, XPhos Pd G2, XPhos, 2 M aq. K_3PO_4 , *i*PrOH, $90\text{ }^\circ\text{C}$, 1 h, 55% (over two steps), > 95% d.e. (x) 1 M HCl in Et_2O , acetone, rt, overnight 79% yield.

Scheme 36: Stereoselective synthetic route for the lead molecule 7.38.

This work reported in sections 5 and 8 enabled the synthesis of molecule **7.38** in a stereoselective fashion from commercial starting materials in 16 steps and 1.9% overall yield, delivering a crystalline solid. The average yield for these transformations

is 78%, and the low overall yield is a consequence of the relatively large number of steps for an advanced lead molecule.

This improved synthetic route was also applied to molecules **7.21**, **7.43** and **7.44** to understand if these molecules could be obtained in a stereoselective fashion. The yields associated with the four final steps of the synthesis are shown in Table 32. Pleasingly, the three molecules were obtained with the desired purity and without the need for chiral separation. The synthesis was conducted on a small scale and some of the yields will likely be improved upon scale up as shown with the synthesis of molecule **7.38**. This was the case for the reductive amination step for molecules **7.21** and **7.43**, where the small scale reductive amination provided the intermediate in 51% yield and a scale-up provided the desired material in 72% yield.



Reaction	Molecule 7.21	Molecule 7.43	Molecule 7.44
Reductive amination	51% - 72%		85%
Borylation – cross-coupling	24%	27%	27%
SEM deprotection	75%	55%	20%

Table 32: Yields for the stereoselective routes for molecules **7.21**, **7.43** and **7.44**.

This new route proved to be robust and was successfully applied to the synthesis of five molecules in this series to supply sufficient quantities of material for biological testing without the need of chiral separation. This route also enabled the evaluation of

the biological profile of molecule **7.44** for which the separation of the diastereomeric mixture was still an outstanding issue.

8.5. Conclusions

The partial racemisation observed at two chiral centres during the SAR synthetic route towards molecule **7.38** was overcome by inverting the order of steps and optimisation of the reductive amination reaction conditions (Figure 53).

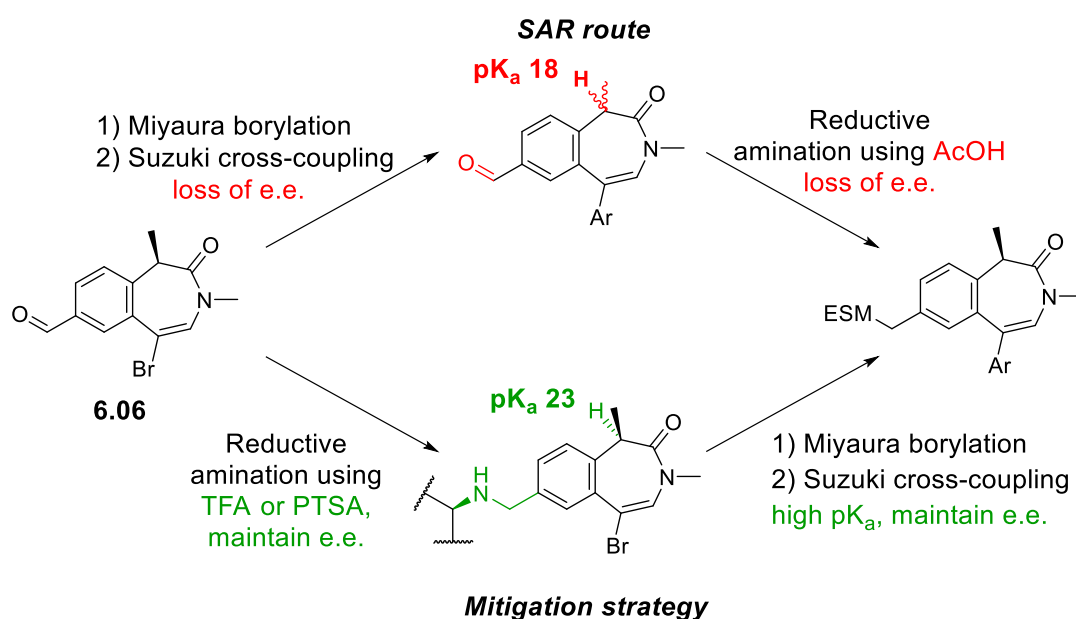
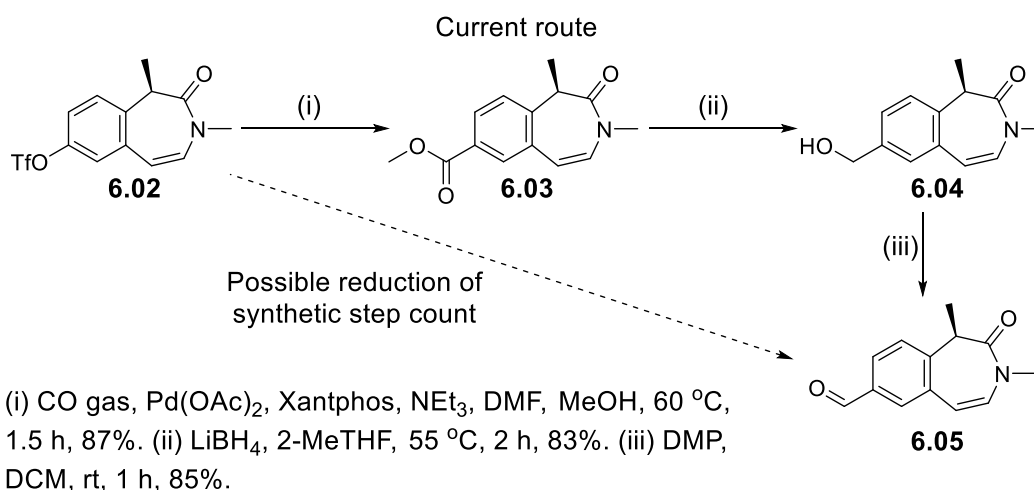


Figure 53: Successful mitigation strategy for the stereoselective synthesis of molecule **7.38**.

Racemisation of amino acids in the presence of a benzaldehyde and acetic acid have been reported previously.^{133,134,135,136} The work reported in this thesis enabled the replacement of the problematic acetic acid by stronger acids such as PTSA or TFA. The more stabilised counter-ions tosylate (TsO^-) and trifluoroacetate (CF_3COO^-) are less prone to remove the proton in the α -position to the amino ester in the imine intermediate. These poorly basic anions are thus able to prevent the racemisation of the more hindered *L-allo*-threonine. Milder reaction conditions (20 °C instead of

50 °C) had to be used to avoid racemisation of the *L*-serine amino ester. By performing first the reductive amination on aldehyde **6.06** to give molecules **8.03** and **8.04**, the pK_a of the CH in the α -position to the amide carbonyl increased compared to molecule **6.06**. The higher pK_a value led to a complete retention of the chiral integrity of the molecule during the borylation and cross coupling steps. The current study enabled the synthesis of molecule **7.38** in 1.9% overall yield in 16 steps and delivered the required amount of material for *in vivo* studies as a crystalline solid. If the molecule was to progress further into pre-clinical safety studies and to enter clinical trials, further route optimisation will be conducted to improve the route, such as a direct formylation from the triflate material **6.02** to the aldehyde **6.05**, aiming to reduce the synthetic step count and increase the overall yield (Scheme 37).



*Scheme 37: Direct formylation of the triflate **6.02** would reduce the synthetic step count.*

This work enabled the synthesis of the three lead molecules in a stereoselective fashion, avoiding the chiral separation step. In addition, no chiral separation methods were identified for molecule **7.44** despite an extensive screening of separation conditions, and this work enabled the synthesis of this challenging molecule with the required purity to progress into biological assays and into *in vivo* studies.

	4.04	5.06	6.26
hWB pIC ₅₀	8.1	7.3	7.3
hWB ΔtBu	+ 0.9	+ 0.2	+ 1.3
CES-2 t _{1/2} (min)	3	> 139	> 139
HLM IVC (-/+ benzil) (mL/min/g)	5.7 / 1.6	1.2 / 0.7	1.2 / 0.6
Heps IVC Cyno (LBF)	95%	74%	55%

Table 33: Profile of three early lead molecules. Decreasing the flexibility and length of the linker to the ESM has enabled increased CES-2 stability. Modification of the ester, amino acid and ZA channel groups have enabled the desired hWB ΔtBu to be reached.

Studies of the impact of the ester, amino acid and ZA channel groups on the esterase turnover proved that the CES-1 turnover (monitored by the hWB ΔtBu value) can successfully be increased whilst maintaining a long CES-2 half-life. This led to the discovery of a new lead molecule **6.26**, combining for the first time in this series the desired CES-1 hydrolysis rate, a long CES-2 half-life and low *in vitro* clearance profile (Figure 54, Table 33).

Further lead optimisation was conducted in this series to reach the desired profile defined at the outset of this work. Two strategies were proposed and implemented: firstly, to identify and remedy potential metabolic soft spots; secondly to improve the potency of known analogues already demonstrating low *in vitro* clearance. These strategies led to the identification of two advanced lead molecules **7.38** and **7.44**, exhibiting excellent *in vitro* profiles (Figure 55, Table 34).

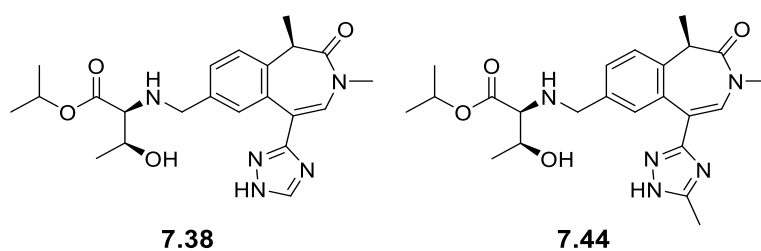


Figure 55: Structures of molecules **7.38** and **7.44**.

	4.04	7.38	7.44	Desired profile
hWB pIC ₅₀	8.1	7.2	7.3	≥ 7.6
hWB ΔtBu	+ 0.9	+ 1.1	+ 1.2	~ + 1.0
Heps IVC human (LBF)	-	49%	64%	≤ 60%
Heps IVC cyno (LBF)	95%	< 38%	38%	≤ 60%
CES-2 t _{1/2} (min)	3	> 139	> 139	> 139

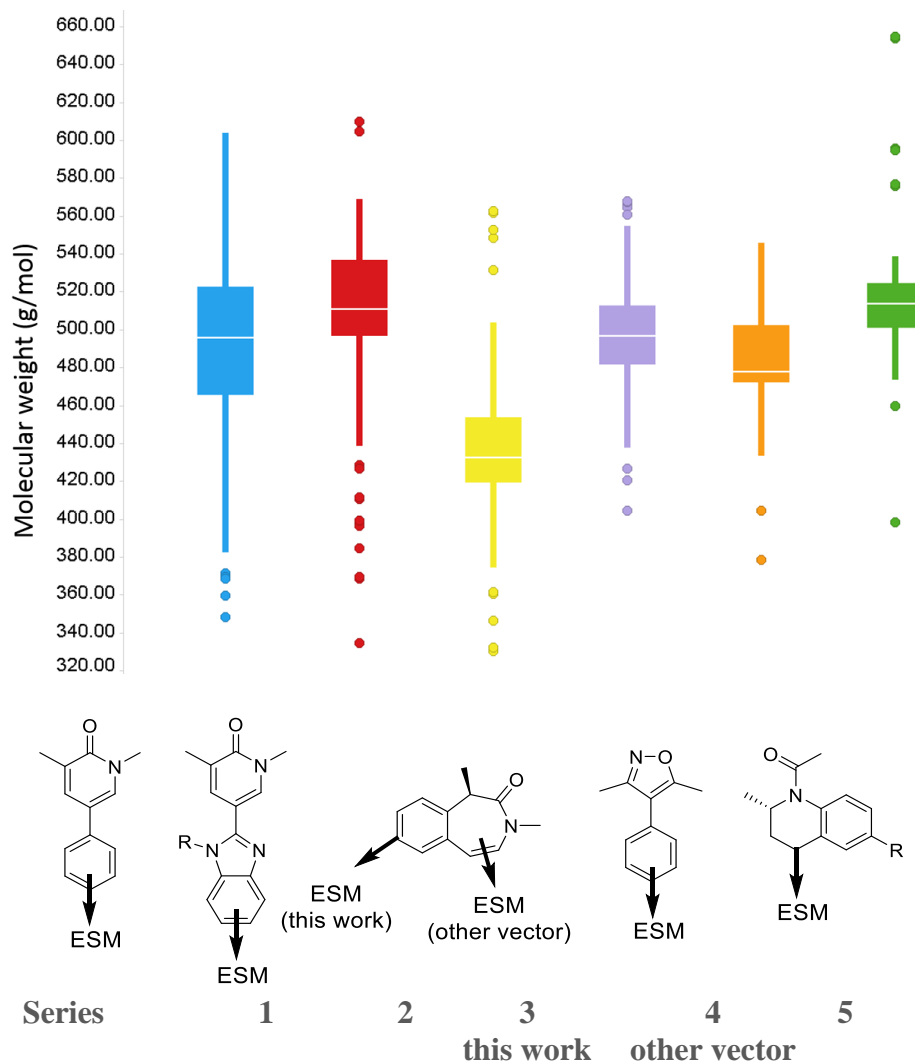
Table 34: Comparison of the profiles of the initial molecule **4.04** and the two lead molecules **7.38** and **7.44**, identified through the work described in this thesis.

Pleasingly, molecules **7.38** and **7.44** demonstrated good to excellent bioavailability in rat, with 69% and 29%, respectively. Unfortunately, following adaptation of the synthetic route for scale-up, progression into monkey PK studies revealed a lack of *in vitro* / *in vivo* clearance correlation in this species. A very high clearance was observed *in vivo* for these two compounds and led to poor bioavailability in monkey for both compounds (F < 10%). The two final molecules **7.38** and **7.44** identified through this work demonstrated higher rat bioavailability and longer half-life than the previous ESM-BET inhibitor **3.01**. As such, these molecules are very valuable tool compounds that could be used in rat models to increase our understanding of ESM-targeted molecules in terms of biology and pharmacokinetics. In particular, they could be used to study the mode of action and the tissue distribution of ESM-molecules in order to better understand their potential applications to macrophage-related diseases.

Through the investigation of this ESM-BET inhibitor series, this work established clear SAR to reach CES-1 vs. CES-2 selectivity. A CES-2 substrate requires a flexible linker to the ester motif in order to access the catalytic triad, whereas the CES-1 active site can accommodate a larger and more rigid linker to the ester motif. Therefore,

CES-1 selectivity can be achieved by modification of the steric bulk and rigidity of the ESM linker. Whilst a directly linked ESM to the benzazepinone motif was not hydrolysed by CES-1, a benzylic linker between these two motifs was found to be optimal in our series. In addition, it was also shown through this work that the BET inhibitor itself has an impact on the CES turnover and can be used to modulate the ester hydrolysis rate, as well as modifications of the ester and amino acid moieties. This CES isoform SAR should be instrumental in the future development of ESM-targeted drugs.

The benzazepinone series developed as part of this study stands out by having excellent physico-chemical properties with lower molecular weight and lower ChromlogD_{7.4} when compared to historical ESM-BET series developed in our laboratories. Figure 56 shows that from the most recent *in-house* ESM-BET series, the series developed in this thesis (yellow) has a significantly lower median molecular weight value (433 g/mol). This demonstrates the possibility of reaching a more conventional drug-like space, enabling permeability and lower lipophilicity to be combined, unlike historical series.^{29,37} This should be a valuable strategy for the optimisation of a future ESM-drug molecule as this will help to reach the desired *in vitro* profile.



	1	2	3	4	5	6
			this work	other vector		
Median MW	496	511	433	497	478	514
Count	460	284	158	129	14	33

Figure 56: Comparison of the molecular weight median and box plots for different GSK series of ESM-BET inhibitors showing the series developed in this thesis has significantly lower molecular weight compounds than the historical and other current series.

Beyond the medicinal chemistry, the synthetic approach to furnish target molecules with the requisite chiral integrity and scale was optimised throughout this work. The synthesis of the benzazepinone building block **5.08** was shortened from 8 to 6 steps and the overall yield increased from 7% to 20% with an excellent enantiomeric excess (Scheme 4, p.56). This optimised route has since delivered more than a kilogram of

the key building block **5.08** to support lead optimisation work of more than thirty chemists across two BET inhibitor programmes in our laboratories.

The initial SAR route established over the course of this work had several synthetic issues in relation to reductive amination yields and partial racemisation of two chiral centres. By understanding the racemisation process, the reductive amination racemisation was overcome by replacing the acetic acid by an acid with a weakly basic counter-ion such as triflate or tosylate. These conditions will be useful for the synthesis of any future ESM-targeted drug molecules. Finally, the racemisation of the chiral centre on the benzazepinone motif itself was overcome by performing the reductive amination before the Miyaura borylation and Suzuki cross-coupling. This led to an increased pK_a of the proton in the α -position to the amide functionality and thus completely suppressed the racemisation. The synthesis of the lead compounds was thus achieved in good yields and with the required enantiomeric excess for *in vivo* studies (Scheme 36, p.164).

Future work

Medicinal chemistry

Additional work on the CES-1 and CES-2 substrate specificity would be valuable for future ESM-drug optimisation programmes (Figure 57). The effect of substitution on the benzylic linker to the ESM has not yet been explored. It would be interesting to understand if substituted linkers are still hydrolysed by CES-1 and the selectivity they can exhibit against the CES-2 isoform. Similarly, it is worth determining if the CES selectivity be modulated by substitution directly on the phenyl ring bearing the ESM.

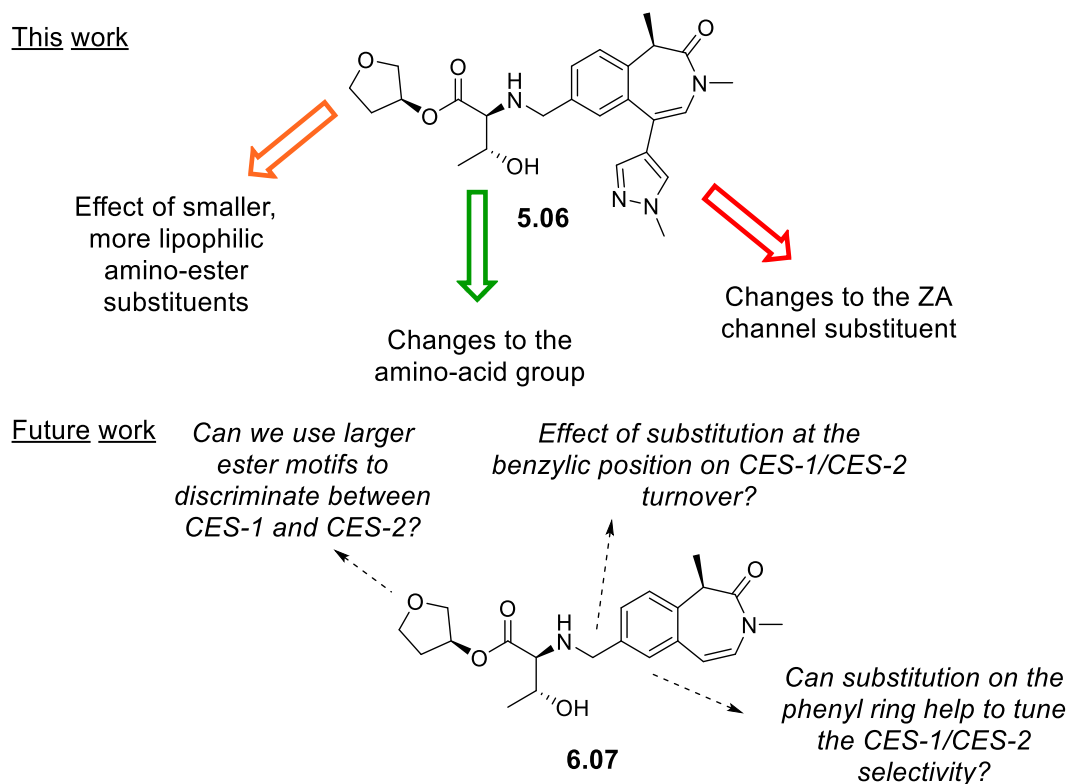


Figure 57: Current CES-1/CES-2 SAR and future work.

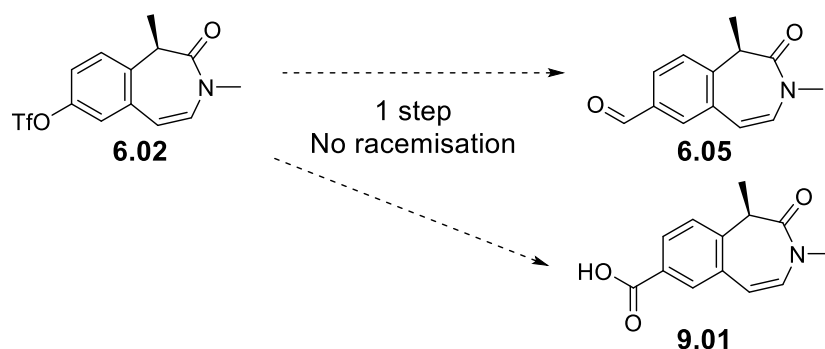
Finally, this study has established that short and constrained linkers are favourable to CES-1 hydrolysis over CES-2. CES-2 is overexpressed in certain cancer lines and is also located in the intestinal membrane.^{47,142} A CES-2 selective ESM could be used to

target drug delivery to patients with cancer or intestinal diseases. The literature suggests that CES-2 can accommodate larger ester motifs than CES-1.^{47,49} By increasing the ester motif, it could be determined if it is possible to increase the affinity for CES-2 over CES-1 and thus investigate the potential of a CES-2 selective ESM drug molecule.

Synthetic chemistry

Further work on reductive amination reactions using an amino ester as the amine starting material is ongoing in our laboratories. A substrate scope is currently being carried out, aiming to identify sterically hindered and/or electron-rich aldehydes. Both factors should reduce their ability to undergo a reductive amination with a weak and hydrophilic amine such as ESM. These substrates are likely to behave like the benzazepinone aldehyde and to provide low yields and potentially racemisation at the amino acid α -position. The reductive amination conditions optimised in this thesis might be suitable for such substrates.

Finally, further work on the benzazepinone derivatization is ongoing within our laboratory. In particular, reaction conditions to obtain the aldehyde or carboxylic acid without racemisation of the chiral centre in the α -position of the lactam moiety are being actively investigated.



Scheme 38: Ongoing investigation within our team to obtain the key building blocks in less steps and without racemisation.

Experimental

Starting materials, reagents and solvents were commercially available and used without further purification. When dry potassium acetate was used, the base was dried overnight in the *vacuum* oven at 40 °C. The synthesis of the amino ester building blocks used in this thesis is described in the literature.⁷⁶ Compounds submitted to biological assays were greater than or equal to 95% pure by NMR and LCMS unless otherwise specified. Intermediates described in the experimental were greater than or equal to 80% pure by ¹H NMR and LCMS unless otherwise specified. ¹H and ¹³C NMR were recorded on a Bruker 400 MHz spectrometer. Chemical shifts are reported in parts per million (ppm) and are internally referenced to the TMS peak. The abbreviations used for NMR analysis are br. = broad, s = singlet, d = doublet, t = triplet, dd = doublet of doublets, qd = quadruplet dedoubled, spt = septuplet, m = multiplet, C_{iv} = quaternary carbon. Optical rotation was measured on a Jasco P1030 polarimeter. Melting points were measured on a Buchi M-565 automated melting point machine. Infra-Red spectroscopy (IR) data was recorded from samples dissolved in chloroform on a Perkin Elmer Spectrum one spectrometer. Only data for strong peaks and main functional groups are reported.

LCMS methods

The UPLC analysis was conducted on an Acquity UPLC CSH C18 column (50 mm x 2.1 mm, 1.7 μm particle diameter) at 40 °C, with a 0.3 μL injection volume. The UV detection was a summed signal from wavelength of 210 nm to 350 nm. The solvents employed were:

High pH method

A = 10 mM ammonium bicarbonate in water adjusted to pH 10 with ammonia solution. **B** = MeCN.

The gradient employed was:

Time (min)	Flow Rate (mL/min)	% A	% B
0.00	1	97	3
0.05	1	97	3
1.50	1	5	95
1.90	1	5	95
2.00	1	97	3

Formic method

A = 0.1% v/v solution of formic acid in water. **B** = 0.1% v/v solution of formic acid in MeCN.

The gradient employed was:

Time (min)	Flow Rate (mL/min)	% A	% B
0.00	1	97	3
1.50	1	5	95
1.90	1	5	95
2.00	1	97	3

The MS analysis was conducted on a Waters ZQ MS with an alternate-scan positive and negative electrospray ionisation mode.

High resolution mass spectrometry (HRMS)

The UPLC analysis was conducted on an Acquity UPLC CSH C18 column (100 mm x 2.1 mm, 1.7 µm particle diameter) at 50 °C, with a 0.2 µL injection volume. The UV detection was a summed signal from wavelength of 210 nm to 350 nm. The solvents employed were:

A = 0.1% v/v solution of formic acid in water. **B** = 0.1% v/v solution of formic acid in MeCN. The gradient employed was:

Time (min)	Flow Rate (mL/min)	% A	% B
0.00	0.8	97	3
8.50	0.8	0	100
9.00	0.8	0	100
9.50	0.8	97	3
10.00	0.8	97	3

The MS analysis was conducted on a Waters XEVO G2-XS Qtof with a positive electrospray ionisation mode.

MDAP (Mass directed auto-preparative chromatography)

The preparative HPLC purification was conducted on an Xbridge C18 column (150 mm x 19 mm, 5 µm particle diameter) at rt. The solvents employed were:

High pH methods. Solvents: A = 10 mM ammonium bicarbonate in water, *B* = MeCN.

TFA method. Solvents: A = 0.1% v/v solution of TFA in water, *B* = 0.1% v/v solution of TFA in MeCN. *Formic methods. Solvents: A* = 0.1% v/v solution of formic acid in

water, *B* = 0.1% v/v solution of formic acid in MeCN. **Gradients:**

<i>High pH extended method A</i>				<i>High pH method C</i>			
Time (min)	Flow Rate (mL/min)	% A	% B	Time (min)	Flow Rate (mL/min)	% A	% B
0.0	40	100	0	0.0	40	30	70
1.0	40	100	0	3.0	40	30	70
20.0	40	75	25	3.5	30	30	70
20.5	40	1	99	24.5	30	15	85
25.0	40	1	99	25.0	30	1	99
				32.0	30	1	99
<i>High pH method B</i>				<i>TFA extended method B</i>			
Time (min)	Flow Rate (mL/min)	% A	% B	Time (min)	Flow Rate (mL/min)	% A	% B
0.0	16	90	10	0.0	40	85	15
10.0	16	50	50	3.0	40	85	15
10.1	16	0	100	22.0	40	45	55
12.0	16	0	100	22.5	40	45	55
12.1	16	90	10	23.0	40	1	99
15.0	16	90	10	23.0	40	1	99
<i>High pH extended method B</i>				<i>Formic extended method A</i>			
Time (min)	Flow Rate (mL/min)	% A	% B	Time (min)	Flow Rate (mL/min)	% A	% B
0.0	40	85	15	0.0	40	100	0
3.0	40	85	15	1.0	40	100	0
22.0	40	45	55	20.0	40	75	25
22.5	40	45	55	20.5	40	1	99
23.0	40	1	99	25.0	40	1	99
27.0	40	1	99				
<i>High pH extended method C</i>				<i>Formic extended method B</i>			
Time (min)	Flow Rate (mL/min)	% A	% B	Time (min)	Flow Rate (mL/min)	% A	% B
0.0	40	70	30	0.0	40	85	15
1.0	40	70	30	1.0	40	85	15
20.0	40	15	85	20.0	40	45	55
20.5	40	1	99	20.5	40	1	99
25.0	40	1	99	25.0	40	1	99

Reductive amination general procedure A1

The aldehyde (1 eq.) and the amino ester (1.5 eq.) were suspended in THF. AcOH (2.5 eq.) and DIPEA (2 eq.) were added to the reaction mixture. The reaction mixture was heated under nitrogen to 40 °C until full formation of the imine was observed (monitored by LCMS, typically 30 min–3 h). The reaction mixture was cooled to rt and sodium triacetoxyborohydride (2.5 eq.) was added. The mixture was stirred at rt, under nitrogen, until complete reduction of the imine to the amine (monitored by LCMS, typically 1-2 h). Additional sodium triacetoxyborohydride (2.5 eq.) was added when necessary to complete the reduction of the imine. The reaction mixture was quenched with methanol and concentrated under reduced pressure to give the crude product.

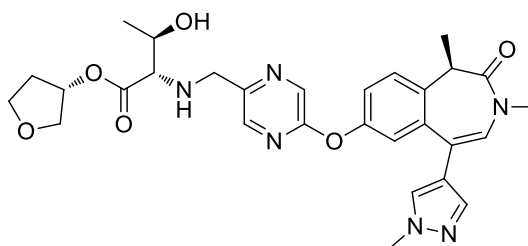
Reductive amination general procedure A2

Same procedure as for general procedure A1 with an aqueous work up. After the methanol quench, the mixture was concentrated under reduced pressure. The crude mixture was partitioned between EtOAc and water (or a 2 M aqueous solution of LiCl). The layers were separated. The aqueous layer was re-extracted with EtOAc. The organic layers were combined, dried through a phase separator and concentrated under reduced pressure to give the crude product.

Reductive amination general procedure B

The aldehyde (1 eq.) and the amino ester (1.5 eq.) were suspended in *i*PrOH and AcOH (10:1 ratio). Picoline borane (1.2 eq.) was added. The mixture was stirred at rt, under nitrogen, until complete formation of the desired product (monitored by LCMS, typically 1-2 h). The reaction mixture was quenched with methanol and concentrated under reduced pressure to give the crude product.

(S)-Tetrahydrofuran-3-yl ((5-(((R)-1,3-dimethyl-5-(1-methyl-1H-pyrazol-4-yl)-2-oxo-2,3-dihydro-1H-benzo[d]azepin-7-yl)oxy)pyrazin-2-yl)methyl)-L-threoninate [5.03]

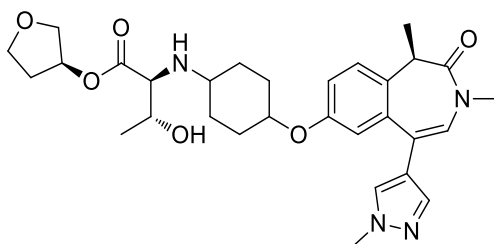


(R)-7-((5-(Hydroxymethyl)pyrazin-2-yl)oxy)-1,3-dimethyl-5-(1-methyl-1H-pyrazol-4-yl)-1,3-dihydro-2H-benzo[d]azepin-2-one [5.41] (203 mg, 0.52 mmol) was dissolved in DCM (5 mL) and the reaction mixture was stirred under nitrogen. Dess-Martin periodinane (330 mg, 0.78 mmol) was added and the reaction mixture stirred at room temperature for 1 h. DCM and a saturated aqueous solution of sodium bicarbonate were added. The layers were separated, the aqueous layer was re-extracted with DCM. The organic layers were combined, dried using a hydrophobic frit and evaporated under reduced pressure to give a pink solid [5.42] (202 mg, quantitative yield). To this solid [5.42] (151 mg, 0.39 mmol) suspended in *i*PrOH (5 mL), was added NEt₃ (0.162 mL, 1.16 mmol) and (S)-tetrahydrofuran-3-yl L-threoninate, hydrochloride (131 mg, 0.58 mmol). The reaction mixture was stirred under nitrogen at rt for 2 h. Picoline borane (62.2 mg, 0.58 mmol) and AcOH (0.56 mL) were added and the reaction mixture stirred under nitrogen for 18 h. The reaction mixture was concentrated under reduced pressure. EtOAc and water were added. The layers were separated, the aqueous layer was re-extracted with EtOAc. The organic layers were combined, dried using a hydrophobic frit and evaporated under reduced pressure. The sample was purified by silica column chromatography, eluted with a gradient of 0-100% EtOAc in cyclohexane, followed by a gradient of 0-25% EtOH in EtOAc. The

relevant fractions were combined and concentrated under reduced pressure. The sample was then further purified by MDAP (high pH, extended method B). The purest fractions were combined, and the solvent was evaporated under reduced pressure to give the title product **[5.03]** as a colourless gum (Batch 1, 11.1 mg, 5% yield). The remaining fractions were combined, concentrated under reduced pressure and purified by MDAP (formic, extended method A). The fractions were combined, and the solvent was evaporated under reduced pressure to give the title product **[5.03]** as the formic salt as a colourless gum (Batch 2, 45.4 mg, 18% yield). **Analysis of batch 1** (analysis of batch 2 is consistent with the formic salt):

¹H NMR (400 MHz, CDCl₃) δ 8.32 (d, *J* = 1.5 Hz, 1H), 8.07 (s, 1H), 7.54 (s, 1H), 7.42 (d, *J* = 8.6 Hz, 1H), 7.37 (s, 1H), 7.23 (dd, *J* = 8.6, 2.6 Hz, 1H), 7.14 (d, *J* = 2.6 Hz, 1H), 6.60 (s, 1H), 5.35-5.30 (m, 1H), 3.99-3.95 (m, 1H), 3.95-3.91 (m, 2H), 3.90 (s, 3H), 3.89-3.87 (m, 1H), 3.86-3.80 (m, 3H), 3.79-3.75 (m, 1H), 3.40 (q, *J* = 6.9 Hz, 1H), 3.13 (s, 3H), 3.09 (d, *J* = 6.7 Hz, 1H), 2.24-2.14 (m, 1H), 2.02-1.95 (m, 1H), 1.70 (d, *J* = 6.9 Hz, 3H), 1.22 (d, *J* = 6.7 Hz, 3H). The signal for one of the two exchangeable protons was not observed. **¹³C NMR** (101 MHz, CDCl₃) δ 173.1 (C=O), 170.3 (C=O), 159.2 (C_{iv}), 151.2 (C_{iv}), 147.9 (C_{iv}), 139.7 (CH), 138.0 (CH), 136.9 (C_{iv}), 134.8 (CH), 134.7 (C_{iv}), 129.0 (CH), 127.0 (CH), 125.6 (CH), 122.0 (CH), 121.3 (C_{iv}), 121.3 (C_{iv}), 120.0 (CH), 75.8 (CH), 73.0 (CH₂), 68.1 (CH), 67.4 (CH₂), 67.0 (CH), 50.8 (CH₂), 40.8 (CH), 39.1 (CH₃), 35.2 (CH₃), 32.8 (CH₂), 19.5 (CH₃), 12.9 (CH₃). **LCMS** (ESI, High pH) *t*_R = 0.86 min, *m/z* 563 [M+H]⁺. **HRMS** (ESI) calculated for C₂₉H₃₅N₆O₆ [M+H]⁺ 563.2619, found 563.2618 (2.63 min). **ν_{max}** (solution in chloroform, cm⁻¹): 3329 (OH), 2997 (CH alkene), 2932 (CH alkane), 1729 (C=O ester), 1659 (C=O amide). **[α_D]**^{21.2 °C}_{589 nm} (c 0.220, MeOH): +53.6°.

(2*S*,3*R*)-(S)-Tetrahydrofuran-3-yl 2-((4-(((*R*)-1,3-dimethyl-5-(1-methyl-1*H*-pyrazol-4-yl)-2-oxo-2,3-dihydro-1*H*-benzo[*d*]azepin-7-yl)oxy)cyclohexyl)amino)-3-hydroxybutanoate [5.04 and 5.05]

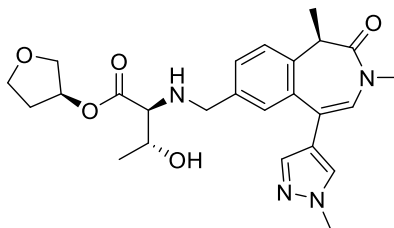


(*R*)-1,3-Dimethyl-5-(1-methyl-1*H*-pyrazol-4-yl)-7-((4-oxocyclohexyl)oxy)-1,3-dihydro-2*H*-benzo[*d*]azepin-2-one [5.47] (80 mg, 0.21 mmol) and (*S*)-tetrahydrofuran-3-yl *L*-threoninate, hydrochloride [5.43] (99 mg, 0.44 mmol) and NET_3 (0.09 mL, 0.63 mmol) were stirred in *i*PrOH (5 mL) under nitrogen at rt for 1 h. AcOH (1.00 mL) and picoline borane (33.8 mg, 0.32 mmol) were added and the reaction mixture was stirred for 1 h at rt, and 1 h at 40 °C. (*S*)-tetrahydrofuran-3-yl *L*-threoninate, hydrochloride [5.43] (99 mg, 0.44 mmol) and picoline borane (33.8 mg, 0.32 mmol) were added and the reaction mixture was stirred at 40 °C for 2 days. The reaction mixture was concentrated under reduced pressure to give a yellow oil. The oil was partitioned between EtOAc and water. The layers were separated. The aqueous layer was re-extracted with EtOAc. The organic layers were combined, dried through a phase separator and concentrated under reduced pressure to give a yellow oil. The product was purified by silica column chromatography, eluted with a gradient of 0-100% EtOAc in cyclohexane, followed by a gradient of 0-25% EtOH in EtOAc. The product was not collected by the automated purification system. The waste was concentrated under reduced pressure to give a yellow oil. The oil was re-purified by two MDAP (high pH, extended method B). The fractions were combined and concentrated under reduced pressure to give two products.

Diastereomeric mixture 1 [**5.04**] as a yellow oil (9.4 mg, 8% yield, d.e. 80% by ^1H NMR): ^1H NMR (400 MHz, CDCl_3) δ 7.54 (s, 1H), 7.34 (s, 1H), 7.27-7.23 (m, 1H)*, 6.97 (dd, $J = 8.6, 2.6$ Hz, 1H), 6.85 (d, $J = 2.5$ Hz, 1H), 6.54 (s, 1H), 5.38-5.34 (m, 1H), 4.15-4.07 (m, 1H), 3.96-3.92 (m, 1H), 3.92 (s, 3H), 3.91-3.89 (m, 1H), 3.82 (br. s, 1H), 3.81 (br. d, $J = 10.8$ Hz, 1H), 3.62-3.54 (m, 1H), 3.33 (q, $J = 7.1$ Hz, 1H), 3.10 (s, 3H), 3.02 (d, $J = 7.6$ Hz, 1H), 2.53-2.45 (m, 1H), 2.27-2.17 (m, 1H), 2.12-1.93 (m, 4H), 1.85 (br. d, $J = 12.5$ Hz, 1H), 1.64 (d, $J = 7.1$ Hz, 3H), 1.50-1.34 (m, 2H), 1.31-1.23 (m, 1H), 1.21 (d, $J = 6.1$ Hz, 3H), 1.19-1.11 (m, 1H). Signals for the exchangeable protons were not observed. NMR showed 10% of the other diastereomer [**5.05**]. This ratio was determined at the two pyrazole CH signals at 7.54 and 7.34 ppm (major diastereomer) and 7.55 and 7.35 ppm (minor diastereomer) . *This signal is perturbed by the residual solvent peak. LCMS (ESI, High pH) $t_{\text{R}} = 0.96$ min, m/z 553 $[\text{M}+\text{H}]^+$.

Diastereomeric mixture 2 [**5.05**] as a yellow oil (8.0 mg, 7% yield, d.e. 80% by ^1H NMR): ^1H NMR (400 MHz, CDCl_3) δ 7.55 (s, 1H), 7.35 (s, 1H), 7.23-7.27 (m, 2H) *, 6.99 (dd, $J = 8.7, 2.6$ Hz, 1H), 6.86 (d, $J = 2.6$ Hz, 1H), 6.55 (s, 1H), 5.35-5.32 (m, 1H), 4.34 (br. s, 1H), 3.93 (s, 3H), 3.92-3.89 (m, 1H), 3.88-3.83 (m, 2H), 3.82 (br. d, $J = 10.8$ Hz, 1H), 3.62-3.54 (m, 1H), 3.34 (q, $J = 6.9$ Hz, 1H), 3.10 (s, 3H), 3.02 (d, $J = 7.6$ Hz, 1H), 2.50 (br. s, 1H), 2.26-2.15 (m, 1H), 2.04-1.91 (m, 4H), 1.64 (d, $J = 6.9$ Hz, 3H), 1.58-1.52 (m, 4H), 1.21 (d, $J = 6.1$ Hz, 3H). Signals for the exchangeable protons were not observed. NMR showed 10% of the other diastereomer [**5.04**]. This ratio was determined at the two pyrazole CH signals at 7.55 and 7.35 ppm (major diastereomer) and 7.54 and 7.34 ppm (minor diastereomer). *This signal is perturbed by the residual solvent peak. LCMS (ESI, High pH) $t_{\text{R}} = 0.98$ min, m/z 553 $[\text{M}+\text{H}]^+$.

(S)-Tetrahydrofuran-3-yl (((R)-1,3-dimethyl-5-(1-methyl-1H-pyrazol-4-yl)-2-oxo-2,3-dihydro-1H-benzo[d]azepin-7-yl)methyl)-L-threoninate [5.06]

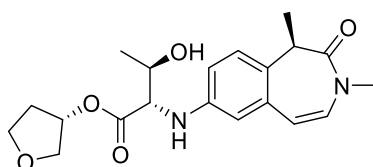


(R)-1,3-Dimethyl-5-(1-methyl-1H-pyrazol-4-yl)-2-oxo-2,3-dihydro-1H-benzo[d]azepine-7-carbaldehyde (82 mg, 0.28 mmol) [5.51], (S)-tetrahydrofuran-3-yl-L-threoninate, hydrochloride [5.43] (94 mg, 0.42 mmol), picoline borane (35.6 mg, 0.33 mmol) and acetic acid (0.5 mL, 8.7 mmol) were stirred in *i*PrOH (5 mL) under nitrogen at rt for 2.5 h. The reaction mixture was quenched with methanol and concentrated under reduced pressure to give a yellow oil. The crude product was purified by MDAP (high pH, extended method B). The relevant fractions were concentrated under reduced pressure to give the title product [5.06] as a colourless oil (62.7 mg, 46% yield).

¹H NMR (400 MHz, CDCl₃) δ 7.57 (s, 1H), 7.37-7.30 (m, 4H), 6.59 (s, 1H), 5.28-5.23 (m, 1H), 3.92 (s, 3H), 3.89-3.80 (m, 4H), 3.74 (br. d, *J* = 10.5 Hz, 1H), 3.67-3.61 (m, 2H), 3.37 (q, *J* = 7.0 Hz, 1H), 3.11 (s, 3H), 2.94 (d, *J* = 7.3 Hz, 1H), 2.22-2.11 (m, 1H), 1.93-1.85 (m, 1H), 1.67 (d, *J* = 7.0 Hz, 3H), 1.17 (d, *J* = 6.1 Hz, 3H). Signals for the exchangeable protons were not observed. ¹³C NMR (101 MHz, CDCl₃) δ 173.3 (C=O), 170.5 (C=O), 137.7 (CH), 137.0 (C_{iv}), 136.9 (C_{iv}), 135.6 (C_{iv}), 129.4 (CH), 129.3 (CH), 127.4 (CH), 126.4 (CH), 124.1 (CH), 122.0 (C_{iv}), 121.5 (C_{iv}), 75.6 (CH), 72.9 (CH₂), 68.0 (CH), 66.9 (CH₂), 66.9 (CH),* 52.1 (CH₂), 40.9 (CH), 39.0 (CH₃), 35.1 (CH₃), 32.8 (CH₂), 19.3 (CH₃), 12.7 (CH₃). *values of 66.93 and 66.90. LCMS

(ESI, High pH) $t_R = 0.79$ min, m/z 469 $[M+H]^+$. **HRMS** (ESI) calculated for $C_{25}H_{33}N_4O_5$ 469.2452 $[M+H]^+$, found 469.2452 (3.86 min). ν_{max} (solution in chloroform, cm^{-1}): 3431 (OH), 2978 (CH alkene), 2938 (CH alkane), 1728 (C=O ester), 1658 (C=O amide). $[\alpha]_D^{20.7}$ $_{589\text{ nm}}$ (c 0.500, MeOH): +84.3°.

(S)-Tetrahydrofuran-3-yl ((R)-1,3-dimethyl-2-oxo-2,3-dihydro-1H-benzo[d]azepin-7-yl)-L-threoninate [5.07]



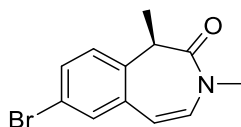
A mixture of (*R*)-7-bromo-1,3-dimethyl-1,3-dihydro-2*H*-benzo[*d*]azepin-2-one [5.15] (200 mg, 0.75 mmol), (*S*)-tetrahydrofuran-3-yl *L*-threoninate, hydrochloride [5.43] (509 mg, 2.25 mmol), cesium carbonate (735 mg, 2.25 mmol) and *t*BuBrettPhos-Pd-G3 (32.1 mg, 0.04 mmol) were suspended in toluene (6 mL) under nitrogen and heated at 100 °C for 20 h. (*S*)-tetrahydrofuran-3-yl *L*-threoninate, hydrochloride [5.43] (169.6 mg, 0.75 mmol) and *t*BuBrettPhos-Pd-G3 (16.05 mg, 0.02 mmol,) were added. A lump of non-dissolved material was observed (likely to be the amino ester) so 1 mL of NEt_3 was added (dissolution of the lump was observed a few minutes after addition), and the reaction mixture was heated at 100 °C under nitrogen for 4 h. The reaction mixture was then heated in a microwave at 100 °C for 30 min. The reaction mixture was concentrated under reduced pressure. EtOAc and water were added to the reaction mixture. The layers were separated, the aqueous layer was re-extracted with EtOAc. The organic layers were combined, dried using a hydrophobic frit and evaporated under reduced pressure. The sample was purified by silica column chromatography, eluted with a gradient of 0-100% EtOAc in cyclohexane. The appropriate fractions

were combined and concentrated under reduced pressure to give a yellow gum. The yellow gum was purified by MDAP (formic, extended method B). The solvent was evaporated under reduced pressure to give the title product **[5.07]** as a pale-yellow gum (7.8 mg, 3% yield).

Analysis of molecule **[5.07]**

¹H NMR (400 MHz, CDCl₃) δ 7.13 (d, $J = 8.3$ Hz, 1H), 6.75 (dd, $J = 8.5, 2.5$ Hz, 1H), 6.56 (d, $J = 2.5$ Hz, 1H), 6.29 (d, $J = 9.2$ Hz, 1H), 6.25 (d, $J = 9.2$ Hz, 1H), 5.37-5.32 (m, 1H), 4.19-4.13 (m, 1H), 3.93 (d, $J = 4.2$ Hz, 1H), 3.91-3.87 (m, 1H), 3.87-3.83 (m, 2H), 3.82-3.78 (m, 1H), 3.21 (br. s, 1H), 3.10 (s, 3H), 2.22-2.12 (m, 1H), 2.00-1.92 (m, 1H), 1.58 (br. d, $J = 5.9$ Hz, 3H), 1.33 (d, $J = 6.4$ Hz, 3H). Signals for the exchangeable protons were not observed. **LCMS** (ESI, High pH) $t_R = 0.81$ min, m/z 375 [M+H]⁺.

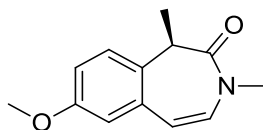
Recovery of molecule **[5.15]**:



Some other fractions from the column chromatography were combined and concentrated under reduced pressure to afford the crude recovered starting material **[5.15]** as a pink solid. The pink solid was purified by MDAP (high pH, extended method C). The solvent was evaporated under reduced pressure to give the recovered starting material (*R*)-7-bromo-1,3-dimethyl-1,3-dihydro-2*H*-benzo[*d*]azepin-2-one **[5.15]** (70.7 mg, 32% yield) as a white solid.

¹H NMR (400 MHz, DMSO-*d*₆) δ 7.49 (dd, $J = 8.3, 2.0$ Hz, 1H), 7.39 (d, $J = 2.0$ Hz, 1H), 7.18 (d, $J = 8.3$ Hz, 1H), 6.33 (s, 2H), 3.23 (br. s, 1H), 3.12 (s, 3H), 1.62 (d, $J = 5.9$ Hz, 3H). **LCMS** (ESI, Formic) $t_R = 1.12$ min, m/z 266/268 [M+H]⁺.

(R)-7-Methoxy-1,3-dimethyl-1,3-dihydro-2H-benzo[d]azepin-2-one [5.08]



(*R,E*)-2-(2-(2-Ethoxyvinyl)-4-methoxyphenyl)-*N*-methylpropanamide [5.22] (78 mg, 0.25 mmol) and 4 M solution of HCl in 1,4-dioxane (5 mL, 20.0 mmol) were stirred under nitrogen at 70 °C for 1 h. The reaction mixture was diluted with EtOAc and water. The layers were separated. The aqueous layer was extracted with EtOAc. The organics were combined, dried through a phase separator and concentrated under reduced pressure to give a crude orange oil. The crude product was purified by silica column chromatography, eluted with a gradient of 0-100% EtOAc in cyclohexane. The appropriate fractions were concentrated under reduced pressure to give the title product [5.08] as a yellow solid (47.3 mg, 82%, e.e. 83% by chiral HPLC).

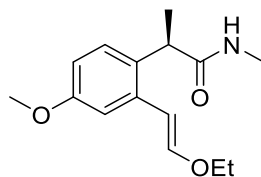
LCMS (ESI, High pH) $t_R = 0.95$ min, m/z 218 [M+H]⁺. **Analytical chiral HPLC** (Chiralpak AD column, 25 cm, rt, 25% EtOH in heptane, injection volume 0.3 μ L) $t_R = 9.39$ min, 91.3%; other enantiomer $t_R = 6.84$ min, 8.6%.

Recrystallisation:

(*R*)-7-Methoxy-1,3-dimethyl-1,3-dihydro-2H-benzo[d]azepin-2-one [5.08] (3.6 g, 15.74 mmol) was suspended in warm MeCN (5 mL). The mixture was heated at reflux for a few minutes. The entire material dissolved. The mixture was then left to slowly cool to rt (for 3 h) allowing the slow formation of white crystals. The supernatant was removed with a pipette. The solid was rinsed with Et₂O twice. The supernatant was removed with a pipette, affording the title product [5.08] as white crystals (2.56 g, 71%, e.e. 99% by chiral HPLC).

¹H NMR (400 MHz, CDCl₃) δ 7.22 (d, *J* = 8.8 Hz, 1H), 6.95 (dd, *J* = 8.8, 2.8 Hz, 1H), 6.76 (d, *J* = 2.8 Hz, 1H), 6.37 (d, *J* = 9.1 Hz, 1H), 6.28 (d, *J* = 9.1 Hz, 1H), 3.80 (s, 3H), 3.23 (br. s, 1H), 3.11 (s, 3H), 1.61 (s, 3H). **¹³C NMR** (101 MHz, CDCl₃) δ 170.0 (C=O), 158.1 (C–O), 130.5 (CH), 128.8 (CH), 116.5 (CH), 115.1 (CH), 111.2 (CH), 55.4 (CH₃), 35.6 (CH₃), 13.3 (CH₃), three quaternary carbons were not observed. **LCMS** (ESI, High pH) *t*_R = 0.95 min, *m/z* 218 [M+H]⁺. **Analytical chiral HPLC** (Chiralpak AD column, 25 cm, rt, 20% EtOH in heptane, injection volume 0.2 μL) *t*_R = 9.83 min, 99.6%; other enantiomer *t*_R = 7.09 min, 0.4%. **HRMS** (ESI) calculated for C₁₃H₁₆NO₂ [M+H]⁺ 218.1181, found 218.1187 (3.86 min). **ν**_{max} (solution in chloroform, cm⁻¹): 2973 (CH alkene), 2943 (CH alkane), 1666 (C=O amide), 1631 (C=C alkene). **[α]_D^{21.9 °C}**_{589 nm} (c 0.500, MeOH): -52.7°. **m.p.** = 120-122 °C.

(*R,E*)-2-(2-(2-Ethoxyvinyl)-4-methoxyphenyl)-*N*-methylpropanamide [5.22]

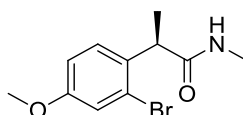


(*R*)-2-(2-Bromo-4-methoxyphenyl)-*N*-methylpropanamide [5.23] (94 mg, 0.31 mmol), (*E*)-2-(2-ethoxyvinyl)-4,4,5,5-tetramethyl-1,3,2-dioxaborolane [5.19] (100 mg, 0.51 mmol), potassium carbonate (80 mg, 0.58 mmol) and tetrakis(triphenylphosphine)palladium (18 mg, 0.016 mmol) were stirred in 1,4-dioxane (5 mL) and water (1 mL) under nitrogen at 120 °C for 2 h. The reaction mixture was cooled to rt and concentrated under reduced pressure to give a brown residue. The residue was partitioned between EtOAc and water. The layers were separated. The aqueous layer was re-extracted with EtOAc. The organics were combined, dried through a phase separator and concentrated under reduced pressure to

give a yellow oil. The crude oil purified by silica column chromatography, eluted with a gradient of 0-100% EtOAc in cyclohexane. The appropriate fractions were concentrated under reduced pressure to give the title product [5.22] as a yellow oil (78.4 mg, 81%).

¹H NMR (400 MHz, CDCl₃) δ 7.20 (d, *J* = 8.6 Hz, 1H), 6.83 (d, *J* = 2.7 Hz, 1H), 6.80 (d, *J* = 12.7 Hz, 1H), 6.75 (dd, *J* = 8.6, 2.7 Hz, 1H), 5.92 (d, *J* = 12.7 Hz, 1H), 5.30 (br. s, 1H), 3.89 (q, *J* = 7.1 Hz, 2H), 3.80 (s, 3H), 3.73 (q, *J* = 7.1 Hz, 1H), 2.70 (d, *J* = 4.5 Hz, 3H), 1.49 (d, *J* = 7.1 Hz, 3H), 1.34 (t, *J* = 7.1 Hz, 3H). LCMS (ESI, High pH) t_R = 0.94 min, *m/z* 264 [M+H]⁺.

(*R*)-2-(2-Bromo-4-methoxyphenyl)-*N*-methylpropanamide [5.23]

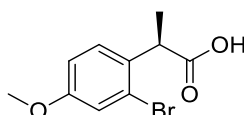


The crude (*R*)-2-(2-bromo-4-methoxyphenyl)propanoic acid [5.24] (5.53 g, 50% pure, 10.7 mmol) was taken in DMF (30 mL) and HATU (4.5 g, 11.7 mmol) and DIPEA (5.6 mL, 32.0 mmol) were added. The reaction mixture was stirred under nitrogen at rt for 5 min. A 2 M solution of methanamine in THF (13.3 mL, 26.7 mmol) was added and the reaction mixture was stirred at rt for 45 min. The reaction mixture was diluted with EtOAc and brine. The layers were separated. The aqueous layer was extracted with EtOAc. The organics were combined, washed with brine, dried through a phase separator and concentrated under reduced pressure to give a crude yellow oil. The crude product was purified by silica column chromatography, eluted with a gradient of 0-60% EtOAc in cyclohexane. The appropriate fractions were concentrated under reduced pressure to give the title product [5.23] as a yellow oil, in two batches (batch 1, 0.82 g, 23% and batch 2, 2.4 g, 58%).

Analysis of batch 2 (analysis of batch 1, matches the data reported below):

¹H NMR (400 MHz, CDCl₃) δ 7.33 (d, J = 8.8 Hz, 1H), 7.11 (d, J = 2.7 Hz, 1H), 6.87 (dd, J = 8.8, 2.7 Hz, 1H), 5.39 (br. s, 1H), 3.96 (q, J = 7.1 Hz, 1H), 3.79 (s, 3H), 2.76 (d, J = 4.9 Hz, 3H), 1.47 (d, J = 7.1 Hz, 3H). **LCMS** (ESI, High pH) t_R = 0.88 min, m/z 272/274 [M+H]⁺.

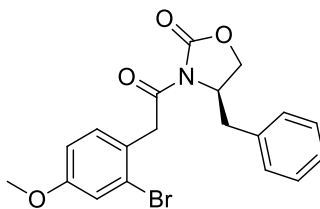
(R)-2-(2-Bromo-4-methoxyphenyl)propanoic acid [5.24]



A 35% aqueous solution of hydrogen peroxide (2 mL, 23.2 mmol) was added to a solution of lithium hydroxide (1.11 g, 46.3 mmol) in water (8 mL) at 0 °C and the solution was stirred for 5 min. This solution was added to a solution of (*R*)-4-benzyl-3-((*R*)-2-(2-bromo-4-methoxyphenyl)propanoyl) oxazolidin-2-one [**5.28**] (5.4 g, 11.6 mmol) in THF (20 mL) at 0 °C. The reaction mixture was stirred for 7 h at rt. A 35% aqueous solution of hydrogen peroxide (2 mL, 23.2 mmol) was added and the reaction mixture was further stirred at rt for 18 h. The reaction mixture was quenched with a 10% sodium thiosulfate solution and was concentrated under reduced pressure. The residual solution was diluted with EtOAc. The layers were separated. The aqueous layer was acidified to pH 1 with a 2 M aqueous solution of HCl and then extracted with EtOAc. The organics were combined, dried through a phase separator and concentrated under reduced pressure to give the title product [**5.24**] as a yellow solid (5.53 g, 50% pure, 92%). This product was used directly in the next step.

LCMS (ESI, High pH) t_R = 0.54 min, m/z 257/259 [M]⁻.

(R)-4-Benzyl-3-(2-(2-bromo-4-methoxyphenyl)acetyl)oxazolidin-2-one [5.27]



The procedures for the different conditions described in Table 6 are described hereafter. The NMR and LCMS analysis of all batches of intermediates **24-A** (different reaction conditions) are identical and are only reported on the largest batch (conditions for entry 2).

Conditions for entry 1 (Table 6)

A mixture of (*R*)-4-benzyloxazolidin-2-one **[5.10]** (1 g, 5.6 mmol), 2-(2-bromo-4-methoxyphenyl)acetic acid **[5.25]** (2.1 g, 8.5 mmol) and triethylamine (3.2 mL, 22.6 mmol) was suspended in toluene (15 mL) and stirred under nitrogen at 110 °C. Pivaloyl chloride (1.0 mL, 8.5 mmol) was dissolved in toluene (5 mL) then added to the reaction mixture. The reaction mixture was stirred under nitrogen at 110 °C for 4 h. The reaction mixture was diluted with methanol and concentrated under reduced pressure to give an orange oil. The residue was partitioned between EtOAc and a saturated solution of sodium bicarbonate. The layers were separated. The aqueous layer was re-extracted with EtOAc. The organic layers were combined, dried using a hydrophobic frit and evaporated under reduced pressure. The crude product was purified by silica column chromatography, eluted with a gradient of 0-100% EtOAc in cyclohexane. The relevant fractions were concentrated under reduced pressure to give the title compound **[5.27]** as an orange gum (1.1 g, 39%).

Conditions for entry 2 (Table 6)

2-(2-Bromo-4-methoxyphenyl)acetic acid [5.25] (25.3 g, 103 mmol), (*R*)-4-benzyloxazolidin-2-one [5.10] (12.4 g, 69.7 mmol) and triethylamine (40 mL, 287 mmol) were stirred in toluene (175 mL) under nitrogen at 80 °C for 5 min. Then, a solution of pivaloyl chloride (12.5 mL, 101 mmol) in toluene (25 mL) was added over 5 min to the reaction mixture at 80 °C. At the end of addition, the reaction mixture was heated at 110 °C for 24 h. The reaction mixture was concentrated under reduced pressure to give a brown oil. The oil was partitioned between EtOAc and a saturated solution of sodium bicarbonate. The layers were separated. The aqueous layer was re-extracted with EtOAc. The organic layers were combined, dried through a phase separator and concentrated under reduced pressure to give a yellow oil. The crude product was purified by silica column chromatography, eluted with a gradient of 0-60% EtOAc in cyclohexane. The relevant fractions were concentrated under reduced pressure to give the title compound [5.27] as a yellow oil (23.5 g, 75%).

¹H NMR (400 MHz, CDCl₃) δ 7.36-7.24 (m, 3H), 7.23-7.19 (m, 2H), 7.17 (d, *J* = 2.8 Hz, 1H), 7.16 (d, *J* = 2.8 Hz, 1H), 6.86 (dd, *J* = 8.6, 2.8 Hz, 1H), 4.75-4.64 (m, 1H), 4.42 (d, *J* = 18.2 Hz, 1H), 4.30 (d, *J* = 18.2 Hz, 1H), 4.25 (d, *J* = 7.8 Hz, 1H), 4.21 (dd, *J* = 9.3, 3.2 Hz, 1H), 3.80 (s, 3H), 3.35 (dd, *J* = 13.3, 3.2 Hz, 1H), 2.80 (dd, *J* = 13.3, 9.3 Hz, 1H). LCMS (ESI, High pH) *t*_R = 1.27 min, *m/z* 402/404 [M]⁻.

Conditions for entry 3 (Table 6)

2-(2-Bromo-4-methoxyphenyl)acetic acid [5.25] (2.1 g, 8.5 mmol), (*R*)-4-benzyloxazolidin-2-one [5.10] (1 g, 5.6 mmol) and triethylamine (3.2 mL, 22.6 mmol) were stirred in toluene (19 mL) under nitrogen at 80 °C. Then a solution of pivaloyl

chloride (1.0 mL, 8.5 mmol) in toluene (5 mL) was added dropwise to the reaction mixture at 80 °C. The reaction mixture was stirred for 1 h at 80 °C and 18 h at 100 °C. The reaction mixture was diluted with methanol and concentrated under reduced pressure to give a brown oil. The oil was partitioned between EtOAc and a saturated solution of sodium bicarbonate. The layers were separated. The aqueous layer was extracted with EtOAc. The organics were dried through a phase separator and concentrated under reduced pressure to give a yellow oil. The crude product was purified by silica column chromatography, eluted with a gradient of 0-100% EtOAc in cyclohexane. The relevant fractions were concentrated under reduced pressure to give the title compound **[5.27]** as a yellow oil (1.18 g, 44%).

Conditions for entry 4 (Table 6)

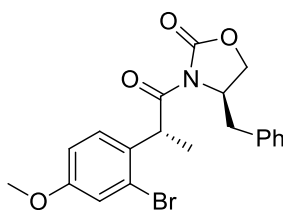
A mixture of (*R*)-4-benzyloxazolidin-2-one **[5.10]** (1 g, 5.6 mmol), 2-(2-bromo-4-methoxyphenyl)acetic acid **[5.25]** (2.8 g, 11.3 mmol) and triethylamine (3.2 mL, 22.6 mmol) was suspended in toluene (15 mL) and stirred under nitrogen at 110 °C. Pivaloyl chloride (1.0 mL, 8.5 mmol) was dissolved in toluene (5 mL) then added to the reaction mixture. The reaction mixture was stirred under nitrogen at 110 °C for 4 h. The reaction mixture was diluted with methanol and concentrated under reduced pressure to give an orange oil. The residue was partitioned between EtOAc and a saturated solution of sodium bicarbonate. The layers were separated. The aqueous layer was re-extracted with EtOAc. The organic layers were combined, dried using a hydrophobic frit and evaporated under reduced pressure. The crude product was purified by silica column chromatography, eluted with a gradient of 0-100% EtOAc in cyclohexane. The relevant fractions were concentrated under reduced pressure to give the title compound **[5.27]** as an orange gum (1.47 g, 58%).

Conditions for entry 5 (Table 6)

2-(2-Bromo-4-methoxyphenyl)acetic acid [5.25] (11.1 g, 45.1 mmol), (*R*)-4-benzyloxazolidin-2-one [5.10] (4 g, 22.6 mmol) and triethylamine (12.6 mL, 90 mmol) were stirred in toluene (75 mL) under nitrogen at 80 °C. Then a solution of pivaloyl chloride (4.2 mL, 33.9 mmol) in toluene (10 mL) was added dropwise to the reaction mixture at 80 °C. The reaction mixture was stirred at 110 °C for 20 h. The reaction mixture was diluted with methanol and concentrated under reduced pressure to give a brown oil. The oil was partitioned between EtOAc and a saturated solution of sodium bicarbonate. The layers were separated. The aqueous layer was extracted with EtOAc. The organics were dried through a phase separator and concentrated under reduced pressure to give a yellow oil. The crude product was purified by silica column chromatography, eluted with a gradient of 0-60% EtOAc in cyclohexane. The relevant fractions were concentrated under reduced pressure to give the title compound [5.27] as a yellow oil (6.83 g, 64%).

(*R*)-4-Benzyl-3-((*R*)-2-(2-bromo-4-methoxyphenyl)propanoyl)oxazolidin-2-one

[5.28]



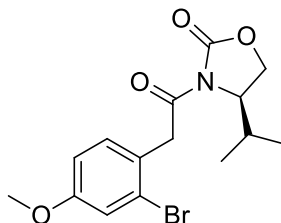
(*R*)-4-Benzyl-3-(2-(2-bromo-4-methoxyphenyl)acetyl)oxazolidin-2-one [5.27] (6.8 g, 14.4 mmol) was dissolved in THF (45 mL) under nitrogen and cooled to -78 °C. A 1 M solution of NaHMDS in THF (17.2 mL, 17.2 mmol) was added dropwise to the reaction mixture. The reaction mixture was stirred for 1.5 h at -78 °C. Methyl iodide (2.7 mL, 43.1 mmol) was added and the reaction mixture was stirred 1 h at -78 °C to

rt. The reaction mixture was quenched with a saturated solution of ammonium chloride. The organic solvent was concentrated under reduced pressure. The residual solution was extracted twice with EtOAc. The organic layers were combined, dried through a phase separator and concentrated under reduced pressure to give a yellow oil. The crude oil was dissolved in THF (45 mL) and cooled under nitrogen to -78 °C. Then a 1 M solution of NaHMDS in THF (17.2 mL, 17.2 mmol) was added dropwise and left to stir at -78 °C for 15 min. The mixture was allowed to warm up to rt for 15 min and then cooled to -78 °C. Methyl iodide (2.69 mL, 43.1 mmol) was added. The reaction mixture was allowed to slowly warm up to rt and was stirred for 6 h at rt. Methyl iodide (2.69 mL, 43.1 mmol) was added and the reaction was stirred overnight at rt. The reaction mixture was quenched with a saturated solution of ammonium chloride. The organic solvent was concentrated under reduced pressure. The residue was partitioned between EtOAc and water. The aqueous layer was extracted with EtOAc. The organic layers were combined, dried through a phase separator and concentrated under reduced pressure to give a yellow oil. The oil was purified by silica column chromatography, eluted with a gradient of 0-80% EtOAc in cyclohexane. The fractions were concentrated under reduced pressure to give the title product **[5.28]** as a yellow oil (5.38 g, 81%, 86% d.e. by ¹H NMR).

¹H NMR (400 MHz, CDCl₃) δ 7.36-7.20 (m, 6H), 7.12 (d, *J* = 2.7 Hz, 1H), 6.86 (dd, *J* = 8.6, 2.7 Hz, 1H), 5.27 (q, *J* = 7.1 Hz, 1H), 4.71-4.63 (m, 1H), 4.16 (d, *J* = 5.1 Hz, 2H), 3.78 (s, 3H), 3.32 (dd, *J* = 13.3, 3.3 Hz, 1H), 2.80 (dd, *J* = 13.3, 9.7 Hz, 1H), 1.55 (d, *J* = 6.8 Hz, 3H). NMR showed 7% of the other diastereomer (*R*)-4-benzyl-3-((*S*)-2-(2-bromo-4-methoxyphenyl)propanoyl)oxazolidin-2-one. This ratio was determined

at the benzylic CH₃ doublet at 1.55 ppm (major diastereomer) and 1.51 ppm (minor diastereomer). LCMS (ESI, High pH) t_R = 1.33 min, m/z 418/420 [M+H]⁺.

(R)-3-(2-(2-Bromo-4-methoxyphenyl)acetyl)-4-isopropylloxazolidin-2-one [5.30]

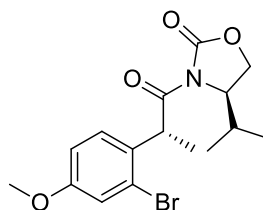


2-(2-Bromo-4-methoxyphenyl)acetic acid [5.25] (1.42 g, 5.8 mmol), (*R*)-4-isopropylloxazolidin-2-one [5.29] (0.5 g, 3.9 mmol) and triethylamine (1.6 mL, 11.6 mmol) and pivaloyl chloride (0.7 mL, 5.8 mmol) were mixed in toluene (11 mL) under nitrogen at rt. The reaction mixture was heated at 110 °C for 24 h. The reaction mixture was concentrated under reduced pressure to give a brown oil. The oil was partitioned between EtOAc and a saturated solution of sodium bicarbonate. The layers were separated. The aqueous layer was re-extracted with EtOAc. The organic layers were combined, dried through a phase separator and concentrated under reduced pressure to give a yellow oil. The crude product was purified by silica column chromatography, eluted with a gradient of 0-70% EtOAc in cyclohexane. The relevant fractions were concentrated under reduced pressure to give the title product [5.30] as a yellow oil (0.47 g, 30%).

¹H NMR (400 MHz, CDCl₃) δ 7.14-7.11 (m, 2H), 6.82 (dd, *J* = 8.6, 2.7 Hz, 1H), 4.47-4.38 (m, 2H), 4.30 (d, *J* = 9.1 Hz, 1H), 4.26 (d, *J* = 4.2 Hz, 1H), 4.22 (dd, *J* = 9.1, 3.2 Hz, 1H), 3.76 (s, 3H), 2.45-2.33 (m, 1H), 0.91 (d, *J* = 4.4 Hz, 3H), 0.89 (d, *J* = 4.7 Hz, 3H). LCMS (ESI, High pH) t_R = 1.21 min, m/z 356/358 [M+H]⁺.

(R)-4-Benzyl-3-((R)-2-(2-bromo-4-methoxyphenyl)propanoyl)oxazolidin-2-one

[5.31]



(R)-3-(2-(2-Bromo-4-methoxyphenyl)acetyl)-4-isopropoxyloxazolidin-2-one [5.30]

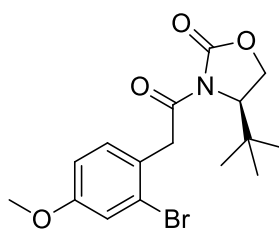
(0.27 g, 0.69 mmol) was dissolved in THF (3.5 mL) under nitrogen and was cooled to -78 °C. A 1 M solution of NaHMDS in THF (0.83 mL, 0.83 mmol) was added and the reaction mixture was stirred 5 min at -78 °C, then the reaction mixture was allowed to warm up to rt for 15 min. The reaction mixture was then cooled to -78 °C and methyl iodide (0.13 mL, 2.1 mmol) was added. The reaction mixture was stirred 30 min at -78 °C and 2 h whilst the acetone-dry ice bath was allowed to warm up to rt. The reaction mixture was quenched with a saturated solution of ammonium chloride. The organic solvent was removed under reduced pressure. The residual suspension was partitioned between EtOAc and water. The layers were separated. The aqueous layer was re-extracted with EtOAc. The organic layers were combined, dried through a phase separator and concentrated under reduced pressure to give a yellow oil. The crude oil was purified by silica column chromatography, eluted with a gradient 0-100% EtOAc in cyclohexane. The appropriate fractions were concentrated under reduced pressure to give the title product [5.31] as a yellow oil (0.11 g, 39%, 80% d.e. by ¹H NMR).

¹H NMR (400 MHz, CDCl₃) δ 7.20 (d, *J* = 8.6 Hz, 1H), 7.12 (d, *J* = 2.7 Hz, 1H), 6.85 (dd, *J* = 8.6, 2.7 Hz, 1H), 5.30 (q, *J* = 7.1 Hz, 1H), 4.46-4.42 (m, 1H), 4.27-4.18 (m, 2H), 3.78 (s, 3H), 2.44-2.34 (m, 1H), 1.54 (d, *J* = 7.1 Hz, 3H), 0.93 (d, *J* = 3.5 Hz, 3H),

0.91 (d, $J = 3.5$ Hz, 3H). NMR showed 10% of the other diastereomer (*R*)-4-benzyl-3-((*S*)-2-(2-bromo-4-methoxyphenyl)propanoyl)oxazolidin-2-one. This ratio was determined at the benzylic CH₃ signal at 1.54 ppm (major diastereomer) and 1.46 ppm (minor diastereomer). LCMS (ESI, High pH) $t_R = 1.29$ min, m/z 370/372 [M+H]⁺.

(*R*)-3-(2-(2-Bromo-4-methoxyphenyl)acetyl)-4-(*tert*-butyl)oxazolidin-2-one

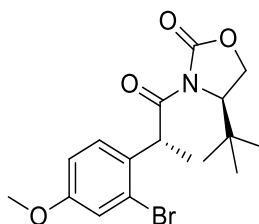
[5.33]



2-(2-Bromo-4-methoxyphenyl)acetic acid **[5.25]** (1.3 g, 5.2 mmol), (*R*)-4-(*tert*-butyl)oxazolidin-2-one **[5.32]** (0.5 g, 3.5 mmol), triethylamine (1.5 mL, 10.5 mmol) and pivaloyl chloride (0.6 mL, 5.2 mmol) were mixed in toluene (11 mL) under nitrogen at rt. The reaction mixture was heated at 110 °C for 24 h. The reaction mixture was concentrated under reduced pressure to give a brown oil. The oil was partitioned between EtOAc and a saturated solution of sodium bicarbonate. The layers were separated. The aqueous layer was re-extracted with EtOAc. The organic layers were dried through a phase separator and concentrated under reduced pressure to give a yellow oil. The crude product was purified by silica column chromatography, eluted with a gradient of 0-60% EtOAc in cyclohexane. The relevant fractions were concentrated under reduced pressure to give the title product as a yellow oil (0.55 g, 30% yield, 70% pure). The product was purified by silica column chromatography, eluted with a gradient of 0-40% EtOAc in cyclohexane. The relevant fractions were concentrated under reduced pressure to give the title product **[5.33]** as a yellow oil (235 mg, 17%).

¹H NMR (400 MHz, CDCl₃) δ 7.14-7.11 (m, 2H), 6.82 (dd, *J* = 8.4, 2.7 Hz, 1H), 4.44-4.37 (m, 2H), 4.31-4.22 (m, 3H), 3.75 (s, 3H), 0.93 (s, 9H). LCMS (ESI, High pH) *t*_R = 1.27 min, *m/z* 370/372 [M+H]⁺.

(*R*)-3-((*R*)-2-(2-Bromo-4-methoxyphenyl)propanoyl)-4-(*tert*-butyl)oxazolidin-2-one [5.34]



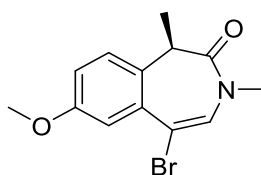
(*R*)-3-(2-(2-Bromo-4-methoxyphenyl)acetyl)-4-(*tert*-butyl)oxazolidin-2-one [5.33]

(131 mg, 0.32 mmol) was dissolved in THF (10 mL) under nitrogen and was cooled to -78 °C. A 1 M solution of NaHMDS in THF (0.38 mL, 0.38 mmol) was added. The reaction mixture was stirred 5 min at -78 °C, then was allowed to warm up to rt for 10 min. The reaction mixture was then cooled to -78 °C and methyl iodide (0.06 mL, 0.96 mmol) was added. The reaction mixture was stirred 30 min at -78 °C and 2 h whilst the acetone-dry ice bath was allowed to warm up to rt. The reaction mixture was quenched with a saturated solution of ammonium chloride. The organic solvent was removed under reduced pressure. The reaction mixture was partitioned between EtOAc and water. The layers were separated. The aqueous layer was re-extracted with EtOAc. The organics were dried through a phase separator and concentrated under reduced pressure to give a yellow oil. The crude product was purified by silica column chromatography, eluted with a gradient 0-100% EtOAc in cyclohexane. The appropriate fractions were concentrated under reduced pressure to give the title product [5.34] as a yellow oil (75 mg, 55%).

¹H NMR (400 MHz, CDCl₃) δ 7.23 (d, *J* = 8.6 Hz, 1H), 7.11 (d, *J* = 2.6 Hz, 1H), 6.86 (dd, *J* = 8.6, 2.6 Hz, 1H), 5.30 (q, *J* = 7.3 Hz, 1H), 4.44 (dd, *J* = 7.4, 1.5 Hz, 1H), 4.29 (dd, *J* = 9.2, 1.5 Hz, 1H), 4.29 (dd, *J* = 9.2, 7.4 Hz, 1H), 3.78 (s, 3H), 1.60 (d, *J* = 7.3 Hz, 3H), 0.95 (s, 9H). None of the opposite diastereomer was observed by ¹H NMR or LCMS. LCMS (ESI, High pH) t_R = 1.34 min, *m/z* 384/386 [M+H]⁺.

(*R*)-5-Bromo-7-methoxy-1,3-dimethyl-1,3-dihydro-2*H*-benzo[*d*]azepin-2-one

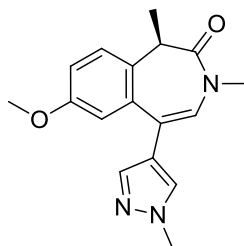
[5.35]



(*R*)-7-Methoxy-1,3-dimethyl-1,3-dihydro-2*H*-benzo[*d*]azepin-2-one **[5.08]** (5.1 g, 23.5 mmol) and PTT (9.3 g, 24.7 mmol) were stirred in MeCN (67 mL) under nitrogen at rt for 30 min. The reaction mixture was concentrated under reduced pressure. The residual orange oil was partitioned between EtOAc and water. The layers were separated. The aqueous layer was re-extracted with EtOAc. The organic layers were combined, dried through a phase separator and concentrated under reduced pressure to give a yellow solid. The product was purified by silica column chromatography eluted with a gradient of 0-50% EtOAc in cyclohexane. The appropriate fractions were concentrated under reduced pressure to give the desired product **[5.35]** as a white solid (6.72 g, 92%)

¹H NMR (400 MHz, CDCl₃) δ 7.22 (d, *J* = 2.7 Hz, 1H), 7.20 (d, *J* = 8.8 Hz, 1H), 7.01 (dd, *J* = 8.8, 2.7 Hz, 1H), 6.82 (s, 1H), 3.83 (s, 3H), 3.32 (q, *J* = 6.8 Hz, 1H), 3.07 (s, 3H), 1.63 (d, *J* = 6.8 Hz, 3H). LCMS (ESI, high pH) t_R = 1.13 min, *m/z* 296/298 [M+H]⁺.

(R)-7-Methoxy-1,3-dimethyl-5-(1-methyl-1H-pyrazol-4-yl)-1,3-dihydro-2H-benzo[d]azepin-2-one [5.37]

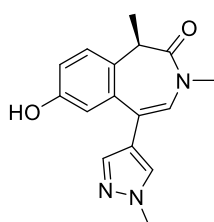


(R)-5-Bromo-7-methoxy-1,3-dimethyl-1,3-dihydro-2H-benzo[d]azepin-2-one [5.35] (2 g, 6.8 mmol), (1-methyl-1H-pyrazol-4-yl)boronic acid [5.36] (1.7 g, 13.5 mmol), potassium carbonate (1.9 g, 13.5 mmol) and Pd(PPh₃)₄ (0.39 g, 0.34 mmol) were suspended in water (5 mL) and 1,4-dioxane (50 mL). The reaction mixture was heated under nitrogen at 120 °C for 2 h. (1-Methyl-1H-pyrazol-4-yl)boronic acid [5.36] (0.85 g, 6.75 mmol) was added to the reaction mixture. The reaction mixture was stirred under nitrogen at 120 °C for 30 min. The reaction mixture was concentrated under reduced pressure. EtOAc and water were added to the residue. The layers were separated, the aqueous layer was re-extracted with EtOAc. The organic layers were combined, dried using a hydrophobic frit and evaporated under reduced pressure. The sample was purified by silica column chromatography, eluted with a gradient of 0-100% EtOAc in cyclohexane. The appropriate fractions were combined and concentrated under reduced pressure to give the desired product [5.37] as a white solid (1.76 g, 79% yield).

¹H NMR (400 MHz, CDCl₃) δ 7.56 (s, 1H), 7.36 (s, 1H), 7.27 (d, *J* = 8.8 Hz, 1H), 7.00 (dd, *J* = 8.8, 2.7 Hz, 1H), 6.88 (d, *J* = 2.7 Hz, 1H), 6.56 (s, 1H), 3.92 (s, 3H), 3.74 (s, 3H), 3.35 (q, *J* = 7.0 Hz, 1H), 3.10 (s, 3H), 1.65 (d, *J* = 7.0 Hz, 3H). ¹³C NMR (101 MHz, CDCl₃) δ 170.9 (C=O), 157.8 (C_{iv}), 138.0 (CH), 136.4 (C_{iv}), 130.5 (C_{iv}), 129.0 (CH), 126.5 (CH), 125.1 (CH), 122.0 (C_{iv}), 121.6 (C_{iv}), 115.4 (CH), 112.5 (CH), 55.5

(CH₃), 40.3 (CH), 39.1 (CH₃), 35.1 (CH₃), 12.8 (CH₃). **LCMS** (ESI, high pH) t_R = 0.87 min, m/z 298 [M+H]⁺. **HRMS** (ESI) calculated for C₁₇H₂₀N₃O₂ [M+H]⁺ 298.1556, found 298.1569 (3.62 min). ν_{max} (neat, cm⁻¹): 3085 (CH alkene), 2938 (CH alkane), 1649 (C=O amide), 1609 (C=C alkene). $[\alpha_D]^{20.5}_{589\text{ nm}}$ (c 0.500, MeOH): +298.7°. **m.p.** = 129-131 °C.

((R)-7-Hydroxy-1,3-dimethyl-5-(1-methyl-1H-pyrazol-4-yl)-1,3-dihydro-2H-benzo[d]azepin-2-one [5.38]

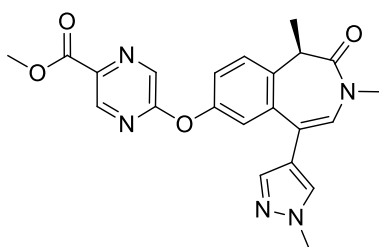


A solution of (*R*)-7-methoxy-1,3-dimethyl-5-(1-methyl-1*H*-pyrazol-4-yl)-1,3-dihydro-2*H*-benzo[*d*]azepin-2-one [5.37] (6.98 g, 20 mmol) in DCM (67 mL) was cooled to -78 °C under a nitrogen atmosphere. A 1 M solution of BBr₃ in DCM (49.9 mL, 49.9 mmol) was added dropwise to the reaction mixture. The reaction mixture was stirred at -78 °C for 1 h, and then was allowed to slowly warm up to rt and stirred for 2 h. The reaction mixture was cooled to -78 °C then a 1 M solution of BBr₃ in DCM (9.9 mL, 9.9 mmol) was added and the reaction mixture was left to stir at -78 °C for 15 min then allowed to slowly warm to rt and stirred for 18 h. The reaction mixture was cooled to 0 °C, quenched with water and diluted with DCM. EtOAc was added to dissolve the solid. The layers were separated. The aqueous layer was re-extracted with EtOAc. The organic layers were combined, dried using a hydrophobic frit and evaporated under reduced pressure to give the desired product [5.38] as an orange solid (7.5 g, 70% pure, 93% yield).

¹H NMR (400 MHz, DMSO-*d*₆) δ 7.73 (s, 1H), 7.56 (s, 1H), 7.10 (d, *J* = 8.6 Hz, 1H),

6.86 (dd, $J = 8.6, 2.7$ Hz, 1H), 6.79 (s, 1H), 6.73 (d, $J = 2.7$ Hz, 1H), 5.72 (br. s, 1H) 3.84 (s, 3H), 3.21 (q, $J = 6.9$ Hz, 1H), 3.00 (s, 3H), 1.47 (d, $J = 6.9$ Hz, 3H). NMR showed an impurity in the aromatic region. LCMS (ESI, high pH) $t_R = 0.73$ min, m/z 284 $[M+H]^+$.

Methyl (*R*)-5-((1,3-dimethyl-5-(1-methyl-1*H*-pyrazol-4-yl)-2-oxo-2,3-dihydro-1*H*-benzo[*d*]azepin-7-yl)oxy)pyrazine-2-carboxylate [5.40]

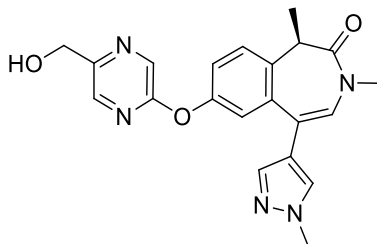


To a mixture of (*R*)-7-hydroxy-1,3-dimethyl-5-(1-methyl-1*H*-pyrazol-4-yl)-1,3-dihydro-2*H*-benzo[*d*]azepin-2-one [5.38] (2.77 g, 6.9 mmol) in DMF (30 mL), was added methyl 5-chloropyrazine-2-carboxylate [5.39] (1.42 g, 8.2 mmol) and potassium carbonate (1.9 g, 13.7 mmol). The reaction mixture was stirred at 110 °C under nitrogen for 1 h. The mixture was concentrated under reduced pressure. EtOAc and water were added. The layers were separated, the aqueous layer was re-extracted with EtOAc. The organic layers were combined, dried using a hydrophobic frit and concentrated under reduced pressure to give the crude product as a brown oil. The sample was purified by silica column chromatography, eluted with a gradient of 0-16% EtOH in EtOAc. The appropriate fractions were combined and concentrated under reduced pressure to give the title product [5.40] as a beige solid (2.5 g, 69% yield).

¹H NMR (400 MHz, CDCl₃) δ 8.81 (d, $J = 1.2$ Hz, 1H), 8.46 (d, $J = 1.2$ Hz, 1H), 7.54 (s, 1H), 7.45 (d, $J = 8.6$ Hz, 1H), 7.37 (s, 1H), 7.28-7.24 (m, 1H)*, 7.17 (d, $J = 2.5$ Hz,

1H), 6.62 (s, 1H), 4.00 (s, 3H), 3.90 (s, 3H), 3.40 (q, $J = 6.9$ Hz, 1H), 3.14 (s, 3H), 1.71 (d, $J = 6.9$ Hz, 3H). *This signal is perturbed by the residual solvent peak. LCMS (ESI, high pH) $t_R = 0.91$ min, m/z 420 $[M+H]^+$.

(R)-7-((5-(Hydroxymethyl)pyrazin-2-yl)oxy)-1,3-dimethyl-5-(1-methyl-1H-pyrazol-4-yl)-1,3-dihydro-2H-benzo[d]azepin-2-one [5.41]



Reduction with NaBH₄:

To a flask containing methyl (R)-5-((1,3-dimethyl-5-(1-methyl-1H-pyrazol-4-yl)-2-oxo-2,3-dihydro-1H-benzo[d]azepin-7-yl)oxy)pyrazine-2-carboxylate [5.40] (2.49 g, 4.75 mmol) in THF (20 mL) was added sodium borohydride (0.36 g, 9.5 mmol) and the reaction mixture was stirred at rt for 5 min. Methanol (10 mL) was added and the reaction mixture was heated under nitrogen at 70 °C for 45 min. Sodium borohydride (0.36 g, 9.5 mmol) was added and the reaction mixture was stirred at rt under nitrogen for 16 h. Sodium borohydride (0.36 g, 9.5 mmol) was added and the reaction mixture was heated under nitrogen at 70 °C for 3 h (until full consumption of the starting material, monitored by LCMS). The reaction was quenched with *i*PrOH and water and concentrated under reduced pressure. EtOAc and water were added. The layers were separated, the aqueous layer was re-extracted with EtOAc. The organic layers were combined, dried using a hydrophobic frit and evaporated under reduced pressure. The sample was loaded in DCM and purified by silica column chromatography, eluted with a gradient of 0-12.5% EtOH in EtOAc. The appropriate fractions were combined and

evaporated under reduced pressure to give the title product **[5.41]** as a yellow gum (0.23 g, 70% pure, 9% yield) and side-product **[5.38]** as a yellow solid (0.78 g, 53% yield).

Analysis of product **[5.41]**: **¹H NMR** (400 MHz, CDCl₃) δ 8.33 (d, J = 1.2 Hz, 1H), 8.12 (s, 1H), 7.54 (s, 1H), 7.42 (d, J = 8.6 Hz, 1H), 7.36 (s, 1H), 7.23 (dd, J = 8.6, 2.5 Hz, 1H), 7.14 (d, J = 2.5 Hz, 1H), 6.60 (s, 1H), 4.77 (s, 2H), 3.89 (s, 3H), 3.40 (q, J = 6.9 Hz, 1H), 3.13 (s, 3H), 2.82 (br. s, 1H), 1.69 (d, J = 6.9 Hz, 3H). The signal for the exchangeable proton was not observed. **LCMS** (ESI, High pH) t_R = 0.79 min, m/z 392 [M+H]⁺.

Product **[5.38]**: NMR and LCMS are consistent with data reported above.

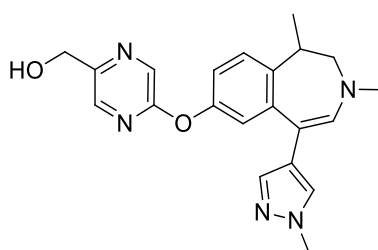
Reduction with DIBAL: To a solution of methyl (*R*)-5-((1,3-dimethyl-5-(1-methyl-1*H*-pyrazol-4-yl)-2-oxo-2,3-dihydro-1*H*-benzo[*d*]azepin-7-yl)oxy)pyrazine-2-carboxylate **[5.40]** (937 mg, 2.0 mmol) in THF (15 mL) at -78 °C, was added dropwise a 1 M solution of DIBAL in THF (4.0 mL, 4.0 mmol). The reaction mixture was stirred under nitrogen for 17 h whilst warming up from -78 °C to rt. A 1 M solution of DIBAL in THF (4.0 mL, 4.0 mmol) was added at -78 °C and the reaction mixture was stirred under nitrogen at rt for 3 h. A 1 M solution of DIBAL in THF (4.0 mL, 4.0 mmol) was added at -78 °C and the reaction mixture was stirred under nitrogen at rt for 2 h. A saturated aqueous solution of sodium potassium tartrate tetrahydrate was added and the reaction mixture was stirred at rt overnight. Water and EtOAc were added. The layers were separated, the aqueous layer was re-extracted with EtOAc. The organic layers were combined, dried using a hydrophobic frit and evaporated under reduced pressure. The sample was purified by silica column chromatography, eluted with a gradient of 0-12.5% EtOH in EtOAc. The appropriate fractions were combined and

evaporated under reduced pressure to give the desired product **[5.41]** and a side-product **[5.44]** (28.3 mg, 4% yield). The desired product was purified by MDAP (high pH, extended method B). The solvent was concentrated under reduced pressure to give the title product **[5.41]** as a yellow gum (46.7 mg, 6% yield).

Product **[5.41]**: NMR and LCMS are consistent with data reported above.

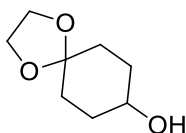
Analysis of product **[5.44]**:

(5-((1,3-Dimethyl-5-(1-methyl-1*H*-pyrazol-4-yl)-2,3-dihydro-1*H*-benzo[*d*]azepin-7-yl)oxy)pyrazin-2-yl)methanol [5.44]



¹H NMR (400 MHz, CDCl₃) δ 8.24 (d, $J = 1.2$ Hz, 1H), 8.12 (d, $J = 1.2$ Hz, 1H), 7.36 (s, 1H), 7.21 (s, 1H), 7.07 (d, $J = 8.1$ Hz, 1H), 6.93 (d, $J = 2.5$ Hz, 1H), 6.73 (dd, $J = 8.1, 2.5$ Hz, 1H), 6.30 (s, 1H), 4.74 (d, $J = 2.9$ Hz, 2H), 3.84 (s, 3H), 3.40-3.39 (m, 1H), 3.31-3.24 (m, 2H), 3.01 (s, 3H), 1.37 (d, $J = 6.6$ Hz, 3H). The signal for the exchangeable proton was not observed. **LCMS** (ESI, High pH) $t_R = 1.02$ min, m/z 378 [M+H]⁺. Due to instability over time of the sample in the NMR tube, further analysis of the compound was not carried out. Chiral analysis of the sample was not carried out, this compound has therefore arbitrarily been drawn as racemic.

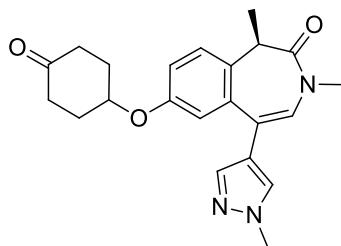
1,4-Dioxaspiro[4.5]decan-8-ol [5.46]⁸⁰



1,4-Dioxaspiro[4.5]decan-8-one **[5.45]** (3 g, 19.21 mmol) was dissolved in methanol (40 mL) under nitrogen at 0 °C. Sodium borohydride (1.1 g, 28.8 mmol) was added

and the reaction mixture was stirred for 20 min. The reaction was monitored by TLC (consumption of the starting material, using a dinitrophenylhydrazine dip). After 2 h of reaction, the reaction mixture was concentrated under reduced pressure to give a white residual suspension. The material was partitioned between EtOAc and water. The layers were separated. The aqueous layer was re-extracted with EtOAc. The organic layers were combined, dried through a phase separator and concentrated under reduced pressure to give the title product **[5.46]** as a colourless oil (2.78 g, 84% yield). $^1\text{H NMR}$ (400 MHz, CDCl_3) δ 3.97-3.90 (m, 4H), 3.83-3.76 (m, 1H), 1.92-1.77 (m, 4H), 1.71-1.53 (m, 4H). The signal for the exchangeable proton was not observed. LCMS (ESI, high pH) $t_R = 0.58$ min, weak ionisation.

(R)-1,3-Dimethyl-5-(1-methyl-1H-pyrazol-4-yl)-7-((4-oxocyclohexyl)oxy)-1,3-dihydro-2H-benzo[d]azepin-2-one [5.47]

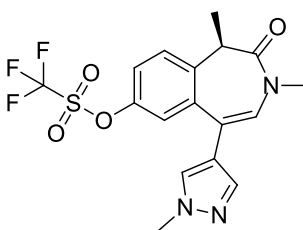


(R)-7-Hydroxy-1,3-dimethyl-5-(1-methyl-1H-pyrazol-4-yl)-1,3-dihydro-2H-benzo[d]azepin-2-one **[5.38]** (250 mg, 0.62 mmol), 1,4-dioxaspiro[4.5]decan-8-ol **[5.46]** (160 mg, 1.0 mmol) and CTBP (224 mg, 0.93 mmol) were heated in toluene (2 mL) under nitrogen at 100 °C for 30 min in the microwave. No product was observed by LCMS. To the reaction mixture was added 1,4-dioxaspiro[4.5]decan-8-ol **[5.46]** (160 mg, 1.0 mmol) and CTBP (224 mg, 0.93 mmol). The reaction mixture was heated at 120 °C for 45 min in the microwave. The reaction mixture was concentrated under reduced pressure. The residue was partitioned between EtOAc and water. The layers

were separated. The aqueous layer was re-extracted with EtOAc. The organic layers were combined, dried through a hydrophobic frit and concentrated under reduced pressure to give a brown oil. The oil was dissolved in a 2 M aqueous solution of HCl (5 mL) and acetone (5 mL) stirred at rt for 2 h and then at 60 °C for 3 h. Then HCl (24% v/v, 3 mL) was added and the reaction mixture was stirred at rt for 1 h and left to stand for 18 h at rt. The reaction mixture was concentrated under reduced pressure to give a dark brown oil. The material was purified by MDAP (formic, extended method B). The appropriate fractions were concentrated under reduced pressure to give the title product [5.47] as a colourless oil (80 mg, 31% yield).

¹H NMR (400 MHz, CDCl₃) δ 7.55 (s, 1H), 7.39 (s, 1H), 7.29 (d, *J* = 8.8 Hz, 1H), 7.06 (dd, *J* = 8.7, 2.7 Hz, 1H), 6.92 (d, *J* = 2.7 Hz, 1H), 6.57 (s, 1H), 4.60 (br. s, 1H), 3.94 (s, 3H), 3.36 (q, *J* = 6.9 Hz, 1H), 3.11 (s, 3H), 2.71-2.58 (m, 2H), 2.34-2.17 (m, 4H), 2.07-1.95 (m, 2H), 1.66 (d, *J* = 6.9 Hz, 3H). LCMS (ESI, formic) t_R = 0.90 min, *m/z* 380 [M+H]⁺.

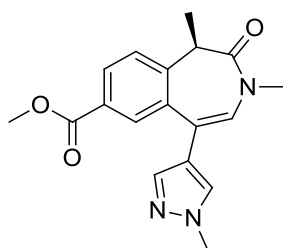
(*R*)-1,3-Dimethyl-5-(1-methyl-1*H*-pyrazol-4-yl)-2-oxo-2,3-dihydro-1*H*-benzo[*d*]azepin-7-yl trifluoromethanesulfonate [5.48]



(*R*)-7-Hydroxy-1,3-dimethyl-5-(1-methyl-1*H*-pyrazol-4-yl)-1,3-dihydro-2*H*-benzo[*d*]azepin-2-one [5.38] (798 mg, 2.8 mmol) and NEt₃ (1.2 mL, 8.5 mmol) were dissolved in DCM (9 mL) under nitrogen at 0 °C. PhN(Tf)₂ (1.2 g, 3.4 mmol) was added and the reaction mixture was stirred 10 min at 0 °C and 2.5 h at rt. The reaction mixture was quenched with a mixture of ice-water. DCM was added and the layers

were separated. The aqueous layer was extracted with DCM. The organic layers were combined, dried through a hydrophobic frit and concentrated under reduced pressure to give a yellow oil. The crude was purified by silica column chromatography, eluted with 0-100% EtOAc in cyclohexane. The relevant fractions were concentrated under reduced pressure to give the title product **[5.48]** as a white foam (803 mg, 62% yield). $^1\text{H NMR}$ (400 MHz, MeOD) δ 7.66 (s, 1H), 7.55 (s, 1H), 7.51 (d, $J = 8.7$ Hz, 1H), 7.43 (dd, $J = 8.7, 2.7$ Hz, 1H), 7.29 (d, $J = 2.7$ Hz, 1H), 6.90 (s, 1H), 3.90 (s, 3H), 3.44 (q, $J = 6.9$ Hz, 1H), 3.10 (s, 3H), 1.63 (d, $J = 6.9$ Hz, 3H). **LCMS** (ESI, High pH) $t_R = 1.11$ min, m/z 416 $[\text{M}+\text{H}]^+$.

Methyl (*R*)-1,3-dimethyl-5-(1-methyl-1*H*-pyrazol-4-yl)-2-oxo-2,3-dihydro-1*H*-benzo[*d*]azepine-7-carboxylate [5.49]



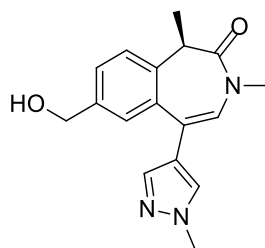
(*R*)-1,3-Dimethyl-5-(1-methyl-1*H*-pyrazol-4-yl)-2-oxo-2,3-dihydro-1*H*-benzo[*d*]azepin-7-yl trifluoromethanesulfonate **[5.48]** (0.80 g, 1.9 mmol), Pd(OAc)₂ (0.04 g, 0.19 mmol) and Xantphos (0.11 g, 0.19 mmol) were suspended in a sealed round bottom flask in DMF (12 mL). The flask was purged with a vacuum-nitrogen cycle 3 times. Methanol (12 mL) and NEt₃ (0.8 mL, 5.8 mmol) were added. The nitrogen atmosphere was replaced by a CO atmosphere by bubbling CO into the solution (with an exit needle in the septum) for 5 min. Then the exit needle was removed and the needle of CO gas was taken out of the solution, but kept in the flask to maintain the CO-atmosphere. The reaction mixture was heated at 60 °C for 3 h.

Pd(OAc)₂ (0.04 g, 0.19 mmol) and Xantphos (0.11 g, 0.19 mmol) were added to the reaction mixture. The flask was purged with a vacuum-nitrogen cycle 3 times. The nitrogen atmosphere was replaced by a CO atmosphere as described above. The reaction mixture was heated at 60 °C for 3 h. The reaction mixture was left to stand at rt for 18 h. Pd(OAc)₂ (0.04 g, 0.19 mmol) was added. The flask was purged with a vacuum-nitrogen cycle 3 times. The nitrogen atmosphere was replaced by a CO atmosphere as described above. The reaction mixture was heated at 60 °C for 4 h. The reaction mixture was concentrated under reduced pressure. The residue was diluted in EtOAc and washed with a 1 M aqueous lithium chloride solution. The layers were separated, the aqueous layer was reextracted with EtOAc. The organic layers were concentrated under reduced pressure. The crude product was purified by silica column chromatography, eluted with a gradient of 0-100% of EtOAc in cyclohexane. The relevant fractions were concentrated under reduced pressure to give the title product **[5.49]** as a yellow oil (383 mg, 52% yield) and some recovered starting material **[5.48]** as a yellow oil in two batches (71.2 mg, 8% yield and 60.8 mg, 6% yield)).

Desired product [5.49]: ¹H NMR (400 MHz, CDCl₃) δ 8.07 (dd, *J* = 8.2, 1.6 Hz, 1H), 8.04 (d, *J* = 1.6 Hz, 1H), 7.56 (s, 1H), 7.44 (d, *J* = 8.2 Hz, 1H), 7.33 (s, 1H), 6.64 (s, 1H), 3.93 (s, 3H), 3.88 (s, 3H), 3.44 (q, *J* = 6.9 Hz, 1H), 3.11 (s, 3H), 1.70 (d, *J* = 6.9 Hz, 3H). LCMS (ESI, High pH) *t*_R = 0.89 min, *m/z* 326 [M+H]⁺.

Recovered starting material [5.48]: analysis matches previous batch described above.

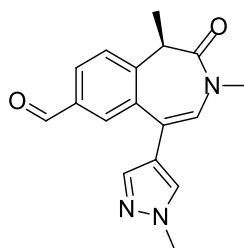
(R)-7-(Hydroxymethyl)-1,3-dimethyl-5-(1-methyl-1H-pyrazol-4-yl)-1,3-dihydro-2H-benzo[d]azepin-2-one [5.50]



Methyl (R)-1,3-dimethyl-5-(1-methyl-1H-pyrazol-4-yl)-2-oxo-2,3-dihydro-1H-benzo[d]azepine-7-carboxylate [5.49] (383 mg, 1.0 mmol) was dissolved in THF under nitrogen. Lithium borohydride (43.6 mg, 2.0 mmol) was added and the reaction mixture was stirred at 55 °C for 18 h. The reaction mixture was quenched with methanol and concentrated under reduced pressure to give a black oil. The oil was dissolved in EtOAc and water. The layers were separated. The aqueous layer was re-extracted with EtOAc. The organic layers were combined, dried through a phase separator and concentrated under reduced pressure to give the title product [5.50] as a white foam (293.6 mg, 94% yield).

¹H NMR (400 MHz, CDCl₃) δ 7.54 (s, 1H), 7.42-7.46 (dd, *J* = 8.1, 1.5 Hz, 1H), 7.39-7.34 (m, 3H), 6.58 (s, 1H), 4.66 (d, *J* = 5.6 Hz, 2H), 3.93 (s, 3H), 3.39 (q, *J* = 6.8 Hz, 1H), 3.10 (s, 3H), 1.68 (d, *J* = 6.8 Hz, 3H). The signal for the exchangeable proton was not observed. LCMS (ESI, High pH) *t*_R = 0.71 min, *m/z* 298 [M+H]⁺.

((R)-1,3-Dimethyl-5-(1-methyl-1H-pyrazol-4-yl)-2-oxo-2,3-dihydro-1H-benzo[d]azepine-7-carbaldehyde [5.51]

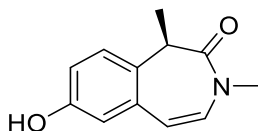


(R)-7-(Hydroxymethyl)-1,3-dimethyl-5-(1-methyl-1H-pyrazol-4-yl)-1,3-dihydro-2H-benzo[d]azepin-2-one [5.50] (293 mg, 0.99 mmol) and DMP (627 mg, 1.5 mmol) were stirred in DCM (5 mL) under nitrogen at 20 °C for 15 min. The reaction mixture was quenched with a saturated solution of sodium bicarbonate and diluted with DCM. The aqueous layer was extracted twice with DCM. The organic layers were combined, dried through a phase separator and concentrated under reduced pressure to give a yellow oil. The crude product was purified by silica column chromatography, eluted with a gradient of 0-100% EtOAc in cyclohexane, followed by 0-25% EtOH in EtOAc. The relevant fractions were concentrated under reduced pressure to give a yellow oil. The product was suspended in methanol and filtered. The filtrate was purified by MDAP (high pH method B). The relevant fractions were combined and concentrated under reduced pressure to give the title product [5.51] as a yellow oil (166.5 mg, 54% yield).

¹H NMR (400 MHz, CDCl₃) δ 9.96 (s, 1H), 7.93 (dd, *J* = 8.3, 1.7 Hz, 1H), 7.88 (d, *J* = 1.7 Hz, 1H), 7.56 (s, 1H), 7.54 (d, *J* = 8.3 Hz, 1H), 7.36 (s, 1H), 6.67 (s, 1H), 3.94 (s, 3H), 3.47 (q, *J* = 6.9 Hz, 1H), 3.13 (s, 3H), 1.72 (d, *J* = 6.9 Hz, 3H). ¹³C NMR (101 MHz, CDCl₃) δ 191.6 (C=O), 169.5 (C=O), 143.5 (CH), 137.9 (CH), 136.2 (C_{iv}), 134.7 (C_{iv}), 129.8 (CH), 129.5 (CH), 129.0 (CH), 127.4 (C_{iv}), 124.9 (CH), 121.4 (C_{iv}), 121.1 (C_{iv}), 41.8 (CH), 39.2 (CH₃), 35.3 (CH₃), 12.7 (CH₃). LCMS (ESI, High pH) t_R = 0.80

min, m/z 296 $[M+H]^+$. **HRMS** (ESI) calculated for $C_{17}H_{18}N_3O_2$ 296.1400 $[M+H]^+$, found 296.1407 (3.24 min). ν_{max} (solution in chloroform, cm^{-1}): 1690 (C=O aldehyde), 1652 (C=O amide), 1596 (C=C alkene). $[\alpha]_D^{20.6}$ $_{589\text{ nm}}$ (c 0.500, MeOH): +302.2°.

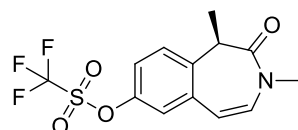
(R)-7-Hydroxy-1,3-dimethyl-1,3-dihydro-2H-benzo[d]azepin-2-one [6.01]



(R)-7-Methoxy-1,3-dimethyl-1,3-dihydro-2H-benzo[d]azepin-2-one **[5.08]** (6.2 g, 28.5 mmol) were dissolved in DCM (100 mL) under nitrogen at -78 °C. A 1 M solution of boron tribromide in DCM (29 mL, 29.0 mmol) was added dropwise to the reaction mixture over 15 min. The reaction mixture was left to warm up slowly from -78 °C to rt and stirred overnight. A 1 M solution of boron tribromide in DCM (15 mL, 15 mmol) was added to the reaction mixture at -78 °C over 5 min. The reaction mixture was stirred 5 min at -78 °C and then warmed up to rt (-78 °C bath was removed) and stirred for 30 min. The reaction mixture was diluted with 10% methanol in water. The layers were separated. The aqueous layer was re-extracted once with DCM, and twice with 10% MeOH in EtOAc. The organic layers were combined, dried through a phase separator and concentrated under reduced pressure to give a beige solid. The solid was purified by silica column chromatography, eluted with a gradient of 0-100% EtOAc in cyclohexane. The relevant fractions were concentrated under reduced pressure to give the title product **[6.01]** as an orange solid (4.73 g, 77%)

¹H NMR (400 MHz, DMSO- d_6) δ 9.35 (br. s, 1H), 7.05 (d, J = 8.6 Hz, 1H), 6.81 (dd, J = 8.6, 2.5 Hz, 1H), 6.68 (d, J = 2.5 Hz, 1H), 6.46 (d, J = 9.3 Hz, 1H), 6.36 (d, J = 9.3 Hz, 1H), 3.12 (br. s, 1H), 3.01 (s, 3H), 1.44 (d, J = 6.6 Hz, 3H). **LCMS** (ESI, High pH) t_R = 0.75 min, m/z 204 $[M+H]^+$.

(R)-1,3-Dimethyl-2-oxo-2,3-dihydro-1H-benzo[d]azepin-7-yltrifluoromethanesulfonate [6.02]

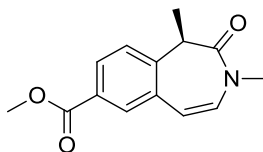


(*R*)-7-Hydroxy-1,3-dimethyl-1,3-dihydro-2*H*-benzo[*d*]azepin-2-one [6.01] (500 mg, 2.5 mmol) was dissolved in DCM (8.2 mL) under nitrogen at 0 °C. 1,1,1-Trifluoro-*N*-phenyl-*N*-((trifluoromethyl)sulfonyl)methanesulfonamide (1.06 g, 2.95 mmol) and pyridine (0.6 mL, 7.4 mmol) were added and the reaction mixture was stirred for 18 h at rt. No reaction occurred. NEt₃ (1 mL, 7.2 mmol) was added and the reaction mixture was stirred for 2 h. The reaction mixture was quenched with a mixture of ice-water. DCM was added and the layers were separated. The aqueous layer was re-extracted with DCM. The organic layers were combined, dried through a hydrophobic frit and concentrated under reduced pressure to give an orange solid. The solid was purified by silica column chromatography, eluted with a gradient of 0-100% EtOAc in cyclohexane. The relevant fractions were concentrated under reduced pressure to give the title product [6.02] as an orange solid (533.8 mg, 62% yield).

¹H NMR (400 MHz, CDCl₃) δ 7.38 (d, *J* = 8.8 Hz, 1H), 7.27 (dd, *J* = 8.8, 2.5 Hz, 1H), 7.17 (d, *J* = 2.5 Hz, 1H), 6.35-6.42 (m, 2H), 3.29 (br. s, 1H), 3.14 (s, 3H), 1.65 (d, *J* = 6.4 Hz, 3H). LCMS (ESI, High pH) t_R = 1.22 min, *m/z* 336 [M+H]⁺.

Methyl (*R*)-1,3-dimethyl-2-oxo-2,3-dihydro-1*H*-benzo[*d*]azepine-7-carboxylate

[6.03]



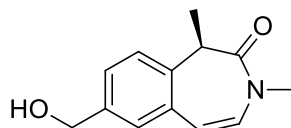
(*R*)-1,3-Dimethyl-2-oxo-2,3-dihydro-1*H*-benzo[*d*]azepin-7-yl

trifluoromethanesulfonate **[6.02]** (2.0 g, 5.4 mmol), Pd(OAc)₂ (0.12 g, 0.54 mmol) and Xantphos (0.31 g, 0.54 mmol) were suspended in a sealed round bottom flask in DMF (9 mL). The flask was purged in a vacuum-nitrogen cycle (repeated 3 times). Methanol (9 mL) and NEt₃ (2.2 mL, 16.1 mmol) were added. The nitrogen atmosphere was replaced by a CO atmosphere by bubbling CO in the solution (with an exit needle in the septum) for 5 min. Then, the exit needle was removed and the needle of CO gas was taken off the solution, but kept in the flask to maintain the CO-atmosphere. The reaction mixture was heated at 60 °C for 1.5 h. The reaction mixture was concentrated under reduced pressure. The residue was diluted in EtOAc and washed with a 1 M aqueous LiCl solution. The layers were separated, the aqueous layer was extracted with EtOAc. The organic layers were dried through a phase separator and concentrated under reduced pressure. The crude product was purified by silica column chromatography, eluted with a gradient of 0-50% of EtOAc in cyclohexane. The relevant fractions were concentrated under reduced pressure to give the title product **[6.03]** as a white solid (1.21 g, 87% yield).

¹H NMR (400 MHz, CDCl₃) δ 8.03 (dd, *J* = 8.3, 1.7 Hz, 1H), 7.95 (d, *J* = 1.7 Hz, 1H), 7.38 (d, *J* = 8.3 Hz, 1H), 6.46 (d, *J* = 9.3 Hz, 1H), 6.36 (d, *J* = 9.3 Hz, 1H), 3.92 (s, 3H), 3.33 (br. s, 1H), 3.13 (s, 3H), 1.67 (d, *J* = 5.9 Hz, 3H). LCMS (ESI, High pH) t_R = 0.98 min, *m/z* 246 [M+H]⁺.

(*R*)-7-(Hydroxymethyl)-1,3-dimethyl-1,3-dihydro-2*H*-benzo[*d*]azepin-2-one

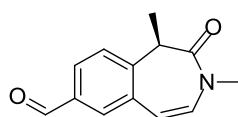
[6.04]



Methyl (*R*)-1,3-dimethyl-2-oxo-2,3-dihydro-1*H*-benzo[*d*]azepine-7-carboxylate **[6.03]** (288.1 mg, 1.12 mmol) and lithium borohydride (77 mg, 3.5 mmol) were stirred in 2-MeTHF (5.8 mL) under nitrogen at 55 °C for 2 h. The reaction mixture was quenched with methanol and concentrated under reduced pressure to give a yellow residue. The residue was partitioned between EtOAc and water. The layers were separated and the aqueous layer was re-extracted with EtOAc. The organic layers were combined, dried through a phase separator and concentrated under reduced pressure to give the title product **[6.04]** as a white solid (249.4 mg, 83% yield).

¹H NMR (400 MHz, CDCl₃) δ 7.37 (dd, *J* = 8.1, 1.2 Hz, 1H), 7.30 (d, *J* = 8.1 Hz, 1H), 7.27 (d, *J* = 1.2 Hz, 1H), 6.42 (d, *J* = 9.1 Hz, 1H), 6.30 (d, *J* = 9.1 Hz, 1H), 4.69 (s, 2H), 3.27 (br. s, 1H), 3.11 (s, 3H), 1.84 (br. s, 1H), 1.64 (d, *J* = 4.9 Hz, 3H). LCMS (ESI, high pH) *t*_R = 0.72 min, *m/z* 218 [M+H]⁺.

(*R*)-5-Bromo-1,3-dimethyl-2-oxo-2,3-dihydro-1*H*-benzo[*d*]azepine-7-carbaldehyde **[6.05]**

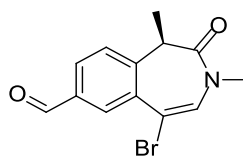


(*R*)-7-(Hydroxymethyl)-1,3-dimethyl-1,3-dihydro-2*H*-benzo[*d*]azepin-2-one **[6.04]** (249.4 mg, 0.98 mmol) and Dess-Martin periodinane (621 mg, 1.5 mmol) were stirred in DCM (5 mL) under nitrogen at 20 °C for 1 h. The reaction mixture was quenched with a saturated solution of sodium bicarbonate. DCM was added. The layers were

separated. The aqueous layer was re-extracted with DCM. The organics were combined, dried through a phase separator and concentrated under reduced pressure to give a yellow oil. The product was purified by column chromatography, eluted with 0-100% EtOAc in cyclohexane. The appropriate fractions were concentrated under reduced pressure to give the title product **[6.05]** as a white solid (188.4 mg, 85%)

$^1\text{H NMR}$ (400 MHz, CDCl_3) δ 10.01 (s, 1H), 7.88 (dd, $J = 8.1, 1.7$ Hz, 1H), 7.77 (d, $J = 1.7$ Hz, 1H), 7.48 (d, $J = 8.1$ Hz, 1H), 6.49 (d, $J = 9.3$ Hz, 1H), 6.41 (d, $J = 9.3$ Hz, 1H), 3.35 (br. s, 1H), 3.15 (s, 3H), 1.69 (d, $J = 6.1$ Hz, 3H). **LCMS** (ESI, High pH) $t_R = 0.87$ min, m/z 216 $[\text{M}+\text{H}]^+$.

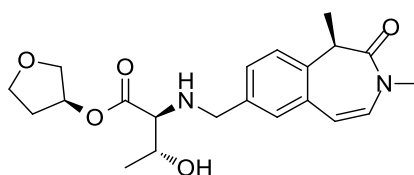
(R)-5-Bromo-1,3-dimethyl-2-oxo-2,3-dihydro-1H-benzo[d]azepine-7-carbaldehyde [6.06]



(*R*)-1,3-Dimethyl-2-oxo-2,3-dihydro-1*H*-benzo[*d*]azepine-7-carbaldehyde **[6.05]** (188.4 mg, 0.88 mmol) and phenyltrimethylaminotribromide (PTT) (345 mg, 0.92 mmol) were stirred in MeCN (10 mL) under nitrogen at 20 °C for 10 min. The reaction mixture was concentrated under reduced pressure. The residual orange oil was partitioned between EtOAc and water. The layers were separated. The aqueous layer was re-extracted with EtOAc. The organic layers were combined, dried through a phase separator and concentrated under reduced pressure to give a yellow solid. The solid was purified by silica column chromatography eluted with a gradient of 0-100% EtOAc in cyclohexane. The appropriate fractions were concentrated under reduced pressure to give the title product **[6.06]** as a white solid (215.6 mg, 80%).

¹H NMR (400 MHz, CDCl₃) δ 10.05 (s, 1H), 8.23 (d, *J* = 1.5 Hz, 1H), 7.95 (dd, *J* = 8.1, 1.5 Hz, 1H), 7.48 (d, *J* = 8.1 Hz, 1H), 6.92 (s, 1H), 3.47 (q, *J* = 6.8 Hz, 1H), 3.11 (s, 3H), 1.71 (d, *J* = 6.8 Hz, 3H). **¹³C NMR** (101 MHz, CDCl₃) δ 191.1 (C=O), 169.0 (C=O), 142.6 (C_{iv}), 135.4 (C_{iv}), 135.1 (C_{iv}), 132.3 (CH), 130.4 (CH)*, 125.1 (CH), 110.3 (C_{iv}), 41.9 (CH), 35.2 (CH₃), 12.8 (CH₃). *HSQC NMR showed correlation to two protons for this signal, indicating there are two CH signals under the peak. **LCMS** (ESI, formic) t_R = 0.99 min, *m/z* 294/296 [M+H]⁺. **HRMS** (ESI) calculated for C₁₃H₁₃BrNO₂ [M+H]⁺ 294.0130, found 294.0133 (4.21 min). ν_{max} (neat, cm⁻¹): 2984 (CH alkene), 1695 (C=O aldehyde), 1671 (C=O amide), 1601 (C=C alkene). [α]_D^{20.5} °C_{589 nm} (c 0.500, MeOH): +136.6°. **m.p.** = 163-167 °C.

(S)-Tetrahydrofuran-3-yl (((R)-1,3-dimethyl-2-oxo-2,3-dihydro-1H-benzo[d]azepin-7-yl)methyl)-L-threoninate [6.07]

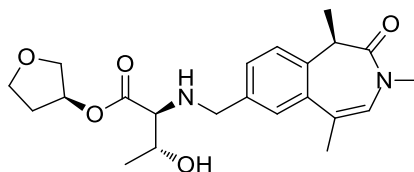


Reductive amination general procedure A2 used on aldehyde **[6.05]** (121 mg, 0.54 mmol) and (S)-tetrahydrofuran-3-yl L-threoninate, hydrochloride **[5.43]** (181 mg, 0.80 mmol). The crude product was purified by silica column chromatography, eluted with a gradient of 0-12.5% EtOAc in EtOH. The fractions were concentrated under reduced pressure. The residue was purified by MDAP (high pH, extended method B) to afford the title product **[6.07]** as a colourless gum (54.5 mg, 25% yield).

¹H NMR (400 MHz, CDCl₃) δ 7.32 (dd, *J* = 8.1, 1.3 Hz, 1H), 7.27 (d, *J* = 8.1 Hz, 1H), 7.20 (d, *J* = 1.3 Hz, 1H), 6.40 (d, *J* = 9.5 Hz, 1H), 6.31 (d, *J* = 9.5 Hz, 1H), 5.29-5.24 (m, 1H), 3.91-3.88 (m, 1H), 3.87-3.84 (m, 2H), 3.83-3.73 (m, 3H), 3.73-3.65 (m, 1H),

3.26 (br. s, 1H), 3.12 (s, 3H), 3.02 (d, $J = 7.1$ Hz, 1H), 2.21-2.11 (m, 1H), 1.93-1.85 (m, 1H), 1.63 (br. s, 3H), 1.21 (d, $J = 6.1$ Hz, 3H). Signals for the exchangeable protons were not observed. ^{13}C NMR (101 MHz, CDCl_3) δ 173.3 (C=O), 169.9 (C=O), 137.2 (C_{iv}), 135.2 (C_{iv}), 134.3 (C_{iv}), 130.5 (CH), 128.7 (CH), 126.7 (CH), 124.8 (C_{iv}), 116.1 (CH), 75.7 (CH_2), 72.9 (CH_2), 68.0 (CH_2), 67.1 (CH_2), 66.9 (CH_2), 52.3 (CH_2), 41.4 (CH), 35.6 (CH_3), 32.7 (CH_2), 19.4 (CH_3), 13.1 (CH_3). LCMS (ESI, high pH) $t_{\text{R}} = 0.83$ min, m/z 389 $[\text{M}+\text{H}]^+$. HRMS (ESI) calculated for $\text{C}_{21}\text{H}_{29}\text{N}_5\text{O}_4$ $[\text{M}+\text{H}]^+$ 389.2077, found 389.2072 (1.74 min). ν_{max} (solution in chloroform, cm^{-1}): 3443 (OH), 2978 (CH alkene), 2936 (CH alkane), 2873 (CH alkane), 1728 (C=O ester), 1660 (C=O amide). $[\alpha]_{\text{D}}^{21.2}$ $^{\circ}\text{C}$ $_{589\text{ nm}}$ (c 0.500, MeOH): -101.3° .

(S)-Tetrahydrofuran-3-yl (((R)-1,3,5-trimethyl-2-oxo-2,3-dihydro-1H-benzo[d]azepin-7-yl)methyl)-L-threoninate [6.08]



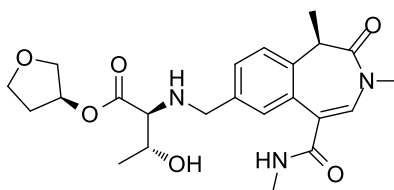
(R)-1,3,5-Trimethyl-2-oxo-2,3-dihydro-1H-benzo[d]azepine-7-carbaldehyde [6.18] (80 mg, 0.33 mmol) and (S)-tetrahydrofuran-3-yl L-threoninate, hydrochloride [5.43] (112 mg, 0.497 mmol) were dissolved THF (5 mL). DIPEA (0.2 mL, 1.15 mmol) and AcOH (0.1 mL, 1.75 mmol) were added. The reaction vessel was placed under a nitrogen atmosphere and stirred at 40 °C for 3 h. Sodium triacetoxyborohydride (176 mg, 0.83 mmol) was added and the reaction mixture was stirred at rt for 1 h. Sodium triacetoxyborohydride (176 mg, 0.83 mmol) was added and the reaction mixture was stirred at 40 °C for 30 min. The reaction mixture was quenched with methanol and concentrated under reduced pressure to give a yellow residue. The residue was

dissolved in methanol and purified by MDAP (high pH, extended method B). The fractions were concentrated under reduced pressure to give the title product [**6.08**] in two batches as two colourless oils (batch 1: 19.5 mg, 14% yield, batch 2: 20.8 mg, 15% yield).

Analysis of batch 2 (analysis of batch 1 matches the data reported below):

¹H NMR (400 MHz, CDCl₃) δ 7.36 (d, $J = 1.5$ Hz, 1H), 7.33 (dd, $J = 8.1, 1.5$ Hz, 1H), 7.28 (d, $J = 8.1$ Hz, 1H), 6.23 (s, 1H), 5.94-5.24 (m, 1H), 3.91-3.88 (m, 1H), 3.88-3.86 (m, 2H), 3.85-3.83 (m, 1H), 3.78-3.66 (m, 3H), 3.27 (q, $J = 7.1$ Hz, 1H), 3.05-2.99 (m, 4H), 2.24 (s, 3H), 2.22-2.11 (m, 1H), 1.94-1.86 (m, 1H), 1.63 (d, $J = 7.1$ Hz, 3H), 1.22 (d, $J = 6.1$ Hz, 3H). Signals for the exchangeable protons were not observed. **¹³C NMR** (101 MHz, CDCl₃) δ 173.4 (C=O), 170.3 (C=O), 137.2 (C_{iv}), 136.7 (C_{iv}), 136.4 (C_{iv}), 128.8 (CH), 127.7 (CH), 124.9 (CH), 124.3 (CH), 124.1 (C_{iv}), 75.7 (CH), 73.0 (CH₂), 68.1 (CH₂), 67.2 (CH), 66.9 (CH₂), 52.5 (CH₂), 40.7 (CH₃), 34.8 (CH₃), 32.8 (CH₂), 20.5 (CH₃), 19.4 (CH₃), 12.8 (CH₃). **LCMS** (ESI, high pH) $t_R = 0.91$ min, m/z 403 [M+H]⁺. **HRMS** (ESI) calculated for C₂₂H₃₁N₂O₅ [M+H]⁺ 403.2234, found 403.2223 (1.98 min). ν_{max} (solution in chloroform, cm⁻¹): 3439 (OH), 2976 (CH alkene), 2936 (CH alkane), 1729 (C=O ester), 1659 (C=O amide). $[\alpha_D]^{21.2}_{589\text{ nm}}$ (c 0.500, MeOH): -74.0°.

(S)-Tetrahydrofuran-3-yl (((R)-1,3-dimethyl-5-(methylcarbamoyl)-2-oxo-2,3-dihydro-1H-benzo[d]azepin-7-yl)methyl)-L-threoninate [6.10]

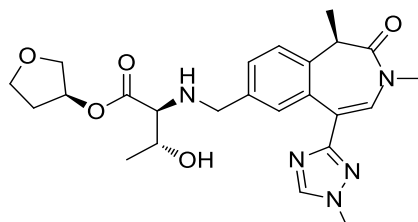


(R)-7-Formyl-N,1,3-trimethyl-2-oxo-2,3-dihydro-1H-benzo[d]azepine-5-carboxamide (88 mg, 0.32 mmol) [6.19], (S)-tetrahydrofuran-3-yl L-threoninate, hydrochloride [5.43] (109 mg, 0.49 mmol), picoline borane (41.5 mg, 0.39 mmol) and acetic acid (0.5 mL, 8.73 mmol) were stirred in *i*PrOH (5 mL) under nitrogen at rt for 1 h. The reaction mixture was concentrated under reduced pressure to give a yellow oil. The crude product was purified by MDAP (high pH, extended method A). The relevant fractions were concentrated under reduced pressure to give the title product [6.10] as a colourless oil (75.9 mg, 50% yield).

¹H NMR (400 MHz, CDCl₃) δ 7.46 (s, 1H), 7.39-7.35 (m, 2H), 7.32 (d, *J* = 8.6 Hz, 1H), 6.00 (br. s, 1H), 5.18 (br. s, 1H), 3.90-3.75 (m, 5H), 3.71-3.64 (m, 2H), 3.28 (q, *J* = 6.9 Hz, 1H), 3.15 (s, 3H), 2.97-2.92 (m, 4H), 2.23-2.12 (m, 1H), 1.94-1.86 (m, 1H), 1.64 (d, *J* = 6.9 Hz, 3H), 1.18 (d, *J* = 6.1 Hz, 3H). Signals for the two of the three exchangeable protons were not observed. ¹³C NMR (101 MHz, CDCl₃) δ 173.2 (C=O), 170.2 (C=O), 166.8 (C=O), 137.7 (C_{iv}), 137.2 (C_{iv}), 136.3 (C_{iv}), 131.9 (CH), 129.7 (CH), 127.3 (CH), 124.6 (CH), 122.1 (C_{iv}), 75.7 (CH), 72.7 (CH), 67.8 (CH₂), 67.3 (CH₂), 66.8 (CH), 52.2 (CH₂), 41.3 (CH), 35.9 (CH₃), 32.7 (CH₂), 26.8 (CH₃), 19.2 (CH₃), 12.6 (CH₃). LCMS (ESI, high pH) *t*_R = 0.69 min, *m/z* 446 [M+H]⁺. HRMS (ESI) calculated for C₂₃H₃₂N₃O₆ [M+H]⁺ 446.2292, found 446.2293 (1.45 min). *ν*_{max} (solution in chloroform, cm⁻¹): 3333 (OH), 2979 (CH alkene), 2939 (CH alkane), 1728

(C=O ester), 1654 (C=O amide), 1612 (C=C alkene). $[\alpha_D]^{20.7}_{589\text{ nm}}$ (c 0.290, MeOH): +74.2°.

(S)-Tetrahydrofuran-3-yl (((R)-1,3-dimethyl-5-(1-methyl-1*H*-1,2,4-triazol-3-yl)-2-oxo-2,3-dihydro-1*H*-benzo[*d*]azepin-7-yl)methyl)-*L*-threoninate [6.11]

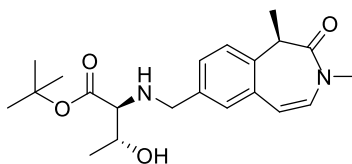


(*R*)-1,3-dimethyl-5-(1-methyl-1*H*-1,2,4-triazol-3-yl)-2-oxo-2,3-dihydro-1*H*-benzo[*d*]azepine-7-carbaldehyde [6.22] (30.2 mg, 0.1 mmol) and (*S*)-tetrahydrofuran-3-yl *L*-threoninate, hydrochloride [5.43] (32.8 mg, 0.15 mmol) were dissolved THF (5 mL). DIPEA (0.2 mL, 1.15 mmol) and AcOH (0.1 mL, 1.7 mmol) were added. The reaction vessel was placed under a nitrogen atmosphere and stirred at 40 °C for 3 h. sodium triacetoxyborohydride (54 mg, 0.26 mmol) was added and the reaction mixture was stirred at 40 °C for 1 h. sodium triacetoxyborohydride (54 mg, 0.26 mmol) was added and the reaction mixture was stirred at 40 °C for 20 min. The reaction mixture was quenched with MeOH and concentrated under reduced pressure to give a yellow residue. The residue was taken in MeOH and purified by MDAP (high pH extended method A, followed by formic, extended method A). The fractions were concentrated under reduced pressure. The product was further purified by silica column chromatography, eluted with a gradient of 0-20% MeOH in DCM. The appropriate fractions were concentrated under reduced to afford the title product [6.11] as a colourless oil (8.3 mg, 17% yield).

¹H NMR (400 MHz, CDCl₃) δ 8.04 (s, 1H), 7.64 (d, *J* = 1.3 Hz, 1H), 7.44 (s, 1H), 7.34 (dd, *J* = 8.2, 1.3 Hz, 1H), 7.31 (d, *J* = 8.2 Hz, 1H), 5.30 (s, 1H), 5.05 (br. s, 2H),

3.95 (s, 3H), 3.92-3.82 (m, 4H), 3.76 (br. d, $J = 10.5$ Hz, 1H), 3.72-3.63 (m, 2H), 3.40 (q, $J = 7.0$ Hz, 1H), 3.19 (s, 3H), 3.02 (d, $J = 7.6$ Hz, 1H), 2.22-2.11 (m, 1H), 1.97-1.89 (m, 1H), 1.65 (d, $J = 7.0$ Hz, 3H), 1.19 (d, $J = 6.4$ Hz, 3H). **LCMS** (ESI, high pH) $t_R = 0.71$ min, m/z 470 $[M+H]^+$.

***Tert*-butyl (((*R*)-1,3-dimethyl-2-oxo-2,3-dihydro-1*H*-benzo[*d*]azepin-7-yl)methyl)-*L*-threoninate [6.12]**

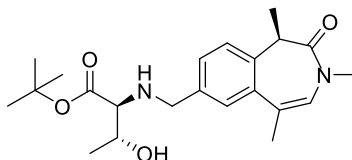


Reductive amination general procedure A2 with aldehyde [6.05] (110 mg, 0.49 mmol) and *tert*-butyl *L*-threoninate, hydrochloride [6.17] (154 mg, 0.73 mmol). The sample was purified by silica column chromatography eluted with a gradient of 0-100% EtOAc in cyclohexane. The relevant fractions were combined and concentrated under reduced pressure to give the title product [6.12] as a colourless gum (108 mg, 56% yield).

¹H NMR (400 MHz, CDCl₃) δ 7.33 (dd, $J = 8.3, 1.5$ Hz, 1H), 7.27 (d, $J = 8.3$ Hz, 1H), 7.21 (d, $J = 1.5$ Hz, 1H), 6.41 (d, $J = 8.8$ Hz, 1H), 6.30 (d, $J = 8.8$ Hz, 1H), 3.83 (d, $J = 13.0$ Hz, 1H), 3.70 (d, $J = 13.0$ Hz, 1H), 3.63 (qd, $J = 7.6, 6.4$ Hz, 1H), 3.26 (br. s, 1H), 3.11 (s, 3H), 2.90 (d, $J = 7.6$ Hz, 1H), 2.87 (br. s, 1H), 1.63 (br. d, $J = 5.6$ Hz, 3H), 1.44 (s, 9H), 1.21 (d, $J = 6.4$ Hz, 3H). The signal for one of the exchangeable protons was not observed. **¹³C NMR** (101 MHz, CDCl₃) δ 172.7 (C=O), 169.9 (C=O), 137.5 (C_{iv}), 135.0 (C_{iv}), 134.2 (C_{iv}), 130.3 (CH), 128.7 (CH), 126.6 (CH), 124.7 (CH), 116.2 (CH), 81.8 (C_{iv}), 68.0 (CH), 52.1 (CH₂), 41.2 (CH), 35.5 (CH₃), 28.0 (CH₃), 19.3 (CH₃), 13.0 (CH₃). One CH was not observed. **LCMS** (ESI, high pH) $t_R = 1.07$ min, m/z 375 $[M+H]^+$. **HRMS** (ESI) calculated for C₂₁H₃₁N₂O₄ $[M+H]^+$ 375.2285, found

375.2281 (2.33 min). ν_{\max} (solution in chloroform, cm^{-1}): 3447 (OH), 3322 (NH), 2976 (CH alkene), 2935 (CH alkane), 1722 (C=O ester), 1660 (C=O amide) and 1636 (C=C alkene). $[\alpha]_D^{21.0\text{ }^\circ\text{C}}_{589\text{ nm}}$ (c 0.493, MeOH): -137.1° .

***Tert*-butyl (((*R*)-1,3,5-trimethyl-2-oxo-2,3-dihydro-1*H*-benzo[*d*]azepin-7-yl)methyl)-*L*-threoninate [6.13]**



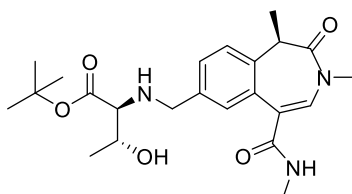
(*R*)-1,3,5-Trimethyl-2-oxo-2,3-dihydro-1*H*-benzo[*d*]azepine-7-carbaldehyde [6.18] (40 mg, 0.17 mmol) and *tert*-butyl *L*-threoninate, hydrochloride [6.17] (55.4 mg, 0.26 mmol) were dissolved in THF (5 mL). Triethylamine (0.07 mL, 0.52 mmol) was added and the reaction mixture was stirred at 50 °C for 18 h. The reaction mixture was cooled to rt and sodium triacetoxyborohydride (111 mg, 0.52 mmol) was added and the reaction mixture was stirred at rt for 6 h. The reaction mixture was quenched with MeOH, concentrated under reduced pressure and the resulting residue was purified by MDAP (high pH, extended method C). The relevant fraction was concentrated under reduced pressure to give the title product [6.13] as a colourless oil (30.9 mg, 43% yield).

$^1\text{H NMR}$ (400 MHz, CDCl_3) δ 7.37 (d, $J = 1.7$ Hz, 1H), 7.48 (dd, $J = 8.1, 1.7$ Hz, 1H), 7.28 (d, $J = 8.1$ Hz, 1H), 6.22 (d, $J = 1.0$ Hz, 1H), 3.85 (d, $J = 13.0$ Hz, 1H), 3.72 (d, $J = 13.0$ Hz, 1H), 3.63 (qd, $J = 7.3, 5.9$ Hz, 1H), 3.27 (q, $J = 6.9$ Hz, 1H), 3.02 (s, 3H), 2.90 (d, $J = 7.3$ Hz, 1H), 2.24 (d, $J = 1.0$ Hz, 3H), 1.63 (d, $J = 6.9$ Hz, 3H), 1.45 (s, 9H), 1.21 (d, $J = 5.9$ Hz, 3H). Signals for the exchangeable protons were not observed.

$^{13}\text{C NMR}$ (101 MHz, CDCl_3) δ 172.8 (C=O), 170.3 (C=O), 137.4 (C_{IV}), 136.7 (C_{IV}),

136.3 (C_{iv}), 128.8 (CH), 127.6 (CH), 124.8 (CH), 124.2 (CH), 124.2 (C_{iv}), 81.9 (C_{iv}), 68.1 (CH), 52.4 (CH₂), 40.7 (CH), 34.7 (CH₃), 28.1 (CH₃), 20.5 (CH₃), 19.3 (CH₃), 12.8 (CH₃). **LCMS** (ESI, high pH) t_R = 1.12 min, m/z 389 [M+H]⁺. **HRMS** (ESI) calculated for C₂₂H₃₃N₂O₄ [M+H]⁺ 389.2441, found 389.2437 (2.56 min). **ν**_{max} (solution in chloroform, cm⁻¹): 3442 (OH), 3322 (NH), 2980 (CH alkene), 2935 (CH alkane), 1723 (C=O ester), 1658 (C=O amide). **[α]_D^{21.3}** °C_{589 nm} (c 0.490, MeOH): -113.4°.

***Tert*-butyl (((*R*)-1,3-dimethyl-5-(methylcarbamoyl)-2-oxo-2,3-dihydro-1*H*-benzo[*d*]azepin-7-yl)methyl)-*L*-threoninate [6.15]**

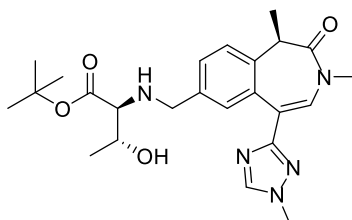


Reductive amination general procedure B with aldehyde **[6.19]** (49 mg, 0.18 mmol) and *tert*-butyl *L*-threoninate, hydrochloride **[6.17]** (57.1 mg, 0.27 mmol). The sample was purified by MDAP (high pH, extended method B), followed by MDAP (formic, extended method B) to afford the title product **[6.15]** as a colourless oil (10 mg, 12% yield).

¹H NMR (400 MHz, MeOD) δ 8.22 (s, 2H), 7.51 (dd, *J* = 8.0, 1.5 Hz, 1H), 7.48 (d, *J* = 1.5 Hz, 1H), 7.39 (d, *J* = 8.0 Hz, 1H), 7.21 (s, 1H), 4.06 (d, *J* = 13.2 Hz, 1H), 3.97 (d, *J* = 13.2 Hz, 1H), 3.91 (qd, *J* = 6.9, 6.4 Hz, 1H), 3.36 (q, *J* = 6.9 Hz, 1H), 3.22 (d, *J* = 6.9 Hz, 1H), 3.13 (s, 3H), 2.87 (s, 3H), 1.62 (d, *J* = 6.9 Hz, 3H), 1.44 (s, 9H), 1.23 (d, *J* = 6.4 Hz, 3H). The signal for one exchangeable proton was not observed. **¹³C NMR** (101 MHz, CDCl₃) δ 172.7 (C=O), 170.3 (C=O), 166.8 (C=O), 138.0 (C_{iv}), 137.3 (C_{iv}), 136.5 (CH), 131.9 (C_{iv}), 129.8 (CH), 127.3 (CH), 124.8 (CH), 122.0 (C_{iv}),

82.1 (C_{iv}), 68.3 (CH), 68.0 (CH), 52.3 (CH₂), 41.4 (CH), 36.0 (CH₃), 28.0 (CH₃), 26.9 (CH₃), 19.1 (CH₃), 12.7 (CH₃). **LCMS** (ESI, high pH) $t_R = 0.86$ min, m/z 432 [M+H]⁺. **HRMS** (ESI) calculated for C₂₃H₃₄N₃O₅ [M+H]⁺ 432.2499, found 432.2496 (1.92 min). ν_{max} (solution in chloroform, cm⁻¹): 3446 (OH), 3322 (NH), 2977 (CH alkene), 2937 (CH alkane), 1723 (C=O ester), 1655 (C=O amide). $[\alpha_D]^{21.7}_{589\text{ nm}}$ (c 0.500, MeOH): +76.3°.

***Tert*-butyl (((*R*)-1,3-dimethyl-5-(1-methyl-1*H*-1,2,4-triazol-3-yl)-2-oxo-2,3-dihydro-1*H*-benzo[*d*]azepin-7-yl)methyl)-*L*-threoninate [6.16]**

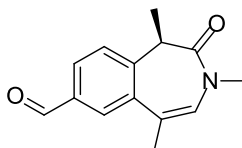


Reductive amination general procedure A2 with aldehyde [6.22] (50 mg, 0.17 mmol) and *tert*-butyl *L*-threoninate, hydrochloride [6.17] (53.6 mg, 0.25 mmol). The sample was purified by MDAP (high pH, extended method B) to afford the title product [6.16] as a colourless gum (36.7 mg, 45% yield).

¹H NMR (400 MHz, CDCl₃) δ 8.04 (s, 1H), 7.66 (d, $J = 1.5$ Hz, 1H), 7.44 (s, 1H), 7.35 (dd, $J = 8.3, 1.5$ Hz, 1H), 7.31 (d, $J = 8.3$ Hz, 1H), 3.95 (s, 3H), 3.89 (d, $J = 13.2$ Hz, 1H), 3.68 (d, $J = 13.2$ Hz, 1H), 3.61 (qd, $J = 7.8, 6.4$ Hz, 1H), 3.40 (q, $J = 6.9$ Hz, 1H), 3.19 (s, 3H), 2.90 (d, $J = 7.8$ Hz, 1H), 1.66 (d, $J = 6.9$ Hz, 3H), 1.45 (s, 9H), 1.19 (d, $J = 6.4$ Hz, 3H). Signals for the exchangeable protons were not observed. **LCMS** (ESI, high pH) $t_R = 0.91$ min, m/z 456 [M+H]⁺.

(R)-1,3,5-Trimethyl-2-oxo-2,3-dihydro-1H-benzo[d]azepine-7-carbaldehyde

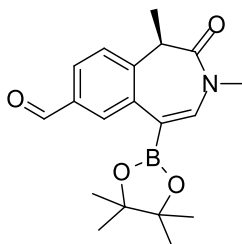
[6.18]



(R)-5-Bromo-1,3-dimethyl-2-oxo-2,3-dihydro-1H-benzo[d]azepine-7-carbaldehyde **[6.06]** (300 mg, 1.0 mmol), 2,4,6-trimethyl-1,3,5,2,4,6-trioxatriborinane (0.29 mL, 2.0 mmol), a 2 M aqueous solution of K_3PO_4 (1.0 mL, 2.0 mmol) and $Pd(PPh_3)_4$ (118 mg, 0.10 mmol) were heated in 1,4-dioxane (5 mL) under nitrogen at 80 °C for 1 h and at 110 °C for 2 h. The reaction mixture was transferred into a microwave vial and heated at 110 °C for 1 h. The reaction mixture was concentrated under reduced pressure to give a black oil. The oil was dissolved in EtOAc and water. The layers were separated. The aqueous layer was re-extracted with EtOAc. The organic layers were combined, dried through a phase separator and concentrated under reduced pressure to give a brown residue. The crude product was purified by silica column chromatography, eluted with a gradient of 0-100% EtOAc in cyclohexane. The appropriate fractions were concentrated under reduced pressure to give the title product **[6.18]** as a yellow solid (99.1 mg, 38%).

1H NMR (400 MHz, $CDCl_3$) δ 10.03 (s, 1H), 7.95 (d, $J = 1.7$ Hz, 1H), 7.89 (dd, $J = 8.1, 1.7$ Hz, 1H), 7.50 (d, $J = 8.1$ Hz, 1H), 6.32 (br. s, 1H), 3.38 (q, $J = 7.0$ Hz, 1H), 3.05 (s, 3H), 2.30 (s, 3H), 1.68 (d, $J = 7.0$ Hz, 3H). LCMS (ESI, high pH) $t_R = 0.94$ min, m/z 230 $[M+H]^+$.

(R)-1,3-Dimethyl-2-oxo-5-(4,4,5,5-tetramethyl-1,3,2-dioxaborolan-2-yl)-2,3-dihydro-1H-benzo[d]azepine-7-carbaldehyde [6.20]

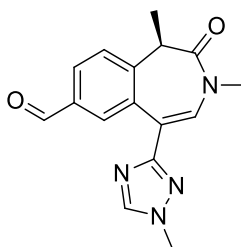


(R)-5-Bromo-1,3-dimethyl-2-oxo-2,3-dihydro-1H-benzo[d]azepine-7-carbaldehyde [6.06] (10.2 g, 34.7 mmol) was dissolved in 1,4-dioxane (100 mL) and heated at 95 °C. 4,4,4',4',5,5,5',5'-octamethyl-2,2'-bi(1,3,2-dioxaborolane) (13.2 g, 52.1 mmol), PdCl₂(dppf).DCM adduct (1.42 g, 1.74 mmol) and KOAc (6.8 g, 69.5 mmol) were added to the solution and the reaction mixture was heated under nitrogen at 95 °C for 2 h. The reaction mixture was concentrated under reduced pressure. The oil was partitioned between EtOAc and a 2 M aqueous solution of LiCl. The layers were separated. The aqueous layer was re-extracted with EtOAc. The organics layers were combined, dried through a phase separator and concentrated under reduced pressure to give a black oil. The crude product was purified by silica column chromatography, eluted with a gradient of 0-60% EtOAc in cyclohexane. The relevant fractions were concentrated under reduced pressure to give the title product [6.20] as a light brown solid (8.3 g, 67% yield) and a side-product [6.05] as a red solid (3.0 g, 32% yield, analysis matching previous batch).

¹H NMR (400 MHz, CDCl₃) δ 10.02 (s, 1H), 8.10 (d, *J* = 1.6 Hz, 1H), 7.87 (dd, *J* = 8.2, 1.6 Hz, 1H), 7.45 (d, *J* = 8.2 Hz, 1H), 7.11 (s, 1H), 3.31 (q, *J* = 7.0 Hz, 1H), 3.16 (s, 3H), 1.67 (d, *J* = 7.0 Hz, 3H), 1.39 (s, 6H), 1.35 (s, 6H). ¹³C NMR (101 MHz, CDCl₃) δ 192.1 (C=O), 170.2 (C=O), 142.4 (C_{iv}), 142.1 (C_{iv}), 136.8 (C_{iv}), 134.6 (CH), 130.6 (CH), 128.3 (CH), 124.6 (CH), 84.2 (C_{iv})*, 42.1 (CH), 35.7 (CH₃), 25.1 (CH₃),

25.0 (CH₃), 24.8 (CH₃), 24.5 (CH₃), 12.8 (CH₃). **LCMS** (ESI, formic) *t_R* = 1.19 min, *m/z* 342 [M+H]⁺. *Only one signal observed for the C_{iv} of the pinacol. One C_{iv} was not observed. **HRMS** (ESI) calculated for C₁₉H₂₅BNO₄ [M+H]⁺ 342.1876, found 342.1887 (5.32 min). *ν*_{max} (neat, cm⁻¹): 2978 (CH alkene), 2937 (CH alkane), 1698 (C=O aldehyde), 1676 (C=O amide), 1596 (C=C alkene), 1348 (B-O). [*α*_D]^{21.2 °C}_{589 nm} (c 0.500, MeOH): +123.9°. **m.p.** = 57-59 °C

(R)-1,3-Dimethyl-5-(1-methyl-1*H*-1,2,4-triazol-3-yl)-2-oxo-2,3-dihydro-1*H*-benzo[*d*]azepine-7-carbaldehyde [6.22]

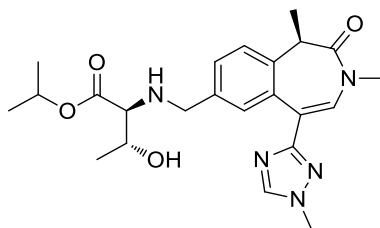


(*R*)-1,3-Dimethyl-2-oxo-5-(4,4,5,5-tetramethyl-1,3,2-dioxaborolan-2-yl)-2,3-dihydro-1*H*-benzo[*d*]azepine-7-carbaldehyde [6.22] (187.9 mg, 0.55 mmol), 3-bromo-1-methyl-1*H*-1,2,4-triazole [6.21] (134 mg, 0.83 mmol), PdCl₂(dppf).DCM adduct (22.5 mg, 0.03 mmol) and K₂CO₃ (228 mg, 1.65 mmol) were suspended in *i*PrOH (4 mL) and water (1 mL) under nitrogen and heated in a microwave at 120 °C for 30 min. The reaction mixture was concentrated under reduced pressure. The black residue was partitioned between EtOAc and water. The layers were separated. The aqueous layer was extracted with EtOAc. The organic layers were combined, dried through a phase separator and concentrated under reduced pressure to give a black oil. The oil was purified by silica column chromatography, eluted with 0-100% EtOAc in cyclohexane. The appropriate fractions were combined and concentrated under reduced pressure to give the deborylated material [6.05] as a yellow oil (40.7 mg, 31% yield). NMR and

LCMS are consistent with data reported above. The column was then eluted with a gradient of 0-25% EtOH in EtOAc. The relevant fractions were combined and concentrated under reduced pressure to give the title product [6.22] as a yellow oil (103.8 mg, 57% yield).

¹H NMR (400 MHz, CDCl₃) δ 10.01 (s, 1H), 8.17 (d, *J* = 1.7 Hz, 1H), 8.09 (s, 1H), 7.95 (dd, *J* = 8.1, 1.5 Hz, 1H), 7.54 (d, *J* = 8.1 Hz, 1H), 7.53 (s, 1H), 3.96 (s, 3H), 3.69 (q, *J* = 6.9 Hz, 1H), 3.21 (s, 3H), 1.71 (d, *J* = 6.9 Hz, 3H). LCMS (ESI, high pH) t_R = 0.72 min, *m/z* 297 [M+H]⁺.

Isopropyl (((R)-1,3-dimethyl-5-(1-methyl-1*H*-1,2,4-triazol-3-yl)-2-oxo-2,3-dihydro-1*H*-benzo[*d*]azepin-7-yl)methyl)-L-threoninate [6.23]

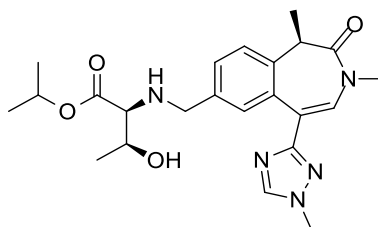


Reductive amination general procedure A2 with aldehyde [6.22] (80.0 mg, 0.27 mmol) and *isopropyl L-threoninate*, hydrochloride [7.06] (80.0 mg, 0.41 mmol). The sample was purified by MDAP (high pH, extended method B) to afford the title product [6.23] as a colourless gum (60 mg, 48% yield).

¹H NMR (400 MHz, CDCl₃) δ 8.04 (s, 1H), 7.65 (d, *J* = 1.3 Hz, 1H), 7.46 (s, 1H), 7.35 (dd, *J* = 8.2, 1.3 Hz, 1H), 7.31 (d, *J* = 8.2 Hz, 1H), 5.06 (spt, *J* = 6.4 Hz, 1H), 3.94 (s, 3H), 3.89 (d, *J* = 13.3 Hz, 1H), 3.68-3.61 (m, 2H), 3.40 (q, *J* = 6.9 Hz, 1H), 3.18 (s, 3H), 2.97 (d, *J* = 7.8 Hz, 1H), 1.65 (d, *J* = 6.9 Hz, 3H), 1.24 (d, *J* = 6.4 Hz, 6H), 1.18 (d, *J* = 6.1 Hz, 3H). Signals for the exchangeable protons were not observed. ¹³C NMR (101 MHz, CDCl₃) δ 173.0 (C=O), 170.7 (C=O), 162.3 (C_{iv}), 143.9 (CH), 137.0 (C_{iv}), 136.6 (C_{iv}), 133.1 (C_{iv}), 131.6 (CH), 129.4 (CH), 128.1 (CH), 123.9 (CH), 119.8 (C_{iv}),

68.7 (CH), 68.0 (CH), 67.4 (CH), 51.9 (CH₂), 41.2 (CH), 36.3 (CH₃), 35.6 (CH₃), 21.9 (CH₃), 21.7 (CH₃), 19.3 (CH₃), 12.7 (CH₃). **LCMS** (ESI, high pH) $t_R = 0.85$ min, m/z 442 [M+H]⁺. **HRMS** (ESI) calculated for C₂₃H₃₂N₅O₄ [M+H]⁺ 442.2455, found 442.2450 (1.96 min). ν_{max} (solution in chloroform, cm⁻¹): 3439 (OH), 2979 (CH), 1724 (C=O ester), 1668 (C=O amide) and 1629 (C=C alkene). $[\alpha_D]^{20.2}_{589\text{ nm}}$ (c 0.500, MeOH): +144.4°.

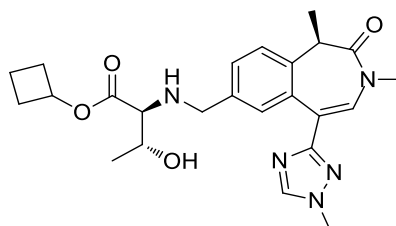
Isopropyl (((R)-1,3-dimethyl-5-(1-methyl-1H-1,2,4-triazol-3-yl)-2-oxo-2,3-dihydro-1H-benzo[d]azepin-7-yl)methyl)-L-allo-threoninate [6.24]



Reductive amination general procedure A2 with aldehyde [6.22] (80.0 mg, 0.27 mmol) and isopropyl *L-allo*-threoninate, hydrochloride [7.07] (80.0 mg, 0.41 mmol). The sample was purified three times by MDAP (high pH extended method B, formic extended method A and finally high pH extended method B) to afford the title product [6.24] as a colourless gum (30.1 mg, 24% yield).

¹H NMR (400 MHz, CDCl₃) δ 8.03 (s, 1H), 7.69 (d, $J = 1.5$ Hz, 1H), 7.45 (s, 1H), 7.36 (dd, $J = 8.1, 1.5$ Hz, 1H), 7.31 (d, $J = 8.1$ Hz, 1H), 5.08 (spt, $J = 6.1$ Hz, 1H), 4.02-3.95 (m, 2H), 3.95 (s, 3H), 3.64 (d, $J = 13.2$ Hz, 1H), 3.39 (q, $J = 7.1$ Hz, 1H), 3.34 (d, $J = 4.7$ Hz, 1H), 3.19 (s, 3H), 1.65 (d, $J = 7.1$ Hz, 3H), 1.27-1.23 (m, 6H), 1.06 (d, $J = 6.6$ Hz, 3H). Signals for the exchangeable protons were not observed. **LCMS** (ESI, high pH) $t_R = 0.83$ min, m/z 442 [M+H]⁺.

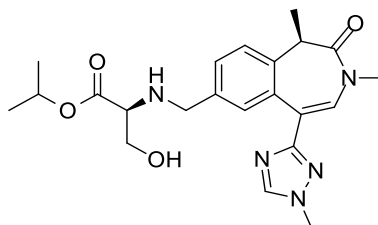
Cyclobutyl (((*R*)-1,3-dimethyl-5-(1-methyl-1*H*-1,2,4-triazol-3-yl)-2-oxo-2,3-dihydro-1*H*-benzo[*d*]azepin-7-yl)methyl)-*L*-threoninate [6.25]



Reductive amination general procedure A2 with aldehyde [6.22] (103 mg, 0.35 mmol) and cyclobutyl *L*-threoninate, 4-methylbenzenesulphonic acid salt [6.28] (180 mg, 0.52 mmol). The sample was purified by MDAP (high pH, extended method B) to afford the title product [6.25] as a colourless gum (26 mg, 16% yield).

¹H NMR (400 MHz, CDCl₃) δ 8.04 (s, 1H), 7.65 (d, *J* = 1.3 Hz, 1H), 7.44 (s, 1H), 7.35 (dd, *J* = 8.2, 1.4 Hz, 1H), 7.31 (d, *J* = 8.2 Hz, 1H), 5.01 (q, *J* = 7.5 Hz, 1H), 3.95 (s, 3H), 3.91 (d, *J* = 13.0 Hz, 1H), 3.69-3.62 (m, 2H), 3.40 (q, *J* = 6.9 Hz, 1H), 3.19 (s, 3H), 2.98 (d, *J* = 7.6 Hz, 1H), 2.41-2.21 (m, 2H), 2.11-1.97 (m, 2H), 1.87-1.77 (m, 1H), 1.69-1.62 (m, 1H), 1.65 (d, *J* = 6.9 Hz, 3H), 1.19 (d, *J* = 6.1 Hz, 3H). Signals for the exchangeable protons were not observed. LCMS (ESI, high pH) *t*_R = 0.88 min, *m/z* 454 [M+H]⁺.

Isopropyl (((*R*)-1,3-dimethyl-5-(1-methyl-1*H*-1,2,4-triazol-3-yl)-2-oxo-2,3-dihydro-1*H*-benzo[*d*]azepin-7-yl)methyl)-*L*-serinate [6.26]

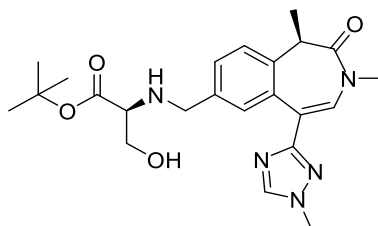


Reductive amination general procedure A2 with aldehyde [6.22] (80 mg, 0.27 mmol) and isopropyl *L*-serinate, tosic acid salt [7.08] (129 mg, 0.41 mmol). MDAP (high pH

extended method B) to afford the title product **[6.26]** as a colourless gum (53.3 mg, 42% yield).

¹H NMR (400 MHz, CDCl₃) δ 8.03 (s, 1H), 7.69 (d, $J = 1.4$ Hz, 1H), 7.46 (s, 1H), 7.36 (dd, $J = 8.2, 1.4$ Hz, 1H), 7.31 (d, $J = 8.2$ Hz, 1H), 5.06 (spt, $J = 6.4$ Hz, 1H), 3.97 (d, $J = 13.5$ Hz, 1H), 3.94 (s, 3H), 3.76-3.69 (m, 2H), 3.59-3.53 (m, 1H), 3.43-3.35 (m, 2H), 3.19 (s, 3H), 1.65 (d, $J = 7.1$ Hz, 3H), 1.25 (d, $J = 6.4$ Hz, 3H), 1.24 (d, $J = 6.4$ Hz, 3H). Signals for the exchangeable protons were not observed. **¹³C NMR** (101 MHz, CDCl₃) δ 172.4 (C=O), 170.7 (C=O), 162.3 (C_{iv}), 143.9 (CH), 137.3 (C_{iv}), 136.6 (C_{iv}), 133.1 (C_{iv}), 131.7 (CH), 129.3 (CH), 128.0 (CH), 124.0 (CH), 119.8 (C_{iv}), 68.9 (CH), 62.5 (CH₂), 62.0 (CH), 51.7 (CH₂), 41.2 (CH), 36.3 (CH₃), 35.6 (CH₃), 21.8 (CH₃)*, 21.8 (CH₃)*, 12.7 (CH₃). *peaks at 21.84 and 21.78 ppm. **LCMS** (ESI, formic) $t_R = 0.51$ min, m/z 428 [M+H]⁺. **HRMS** (ESI) calculated for C₂₂H₃₀N₅O₄ [M+H]⁺ 428.2299, found 428.2290 (1.82 min). ν_{max} (solution in chloroform, cm⁻¹): 3427 (OH), 3260 (NH), 2980 (CH alkene), 2934 (CH alkane), 1725 (C=O ester), 1667 (C=O amide), 1630 (C=C alkene). $[\alpha_D]^{20.2}_{589\text{ nm}}$ (c 0.500, MeOH): +197.1°.

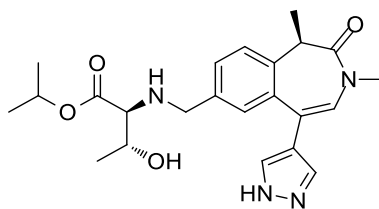
Tert*-butyl (((*R*)-1,3-dimethyl-5-(1-methyl-1*H*-1,2,4-triazol-3-yl)-2-oxo-2,3-dihydro-1*H*-benzo[*d*]azepin-7-yl)methyl)-*L*-serinate **[6.27]*



Reductive amination general procedure A2 with aldehyde **[6.22]** (50 mg, 0.17 mmol) and *tert*-butyl *L*-serinate, hydrochloride **[7.11]** (50 mg, 0.25 mmol). The sample was purified by MDAP (high pH, extended method B) to afford the title product **[6.27]** as a colourless gum (26.3 mg, 34% yield).

¹H NMR (400 MHz, CDCl₃) δ 8.04 (s, 1H), 7.69 (d, *J* = 1.5 Hz, 1H), 7.45 (s, 1H), 7.35 (dd, *J* = 7.8, 1.5 Hz, 1H), 7.31 (d, *J* = 7.8 Hz, 1H), 3.95 (d, *J* = 13.7 Hz, 1H), 3.94 (s, 3H), 3.71 (d, *J* = 13.7 Hz, 1H), 3.69 (dd, *J* = 10.8, 4.4 Hz, 1H), 3.52 (dd, *J* = 10.8, 6.9 Hz, 1H), 3.39 (q, *J* = 6.9 Hz, 1H), 3.29 (dd, *J* = 6.9, 4.4 Hz, 1H), 3.18 (s, 3H), 2.13 (br. s, 2H), 1.65 (d, *J* = 6.9 Hz, 3H), 1.45 (s, 9H). LCMS (ESI, high pH) t_R = 0.85 min, *m/z* 442 [M+H]⁺.

Isopropyl (((*R*)-1,3-dimethyl-2-oxo-5-(1*H*-pyrazol-4-yl)-2,3-dihydro-1*H*-benzo[*d*]azepin-7-yl)methyl)-*L*-threoninate [7.01]



Reductive amination general procedure A1 with aldehyde [7.05] (181.4 mg, 0.40 mmol) and isopropyl *L*-threoninate, hydrochloride [7.06] (118 mg, 0.60 mmol). The product was purified by silica column chromatography, eluted with 0-100% EtOAc in cyclohexane. The relevant fractions were concentrated under reduced pressure to give isopropyl (((*R*)-1,3-dimethyl-2-oxo-5-(1-((2-(trimethylsilyl)ethoxy)methyl)-1*H*-pyrazol-4-yl)-2,3-dihydro-1*H*-benzo[*d*]azepin-7-yl)methyl)-*L*-threoninate [7.12] as a colourless oil (101.8 mg, 46% yield). LCMS (ESI, high pH) t_R = 1.33 min, *m/z* 557 [M+H]⁺.

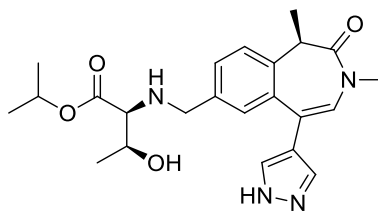
Deprotection reaction:

Isopropyl (((*R*)-1,3-dimethyl-2-oxo-5-(1-((2-(trimethylsilyl)ethoxy)methyl)-1*H*-pyrazol-4-yl)-2,3-dihydro-1*H*-benzo[*d*]azepin-7-yl)methyl)-*L*-threoninate [7.12] (101 mg, 0.18 mmol) and a 1 M solution of boron tribromide in DCM (272 μL, 0.27 mmol) were stirred in DCM (5 mL) under nitrogen at -78 °C for 30 min. Then, the reaction

mixture was stirred at rt for 15 min. The reaction mixture was cooled to -78 °C and was quenched with water and methanol. The layers were separated. The aqueous layer was re-extracted with DCM containing 10% MeOH, followed by an extraction with EtOAc. The organic layers were combined, dried through a phase separator and concentrated under reduced pressure to give a colourless oil. (NB: an LCMS of the aqueous layer showed some remaining product in the aqueous layer). The crude oil was purified by MDAP (high pH, extended method B) to afford the title product **[7.01]** as a yellow oil (14 mg, 17% yield).

¹H NMR (400 MHz, CDCl₃) δ 7.65 (br. s, 2H), 7.34 (d, *J* = 1.8 Hz, 1H), 7.33 (dd, *J* = 8.2, 1.8 Hz, 1H), 7.32 (d, *J* = 8.2 Hz, 1H), 7.26 (s, 2H)*, 6.63 (s, 1H), 5.03 (spt, *J* = 6.3 Hz, 1H), 3.82 (d, *J* = 13.0 Hz, 1H), 3.62 (d, *J* = 13.0 Hz, 1H), 3.62 (qd, *J* = 8.1, 6.3 Hz, 1H), 3.40 (q, *J* = 6.8 Hz, 1H), 3.13 (s, 3H), 2.89 (d, *J* = 8.1 Hz, 1H), 1.68 (d, *J* = 6.8 Hz, 3H), 1.23 (d, *J* = 6.3 Hz, 3H), 1.22 (d, *J* = 6.3 Hz, 3H), 1.17 (d, *J* = 6.3 Hz, 3H). *Same chemical shift than residual solvent peak. The signal for one of the exchangeable protons was not observed. LCMS (ESI, high pH) t_R = 0.86 min, *m/z* 427 [M+H]⁺.

Isopropyl (((*R*)-1,3-dimethyl-2-oxo-5-(1*H*-pyrazol-4-yl)-2,3-dihydro-1*H*-benzo[*d*]azepin-7-yl)methyl)-*L*-allo-threoninate [7.02]



Reductive amination general procedure A1 with aldehyde **[7.05]** (181.4 mg, 0.40 mmol) and isopropyl *L*-allo-threoninate, hydrochloride **[7.07]** (118 mg, 0.60 mmol). The product was purified by MDAP (high pH, extended method C). The relevant

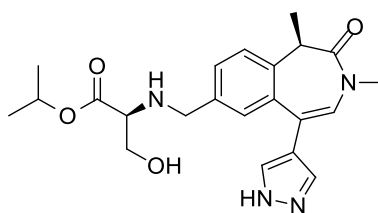
fractions were concentrated under reduced pressure to give isopropyl (((*R*)-1,3-dimethyl-2-oxo-5-(1-((2-(trimethylsilyl)ethoxy)methyl)-1*H*-pyrazol-4-yl)-2,3-dihydro-1*H*-benzo[*d*]azepin-7-yl)methyl)-*L*-allo-threoninate [**7.13**] as a white solid (100.6 mg, 67% yield). The product was used without further purification in the deprotection reaction. LCMS (ESI, high pH) $t_R = 1.30$ min, m/z 557 [M+H]⁺.

Deprotection reaction:

Isopropyl (((*R*)-1,3-dimethyl-2-oxo-5-(1-((2-(trimethylsilyl)ethoxy)methyl)-1*H*-pyrazol-4-yl)-2,3-dihydro-1*H*-benzo[*d*]azepin-7-yl)methyl)-*L*-allo-threoninate [**7.13**] (100.6 mg, 0.16 mmol) and a 1 M solution of boron tribromide in DCM (0.24 mL, 0.24 mmol) were stirred in DCM (5 mL) under nitrogen at -78 °C for 15 min and then the reaction mixture was stirred at rt for 15 min. The reaction mixture was quenched with a saturated solution of sodium bicarbonate and diluted with DCM. The layers were separated. The aqueous layer was re-extracted with DCM. The organic layers were combined, dried through a phase separator and concentrated under reduced pressure to give the crude product as a colourless oil. The oil was purified by MDAP (high pH, extended method B). The relevant fractions were concentrated under reduced pressure to give the title product [**7.02**] as a colourless oil (3.5 mg, 5% yield). The aqueous layer was re-extracted with EtOAc + 10% MeOH. A 2 M aqueous solution of LiCl was added. The layers were separated. The organic layer was dried through a phase separator and concentrated under reduced pressure to give a white residual oil. The oil was purified by MDAP (high pH method B). The relevant fractions were concentrated under reduced pressure to give the title product [**7.02**] as a colourless oil (29.8 mg, 41% yield).

¹H NMR (400 MHz, CDCl₃) δ 7.63 (s, 2H), 7.34 (s, 3H), 6.63 (s, 1H), 5.04 (spt, *J* = 6.4 Hz, 1H), 3.83 (d, *J* = 13.1 Hz, 1H), 3.64 (qd, *J* = 7.8, 6.1 Hz, 1H), 3.63 (d, *J* = 13.1 Hz, 1H), 3.40 (q, *J* = 6.9 Hz, 1H), 3.13 (s, 3H), 2.91 (d, *J* = 7.8 Hz, 1H), 1.68 (d, *J* = 6.9 Hz, 3H), 1.23 (d, *J* = 6.4 Hz, 3H), 1.22 (d, *J* = 6.4 Hz, 3H), 1.17 (d, *J* = 6.1 Hz, 3H). The signals for the exchangeable protons were not observed. ¹³C NMR (101 MHz, CDCl₃) δ 173.0 (C=O), 170.5 (C=O), 137.2 (C_{iv}), 136.9 (C_{iv}), 135.6 (C_{iv}), 132.9 (CH), 132.9 (CH), 129.6 (CH), 127.4 (CH), 126.8 (CH), 124.2 (CH), 121.8 (C_{iv}), 121.1 (C_{iv}), 68.8 (CH), 68.0 (CH), 67.2 (CH), 51.9 (CH₂), 41.0 (CH), 35.2 (CH₃), 21.9 (CH₃), 21.7 (CH₃), 19.2 (CH₃), 12.7 (CH₃). LCMS (ESI, formic) t_R = 0.51 min, *m/z* 427 [M+H]⁺. HRMS (ESI) calculated for C₂₃H₃₁N₄O₄ [M+H]⁺ 427.2349, found 427.2343 (2.10 min). ν_{max} (solution in chloroform, cm⁻¹): 3438 (OH), 3223 (NH), 2978 (CH alkene), 2935 (CH alkane), 1723 (C=O ester), 1646 (C=O amide). [α]_D^{20.5 °C}_{589 nm} (c 0.500, MeOH): +96.4°.

Isopropyl (((*R*)-1,3-dimethyl-2-oxo-5-(1*H*-pyrazol-4-yl)-2,3-dihydro-1*H*-benzo[*d*]azepin-7-yl)methyl)-*L*-serinate [7.03]

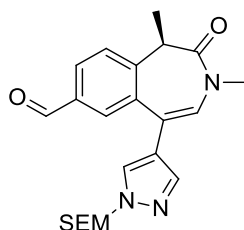


Isopropyl (((*R*)-1,3-dimethyl-2-oxo-5-(1-((2-(trimethylsilyl)ethoxy)methyl)-1*H*-pyrazol-4-yl)-2,3-dihydro-1*H*-benzo[*d*]azepin-7-yl)methyl)-*L*-serinate [7.14] (152 mg, 0.25 mmol) was dissolved in DCM (5 mL) under nitrogen at -78 °C. A 1 M solution of BBr₃ in DCM (0.63 mL, 0.63 mmol) was added and the reaction mixture was stirred 20 min at -78 °C. The reaction mixture was quenched with a saturated solution of sodium bicarbonate. DCM was added. The layers were separated. The

aqueous layer was re-extracted with EtOAc. The organic layers were combined, dried through a phase separator and concentrated under reduced pressure to give the crude product as a white solid. The solid was purified by MDAP (high pH, extended method B). The relevant fractions were concentrated under reduced pressure to give the title product **[7.03]** as a colourless oil (20.4 mg, 19% yield).

¹H NMR (400 MHz, CDCl₃) δ 7.58 (s, 2H), 7.37 (dd, $J = 8.4, 1.7$ Hz, 1H), 7.35 (d, $J = 8.4$ Hz, 1H), 7.34 (s, 1H), 6.61 (s, 1H), 5.04 (spt, $J = 6.2$ Hz, 1H), 3.87 (d, $J = 13.2$ Hz, 1H), 3.73 (dd, $J = 10.8, 4.5$ Hz, 1H), 3.69 (d, $J = 13.2$ Hz, 1H), 3.59 (dd, $J = 10.8, 6.4$ Hz, 1H), 3.39 (q, $J = 6.9$ Hz, 1H), 3.32 (dd, $J = 6.4, 4.5$ Hz, 1H), 3.12 (s, 3H), 1.68 (d, $J = 6.9$ Hz, 3H), 1.23 (d, $J = 6.2$ Hz, 3H), 1.22 (d, $J = 6.2$ Hz, 3H). The signals for the exchangeable protons were not observed. **¹³C NMR** (101 MHz, MeOD) δ 172.2 (C=O), 140.5 (CH), 137.6 (C_{iv}) 134.2 (C_{iv}), 132.4 (CH), 130.9 (CH), 130.4 (C_{iv}), 129.2 (CH), 126.0 (CH), 123.1 (CH), 72.6 (CH), 62.2 (CH₂), 59.9 (CH), 42.4 (CH), 35.6 (CH₃), 22.0 (CH₃), 21.9 (CH₃), 13.1 (CH₃). The signal for the benzylic CH₂ was hidden under the residual methanol signal (observed by HSQC ¹H-¹³C NMR). The signals for three quaternary carbons were not observed. **LCMS** (ESI, high pH) $t_R = 0.80$ min, m/z 413 [M+H]⁺. **HRMS** (ESI) calculated for C₂₂H₂₉N₄O₄ [M+H]⁺ 413.2189, found 413.2183 (1.92 min). ν_{\max} (solution in methanol, cm⁻¹): 3367 (OH), 3233 (NH), 2981 (CH alkene), 2935 (CH alkane), 1738 (C=O ester), 1644 (C=O amide), 1561 (C=C). $[\alpha_D]^{20.5}_{589\text{ nm}}$ (c 0.498, MeOH): +80.3°.

(R)-1,3-Dimethyl-2-oxo-5-(1-((2-(trimethylsilyl)ethoxy)methyl)-1H-pyrazol-4-yl)-2,3-dihydro-1H-benzo[d]azepine-7-carbaldehyde [7.05]

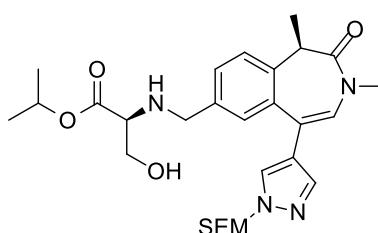


(R)-5-Bromo-1,3-dimethyl-2-oxo-2,3-dihydro-1H-benzo[d]azepine-7-carbaldehyde [6.06] (122 mg, 0.42 mmol), potassium carbonate (115 mg, 0.83 mmol), 4-(4,4,5,5-tetramethyl-1,3,2-dioxaborolan-2-yl)-1-((2-(trimethylsilyl)ethoxy)methyl)-1H-pyrazole [7.04] (269 mg, 0.83 mmol), and Pd(PPh₃)₄ (24 mg, 0.02 mmol) were suspended in water (1 mL) and 1,4-dioxane (5 mL). The reaction mixture was stirred under nitrogen at 120 °C for 1 h. The reaction mixture was concentrated under reduced pressure. EtOAc and water were added to the residue. The layers were separated and the aqueous layer was extracted with EtOAc. The organic layers were combined, washed with brine, dried using a hydrophobic frit and concentrated under reduced pressure to give a yellow oil. The crude product was purified by silica column chromatography, eluted with a gradient of 0-40% EtOAc in cyclohexane. The relevant fractions were concentrated under reduced pressure to afford the title product [7.05] as a colourless oil (181.4 mg, 96% yield).

¹H NMR (400 MHz, CDCl₃) δ 9.93 (s, 1H), 7.93 (dd, *J* = 8.1, 1.5 Hz, 1H), 7.84 (d, *J* = 1.5 Hz, 1H), 7.60 (s, 1H), 7.54 (s, 1H), 7.54 (d, *J* = 8.1 Hz, 1H), 6.68 (s, 1H), 5.43 (s, 2H), 3.62 (t, *J* = 8.2, 2H), 3.47 (q, *J* = 6.9 Hz, 1H), 3.12 (s, 3H), 1.72 (d, *J* = 6.9 Hz, 3H), 0.92 (t, *J* = 8.2 Hz, 2H), -0.01 (s, 9H). ¹³C NMR (101 MHz, CDCl₃) δ 191.41 (C=O), 169.54 (C=O), 143.48 (C_{iv}), 138.51 (CH), 136.05 (C_{iv}), 134.73 (C_{iv}), 129.70 (CH), 129.47 (CH), 128.31 (CH), 127.83 (CH), 124.99 (CH), 122.06 (C_{iv}), 121.05

(C_{iv}), 80.46 (CH₂), 67.02 (CH₂), 41.78 (CH), 35.29 (CH₃), 17.78 (CH₂), 12.71 (CH₃), -1.45 (Si(CH₃)₃). **LCMS** (ESI, high pH) *t_R* = 1.28 min, *m/z* 412 [M+H]⁺. **HRMS** (ESI) calculated for C₂₂H₃₀N₃O₃Si [M+H]⁺ 412.2057, found 412.2049 (5.74 min). **ν_{max}** (solution in chloroform, cm⁻¹): 2947 (CH alkene), 2889 (CH alkane), 1699 (C=O aldehyde), 1661 (C=O amide), 1600 (C=C). **[α]_D**^{20.5 °C}_{589 nm} (c 0.500, MeOH): +213.8°.

Isopropyl (((*R*)-1,3-dimethyl-2-oxo-5-(1-((2-(trimethylsilyl)ethoxy)methyl)-1*H*-pyrazol-4-yl)-2,3-dihydro-1*H*-benzo[*d*]azepin-7-yl)methyl)-*L*-serinate [7.14]

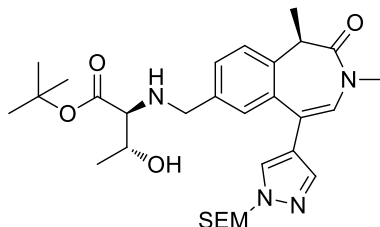


Reductive amination general procedure A1 with aldehyde [7.05] (178.9 mg, 0.39 mmol) and isopropyl *L*-serinate, tosic acid salt [7.08] (187 mg, 0.59 mmol). The product was purified by silica column chromatography, eluted with 0-100% EtOAc in cyclohexane. The relevant fractions were concentrated under reduced pressure and purified by MDAP (high pH, extended method C). The relevant fractions were concentrated under reduced pressure to give the title product [7.14] as a colourless oil (152.1 mg, 65% yield).

¹H NMR (400 MHz, CDCl₃) δ 7.62 (s, 1H), 7.56 (s, 1H), 7.38 (dd, *J* = 8.1, 1.5 Hz, 1H), 7.33 (d, *J* = 8.1 Hz, 1H), 7.32 (d, *J* = 1.5 Hz, 1H), 6.62 (s, 1H), 5.43 (s, 2H), 5.03 (spt, *J* = 6.4 Hz, 1H), 3.86 (d, *J* = 13.2 Hz, 1H), 3.70 (dd, *J* = 10.8, 4.5 Hz, 1H), 3.68 (d, *J* = 13.2 Hz, 1H), 3.63 (d, *J* = 7.9 Hz, 1H), 3.61 (d, *J* = 7.9 Hz, 1H), 3.53 (dd, *J* = 10.8, 6.8 Hz, 1H), 3.39 (q, *J* = 6.9 Hz, 1H), 3.30 (dd, *J* = 6.8, 4.5 Hz, 1H), 3.11 (s, 3H), 2.69 (br. s, 1H), 1.67 (d, *J* = 6.9 Hz, 3H), 1.23 (d, *J* = 6.4 Hz, 3H), 1.22 (d, *J* = 6.4 Hz, 3H), 0.94 (d, *J* = 7.9 Hz, 1H), 0.92 (d, *J* = 7.9 Hz, 1H), -0.02 (m, 9H). The signal for

one of the exchangeable protons was not observed. LCMS (ESI, high pH) $t_R = 1.25$ min, m/z 543 $[M+H]^+$.

Isopropyl (((R)-1,3-dimethyl-2-oxo-5-(1-((2-(trimethylsilyl)ethoxy)methyl)-1H-pyrazol-4-yl)-2,3-dihydro-1H-benzo[d]azepin-7-yl)methyl)-L-serinate [7.15]

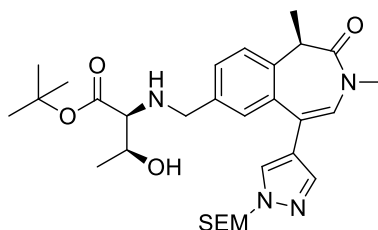


Reductive amination general procedure A1 with aldehyde [7.05] (150 mg, 0.35 mmol) and *tert*-butyl *L*-threoninate, hydrochloride [7.09] (110 mg, 0.52 mmol). The product was purified by MDAP (high pH, extended method C). *NB*: one of the MDAP runs had a pump failure during the injection and the product was lost. The relevant fractions were concentrated under reduced pressure to give the title product [7.15] as a white solid (75.5 mg, 36% yield).

$^1\text{H NMR}$ (400 MHz, CDCl_3) δ 7.62 (s, 1H), 7.55 (s, 1H), 7.35 (dd, $J = 8.0, 1.5$ Hz, 1H), 7.32 (d, $J = 8.0$ Hz, 1H), 7.31 (d, $J = 1.5$ Hz, 1H), 6.62 (s, 1H), 5.44 (d, $J = 10.9$ Hz, 1H), 5.40 (d, $J = 10.9$ Hz, 1H), 3.80 (d, $J = 13.2$ Hz, 1H), 3.63 (d, $J = 13.2$ Hz, 1H), 3.62 (d, $J = 7.6$ Hz, 1H), 3.61 (d, $J = 7.6$ Hz, 1H), 3.56 (qd, $J = 7.8, 6.4$ Hz, 1H), 3.38 (q, $J = 6.9$ Hz, 1H), 3.10 (s, 3H), 2.80 (d, $J = 7.8$ Hz, 1H), 1.98 (br. s, 2H), 1.66 (d, $J = 6.9$ Hz, 3H), 1.41 (s, 9H), 1.16 (d, $J = 6.4$ Hz, 3H), 0.93 (d, $J = 7.6$ Hz, 1H), 0.90 (d, $J = 7.6$ Hz, 1H), -0.02 (s, 9H). LCMS (ESI, high pH) $t_R = 1.38$ min, m/z 571 $[M+H]^+$.

***Tert*-butyl (((*R*)-1,3-dimethyl-2-oxo-5-(1-((2-(trimethylsilyl)ethoxy)methyl)-1*H*-pyrazol-4-yl)-2,3-dihydro-1*H*-benzo[*d*]azepin-7-yl)methyl)-*L*-allo-threoninate**

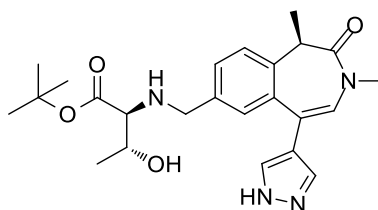
[7.16]



Reductive amination general procedure A1 with aldehyde [7.05] (101 mg, 0.23 mmol) and *tert*-butyl *L*-allo-threoninate, hydrochloride [7.10] (74.0 mg, 0.35 mmol). The product was purified by silica column chromatography eluted with a gradient of 0-100% EtOAc in cyclohexane. The relevant fractions were concentrated under reduced pressure to give the title product [7.16] as a yellow oil (57.5 mg, 37% yield).

¹H NMR (400 MHz, CDCl₃) δ : 7.62 (s, 1H), 7.55 (s, 1H), 7.37 (dd, *J* = 8.0, 1.5 Hz, 1H), 7.32 (d, *J* = 8.0 Hz, 1H), 7.30 (br. s, 1H), 6.61 (s, 1H), 5.42 (s, 2H), 3.93 (qd, *J* = 6.5, 4.5 Hz, 1H), 3.83 (d, *J* = 13.1 Hz, 1H), 3.62 (d, *J* = 13.1 Hz, 1H), 3.61 (d, *J* = 7.5 Hz, 1H), 3.60 (d, *J* = 7.5 Hz, 1H), 3.38 (q, *J* = 6.9 Hz, 1H), 3.19 (d, *J* = 4.5 Hz, 1H), 3.10 (s, 3H), 1.66 (d, *J* = 6.9 Hz, 3H), 1.42 (s, 9H), 1.04 (d, *J* = 6.5 Hz, 3H), 0.93 (d, *J* = 7.5 Hz, 1H), 0.91 (d, *J* = 7.5 Hz, 1H), -0.02 (s, 9H). The signals for the exchangeable protons were not observed. LCMS (ESI, high pH) *t*_R = 1.35 min, *m/z* 571 [M+H]⁺.

***Tert*-butyl (((*R*)-1,3-dimethyl-2-oxo-5-(1*H*-pyrazol-4-yl)-2,3-dihydro-1*H*-benzo[*d*]azepin-7-yl)methyl)-*L*-threoninate [7.17]**



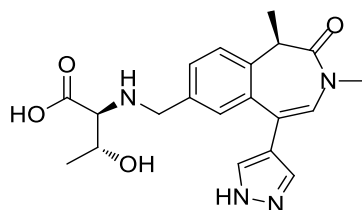
Tert-butyl (((*R*)-1,3-dimethyl-2-oxo-5-(1-((2-(trimethylsilyl)ethoxy)methyl)-1*H*-pyrazol-4-yl)-2,3-dihydro-1*H*-benzo[*d*]azepin-7-yl)methyl)-*L*-threoninate [7.15]

(75.5 mg, 0.132 mmol) and a 1 M solution of boron tribromide in DCM (0.20 mL, 0.20 mmol) were stirred in DCM (5 mL) under nitrogen at -78 °C for 15 min and then the reaction mixture was stirred at rt for 30 min. The reaction mixture was quenched with a saturated solution of sodium bicarbonate and diluted with DCM. The layers were separated. The aqueous layer was re-extracted with DCM. The organic layers were combined, dried through a phase separator and concentrated under reduced pressure to give the crude product as a colourless oil. The oil was purified by MDAP (high pH, extended method B). The relevant fractions were concentrated under reduced pressure to give the title product [7.17] as yellow oil (2.8 mg, 5% yield).

¹H NMR (400 MHz, CDCl₃) δ 7.63 (s, 2H), 7.36 (dd, *J* = 8.4, 1.7 Hz, 1H), 7.35 (d, *J* = 1.7 Hz, 1H), 7.34 (d, *J* = 8.4 Hz, 1H), 6.63 (s, 1H), 3.82 (d, *J* = 13.2 Hz, 1H), 3.63 (d, *J* = 13.2 Hz, 1H), 3.58 (qd, *J* = 8.0, 6.1 Hz, 1H), 3.40 (q, *J* = 7.0 Hz, 1H), 3.12 (s, 3H), 2.81 (d, *J* = 8.0 Hz, 1H), 1.68 (d, *J* = 7.0 Hz, 3H), 1.44 (s, 9H), 1.17 (d, *J* = 6.1 Hz, 3H). The signals for the exchangeable protons were not observed. LCMS (ESI, high pH) *t*_R = 0.92 min, *m/z* 441 [M+H]⁺.

Isolation of the carboxylic acid product:

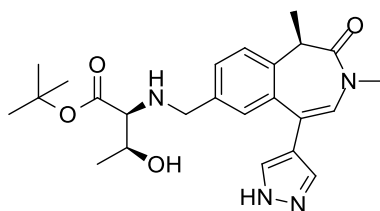
(((*R*)-1,3-Dimethyl-2-oxo-5-(1*H*-pyrazol-4-yl)-2,3-dihydro-1*H*-benzo[*d*]azepin-7-yl)methyl)-*L*-threonine



The aqueous layer was concentrated under reduced pressure to give a white residue. The white solid was suspended in MeOH + 2 drops of DMSO. The suspension was filtered through a phase separator and the filtrate was evaporated under reduced pressure to give the crude product in DMSO. This fraction was purified by MDAP (formic, extended method A). The relevant fractions were concentrated under reduced pressure to give the title product as a colourless oil (5.8 mg, 10% yield).

¹H NMR (400 MHz, MeOD) δ 7.72 (br. s, 2H), 7.60 (br. d, $J = 7.7$ Hz, 1H), 7.53 (br. s, 1H), 7.46 (d, $J = 7.7$ Hz, 1H), 6.89 (s, 1H), 4.25 (d, $J = 12.3$ Hz, 1H), 4.16 (d, $J = 12.3$ Hz, 1H), 3.95 (br. s, 1H), 3.47 (q, $J = 6.9$ Hz, 1H), 3.18 (br. s, 1H), 3.09 (s, 3H), 1.64 (d, $J = 6.9$ Hz, 3H), 1.27 (br. s, 3H). The signals for the exchangeable protons were observed as very broad peaks under other signals. LCMS (ESI, high pH) $t_R = 0.52$ min, m/z 385 [M+H]⁺.

***Tert*-butyl (((*R*)-1,3-dimethyl-2-oxo-5-(1*H*-pyrazol-4-yl)-2,3-dihydro-1*H*-benzo[*d*]azepin-7-yl)methyl)-*L*-*allo*-threoninate [7.18]**



Tert-butyl (((*R*)-1,3-dimethyl-2-oxo-5-(1-((2-(trimethylsilyl)ethoxy)methyl)-1*H*-pyrazol-4-yl)-2,3-dihydro-1*H*-benzo[*d*]azepin-7-yl)methyl)-*L*-*allo*-threoninate [7.16]

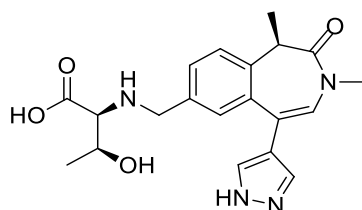
(57.4 mg, 0.09 mmol) and a 1 M solution of boron tribromide in DCM (0.13 mL, 0.13 mmol) were stirred in DCM (5 mL) under nitrogen at -78 °C for 30 min. The reaction mixture was warmed up to rt and stirred for 15 min. The reaction mixture was quenched with a saturated solution of sodium bicarbonate and diluted with DCM. The layers were separated. The aqueous layer was re-extracted with DCM. The organic layers were combined, dried through a phase separator and concentrated under reduced pressure to give the crude product as a colourless oil. The oil was purified by MDAP (high pH, extended method B). The relevant fraction was concentrated under reduced pressure to give the title product **[7.18]** as colourless oil (2.5 mg, 6% yield).

¹H NMR (400 MHz, CDCl₃) δ 7.63 (s, 2H), 7.38 (d, $J = 8.1, 1.5$ Hz, 1H), 7.34 (d, $J = 8.1$ Hz, 1H), 7.32 (br. s, 1H), 6.63 (s, 1H), 3.94 (qd, $J = 6.4, 4.7$ Hz, 1H), 3.85 (d, $J = 13.0$ Hz, 1H), 3.62 (d, $J = 13.0$ Hz, 1H), 3.39 (q, $J = 6.9$ Hz, 1H), 3.21 (d, $J = 4.7$ Hz, 1H), 3.12 (s, 3H), 2.67 (br. s, 1H), 1.68 (d, $J = 6.9$ Hz, 3H), 1.44 (s, 9H), 1.04 (d, $J = 6.4$ Hz, 3H). The signals for two of the exchangeable protons were not observed.

LCMS (ESI, high pH) $t_R = 0.90$ min, m/z 441 [M+H]⁺.

Isolation of the carboxylic acid product:

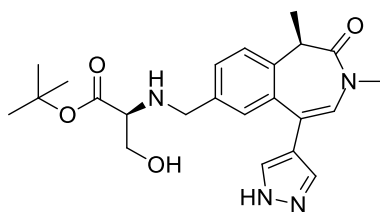
(((R)-1,3-Dimethyl-2-oxo-5-(1H-pyrazol-4-yl)-2,3-dihydro-1H-benzo[d]azepin-7-yl)methyl)-L-allo-threonine



The aqueous layer was concentrated under reduced pressure to give a white residue. The white solid was suspended in methanol and DCM. The suspension was filtered through a phase separator and the filtrate was concentrated under reduced pressure to

give the crude carboxylic acid product. The by-product was purified by MDAP (formic, extended method A). The relevant fractions were concentrated under reduced pressure to give the title product as a colourless oil in two batches (3.0 mg, 9% yield and 2.5 mg, 7% yield). $^1\text{H NMR}$ (400 MHz, MeOD) δ 8.16 (s, 1H), 7.72 (s, 2H), 7.60 (dd, $J = 8.1, 1.7$ Hz, 1H), 7.51 (d, $J = 1.7$ Hz, 1H), 7.47 (d, $J = 8.1$ Hz, 1H), 6.89 (s, 1H), 4.29 (d, $J = 13.2$ Hz, 1H), 4.19 (d, $J = 13.2$ Hz, 1H), 4.22 (qd, $J = 6.6, 3.9$ Hz, 1H), 3.47 (q, $J = 6.9$ Hz, 1H), 3.44 (d, $J = 3.9$ Hz, 1H), 3.09 (s, 3H), 1.64 (d, $J = 6.9$ Hz, 3H), 1.17 (d, $J = 6.6$ Hz, 3H). The signals for three of the four exchangeable protons were not observed. LCMS (ESI, formic) $t_R = 0.47$ min, m/z 385 $[\text{M}+\text{H}]^+$.

***Tert*-butyl (((*R*)-1,3-dimethyl-2-oxo-5-(1*H*-pyrazol-4-yl)-2,3-dihydro-1*H*-benzo[*d*]azepin-7-yl)methyl)-*L*-serinate [7.19]**

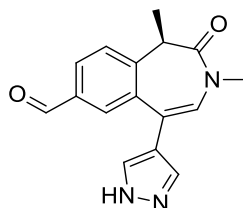


Reductive amination general procedure A1 with aldehyde [7.20] (11.7 mg, 0.035 mmol) and *tert*-butyl *L*-serinate, hydrochloride [7.11] (10.5 mg, 0.05 mmol). The product was purified by silica column chromatography eluted with 0-100% EtOAc in cyclohexane, followed by a gradient of 0-25% EtOH in EtOAc. The relevant fractions were concentrated under reduced pressure and further purified by MDAP (high pH, extended method B). The relevant fractions were concentrated under reduced pressure to give the title product [7.19] as a colourless oil (7.6 mg, 48% yield).

$^1\text{H NMR}$ (400 MHz, CDCl_3) δ . 7.60 (s, 2H), 7.38 (dd, $J = 8.1, 1.5$ Hz, 1H), 7.34 (d, $J = 8.1$ Hz, 1H), 7.33 (d, $J = 1.5$ Hz, 1H), 6.62 (s, 1H), 3.86 (d, $J = 13.2$ Hz, 1H), 3.68 (d, $J = 13.2$ Hz, 1H), 3.70 (dd, $J = 10.5, 4.5$ Hz, 1H), 3.52 (dd, $J = 10.5, 6.6$ Hz, 1H),

3.40 (q, $J = 7.1$ Hz, 1H), 3.25 (dd, $J = 6.6, 4.5$ Hz, 1H), 3.12 (s, 3H), 1.68 (d, $J = 7.1$ Hz, 3H), 1.44 (s, 9H). The signals for the exchangeable protons were not observed. LCMS (ESI, high pH) $t_R = 0.85$ min, m/z 427 $[M+H]^+$.

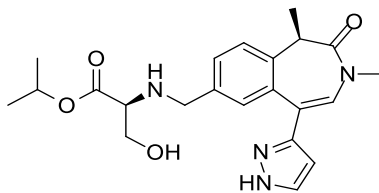
(R)-1,3-Dimethyl-2-oxo-5-(1H-pyrazol-4-yl)-2,3-dihydro-1H-benzo[d]azepine-7-carbaldehyde [7.20]



(R)-1,3-Dimethyl-2-oxo-5-(1-((2-(trimethylsilyl)ethoxy)methyl)-1H-pyrazol-4-yl)-2,3-dihydro-1H-benzo[d]azepine-7-carbaldehyde [7.05] (90 mg, 0.20 mmol) was dissolved in DCM (5 mL) under nitrogen at -78 °C. A 1 M solution of BBr_3 in DCM (0.50 mL, 0.50 mmol) was added and the reaction mixture was stirred at -78 °C for 15 min and then at rt for 30 min. The reaction mixture was quenched with a saturated aqueous solution of sodium bicarbonate. DCM was added. The layers were separated. The aqueous layer was re-extracted with EtOAc. The organic layers were combined, dried through a phase separator and concentrated under reduced pressure to give the crude product as a yellow solid. The product was dissolved in MeCN and purified by MDAP (high pH, extended method A). The relevant fractions were concentrated under reduced pressure to give the title product [7.20] as a yellow solid (11.7 mg, 18% yield). 1H NMR (400 MHz, $CDCl_3$) δ 9.95 (s, 1H), 7.94 (dd, $J = 8.2, 1.7$ Hz, 1H), 7.86 (d, $J = 1.7$ Hz, 1H), 7.63 (s, 2H), 7.56 (d, $J = 8.2$ Hz, 1H), 6.70 (s, 1H), 3.49 (q, $J = 7.1$ Hz, 1H), 3.15 (s, 3H), 3.14-3.10 (m, 1H), 1.74 (d, $J = 7.1$ Hz, 3H). LCMS (ESI, high pH) $t_R = 0.75$ min, m/z 282 $[M+H]^+$.

Stereoselective synthesis of molecule [7.21]:

Isopropyl (((*R*)-1,3-dimethyl-2-oxo-5-(1*H*-pyrazol-3-yl)-2,3-dihydro-1*H*-benzo[*d*]azepin-7-yl)methyl)-*L*-serinate [7.21]

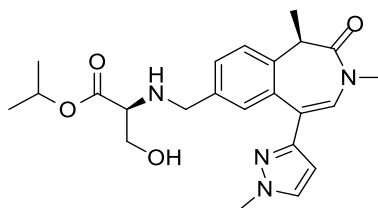


Isopropyl (((*R*)-1,3-dimethyl-2-oxo-5-(1-((2-(trimethylsilyl)ethoxy)methyl)-1*H*-pyrazol-3-yl)-2,3-dihydro-1*H*-benzo[*d*]azepin-7-yl)methyl)-*L*-serinate [8.09] (47.7 mg, 0.09 mmol) was dissolved in acetone (2 mL) at rt. A 1 M solution of HCl in Et₂O (4 mL, 132 mmol) was added and the reaction mixture was stirred for 18 h. The reaction mixture was concentrated under reduced pressure to give a pale yellow solid. The crude product was purified by MDAP (high pH, extended method B). The relevant fractions were concentrated under reduced pressure to give the title product [7.21] as a colourless oil (28.6 mg, 75% yield).

¹H NMR (400 MHz, MeOD) δ 7.66 (d, $J = 2.1$ Hz, 1H), 7.47 (dd, $J = 8.1, 1.6$ Hz, 1H), 7.36 (d, $J = 8.1$ Hz, 1H), 7.29 (d, $J = 1.6$ Hz, 1H), 7.00 (s, 1H), 6.39 (d, $J = 2.1$ Hz, 1H), 4.98 (spt, $J = 6.4$ Hz, 1H), 3.82 (d, $J = 13.0$ Hz, 1H), 3.68 (dd, $J = 5.1, 1.5$ Hz, 2H), 3.68 (d, $J = 13.0$ Hz, 1H), 3.43 (q, $J = 6.9$ Hz, 1H), 3.27 (t, $J = 5.1$ Hz, 1H), 3.13 (s, 3H), 1.64 (d, $J = 6.9$ Hz, 3H), 1.21 (d, $J = 6.4$ Hz, 3H), 1.19 (d, $J = 6.4$ Hz, 3H). The exchangeable protons were not observed. ¹³C NMR (101 MHz, MeOD) δ 173.9 (C=O), 172.6 (C=O), 138.7 (C_{iv}), 138.0 (C_{iv}), 135.9 (C_{iv}), 131.1 (CH), 130.3 (CH), 129.4 (CH), 125.0 (CH), 106.2 (CH), 70.1 (CH), 63.9 (CH₂), 63.4 (CH), 52.3 (CH₂), 42.3 (CH), 35.7 (CH₃), 22.2 (CH₃), 22.1 (CH₃), 13.2 (CH₃). The signals for a methine and two quaternary carbons were not observed. LCMS (ESI, high pH) $t_R = 0.81$ min, m/z 413 [M+H]⁺. HRMS (ESI) calculated for C₂₂H₂₉N₄O₄ [M+H]⁺ 413.2189, found

413.2188 (2.06 min). ν_{\max} (solution in chloroform, cm^{-1}): 3218 (OH), 2981 (CH alkene), 2934 (CH alkane), 1725 (C=O ester), 1651 (C=O amide). $[\alpha]_D^{21.6}$ (c 0.500, MeOH): +139.2°.

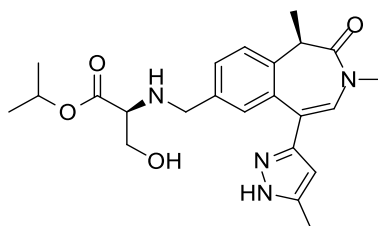
Isopropyl (((*R*)-1,3-dimethyl-5-(1-methyl-1*H*-pyrazol-3-yl)-2-oxo-2,3-dihydro-1*H*-benzo[*d*]azepin-7-yl)methyl)-*L*-serinate [7.23]



Reductive amination general procedure A1 with aldehyde [7.46] (90 mg, 0.27 mmol) and isopropyl *L*-serinate, tosic acid salt [7.08] (130 mg, 0.41 mmol). The product was purified silica column chromatography eluted with a gradient of 0-100% EtOAc in cyclohexane, followed by a gradient of 0-25% EtOH in EtOAc. The relevant fractions were concentrated under reduced pressure and purified by HPLC (Chiralpak AD-H column, 30% EtOH (containing 2% *i*PrNH₂) in heptane (containing 2% *i*PrNH₂)). The relevant fractions were concentrated under reduced pressure to give the title product [7.23] as a colourless oil (83 mg, 72% yield).

¹H NMR (400 MHz, MeOD) δ 7.61 (d, $J = 2.4$ Hz, 1H), 7.46 (dd, $J = 8.3, 1.6$ Hz, 1H), 7.34 (d, $J = 8.3$ Hz, 1H), 7.33 (d, $J = 1.6$ Hz, 1H), 7.00 (s, 1H), 6.33 (d, $J = 2.4$ Hz, 1H), 4.99 (spt, $J = 6.4$ Hz, 1H), 3.91 (s, 3H), 3.81 (d, $J = 13.2$ Hz, 1H), 3.65 (d, $J = 13.2$ Hz, 1H), 3.68 (dd, $J = 7.1, 5.1$ Hz, 1H), 3.61 (dd, $J = 7.1, 5.1$ Hz, 1H), 3.41 (q, $J = 7.0$ Hz, 1H), 3.24 (t, $J = 5.1$ Hz, 1H), 3.12 (s, 3H), 1.63 (d, $J = 7.0$ Hz, 3H), 1.21 (d, $J = 6.4$ Hz, 3H), 1.19 (d, $J = 6.4$ Hz, 3H). The signals for the exchangeable protons were not observed. LCMS (ESI, high pH) $t_R = 0.88$ min, m/z 427 [M+H]⁺.

Isopropyl (((*R*)-1,3-dimethyl-5-(5-methyl-1*H*-pyrazol-3-yl)-2-oxo-2,3-dihydro-1*H*-benzo[*d*]azepin-7-yl)methyl)-*L*-serinate [7.25]



Isopropyl (((*R*)-1,3-dimethyl-5-(5-methyl-1-((2-(trimethylsilyl)ethoxy)methyl)-1*H*-pyrazol-3-yl)-2-oxo-2,3-dihydro-1*H*-benzo[*d*]azepin-7-yl)methyl)-*L*-serinate [7.69]

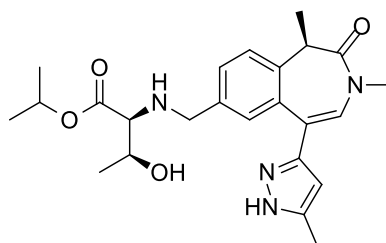
(30 mg, 0.043 mmol) was dissolved in DCM (5 mL) under nitrogen and the reaction mixture was cooled to -78 °C. A 1 M solution of boron tribromide in DCM (0.13 mL, 0.13 mmol) was added and the reaction mixture was stirred at -78 °C for 8 min and at rt for 1 h. The reaction mixture was quenched with MeOH and concentrated under reduced pressure. The resulting residue was purified by MDAP (High pH, extended method B). The relevant fractions were combined and concentrated under reduced pressure and further purified by HPLC (Chiralpak AD-H column, 30% EtOH in heptane). The relevant fractions were concentrated under reduced pressure to give the title product [7.25] as a white solid (8 mg, 36% yield).

¹H NMR (400 MHz, CDCl₃) δ 7.39 (br. s, 1H), 7.37 (br. d, *J* = 8.0 Hz, 1H), 7.32 (br. d, *J* = 8.0 Hz, 1H), 6.88 (s, 1H), 6.14 (s, 1H), 5.03 (spt, *J* = 6.4 Hz, 1H), 3.89 (d, *J* = 13.2 Hz, 1H), 3.71 (d, *J* = 13.2 Hz, 1H), 3.70 (dd, *J* = 10.8, 5.1 Hz, 1H), 3.68 (br. s, 1H), 3.53 (dd, *J* = 10.8, 6.7 Hz, 1H), 3.39 (q, *J* = 7.1 Hz, 1H), 3.31 (dd, *J* = 6.7, 5.1 Hz, 1H), 3.14 (s, 3H), 2.34 (br. s, 3H), 1.67 (d, *J* = 7.1 Hz, 3H), 1.24 (d, *J* = 6.4 Hz, 3H), 1.23 (d, *J* = 6.4 Hz, 3H). Two of the three exchangeable protons were not observed. ¹³C NMR (101 MHz, CDCl₃) δ 170.5 (C=O), 136.8 (C_{iv}), 134.2 (C_{iv}), 129.5 (CH), 128.7 (CH), 127.8 (CH), 124.2 (CH), 103.8 (CH), 100.0 (C_{iv}), 69.0 (CH), 62.4

(CH₂), 62.0 (CH), 51.7 (CH₂), 41.1 (CH), 35.3(CH₃), 21.8 (CH₃), 21.8 (CH₃), 12.7 (CH₃). The signals for one CH₃ and four C_{iv} were not observed. **LCMS** (ESI, high pH) $t_R = 0.87$ min, m/z 427 [M+H]⁺. **HRMS** (ESI) calculated for C₂₃H₃₁N₄O₄ [M+H]⁺ 427.2349, found 427.2341 (2.28 min). ν_{max} (solution in chloroform, cm⁻¹): 3242 (OH), 3139 (NH), 2981 (CH alkene), 2936 (CH alkane), 1724 (C=O ester), 1647 (C=O amide), 1579 (C=C). $[\alpha_D]^{25.0 \text{ } ^\circ\text{C}}_{589 \text{ nm}}$ (c 0.500, MeOH): +128.5°. **m.p.** = 98-99 °C.

Isopropyl (((R)-1,3-dimethyl-5-(5-methyl-1H-pyrazol-3-yl)-2-oxo-2,3-dihydro-1H-benzo[d]azepin-7-yl)methyl)-L-allo-threoninate, trifluoroacetic acid salt

[7.26]

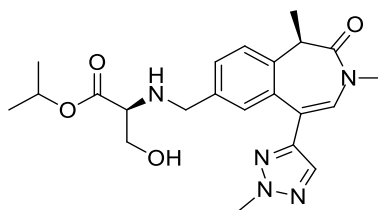


Reductive amination general procedure B with aldehyde [7.47] (mixture of SEM-regioisomers) (121 mg, 0.27 mmol) and isopropyl *L-allo*-threoninate, hydrochloride [7.07] (80 mg, 0.41 mmol). The product was purified silica column chromatography eluted with a gradient of 0-100% EtOAc in cyclohexane, followed by a gradient of 0-25% EtOH in EtOAc. The relevant fractions were concentrated under reduced pressure and further purified by MDAP (high pH, extended method C). The relevant fractions were concentrated under reduced pressure to give the SEM-protected crude product as a colourless oil (46 mg, 30% yield). The product was dissolved in a 4 M solution of HCl in 1,4-dioxane (3 mL, 12.0 mmol) and the reaction mixture was stirred at 40 °C for 5 h. The reaction mixture was concentrated under reduced pressure and purified by MDAP (high pH, extended method B). The relevant fractions were combined and

concentrated under reduced pressure and further purified by HPLC (Xbridge column, gradient of 3-100% MeCN (containing TFA 0.1% v/v) in water (containing TFA 0.1% v/v)). The relevant fractions were concentrated under reduced pressure to give the title product **[7.26]** as a colourless oil (31 mg, 20% yield).

¹H NMR (400 MHz, MeOD) δ 7.59 (dd, $J = 8.0, 1.7$ Hz, 1H), 7.48 (d, $J = 8.0$ Hz, 1H), 7.48 (d, $J = 1.7$ Hz, 1H), 7.07 (s, 1H), 6.33 (s, 1H), 5.06 (spt, $J = 6.4$ Hz, 1H), 4.27 (d, $J = 13.2$ Hz, 1H), 4.26 (d, $J = 13.2$ Hz, 1H), 4.25 (dd, $J = 6.1, 3.4$ Hz, 1H), 3.87 (d, $J = 3.4$ Hz, 1H), 3.47 (q, $J = 7.0$ Hz, 1H), 3.13 (s, 3H), 2.36 (s, 3H), 1.65 (d, $J = 7.0$ Hz, 3H), 1.27 (d, $J = 6.4$ Hz, 3H), 1.26 (d, $J = 6.4$ Hz, 3H), 1.21 (d, $J = 6.1$ Hz, 3H). The signals for the exchangeable protons were not observed. **¹³C NMR** (101 MHz, CDCl₃) δ 170.0 (C=O), 139.0 (C_{iv}), 133.8 (C_{iv}), 132.1 (CH), 131.6 (CH), 129.4 (CH), 128.4 (C_{iv}), 125.1 (CH), 117.5 (C_{iv}), 104.2 (CH), 71.6 (CH), 67.4 (CH), 64.6 (CH), 50.5 (CH₂), 41.5 (CH), 35.7 (CH₃), 21.5 (CH₃), 21.5 (CH₃), 18.7 (CH₃), 12.5 (CH₃), 11.1 (CH₃). The signals for three quaternary carbons were not observed. **LCMS** (ESI, formic) $t_R = 0.58$ min, m/z 441 [M+H]⁺. **HRMS** (ESI) calculated for C₂₄H₃₃N₄O₄ [M+H]⁺ 441.2499, found 441.2498 (2.37 min). ν_{max} (solution in chloroform, cm⁻¹): 3377 (OH), 3243 (NH), 2986 (CH alkene), 2937 (CH alkane), 1736 (C=O ester), 1630 (C=O amide). **[α]_D**^{24.2 °C}_{589 nm} (c 0.500, MeOH): +72.6°.

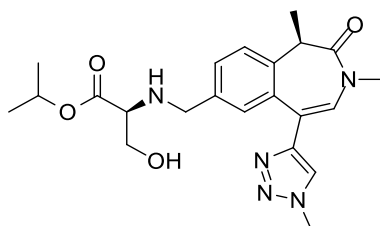
Isopropyl (((*R*)-1,3-dimethyl-5-(2-methyl-2*H*-1,2,3-triazol-4-yl)-2-oxo-2,3-dihydro-1*H*-benzo[*d*]azepin-7-yl)methyl)-*L*-serinate [7.33]



Reductive amination general procedure A1 with aldehyde [7.48] (100 mg, 0.32 mmol) and isopropyl *L*-serinate, tosic acid salt [7.08] (154 mg, 0.48 mmol). The crude was suspended in DCM and filtered. The filtrate was purified by silica column chromatography, eluted with a gradient of 0-100% EtOAc in cyclohexane, followed by a gradient of 0-25% EtOH in EtOAc. The relevant fractions were concentrated under reduced pressure to give the title product [7.33] as two colourless oils (38.7 mg, 27% yield and 41.9 mg, 28% yield).

¹H NMR (400 MHz, CDCl₃) δ 7.53 (s, 1H), 7.41 (dd, *J* = 8.1, 1.5 Hz, 1H), 7.352 (d, *J* = 8.1 Hz, 1H)*, 7.345 (d, *J* = 1.5 Hz, 1H)*, 7.01 (s, 1H), 5.05 (spt, *J* = 6.1 Hz, 1H), 4.24 (s, 3H), 3.88 (d, *J* = 13.2 Hz, 1H), 3.71 (dd, *J* = 10.6, 4.5 Hz, 1H), 3.70 (d, *J* = 13.2 Hz, 1H), 3.55 (dd, *J* = 10.6, 6.7 Hz, 1H), 3.39 (q, *J* = 7.0 Hz, 1H), 3.33 (dd, *J* = 6.7, 4.5 Hz, 1H), 3.16 (s, 3H), 2.60 (br. s, 1H), 1.68 (d, *J* = 7.0 Hz, 3H), 1.23 (d, *J* = 6.1 Hz, 6H). *3 decimals were given to differentiate the chemical shift between the two signals. One of the two exchangeable protons was not observed. LCMS (ESI, high pH) t_R = 0.90 min, *m/z* 428 [M+H]⁺.

Isopropyl (((*R*)-1,3-dimethyl-5-(1-methyl-1*H*-1,2,3-triazol-4-yl)-2-oxo-2,3-dihydro-1*H*-benzo[*d*]azepin-7-yl)methyl)-*L*-serinate [7.35]

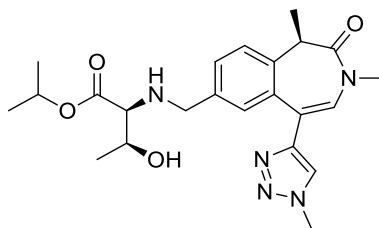


Reductive amination general procedure A1 with aldehyde [7.49] (75 mg, 0.22 mmol) and isopropyl *L*-serinate, tosic acid salt [7.08] (103 mg, 0.32 mmol). The crude was purified by silica column chromatography, eluted with a gradient of 0-100% EtOAc in cyclohexane, followed by a gradient of 0-25% EtOH in EtOAc. The relevant fractions were concentrated under reduced pressure and the product was further purified by HPLC (Chiralpak AD-H column, 30% EtOH (containing 0.2% *i*PrNH₂) in heptane (containing 0.2% *i*PrNH₂)). The relevant fractions were concentrated under reduced pressure to give the title product [7.35] as a colourless oil (39 mg, 42% yield).

¹H NMR (400 MHz, MeOD) δ 7.93 (s, 1H), 7.47 (dd, $J = 8.3, 1.7$ Hz, 1H), 7.37 (d, $J = 8.3$ Hz, 1H), 7.36 (d, $J = 1.7$ Hz, 1H), 7.21 (s, 1H), 4.99 (spt, $J = 6.4$ Hz, 1H), 4.13 (s, 3H), 3.83 (d, $J = 13.2$ Hz, 1H), 3.72 (d, $J = 5.1$ Hz, 1H), 3.71 (d, $J = 13.2$ Hz, 1H), 3.70 (d, $J = 5.1$ Hz, 1H), 3.43 (q, $J = 6.9$ Hz, 1H), 3.27 (t, $J = 5.1$ Hz, 1H), 3.14 (s, 3H), 1.63 (d, $J = 6.9$ Hz, 3H), 1.21 (d, $J = 6.4$ Hz, 3H), 1.20 (d, $J = 6.4$ Hz, 3H). The two exchangeable protons were not observed. **¹³C NMR** (101 MHz, CDCl₃) δ 172.4 (C=O), 170.3 (C=O), 146.6 (C_{iv}), 137.6 (C_{iv}), 136.9 (C_{iv}), 134.3 (C_{iv}), 129.6 (CH), 128.9 (CH), 126.4 (CH), 124.3 (CH), 123.3 (CH), 119.0 (C_{iv}), 69.0 (CH), 62.5 (CH₂), 61.8 (CH), 51.6 (CH₂), 41.0 (CH), 36.7 (CH₃), 35.3 (CH₃), 21.8 (CH₃), 21.7 (CH₃), 12.7 (CH₃). **LCMS** (ESI, high pH) $t_R = 0.82$ min, m/z 428 [M+H]⁺. **HRMS** (ESI) calculated for C₂₂H₃₀N₅O₄ [M+H]⁺ 428.2299, found 428.2294 (1.91 min). ν_{max}

(solution in chloroform, cm^{-1}): 3433 (OH), 3312 (NH), 2976 (CH alkene), 2934 (CH alkane), 1724 (C=O ester), 1657 (C=O amide). $[\alpha]_D^{24.7}$ $_{589 \text{ nm}}$ (c 0.500, MeOH): +184.7°.

Isopropyl (((*R*)-1,3-dimethyl-5-(1-methyl-1*H*-1,2,3-triazol-4-yl)-2-oxo-2,3-dihydro-1*H*-benzo[*d*]azepin-7-yl)methyl)-*L*-allo-threoninate [7.36]

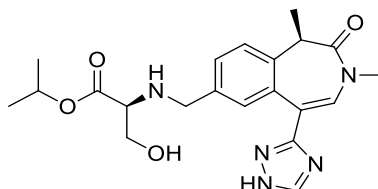


Reductive amination general procedure A1 with aldehyde [7.49] (100 mg, 0.34 mmol) and isopropyl *L*-allo-threoninate, hydrochloride [7.07] (100 mg, 0.51 mmol). The crude was purified by silica column chromatography, eluted with 0-100% EtOAc in cyclohexane. The relevant fractions were concentrated under reduced pressure to give the title product [7.36] as a colourless oil (101 mg, 64% yield).

¹H NMR (400 MHz, MeOD) δ 7.92 (s, 1H), 7.45 (dd, $J = 8.1, 1.5$ Hz, 1H), 7.35 (d, $J = 8.1$ Hz, 1H), 7.34 (br. s, 1H), 7.19 (s, 1H), 4.98 (spt, $J = 6.4$ Hz, 1H), 4.12 (s, 3H), 3.89 (dq, $J = 6.4, 5.1$ Hz, 1H), 3.80 (d, $J = 13.3$ Hz, 1H), 3.64 (d, $J = 13.3$ Hz, 1H), 3.42 (q, $J = 6.9$ Hz, 1H), 3.13 (s, 3H), 3.12 (d, $J = 5.1$ Hz, 1H), 1.62 (d, $J = 6.9$ Hz, 3H), 1.21 (d, $J = 6.4$ Hz, 3H), 1.19 (d, $J = 6.4$ Hz, 3H), 1.16 (d, $J = 6.4$ Hz, 3H). The two exchangeable protons were not observed. **¹³C NMR** (101 MHz, CDCl₃) δ 172.3 (C=O), 170.3 (C=O), 146.6 (C_{iv}), 137.4 (C_{iv}), 136.9 (C_{iv}), 134.3 (C_{iv}), 129.7 (CH), 128.9 (CH), 126.5 (CH), 124.3 (CH), 123.4 (CH), 119.1 (C_{iv}), 68.8 (CH), 67.0 (CH), 64.9 (CH), 51.9 (CH₂), 41.0 (CH), 36.7 (CH₃), 35.3 (CH₃), 21.8 (CH₃), 21.7 (CH₃), 18.5 (CH₃), 12.7 (CH₃). **LCMS** (ESI, high pH) $t_R = 0.86$ min, m/z 442 [M+H]⁺. **HRMS** (ESI) calculated for C₂₃H₃₂N₅O₄ [M+H]⁺ 442.2459, found 442.2453 (2.06 min). ν_{max}

(solution in chloroform, cm^{-1}): 3438 (OH), 3328 (NH), 2979 (CH alkene), 2937 (CH alkane), 1723 (C=O ester), 1660 (C=O amide). $[\alpha]_D^{24.7}$ $_{589 \text{ nm}}$ (c 0.500, MeOH): +144.6°.

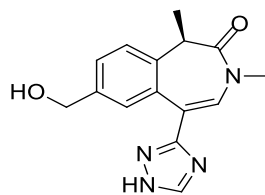
Isopropyl (((*R*)-1,3-dimethyl-2-oxo-5-(1*H*-1,2,4-triazol-3-yl)-2,3-dihydro-1*H*-benzo[*d*]azepin-7-yl)methyl)-*L*-serinate [7.37]



Reductive amination general procedure B with aldehyde [7.71] (267 mg, 0.95 mmol) and isopropyl *L*-serinate, tosic acid salt [7.08] (453 mg, 1.42 mmol), in a 20:1 mixture of *i*PrOH: AcOH. The crude was purified by reverse phase C18 column chromatography, eluted with 0-20% MeCN in a 10 mM aqueous solution of ammonium carbonate. The relevant fractions were concentrated under reduced pressure and the product was further purified by HPLC (Chiralpak AD-H column, 25% EtOH (containing 0.2% *i*PrNH₂) in heptane (containing 0.2% *i*PrNH₂)). The relevant fractions were concentrated under reduced pressure to give the title product [7.37] as a colourless oil (37.9 mg, 9% yield).

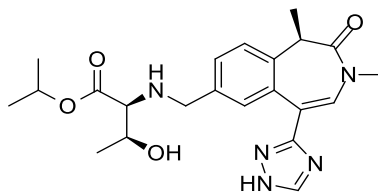
¹H NMR (400 MHz, MeOD) δ 8.34 (s, 1H), 7.49 (dd, $J = 8.1, 1.5$ Hz, 1H), 7.37 (d, $J = 8.1$ Hz, 1H), 7.37 (s, 1H), 7.36 (d, $J = 1.5$ Hz, 1H), 4.99 (spt, $J = 6.4$ Hz, 1H), 3.84 (d, $J = 13.0$ Hz, 1H), 3.71 (dd, $J = 10.8, 5.1$ Hz, 1H), 3.69 (d, $J = 13.0$ Hz, 1H), 3.67 (dd, $J = 10.8, 5.1$ Hz, 1H), 3.43 (q, $J = 6.9$ Hz, 1H), 3.29 (t, $J = 5.1$ Hz, 1H), 3.17 (s, 3H), 1.64 (d, $J = 6.9$ Hz, 3H), 1.21 (d, $J = 6.4$ Hz, 3H), 1.20 (d, $J = 6.4$ Hz, 3H). The three exchangeable protons were not observed. LCMS (ESI, high pH) $t_R = 0.71$ min, m/z 414 [M+H]⁺.

Reverse phase column chromatography also enabled the recovery of (*R*)-7-(hydroxymethyl)-1,3-dimethyl-5-(1*H*-1,2,4-triazol-3-yl)-1,3-dihydro-2*H*-benzo[*d*]azepin-2-one (150.8 mg, 48% yield).



$^1\text{H NMR}$ (400 MHz, CDCl_3) δ 7.98 (s, 1H), 7.49 (s, 1H), 7.46 (d, $J = 1.2$ Hz, 1H), 7.34 (dd, $J = 8.2, 1.2$ Hz, 1H), 7.31 (d, $J = 8.2$ Hz, 1H), 5.20 (br. s, 2H), 4.55 (d, $J = 12.6$ Hz, 1H), 4.49 (d, $J = 12.6$ Hz, 1H), 3.32 (q, $J = 6.9$ Hz, 1H) 3.14 (s, 3H), 1.62 (d, $J = 6.9$ Hz, 3H). **LCMS** (ESI, high pH) $t_{\text{R}} = 0.53$ min, m/z 285 $[\text{M}+\text{H}]^+$.

Isopropyl (((*R*)-1,3-dimethyl-2-oxo-5-(1*H*-1,2,4-triazol-3-yl)-2,3-dihydro-1*H*-benzo[*d*]azepin-7-yl)methyl)-*L*-allo-threoninate [7.38]



Isopropyl (((*R*)-1,3-dimethyl-2-oxo-5-(1-((2-(trimethylsilyl)ethoxy)methyl)-1*H*-1,2,4-triazol-3-yl)-2,3-dihydro-1*H*-benzo[*d*]azepin-7-yl)methyl)-*L*-allo-threoninate [7.78] (100 mg, 0.14 mmol) was dissolved in DCM (5 mL) under nitrogen at -78 °C. A 1 M solution of boron tribromide in DCM (0.43 mL, 0.43 mmol) was added to the reaction mixture and the reaction mixture was stirred at -78 °C for 5 min and at rt for 5 min. The reaction was quenched with MeOH and concentrated under reduced pressure to give a yellow oil. The oil was purified by MDAP (high pH, extended method B). The relevant fractions were concentrated under reduced pressure to give two colourless oils (22 mg, 34% yield; 27.5 mg, 43% yield) showing 5% of a diastereomer by $^1\text{H NMR}$. This ratio was determined at the benzylic CH_2 signal at 3.62

ppm (major diastereomer) and 3.64 ppm (minor diastereomer). (**Table 31, entry 1, p.161**). These oils were combined and further purified by HPLC (Chiralpak AD-H column, 20% EtOH (containing 0.2% *i*PrNH₂) in heptane (containing 0.2% *i*PrNH₂)). The relevant fractions were concentrated under reduced pressure to give the title product **[7.38]** as a colourless oil (16 mg, 25% yield).

¹H NMR (400 MHz, MeOD) δ 8.33 (s, 1H), 7.48 (dd, $J = 8.2, 1.4$ Hz, 1H), 7.37 (d, $J = 8.2$ Hz, 1H), 7.35 (s, 1H), 7.33 (d, $J = 1.4$ Hz, 1H), 5.00 (spt, $J = 6.5$ Hz, 1H), 3.87 (qd, $J = 6.5, 5.4$ Hz, 1H), 3.81 (d, $J = 13.2$ Hz, 1H), 3.62 (d, $J = 13.2$ Hz, 1H), 3.44 (q, $J = 6.9$ Hz, 1H), 3.18 (s, 3H), 3.11 (d, $J = 5.4$ Hz, 1H), 1.65 (d, $J = 6.9$ Hz, 3H), 1.21 (d, $J = 6.5$ Hz, 3H), 1.19 (d, $J = 6.5$ Hz, 3H), 1.16 (d, $J = 6.5$ Hz, 3H). The signals for the three exchangeable protons were not observed. **¹³C NMR** (CDCl₃, 101 MHz) δ 172.4 (C=O), 170.4 (C=O), 138.0 (C_{iv}), 136.9 (C_{iv}), 132.9 (CH), 132.5 (C_{iv}), 130.1 (CH), 127.3 (CH), 124.4 (CH), 69.0 (CH), 67.3 (CH), 64.9 (CH), 52.0 (CH₂), 41.3 (CH), 35.7 (CH₃), 21.9 (CH₃), 21.7 (CH₃), 18.4 (CH₃), 12.7 (CH₃). Two quaternary carbons and one methine were not observed. **LCMS** (ESI, high pH) $t_R = 0.74$ min, m/z 428 [M+H]⁺. **HRMS** (ESI) calculated for C₂₂H₃₀N₅O₄ [M+H]⁺ 428.2299, found 428.2296 (1.82 min). ν_{max} (solution in chloroform, cm⁻¹): 3443 (OH), 3139 (NH), 2980 (CH alkene), 2934 (CH alkane), 1724 (C=O ester), 1663 (C=O amide), 1628 (C=C alkene). $[\alpha_D]^{24.7}_{589\text{ nm}}$ (c 0.500, MeOH): +153.3°.

Procedure for preparation of molecule [7.38], Table 31, entry 2, p.161

Isopropyl (((*R*)-1,3-dimethyl-2-oxo-5-(1-((2-(trimethylsilyl)ethoxy)methyl)-1*H*-1,2,4-triazol-3-yl)-2,3-dihydro-1*H*-benzo[*d*]azepin-7-yl)methyl)-*L*-allo-threoninate **[7.78]** (1.82 g, 3.3 mmol) and a 4 M solution of HCl in 1,4-dioxane (10 mL, 40.0 mmol) were stirred at 40 °C for 1 h. The white slurry was concentrated under reduced

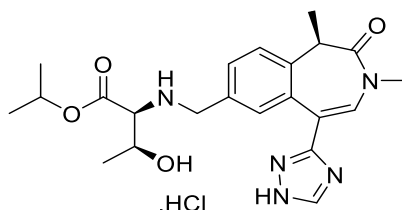
pressure. The white solid was suspended in water. (pH = 1 (pH paper)). The solution was brought to pH 9 (pH paper) with NEt₃ and purified by reverse phase column chromatography, eluted with a gradient of 5-20% MeCN in a 10 mM aqueous solution of ammonium carbonate. The relevant fractions were concentrated under reduced pressure to give molecule **[7.38]** in two batches, as two white solids (581.5 mg, 40% yield and 253.8 mg, 17% yield). The analysis of the second batch matches the LCMS data reported below.

LCMS (ESI, formic, 10 min method) t_R = 1.94 min, m/z 428 [M+H]⁺.

Stereoselective synthesis of molecule **[7.38]**:

Isopropyl (((*R*)-1,3-dimethyl-2-oxo-5-(1*H*-1,2,4-triazol-3-yl)-2,3-dihydro-1*H*-benzo[*d*]azepin-7-yl)methyl)-*L*-allo-threoninate, hydrochloride salt **[7.38]**, (Table

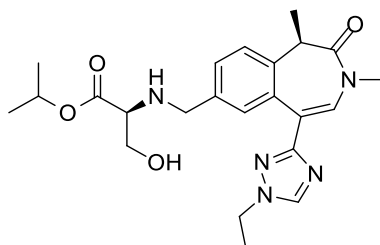
31, entry 4, p.161)



A 1 M solution of HCl in Et₂O (5 mL, 5.0 mmol) was added to a flask containing *isopropyl* (((*R*)-1,3-dimethyl-2-oxo-5-(1-((2-(trimethylsilyl)ethoxy)methyl)-1*H*-1,2,4-triazol-3-yl)-2,3-dihydro-1*H*-benzo[*d*]azepin-7-yl)methyl)-*L*-allo-threoninate **[7.78]** (582.5 mg, 1.04 mmol). EtOAc (3 mL) and acetone (3 mL) were added to help dissolution of the starting material. The reaction mixture was stirred at rt for 20 h. A 1 M solution of HCl in Et₂O (5 mL, 5.0 mmol) was added and the reaction mixture was further stirred at rt for 3 h. A 1 M solution of HCl in Et₂O (5 mL, 5.00 mmol) was added and the reaction mixture was stirred at rt for 3 h. The suspension was filtered

through celite and rinsed with acetone (6 mL), followed by Et₂O (6 mL) to afford the title product **[7.38]** as the HCl salt, as a crystalline white solid (401.5 mg, 79% yield). ¹H NMR (400 MHz, MeOD) δ 9.15 (br. s, 1H), 7.67 (d, *J* = 7.6 Hz, 1H), 7.59 (br. s, 1H), 7.56 (br. s, 1H), 7.55 (d, *J* = 7.6 Hz, 1H), 5.06 (br. spt, *J* = 5.9 Hz, 1H), 4.31 (br. s, 3H), 3.94 (br. s, 1H), 3.53 (br. s, 1H), 3.22 (s, 3H), 1.69 (br. s, 3H), 1.28 (br. d, *J* = 5.9 Hz, 6H), 1.22 (br. d, *J* = 5.9 Hz, 3H). The three exchangeable protons were not observed. LCMS (ESI, high pH) t_R = 0.72 min, *m/z* 428 [M+H]⁺.

Isopropyl (((*R*)-5-(1-ethyl-1*H*-1,2,4-triazol-3-yl)-1,3-dimethyl-2-oxo-2,3-dihydro-1*H*-benzo[*d*]azepin-7-yl)methyl)-*L*-serinate [7.39]

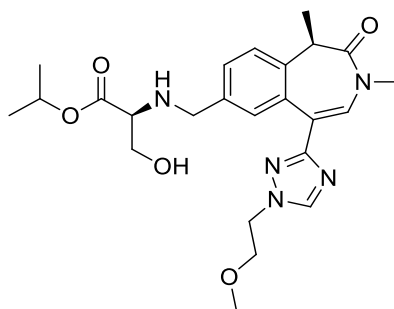


Reductive amination general procedure B with aldehyde **[7.51]** (132.8 mg, 0.36 mmol) and isopropyl *L*-serinate, tosic acid salt **[7.08]** (194 mg, 0.55 mmol) in a 25:1 mixture of *i*PrOH: AcOH. The reaction mixture was quenched with methanol and concentrated under reduced pressure. The crude product was taken in DCM, sonicated and purified by silica column chromatography eluted with a gradient of 0-100% EtOAc in cyclohexane, followed by a gradient of 0-25% EtOH in EtOAc. The relevant fractions were concentrated under reduced pressure and further purified by MDAP (high pH, extended method B). The relevant fractions were concentrated under reduced pressure to give the title product **[7.39]** as a colourless oil (30.8 mg, 18% yield).

¹H NMR (400 MHz, MeOD) δ 8.46 (s, 1H), 7.47 (dd, *J* = 7.8, 1.7 Hz, 1H), 7.46 (s, 1H), 7.36 (s, 1H), 7.35 (d, *J* = 7.8 Hz, 1H), 5.00 (spt, *J* = 6.4 Hz, 1H), 4.27 (q, *J* = 7.3

Hz, 2H), 3.85 (d, $J = 13.2$ Hz, 1H), 3.69 (d, $J = 13.2$ Hz, 1H), 3.70 (dd, $J = 10.8, 5.1$ Hz, 1H), 3.68 (dd, $J = 10.8, 5.1$ Hz, 1H), 3.41 (q, $J = 6.9$ Hz, 1H), 3.30 (t, $J = 5.1$ Hz, 1H), 3.16 (s, 3H), 1.63 (d, $J = 6.9$ Hz, 3H), 1.51 (t, $J = 7.3$ Hz, 3H), 1.21 (d, $J = 6.4$ Hz, 3H), 1.20 (d, $J = 6.4$ Hz, 3H). The two exchangeable protons were not observed. ^{13}C NMR (101 MHz, CDCl_3) δ 172.4 (C=O), 170.7 (C=O), 162.0 (C_{iv}), 142.5 (CH), 137.3 (C_{iv}), 136.5 (C_{iv}), 133.2 (C_{iv}), 131.6 (CH), 129.2 (CH), 128.1 (CH), 124.0 (CH), 119.9 (C_{iv}), 68.9 (CH), 62.5 (CH_2), 62.1 (CH), 51.7 (CH_2), 44.9 (CH_2), 41.2 (CH), 35.6 (CH_3), 21.84 (CH_3), 21.78 (CH_3), 15.2 (CH_3), 12.7 (CH_3). LCMS (ESI, high pH) $t_{\text{R}} = 0.83$ min, m/z 442 $[\text{M}+\text{H}]^+$. HRMS (ESI) calculated for $\text{C}_{23}\text{H}_{32}\text{N}_5\text{O}_4$ $[\text{M}+\text{H}]^+$ 442.2459, found 442.2453 (2.12 min). ν_{max} (solution in chloroform, cm^{-1}): 3438 (OH), 3334 (NH), 2980 (CH alkene), 2937 (CH alkane), 1727 (C=O ester), 1667 (C=O amide), 1629 (C=C). $[\alpha_{\text{D}}]^{24.2}_{589 \text{ nm}}$ (c 0.500, MeOH): +120.4°.

Isopropyl (((*R*)-5-(1-(2-methoxyethyl)-1*H*-1,2,4-triazol-3-yl)-1,3-dimethyl-2-oxo-2,3-dihydro-1*H*-benzo[*d*]azepin-7-yl)methyl)-*L*-serinate [7.41]

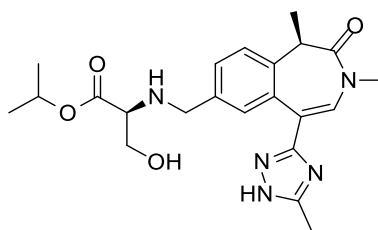


Reductive amination general procedure B with aldehyde [7.53] (110 mg, 0.26 mmol) and isopropyl *L*-serinate, tosic acid salt [7.08] (138 mg, 0.39 mmol). The reduced aldehyde was observed by HPLC analysis of the reaction mixture. The reaction mixture was quenched with methanol and concentrated under reduced pressure. The residue was partitioned between EtOAc and water. The two layers were separated and the aqueous layer was extracted with EtOAc three times. The aqueous layer was then

extracted with 10% EtOH in EtOAc, three times. The aqueous layer was neutralised with a saturated solution of sodium bicarbonate and was extracted with EtOAc three times. The organics were combined, dried through a phase separator and concentrated under reduced pressure. The crude product was purified by MDAP (high pH, extended method B). The relevant fractions were concentrated under reduced pressure to give the title product **[7.41]** as a colourless oil (9.2 mg, 7% yield).

¹H NMR (400 MHz, MeOD) δ 8.44 (s, 1H), 7.49 (br. s, 1H), 7.48 (dd, $J = 8.5, 1.7$ Hz, 1H), 7.39 (s, 1H), 7.36 (d, $J = 8.5$ Hz, 1H), 5.00 (spt, $J = 6.4$ Hz, 1H), 4.40 (t, $J = 5.0$ Hz, 2H), 3.88 (d, $J = 12.6$ Hz, 1H), 3.77 (dd, $J = 4.9$ Hz, 1H), 3.77 (dd, $J = 4.9$ Hz, 1H), 3.76 (d, $J = 12.6$ Hz, 1H), 3.72 (t, $J = 5.0$ Hz, 1H), 3.71 (t, $J = 5.0$ Hz, 1H), 3.42 (q, $J = 6.9$ Hz, 1H), 3.36 (s, 3H), 3.34 (t, $J = 4.9$ Hz, 1H), 3.17 (s, 3H), 1.64 (d, $J = 6.9$ Hz, 3H), 1.22 (d, $J = 6.4$ Hz, 3H), 1.20 (d, $J = 6.4$ Hz, 3H). The two exchangeable protons were not observed. **LCMS** (ESI, high pH) $t_R = 0.82$ min, m/z 472 $[M+H]^+$.

Isopropyl (((*R*)-1,3-dimethyl-5-(5-methyl-1*H*-1,2,4-triazol-3-yl)-2-oxo-2,3-dihydro-1*H*-benzo[*d*]azepin-7-yl)methyl)-*L*-serinate [7.43]

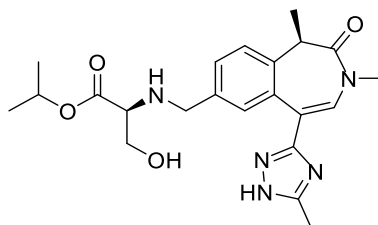


Reductive amination general procedure A1 with aldehyde **[7.52]** (120 mg, 0.18 mmol) and isopropyl *L*-serinate, tosic acid salt **[7.08]** (88 mg, 0.27 mmol). The reaction mixture was quenched with methanol and concentrated under reduced pressure to give a yellow residue. The residue was taken in DCM and cooled to -78 °C. A 1 M solution of boron tribromide in DCM (0.55 mL, 0.55 mmol) was added and the reaction was stirred for 5 min at -78 °C, and 1 h at rt. HPLC analysis of the reaction mixture showed

presence of aldehyde starting material. The reaction mixture was quenched with a saturated aqueous sodium bicarbonate solution. The layers were separated. The aqueous layer was extracted with EtOAc + 10% methanol. The organic layers were combined, dried through a phase separator and concentrated under reduced pressure to give a yellow oil. The oil was purified by MDAP (high pH, extended method A), the relevant fractions were concentrated under reduced pressure. The product was further purified by MDAP (high pH, extended method B), the relevant fractions were concentrated under reduced pressure. The product was further purified by HPLC (Chiralpak IA5 column, 30% EtOH (containing 0.2% *i*PrNH₂) in heptane (containing 0.2% *i*PrNH₂)). The relevant fractions were concentrated under reduced pressure to give the title product **[7.43]** as a colourless oil (3 mg, 3% yield). The full analysis of this batch matches the data reported below, but with the presence of 5% of a diastereomer observed by small shoulders on several peaks notably ¹H NMR (400 MHz, MeOD) δ 3.18 ppm for the diastereomeric impurity and 3.17 ppm for methyl signal of the amide.

Stereoselective synthesis of molecule [7.43]:

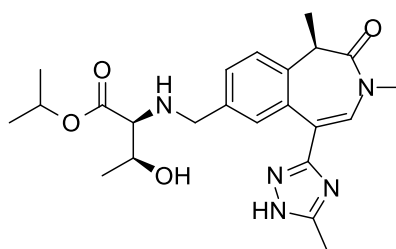
Isopropyl (((R)-1,3-dimethyl-5-(5-methyl-1H-1,2,4-triazol-3-yl)-2-oxo-2,3-dihydro-1H-benzo[d]azepin-7-yl)methyl)-L-serinate [7.43]



Isopropyl (((R)-1,3-dimethyl-5-(5-methyl-1-((2-(trimethylsilyl)ethoxy)methyl)-1H-1,2,4-triazol-3-yl)-2-oxo-2,3-dihydro-1H-benzo[d]azepin-7-yl)methyl)-L-serinate [8.07] (18 mg, 0.02 mmol) was dissolved in DCM (3 mL). A 4 M solution of HCl in

1,4-dioxane (3 mL, 12.0 mmol) was added and the reaction mixture was stirred at rt for 40 min. The solution was concentrated under reduced pressure and purified by MDAP (high pH, extended method B). The relevant fractions were concentrated under reduced pressure to give the title product [**7.43**] as a white solid (4.8 mg, 55% yield). ¹H NMR (400 MHz, MeOD) δ 7.48 (dd, $J = 8.1, 1.7$ Hz, 1H), 7.38 (br. s, 1H), 7.36 (d, $J = 8.1$ Hz, 1H), 7.30 (s, 1H), 5.00 (spt, $J = 6.2$ Hz, 1H), 3.84 (d, $J = 13.0$ Hz, 1H), 3.71 (dd, $J = 10.8, 5.1$ Hz, 1H), 3.68 (d, $J = 13.0$ Hz, 1H), 3.67 (dd, $J = 10.8, 5.1$ Hz, 1H), 3.42 (q, $J = 6.9$ Hz, 1H), 3.28 (t, $J = 5.1$ Hz, 1H), 3.17 (s, 3H), 2.46 (s, 3H), 1.64 (d, $J = 6.9$ Hz, 3H), 1.21 (d, $J = 6.2$ Hz, 3H), 1.20 (d, $J = 6.2$ Hz, 3H). The three exchangeable protons were not observed. ¹³C NMR (101 MHz, CDCl₃) δ 136.8 (C_{iv}), 132.6 (CH), 129.7 (CH), 127.6 (CH), 124.3 (CH), 100.0 (C_{iv}), 69.1 (CH), 62.4 (CH₂), 62.2 (CH), 51.8 (CH₂), 41.2 (CH), 35.6 (CH₃), 21.8 (CH₃), 21.7 (CH₃), 12.9 (CH₃), 12.7 (CH₃). Six quaternary carbons were not observed. LCMS (ESI, high pH) $t_R = 0.71$ min, m/z 428 [M+H]⁺. HRMS (ESI) calculated for C₂₂H₃₀N₅O₄ [M+H]⁺ 428.2299, found 428.2294 (1.78 min). ν_{max} (solution in chloroform, cm⁻¹): 3252 (OH), 3076 (NH), 2980 (CH alkene), 2934 (CH alkane), 1724 (C=O ester), 1651 (C=O amide), 1629 (C=C alkene). $[\alpha_D]^{24.6}_{589\text{ nm}}$ (c 0.500, MeOH): +179.5°. **m.p.** = 136-137 °C.

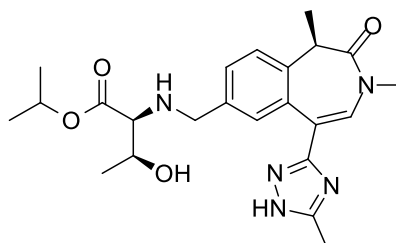
Isopropyl (((*R*)-1,3-dimethyl-5-(5-methyl-1*H*-1,2,4-triazol-3-yl)-2-oxo-2,3-dihydro-1*H*-benzo[*d*]azepin-7-yl)methyl)-*L*-allo-threoninate [7.44**]**



Reductive amination general procedure B with aldehyde **[7.74]** (50 mg, 0.17 mmol) and *isopropyl L-allo-threoninate*, tosic salt **[7.07]** (50 mg, 0.25 mmol) in AcOH (0.2 mL) and *i*PrOH (5 mL). The reaction mixture was concentrated under reduced pressure to give white residue. The residue was purified by MDAP (high pH, extended method B). The relevant fraction was concentrated under reduced pressure and further purified by MDAP (high pH, extended method A). The relevant fraction was concentrated under reduced pressure to give the title product **[7.44]** as a yellow oil (11.2 mg, 12% yield). The NMR and LCMS analysis of this batch matches the data reported below, but the NMR showed the presence of 27% of a diastereomer, determined at ^1H NMR (400 MHz, MeOD) δ 5.06 ppm (spt, minor diastereomer) and 5.00 ppm (spt, major diastereomer).

Stereoselective synthesis of molecule **[7.44]**

*Isopropyl (((R)-1,3-dimethyl-5-(5-methyl-1H-1,2,4-triazol-3-yl)-2-oxo-2,3-dihydro-1H-benzo[d]azepin-7-yl)methyl)-L-allo-threoninate **[7.44]***



The pinacol boronic ester **[8.05]** was prepared following the procedure described p.295. The yield indicated below is calculated over the borylation and cross-coupling steps.

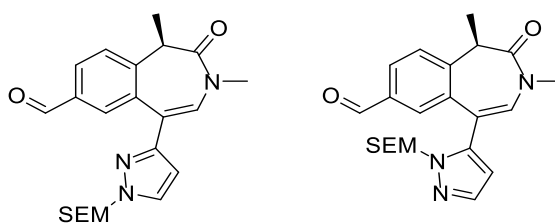
*Isopropyl (((R)-1,3-dimethyl-2-oxo-5-(4,4,5,5-tetramethyl-1,3,2-dioxaborolan-2-yl)-2,3-dihydro-1H-benzo[d]azepin-7-yl)methyl)-L-allo-threoninate **[8.05]*** (470 mg, 0.97 mmol), 3-bromo-5-methyl-1-((2-(trimethylsilyl)ethoxy)methyl)-1H-1,2,4-triazole

[7.60] (565 mg, 1.93 mmol), Pd Xphos G2 (76 mg, 0.10 mmol), Xphos (92 mg, 0.19 mmol), a 2 M aqueous solution of K₃PO₄ (1.5 mL, 2.9 mmol) were suspended in *i*PrOH (20 mL) and water (4 mL). The reaction mixture was placed under nitrogen atmosphere by three cycles of vacuum-nitrogen. The mixture was stirred at 90 °C for 18 h. The reaction mixture was cooled to rt and concentrated under reduced pressure to give a black oil. The residue was partitioned between DCM and water. The aqueous layer was extracted with DCM. The organic layers were combined, dried through a phase separator and concentrated under reduced pressure to give a brown oil. A 120g silica column was conditioned with 3% NEt₃ in cyclohexane. The product dissolved in DCM was loaded on the column and eluted with a gradient of 0-100% EtOAc in 3% NEt₃ in cyclohexane. The relevant fractions were concentrated under reduced pressure to give *isopropyl* (((*R*)-1,3-dimethyl-5-(5-methyl-1-((2-(trimethylsilyl)ethoxy)methyl)-1*H*-1,2,4-triazol-3-yl)-2-oxo-2,3-dihydro-1*H*-benzo[*d*]azepin-7-yl)methyl)-*L*-allo-threoninate (245.5 mg, 27% yield). LCMS (ESI, high pH) *t*_R = 1.25 min, *m/z* 572 [M+H]⁺. This material was dissolved in a 1 M solution of hydrochloric acid in Et₂O (10 mL, 10.0 mmol) and left to stir at rt for 2 days. The reaction mixture was concentrated under reduced pressure to give a yellow oil, which was purified by MDAP (high pH, extended method B). The product was not collected and the recovered MDAP waste was concentrated under reduced pressure to give the crude material. This material was purified by MDAP (high pH, extended method B). The relevant fractions were concentrated under reduced pressure to give the title product [7.44] as a white solid (90 mg, 20% yield).

¹H NMR (400 MHz, MeOD) δ 7.47 (dd, *J* = 8.3, 1.7 Hz, 1H), 7.36 (d, *J* = 1.7 Hz, 1H), 7.35 (d, *J* = 8.3 Hz, 1H), 7.29 (s, 1H), 5.00 (spt, *J* = 6.5 Hz, 1H), 3.88 (dt, *J* = 6.8, 5.4

Hz, 1H), 3.82 (d, $J = 13.2$ Hz, 1H), 3.62 (d, $J = 13.2$ Hz, 1H), 3.42 (q, $J = 6.9$ Hz, 1H), 3.16 (s, 3H), 3.11 (d, $J = 5.4$ Hz, 1H), 2.46 (s, 3H), 1.64 (d, $J = 6.8$ Hz, 3H), 1.21 (d, $J = 6.5$ Hz, 3H), 1.20 (d, $J = 6.9$ Hz, 3H), 1.16 (d, $J = 6.5$ Hz, 3H). The three exchangeable protons were not observed. ^{13}C NMR (101 MHz, MeOD) δ 174.3 (C=O), 172.6 (C=O), 160.9 (C_{iv}), 157.0 (C_{iv}), 139.2 (C_{iv}), 137.7 (C_{iv}), 134.5 (C_{iv}), 133.2 (CH), 131.2 (CH), 129.3 (CH), 125.0 (CH), 120.9 (C_{iv}), 69.8 (CH), 69.7 (CH), 67.7 (CH), 52.6 (CH₂), 42.5 (CH), 36.0 (CH₃), 22.3 (CH₃), 22.2 (CH₃), 20.2 (CH₃), 13.2 (CH₃), 12.1 (CH₃). LCMS (ESI, high pH) $t_R = 0.76$ min, m/z 442 [M+H]⁺. HRMS (ESI) calculated for C₂₃H₃₂N₅O₄ [M+H]⁺ 442.2459, found 442.2455 (1.91 min). ν_{max} (solution in chloroform, cm⁻¹): 3175 (OH), 3079 (NH), 2979 (CH alkene), 2931 (CH alkane), 1723 (C=O ester), 1656 (C=O amide), 1629 (C=C). $[\alpha]_D^{23.7}$ °C_{589 nm} (c 0.500, MeOH): +134.0°. m.p. = 106-108 °C.

(R)-1,3-Dimethyl-2-oxo-5-(1-((2-(trimethylsilyl)ethoxy)methyl)-1H-pyrazol-3-yl)-2,3-dihydro-1H-benzo[d]azepine-7-carbaldehyde
and (R)-1,3-dimethyl-2-oxo-5-(1-((2-(trimethylsilyl)ethoxy)methyl)-1H-pyrazol-5-yl)-2,3-dihydro-1H-benzo[d]azepine-7-carbaldehyde [7.45]

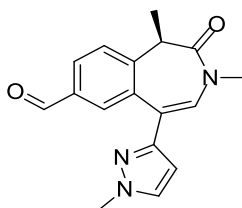


(R)-1,3-dimethyl-2-oxo-5-(4,4,5,5-tetramethyl-1,3,2-dioxaborolan-2-yl)-2,3-dihydro-1H-benzo[d]azepine-7-carbaldehyde [6.20] (500 mg, 75% pure, 1.1 mmol), 3-bromo-1-((2-(trimethylsilyl)ethoxy)methyl)-1H-pyrazole [7.55] (1.33 g, 4.6 mmol), a 2 M aqueous solution of K₃PO₄ (1.7 mL, 3.3 mmol), Xphos (262 mg, 0.55 mmol) and Pd Xphos G2 (8.65 mg, 11.0 μmol) were suspended in *isopropanol* (3 mL) under nitrogen.

The reaction mixture was split into two microwave vials. The first vial was heated in the microwave for 30 min at 120 °C, and the second vial was heated twice in the microwave for 30 min at 120 °C. The two reaction mixtures were concentrated under reduced pressure. The residues were partitioned between EtOAc and water. The layers were separated and the aqueous layers were extracted with EtOAc. The organic layers were concentrated under reduced pressure. The crude products were purified by silica column chromatography, eluted with a gradient of 0-100% EtOAc in cyclohexane. The relevant fractions were combined and concentrated to give two colourless oils. The oils were further purified by MDAP (high pH, method C). The relevant fractions were combined and concentrated to give the title products **[7.45]** as a mixture of regioisomers in a 1:1 ratio, as a brown oil (321.5 mg, 68% yield). The ratio was determined at the ¹H NMR aldehyde signals.

¹H NMR (400 MHz, CDCl₃) δ 9.93 (s, 1H), 9.88 (s, 1H), 7.93 (dd, *J* = 8.2, 1.5 Hz, 1H), 7.91 (dd, *J* = 8.2, 1.5 Hz, 1H), 7.91 (d, *J* = 1.5 Hz, 1H), 7.60 (d, *J* = 2.3 Hz, 1H), 7.58 (d, *J* = 1.7 Hz, 1H), 7.55 (d, *J* = 8.2 Hz, 1H), 7.52 (d, *J* = 8.2 Hz, 1H), 7.49 (d, *J* = 1.5 Hz, 1H), 7.05 (s, 1H), 6.84 (s, 1H), 6.37 (d, *J* = 1.7 Hz, 1H), 6.31 (d, *J* = 2.3 Hz, 1H), 5.44 (s, 2H), 5.27 (d, *J* = 11.0 Hz, 1H), 5.08 (d, *J* = 11.0 Hz, 1H), 3.65 (dd, *J* = 9.5, 8.0 Hz, 1H), 3.62 (d, *J* = 9.5, 8.0 Hz, 1H), 3.59 (q, *J* = 6.9 Hz, 1H), 3.46 (q, *J* = 6.9 Hz, 1H), 3.51-3.47 (m, 2H), 3.17 (s, 3H), 3.16 (s, 3H), 1.75 (d, *J* = 6.9 Hz, 3H), 1.71 (d, *J* = 6.9 Hz, 3H), 0.95 (d, *J* = 8.0 Hz, 1H), 0.92 (d, *J* = 8.0 Hz, 1H), 0.76-0.71 (m, 2H), -0.01 (s, 9H), -0.07 (s, 9H). **LCMS** (ESI, high pH) *t_R* = 1.28 and 1.30 min, *m/z* 412 [M+H]⁺.

(R)-1,3-Dimethyl-5-(1-methyl-1H-pyrazol-3-yl)-2-oxo-2,3-dihydro-1H-benzo[d]azepine-7-carbaldehyde [7.46]



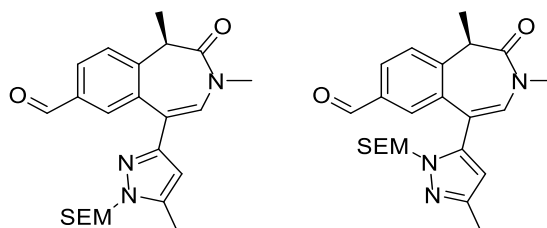
(R)-1,3-Dimethyl-2-oxo-5-(4,4,5,5-tetramethyl-1,3,2-dioxaborolan-2-yl)-2,3-dihydro-1H-benzo[d]azepine-7-carbaldehyde **[6.20]** (458 mg, 70% pure, 0.94 mmol), 3-bromo-1-methyl-1H-pyrazole (779 mg, 4.84 mmol), a 2 M aqueous solution of potassium phosphate tribasic (1.0 mL, 2.0 mmol), Pd Xphos G2 (80 mg, 0.10 mmol) and Xphos (27 mg, 0.06 mmol) were suspended in *i*PrOH (4 mL) under nitrogen. The reaction mixture was heated in a microwave at 120 °C for 30 min. The reaction mixture was concentrated under reduced pressure. The residue was partitioned between EtOAc and water. The layers were separated, the aqueous layer was re-extracted with EtOAc. The organic layers were combined, dried using a hydrophobic frit and concentrated under reduced pressure. The crude product was purified by silica column chromatography eluted with a gradient of 0-100% EtOAc in cyclohexane. The relevant fractions were combined and concentrated under reduced pressure to give the title product **[7.46]** a colourless oil (148.1 mg, 48% yield).

¹H NMR (400 MHz, CDCl₃) δ 9.96 (s, 1H), 7.94 (br. s, 1H), 7.93 (dd, *J* = 7.8, 1.7 Hz, 1H), 7.54 (d, *J* = 7.8 Hz, 1H), 7.40 (d, *J* = 2.2 Hz, 1H), 7.03 (s, 1H), 6.23 (d, *J* = 2.2 Hz, 1H), 3.95 (s, 3H), 3.50 (q, *J* = 6.9 Hz, 1H), 3.17 (s, 3H), 1.72 (d, *J* = 6.9 Hz, 3H).

LCMS (ESI, formic) *t*_R = 0.82 min, *m/z* 296 [M+H]⁺.

(R)-1,3-Dimethyl-5-(5-methyl-1-((2-(trimethylsilyl)ethoxy)methyl)-1H-pyrazol-3-yl)-2-oxo-2,3-dihydro-1H-benzo[d]azepine-7-carbaldehyde, as the main regioisomer

and (R)-1,3-dimethyl-5-(3-methyl-1-((2-(trimethylsilyl)ethoxy)methyl)-1H-pyrazol-5-yl)-2-oxo-2,3-dihydro-1H-benzo[d]azepine-7-carbaldehyde [7.47]



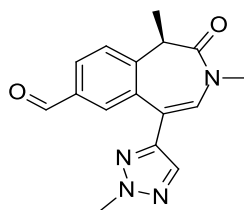
(R)-1,3-Dimethyl-2-oxo-5-(4,4,5,5-tetramethyl-1,3,2-dioxaborolan-2-yl)-2,3-dihydro-1H-benzo[d]azepine-7-carbaldehyde [6.20] (500 mg, 1.25 mmol), 3-bromo-5-methyl-1-((2-(trimethylsilyl)ethoxy)methyl)-1H-pyrazole [7.57] (1.53 g, 4.98 mmol), a 2 M aqueous solution of K₃PO₄ (1.87 mL, 3.74 mmol), Xphos (29.7 mg, 0.06 mmol) and Pd Xphos G2 (98 mg, 0.13 mmol) were suspended in *i*PrOH (3 mL) under nitrogen and the reaction mixture was heated at 120 °C for 30 min in the microwave. The reaction mixture was concentrated and partitioned between EtOAc and water. The layers were separated and the aqueous layer was re-extracted with EtOAc. The organic layer was dried through a phase separator and concentrated under reduced pressure. The crude was purified by silica column chromatography, eluting with a gradient of 0-25% EtOAc in cyclohexane. The relevant fractions were combined to give the title product [7.47] as yellow oil (157 mg, 24% yield, regioisomer 2 containing 15% of regioisomer 1) and a less pure batch. The impure batch was purified by silica column chromatography, eluting with a gradient of 0-25% EtOAc in cyclohexane. The UV detection failed and the product was sent to the waste bottle. This solution was concentrated under reduced pressure and was purified by silica column

chromatography, eluting with a gradient of 0-25% EtOAc in cyclohexane, followed by a purification by MDAP (high pH, extended method C). The relevant fractions were concentrated under reduced pressure to afford regioisomer 1 as a yellow oil (82.6 mg, 15% yield).

Regioisomer 1 (82.6 mg, 15% yield): $^1\text{H NMR}$ (400 MHz, CDCl_3) δ 9.92 (s, 1H), 7.94 (dd, $J = 8.0, 1.5$ Hz, 1H), 7.55 (d, $J = 8.0$ Hz, 1H), 7.55 (d, $J = 1.5$ Hz, 1H), 6.83 (s, 1H), 6.17 (s, 1H), 5.19 (d, $J = 11.0$ Hz, 1H), 5.00 (d, $J = 11.0$ Hz, 1H), 3.53 (q, $J = 6.9$ Hz, 1H), 3.49 (t, $J = 9.2$ Hz, 1H), 3.47 (t, $J = 9.2$ Hz, 1H), 3.17 (s, 3H), 2.33 (s, 3H), 1.75 (d, $J = 6.9$ Hz, 3H), 0.75 (t, $J = 9.2$ Hz, 1H), 0.74 (t, $J = 9.2$ Hz, 1H), -0.06 (m, 9H). **LCMS** (ESI, high pH) $t_{\text{R}} = 1.31$ min, m/z 426 $[\text{M}+\text{H}]^+$.

Regioisomer 2 (157 mg, 24% yield, containing 15% of regioisomer 1): $^1\text{H NMR}$ (400 MHz, CDCl_3) δ 9.95 (s, 1H), 7.93 (dd, $J = 8.4, 1.7$ Hz, 1H), 7.92 (d, $J = 1.7$ Hz, 1H), 7.53 (d, $J = 8.4$ Hz, 1H), 7.00 (s, 1H), 6.08 (s, 1H), 5.44 (d, $J = 11.0$ Hz, 1H), 5.40 (d, $J = 11.0$ Hz, 1H), 3.65 (td, $J = 9.5, 7.8$ Hz, 1H), 3.63 (td, $J = 9.5, 7.8$ Hz, 1H), 3.48 (q, $J = 7.0$ Hz, 1H), 3.17 (s, 3H), 2.39 (s, 3H), 1.72 (d, $J = 7.0$ Hz, 3H), 0.95 (d, $J = 7.8$ Hz, 1H), 0.92 (d, $J = 7.8$ Hz, 1H), -0.01 (s, 9H). The regioisomer ratio was determined at the aldehyde signals. **LCMS** (ESI, high pH) $t_{\text{R}} = 1.31$ min, m/z 426 $[\text{M}+\text{H}]^+$ and $t_{\text{R}} = 1.36$ min, m/z 426 $[\text{M}+\text{H}]^+$.

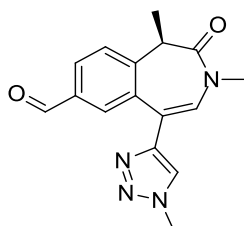
(R)-1,3-Dimethyl-5-(2-methyl-2H-1,2,3-triazol-4-yl)-2-oxo-2,3-dihydro-1H-benzo[d]azepine-7-carbaldehyde [7.48]



(R)-1,3-Dimethyl-2-oxo-5-(4,4,5,5-tetramethyl-1,3,2-dioxaborolan-2-yl)-2,3-dihydro-1H-benzo[d]azepine-7-carbaldehyde **[6.20]** (500 mg, 1.099 mmol), 4-bromo-2-methyl-2H-1,2,3-triazole (890 mg, 5.50 mmol), a 2 M aqueous solution of K_3PO_4 (1.65 mL, 3.30 mmol), Xphos (26.2 mg, 0.06 mmol) and Pd Xphos G2 (86 mg, 0.11 mmol) were stirred in *i*PrOH (5.5 mL) at 120 °C for 30 min in a microwave. The reaction mixture was concentrated under reduced pressure. EtOAc and water were added to the residue. The layers were separated and the aqueous layer was extracted with EtOAc. The organic layers were combined, dried through a hydrophobic frit and concentrated under reduced pressure. The crude product was purified by silica column chromatography eluted with a gradient of 0-100% EtOAc in cyclohexane, followed by a gradient of 0-25% EtOH in EtOAc. The relevant fractions were combined and concentrated under reduced pressure to give the title product **[7.48]** as a white solid (305 mg, 89% yield).

1H NMR (400 MHz, $CDCl_3$) δ 9.97 (s, 1H), 7.96 (dd, $J = 8.3, 1.7$ Hz, 1H), 7.88 (d, $J = 1.7$ Hz, 1H), 7.56 (d, $J = 8.3$ Hz, 1H), 7.54 (s, 1H), 7.07 (s, 1H), 4.24 (s, 3H), 3.48 (q, $J = 7.0$ Hz, 1H), 3.18 (s, 3H), 1.73 (d, $J = 7.0$ Hz, 3H). LCMS (ESI, formic) $t_R = 0.82$ min, m/z 297 $[M+H]^+$.

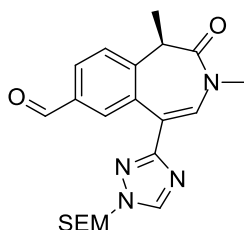
(R)-1,3-Dimethyl-5-(1-methyl-1H-1,2,3-triazol-4-yl)-2-oxo-2,3-dihydro-1H-benzo[d]azepine-7-carbaldehyde [7.49]



(R)-1,3-Dimethyl-2-oxo-5-(4,4,5,5-tetramethyl-1,3,2-dioxaborolan-2-yl)-2,3-dihydro-1H-benzo[d]azepine-7-carbaldehyde **[6.20]** (200 mg, 0.54 mmol), 4-bromo-1-methyl-1H-1,2,3-triazole (262 mg, 1.62 mmol), a 2 M aqueous solution of K_3PO_4 (2 mL, 4.0 mmol), Pd Xphos G2 (54 mg, 0.07 mmol) and Xphos (22 mg, 0.05 mmol) were suspended in *i*PrOH (5 mL) under nitrogen. The reaction mixture was heated in the microwave at 120 °C for 75 min. The reaction mixture was concentrated under reduced pressure. The residue was partitioned between EtOAc and water. The layers were separated, the aqueous layer was extracted with EtOAc. The organic layers were combined, dried using a hydrophobic frit and concentrated under reduced pressure. The crude product was purified by silica column chromatography eluted with a gradient of 0-100% EtOAc in cyclohexane, followed by a gradient of 0-25% EtOH in EtOAc. The appropriate fractions were combined and concentrated under reduced pressure to give the title product **[7.49]** as a colourless oil (105 mg, 56% yield).

1H NMR (400 MHz, $CDCl_3$) δ 9.98 (s, 1H), 7.95 (dd, $J = 8.2, 1.6$ Hz, 1H), 7.92 (d, $J = 1.6$ Hz, 1H), 7.57 (d, $J = 8.2$ Hz, 1H), 7.47 (s, 1H), 7.38 (s, 1H), 4.14 (s, 3H), 3.49 (q, $J = 6.9$ Hz, 1H), 3.19 (s, 3H), 1.72 (d, $J = 6.9$ Hz, 3H). LCMS (ESI, high pH) $t_R = 0.75$ min, m/z 297 $[M+H]^+$.

(R)-1,3-Dimethyl-2-oxo-5-(1-((2-(trimethylsilyl)ethoxy)methyl)-1H-1,2,4-triazol-3-yl)-2,3-dihydro-1H-benzo[d]azepine-7-carbaldehyde [7.50]

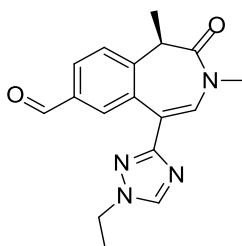


(R)-1,3-Dimethyl-2-oxo-5-(4,4,5,5-tetramethyl-1,3,2-dioxaborolan-2-yl)-2,3-dihydro-1H-benzo[d]azepine-7-carbaldehyde **[6.20]** (500 mg, 71% pure, 1.04 mmol), 3-bromo-1-((2-(trimethylsilyl)ethoxy)methyl)-1H-1,2,4-triazole **[7.59]** (1.2 g, 4.3 mmol), a 2 M aqueous solution of K_3PO_4 (0.88 mL, 1.76 mmol), Pd Xphos G2 (82 mg, 0.10 mmol) and Xphos (24.8 mg, 0.05 mmol) was suspended in *i*PrOH (4 mL) under nitrogen. (NB reaction was carried out in two microwave vials and combined for work up). The reaction mixtures were sonicated for a few minutes and heated in the microwave at 120 °C for 30 min. The combined reaction mixtures were concentrated under reduced pressure. The residue was partitioned between EtOAc and water twice. The organic layers were combined, dried using a hydrophobic frit and concentrated under reduced pressure. The crude product was purified by silica column chromatography eluted with a gradient of 0-100% EtOAc in cyclohexane. The appropriate fractions were combined and concentrated under reduced pressure to give the title product **[7.50]** as a colourless oil (465.5 mg, 98% yield).

1H NMR (400 MHz, $CDCl_3$) δ 9.96 (s, 1H), 8.25 (s, 1H), 8.16 (d, $J = 1.5$ Hz, 1H), 7.92 (dd, $J = 8.2, 1.5$ Hz, 1H), 7.55 (s, 1H), 7.50 (d, $J = 8.2$ Hz, 1H), 5.49 (d, $J = 11.0$ Hz, 1H), 5.46 (d, $J = 11.0$ Hz, 1H), 3.67 (dt, $J = 9.3, 8.2$ Hz, 2H), 3.47 (q, $J = 6.9$ Hz, 1H), 3.18 (s, 3H), 1.68 (d, $J = 6.9$ Hz, 3H), 0.93 (t, $J = 8.2$ Hz, 2H), -0.03 (s, 9H).

LCMS (ESI, high pH) $t_R = 1.22$ min, m/z 413 $[M+H]^+$.

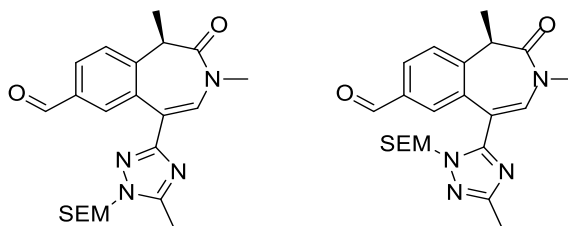
(R)-5-(1-Ethyl-1H-1,2,4-triazol-3-yl)-1,3-dimethyl-2-oxo-2,3-dihydro-1H-benzo[d]azepine-7-carbaldehyde [7.51]



(R)-1,3-Dimethyl-2-oxo-5-(4,4,5,5-tetramethyl-1,3,2-dioxaborolan-2-yl)-2,3-dihydro-1H-benzo[d]azepine-7-carbaldehyde **[6.20]** (564.8 mg, 71% pure, 1.18 mmol), 3-bromo-1-ethyl-1H-1,2,4-triazole (414 mg, 2.35 mmol), a 2 M aqueous solution of K_3PO_4 (0.5 mL, 1.0 mmol), Xphos (28.0 mg, 0.06 mmol) and Pd Xphos G2 (92 mg, 0.12 mmol) were heated at 120 °C, under nitrogen for 30 min in a microwave. The reaction mixture was concentrated under reduced pressure and the resulting residue was partitioned between EtOAc and water. The two layers were separated and the aqueous layer was extracted with EtOAc three times. The organics were combined, dried through a hydrophobic frit and concentrated under reduced pressure. The crude was purified by silica column chromatography, eluted with a gradient of 0-100% EtOAc in cyclohexane, followed by a gradient of 0-25% EtOH in EtOAc. The relevant fractions were combined and concentrated under reduced pressure to give the title product **[7.51]** as a colourless oil (132.8 mg, 31% yield).

1H NMR (400 MHz, MeOD) δ 9.96 (s, 1H), 8.49 (s, 1H), 8.06 (d, $J = 1.6$ Hz, 1H), 8.01 (dd, $J = 8.2, 1.6$ Hz, 1H), 7.60 (d, $J = 8.2$ Hz, 1H), 7.49 (s, 1H), 4.29 (q, $J = 7.3$ Hz, 2H), 3.53 (q, $J = 6.9$ Hz, 1H), 3.19 (s, 3H), 1.69 (d, $J = 6.9$ Hz, 3H), 1.52 (t, $J = 7.3$ Hz, 3H). **LCMS** (ESI, high pH) $t_R = 0.79$ min, m/z 311 $[M+H]^+$.

(R)-1,3-Dimethyl-5-(5-methyl-1-((2-(trimethylsilyl)ethoxy)methyl)-1H-1,2,4-triazol-3-yl)-2-oxo-2,3-dihydro-1H-benzo[d]azepine-7-carbaldehyde [7.52]



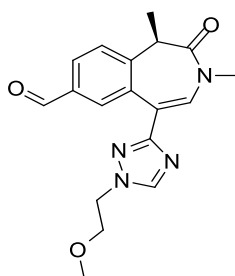
Main regioisomer (82%)

(R)-1,3-Dimethyl-2-oxo-5-(4,4,5,5-tetramethyl-1,3,2-dioxaborolan-2-yl)-2,3-dihydro-1H-benzo[d]azepine-7-carbaldehyde [6.20] (500 mg, 1.47 mmol), 3-bromo-5-methyl-1-((2-(trimethylsilyl)ethoxy)methyl)-1H-1,2,4-triazole [7.60] (1.29 g, 4.40 mmol), a 2 M aqueous solution of K_3PO_4 (2.2 mL, 4.40 mmol), Pd Xphos G2 (115 mg, 0.15 mmol) and Xphos (34.9 mg, 0.07 mmol) was suspended in *i*PrOH (5 mL) under nitrogen. The reaction mixture was split into two microwave vials and heated in the microwave for 30 min at 120 °C (NB: one of the vials was sonicated to help solubilisation of the boronic ester starting material). The crude was partitioned between EtOAc and water. The aqueous layer was extracted twice with EtOAc. The organic layers were combined, dried through a phase separator and concentrated under reduced pressure to give a yellow oil. The crude product was purified by silica column chromatography, eluted with a gradient of 0-100% EtOAc in cyclohexane. The relevant fractions were concentrated under reduced pressure to give the title product [7.52] as a yellow oil (0.48 g, 65% pure, 50% yield).

1H NMR (400 MHz, $CDCl_3$) δ . 9.96 (s, 1H), 8.13 (d, $J = 1.7$ Hz, 1H), 7.92 (dd, $J = 8.1, 1.7$ Hz, 1H), 7.51 (d, $J = 8.1$ Hz, 1H), 7.47 (s, 1H), 5.44 (d, $J = 11.3$ Hz, 1H), 5.40 (d, $J = 11.3$ Hz, 1H), 3.65 (td, $J = 9.3, 7.8$ Hz, 2H), 3.46 (q, $J = 6.9$ Hz, 1H), 3.19 (s, 3H), 2.56 (s, 3H), 1.68 (d, $J = 6.9$ Hz, 3H), 0.93 (d, $J = 7.8$ Hz, 1H), 0.91 (d, $J = 7.8$

Hz, 1H), -0.02 (s, 9H). NMR showed presence of 18% of the minor SEM regioisomer, determined at peaks 9.96 ppm (major regioisomer) and 9.92 ppm (minor regioisomer). LCMS (ESI, high pH) $t_R = 1.24$ min, m/z 427 $[M+H]^+$.

(R)-5-(1-(2-Methoxyethyl)-1H-1,2,4-triazol-3-yl)-1,3-dimethyl-2-oxo-2,3-dihydro-1H-benzo[d]azepine-7-carbaldehyde [7.53]



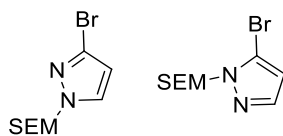
(R)-1,3-Dimethyl-2-oxo-5-(4,4,5,5-tetramethyl-1,3,2-dioxaborolan-2-yl)-2,3-dihydro-1H-benzo[d]azepine-7-carbaldehyde **[6.20]** (250 mg, 71% purity, 0.52 mmol), 3-bromo-1-(2-methoxyethyl)-1H-1,2,4-triazole **[7.65]** (475 mg, 2.08 mmol), a 2 M aqueous solution of K_3PO_4 (0.5 mL, 1.0 mmol), Xphos (12.4 mg, 0.03 mmol) and Pd Xphos G2 (40.9 mg, 0.05 mmol) were heated at 120 °C for 30 min in a microwave. The reaction mixture was filtered through a hydrophobic frit and the filtrate was concentrated under reduced pressure. The resulting residue was partitioned between EtOAc and water and the two layers were separated. The aqueous layer was extracted with EtOAc three times. The organic layers were combined, dried through a hydrophobic frit and concentrated under reduced pressure. The crude product was taken in DCM, sonicated and purified by silica column chromatography, eluting with a gradient of 0-100% EtOAc in cyclohexane, followed by a gradient of 0-25% EtOH in EtOAc. The relevant fractions were combined and concentrated under reduced pressure to give the title product **[7.53]** as a colourless oil (74.5 mg, 34% yield) and a second batch, less pure. This second batch was further purified by MDAP (high pH,

extended method A). The relevant fractions were concentrated under reduced pressure to give the title product **[7.53]** as a colourless oil in two batches (27 mg, 12% yield and 9 mg, 4% yield).

The analysis of the largest batch will be here reported but matches the data for the two smaller batches.

¹H NMR (400 MHz, MeOD) δ 9.95 (s, 1H), 8.46 (s, 1H), 8.08 (d, $J = 1.7$ Hz, 1H), 7.99 (dd, $J = 8.3, 1.7$ Hz, 1H), 7.59 (d, $J = 8.3$ Hz, 1H), 7.50 (s, 1H), 4.40 (t, $J = 5.0$ Hz, 2H), 3.77 (t, $J = 5.0$ Hz, 2H), 3.52 (q, $J = 6.9$ Hz, 1H), 3.35 (s, 3H), 3.18 (s, 3H), 1.67 (d, $J = 6.9$ Hz, 3H). LCMS (ESI, high pH) $t_R = 0.77$ min, m/z 341 [M+H]⁺.

**3-Bromo-1-((2-(trimethylsilyl)ethoxy)methyl)-1H-pyrazole and
5-bromo-1-((2-(trimethylsilyl)ethoxy)methyl)-1H-pyrazole [7.55]¹¹⁹**

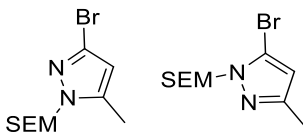


3-Bromo-1H-pyrazole **[7.54]** (2 g, 13.6 mmol) was dissolved THF (40 mL), placed under nitrogen and cooled to 0 °C. Sodium hydride (60% in mineral oil, 0.82 g, 20.4 mmol) was added. The reaction mixture was stirred at 0 °C for 10 min. (2-(chloromethoxy)ethyl)trimethylsilane (3.61 mL, 20.4 mmol) was added and the reaction mixture was stirred overnight, the ice bath slowly warming up to rt. The reaction mixture was quenched with MeOH and concentrated under reduced pressure. The crude was then partitioned between DCM and water and the layers were separated. The aqueous layer was extracted with DCM. The organic layers were combined and concentrated under reduced pressure to give a pale-yellow oil. The crude product was purified by silica column chromatography eluted with a gradient of 0-40% EtOAc in cyclohexane (containing 1% Et₃N). The relevant fractions were concentrated under

reduced pressure to give the title products [7.55] as a mixture of regioisomers in a 2:1 ratio as a colourless oil (3.15 g, 71% yield). The ratio of regioisomers was determined at the SEM methylene signals at 5.37 ppm and 5.47 ppm.

Regioisomer 1 (major): $^1\text{H NMR}$ (400 MHz, CDCl_3) δ 7.44 (d, $J = 2.5$ Hz, 1H), 6.32 (d, $J = 2.5$ Hz, 1H), 5.35 (s, 2H), 3.57 (d, $J = 8.2$ Hz, 1H), 3.55 (d, $J = 8.2$ Hz, 1H), 0.89 (d, $J = 8.2$ Hz, 1H), 0.87 (d, $J = 8.2$ Hz, 1H), -0.03 (s, 9H). **LCMS** (ESI, high pH) $t_{\text{R}} = 1.30$ min, m/z 277/279 $[\text{M}+\text{H}]^+$. **Regioisomer 2 (minor):** $^1\text{H NMR}$ (400 MHz, CDCl_3) δ 7.51 (d, $J = 2.0$ Hz, 1H), 6.32 (d, $J = 2.0$ Hz, 1H), 5.47 (s, 2H), 3.60 (d, $J = 8.1$ Hz, 1H), 3.56 (d, $J = 8.1$ Hz, 1H), 0.90 (d, $J = 8.1$ Hz, 1H), 0.88 (d, $J = 8.1$ Hz, 1H), -0.04 (s, 9H). **LCMS** (ESI, high pH) $t_{\text{R}} = 1.31$ min, m/z 277/279 $[\text{M}+\text{H}]^+$.

**3-Bromo-5-methyl-1-((2-(trimethylsilyl)ethoxy)methyl)-1H-pyrazole and
5-bromo-3-methyl-1-((2-(trimethylsilyl)ethoxy)methyl)-1H-pyrazole [7.57]¹¹⁶**



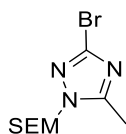
3-Bromo-5-methyl-1H-pyrazole [7.56] (1 g, 6.2 mmol) was dissolved in THF (20 mL), placed under nitrogen and cooled to 0 °C. Sodium hydride (60% in mineral oil, 0.37 g, 9.3 mmol) was added and the reaction mixture was stirred at 0 °C for 15 min. SEM-Cl (1.7 mL, 9.3 mmol) was added and the reaction mixture was stirred at 0 °C for 1.5 h and at rt for 2 h. The reaction mixture was quenched with MeOH and concentrated under reduced pressure. The oil was partitioned between EtOAc and water. The aqueous layer was extracted with EtOAc. The organic layers were combined, dried through a hydrophobic frit and concentrated under reduced pressure. The crude product was purified by silica column chromatography, eluted with a gradient of 0-100% of EtOAc in cyclohexane. The relevant fractions were concentrated under

reduced pressure to give the title products [7.57] as a mixture of regioisomers as two yellow oils, both in a 55:45 ratio (1.09 g, 57% yield and 434.4 mg, 23% yield). The ratio of regioisomers was determined at the aromatic proton signal. The analysis of the larger batch was reported below.

Regioisomer 1: $^1\text{H NMR}$ (400 MHz, CDCl_3) δ 5.98 (s, 1H), 5.24 (s, 2H), 3.49 (t, $J = 8.1$ Hz, 2H), 2.23 (s, 3H), 0.79 (t, $J = 8.1$ Hz, 2H), -0.10 (s, 9H). **Regioisomer 2:** $^1\text{H NMR}$ (400 MHz, CDCl_3) δ 6.03 (s, 1H), 5.30 (s, 2H), 3.53 (t, $J = 8.1$ Hz, 2H), 2.16 (s, 3H), 0.82 (t, $J = 8.1$ Hz, 2H), -0.10 (s, 9H). **LCMS** (ESI, high pH) $t_R = 1.38$ min (broad peak), m/z 291/293 $[\text{M}+\text{H}]^+$.

3-Bromo-5-methyl-1-((2-(trimethylsilyl)ethoxy)methyl)-

1H-1,2,4-triazole [7.62]¹¹⁷

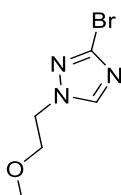


Major regioisomer

3-Bromo-5-methyl-1H-1,2,4-triazole [7.61] (2.0 g, 12.4 mmol) was dissolved in THF (41 mL) under nitrogen at 0 °C. Sodium hydride (60% in mineral oil, 0.74 g, 18.5 mmol) was added and the reaction mixture was stirred at 0 °C for 15 min. SEM-Cl (3.3 ml, 18.5 mmol) was added and the reaction mixture was stirred 0 °C for 30 min. The reaction mixture was concentrated under reduced pressure. The oil was partitioned between EtOAc and water. The organic layer was dried through a phase separator and concentrated under reduced pressure. The crude product was purified by silica column chromatography, eluted with a gradient of 0-100% EtOAc in cyclohexane. The relevant fractions were concentrated under reduced pressure to give the title product [7.62] as the major regioisomer, as a yellow oil (1.97 g, 52% yield).

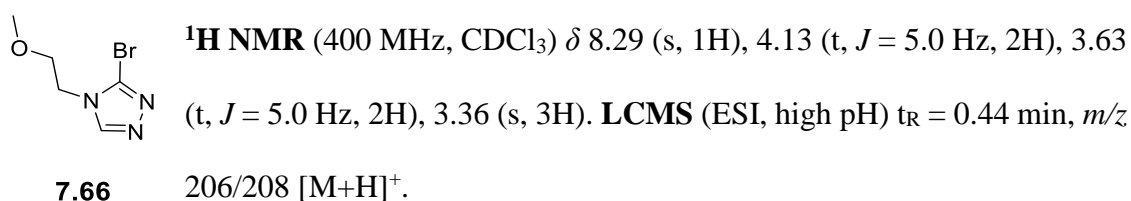
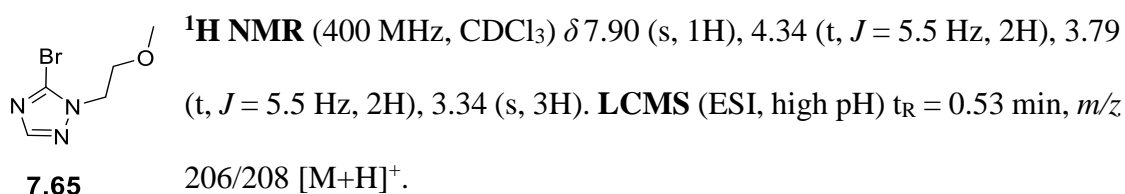
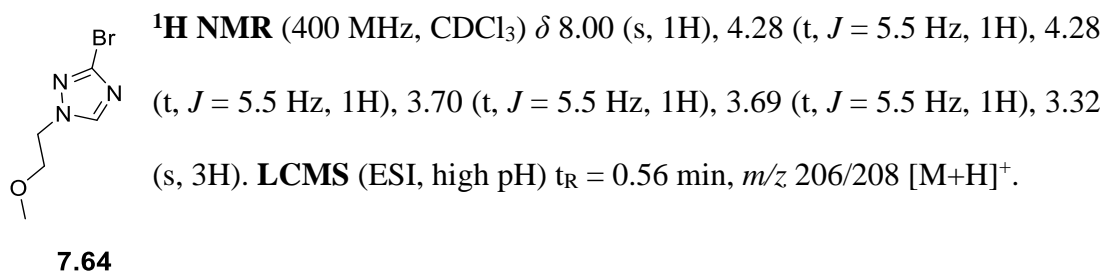
Regioisomer 1 (major): $^1\text{H NMR}$ (400 MHz, CDCl_3) δ 5.32 (s, 2H), 3.56 (t, $J = 8.2$ Hz, 2H), 2.45 (s, 3H), 0.84 (t, $J = 8.2$ Hz, 2H), -0.06 (s, 9H). **Regioisomer 2 (minor):** $^1\text{H NMR}$ (400 MHz, CDCl_3) δ 5.35 (s, 2H), 3.59 (t, $J = 8.2$ Hz, 2H), 2.32 (s, 3H), 0.87 (t, $J = 8.2$ Hz, 2H), -0.06 (s, 9H). The relative ratio of regioisomers was determined as 2:1, at the methyl signals. **LCMS** (ESI, high pH) $t_{\text{R}} = 1.22$ min, m/z 292/294 $[\text{M}+\text{H}]^+$.

3-Bromo-1-(2-methoxyethyl)-1H-1,2,4-triazole [7.64]

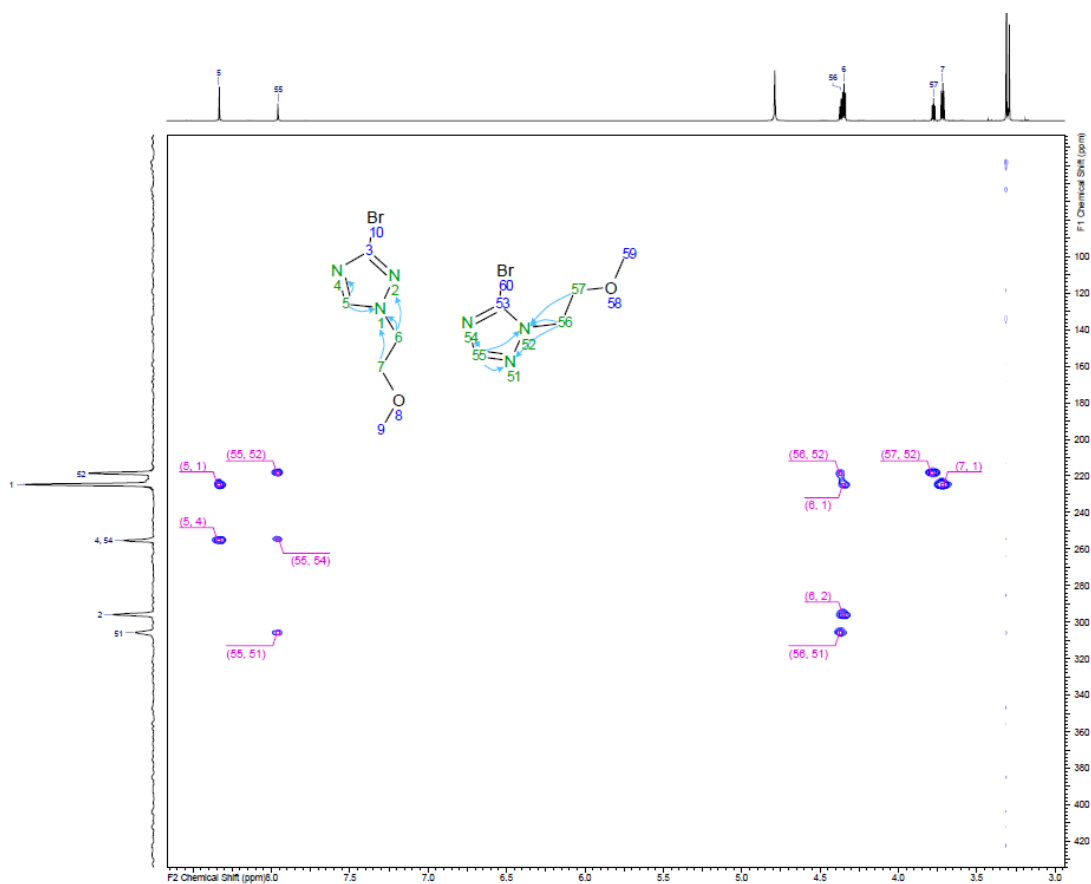


3-Bromo-1H-1,2,4-triazole [7.58] (200 mg, 1.4 mmol) in DMF (5 mL) was treated with *t*BuOK (228 mg, 2.0 mmol) and the reaction mixture was stirred under nitrogen at rt for 15 min. 1-Bromo-2-methoxyethane [7.63] (0.64 mL, 6.8 mmol) was added and the reaction mixture was stirred at 40 °C for 3 h. Acetone (1 mL) was added and the reaction mixture was stirred at 40 °C under nitrogen for 1.5 h. The reaction mixture was transferred into a microwave vial, the flask was rinsed with MeOH and the vial was sealed. 1-Bromo-2-methoxyethane [7.63] (0.64 mL, 6.8 mmol) was added to the reaction mixture and was stirred at 60 °C for 15 h. 1-Bromo-2-methoxyethane [7.63] (0.64 mL, 6.8 mmol) was added and the reaction mixture was stirred at 60 °C for 4 h. 1-Bromo-2-methoxyethane [7.63] (0.64 mL, 6.8 mmol) was added and the reaction was stirred at 60 °C for 16 h. 1-bromo-2-methoxyethane [7.63] (0.64 mL, 6.8 mmol) was added and the reaction mixture was stirred at 60 °C for 5 h. 1-Bromo-2-methoxyethane [7.63] (0.64 mL, 6.8 mmol) was added and the reaction was stirred at 60 °C for 3 h. The reaction mixture was concentrated under reduced pressure. The residue was taken in MeOH, filtered through a phase separator and concentrated under

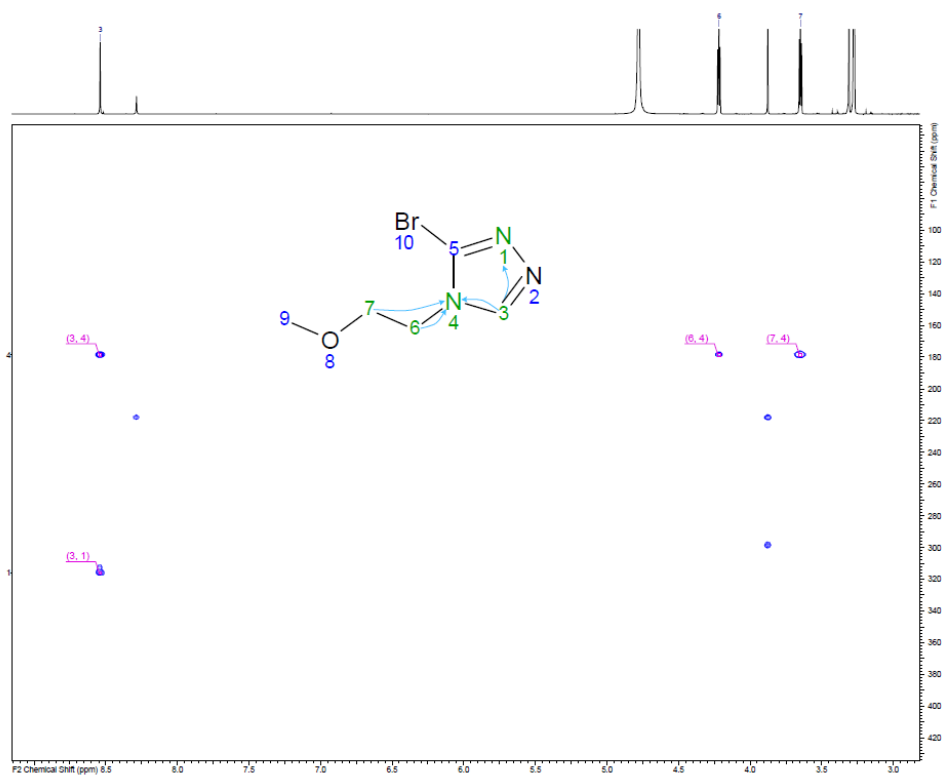
reduced pressure. The residue was purified by MDAP (High pH, extended method A). The relevant fractions were combined and concentrated to give the title product **[7.64]** as a white solid (177.4 mg, 57% yield), 5-bromo-1-(2-methoxyethyl)-1*H*-1,2,4-triazole **[7.65]** as a white solid (54 mg, 18% yield) and 3-bromo-4-(2-methoxyethyl)-4*H*-1,2,4-triazole **[7.66]** as a white solid (16.6 mg, 75% pure, 5% yield).



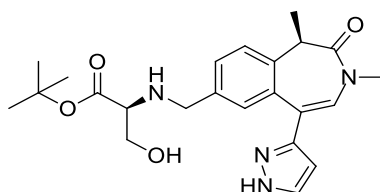
¹⁵N HMBC (MeOD) are shown below for one of the first batch, where products **7.64** and **7.65** were analysed as a 2:1 mixture. The ratio of product **7.64** and **7.65** enabled the attribution of the ¹H NMR signals for each regioisomer and then enabled analysis of the ¹⁵N HMBC.



¹⁵N HMBC (MeOD) of product **7.66** is shown below.



***Tert*-butyl (((*R*)-1,3-dimethyl-2-oxo-5-(1*H*-pyrazol-3-yl)-2,3-dihydro-1*H*-benzo[*d*]azepin-7-yl)methyl)-*L*-serinate [7.67]**

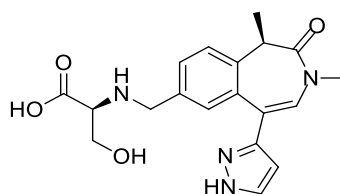


(*R*)-1,3-Dimethyl-2-oxo-5-(1-((2-(trimethylsilyl)ethoxy)methyl)-1*H*-pyrazol-3-yl)-2,3-dihydro-1*H*-benzo[*d*]azepine-7-carbaldehyde [7.45] (157 mg, 0.38 mmol), *tert*-butyl *L*-serinate, hydrochloride [7.11] (113 mg, 0.57 mmol), DIPEA (0.13 mL, 0.76 mmol) and acetic acid (0.055 mL, 0.95 mmol) were stirred in THF (5 mL) under nitrogen at 40 °C for 2.5 h. The reaction mixture was cooled to rt and sodium triacetoxyborohydride (202 mg, 0.95 mmol) was added and the reaction mixture was stirred for 1.5 h at rt. The reaction mixture was quenched with MeOH and concentrated under reduced pressure to give a yellow residue. The residue was dissolved in DCM and washed with water. The organic layer was dried through a phase separator and concentrated under reduced pressure to give a yellow oil. The oil was taken in DCM and cooled to -78 °C under nitrogen. A 1 M solution of BBr₃ in DCM (1.1 mL, 1.1 mmol) was added and the reaction mixture was stirred 10 min at -78 °C and then was warmed up to rt and stirred for 6 h. The reaction mixture was quenched with a saturated aqueous solution of sodium bicarbonate. The layers were separated. The aqueous layer was re-extracted with DCM. The organic layers were combined, dried through a phase separator and concentrated under reduced pressure to give a yellow oil. The crude product was purified by MDAP (high pH, extended method B). The relevant fractions were concentrated under reduced pressure to give the title product [7.67] as a colourless oil (13.2 mg, 8% yield).

¹H NMR (400 MHz, MeOD) δ 7.66 (d, J = 1.6 Hz, 1H), 7.48 (dd, J = 8.1, 1.5 Hz, 1H), 7.36 (d, J = 8.1 Hz, 1H), 7.29 (d, J = 1.5 Hz, 1H), 7.01 (s, 1H), 6.39 (d, J = 1.6 Hz, 1H), 3.81 (d, J = 13.2 Hz, 1H), 3.67 (d, J = 13.2 Hz, 1H), 3.65 (d, J = 5.1 Hz, 2H), 3.43 (q, J = 6.9 Hz, 1H), 3.17 (t, J = 5.1 Hz, 1H), 3.13 (s, 3H), 1.64 (d, J = 6.9 Hz, 3H), 1.41 (s, 9H). The signals for the exchangeable protons were not observed. LCMS (ESI, high pH) t_R = 0.88 min, m/z 427 [M+H]⁺.

Isolation and characterisation of the carboxylic acid by-product:

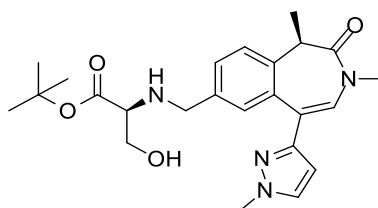
(((*R*)-1,3-Dimethyl-2-oxo-5-(1*H*-pyrazol-3-yl)-2,3-dihydro-1*H*-benzo[*d*]azepin-7-yl)methyl)-*L*-serine



The aqueous layer was concentrated under reduced pressure to give a white solid. The solid was suspended in methanol and filtered. The filtrate was concentrated under reduced pressure to give a white solid. This solid was purified by MDAP (high pH, extended method A). The relevant fractions were concentrated under reduced pressure to give the title product as a white solid (11.6 mg, 8% yield).

¹H NMR (400 MHz, MeOD) δ 7.67 (d, J = 1.9 Hz, 1H), 7.61 (dd, J = 8.3, 1.7 Hz, 1H), 7.47 (br. s, 1H), 7.46 (d, J = 8.3 Hz, 1H), 7.06 (s, 1H), 6.47 (d, J = 1.9 Hz, 1H), 4.20 (d, J = 13.2 Hz, 1H), 4.15 (d, J = 13.2 Hz, 1H), 3.92 (dd, J = 11.7, 3.9 Hz, 1H), 3.83 (dd, J = 11.7, 6.6 Hz, 1H), 3.47 (q, J = 6.9 Hz, 1H), 3.47 (dd, J = 6.6, 3.9 Hz, 1H), 3.13 (s, 3H), 1.65 (d, J = 6.9 Hz, 3H). The signals for the exchangeable protons were not observed. LCMS (ESI, high pH) t_R = 0.52 min, m/z 371 [M+H]⁺.

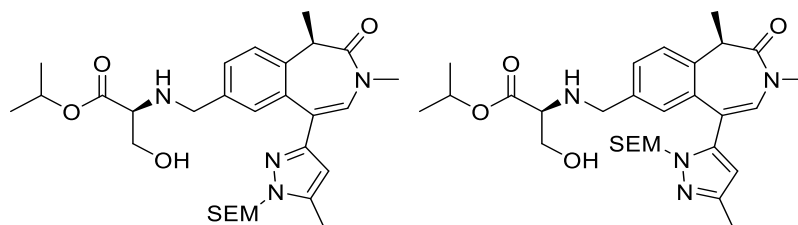
***Tert*-butyl (((*R*)-1,3-dimethyl-5-(1-methyl-1*H*-pyrazol-3-yl)-2-oxo-2,3-dihydro-1*H*-benzo[*d*]azepin-7-yl)methyl)-*L*-serinate [7.68]**



Reductive amination general procedure A1 with aldehyde [7.46] (58 mg, 0.18 mmol) and *tert*-butyl *L*-serinate, hydrochloride [7.11] (51.8 mg, 0.26 mmol). The product was purified silica column chromatography eluted with a gradient of 0-100% EtOAc in cyclohexane, followed by a gradient of 0-25% EtOH in EtOAc. The relevant fractions were concentrated under reduced pressure and purified by HPLC (Chiralpak IC5 column, 20% EtOH (containing 2% *i*PrNH₂) in heptane (containing 2% *i*PrNH₂)). The relevant fractions were concentrated under reduced pressure to give the title product [7.68] as a colourless oil (14.8 mg, 19% yield).

¹H NMR (400 MHz, CDCl₃) δ 7.40 (d, *J* = 1.4 Hz, 1H), 7.37 (dd, *J* = 8.1, 1.4 Hz, 1H), 7.30 (d, *J* = 2.5 Hz, 1H), 7.32 (d, *J* = 8.1 Hz, 1H), 6.97 (s, 1H), 6.21 (d, *J* = 2.5 Hz, 1H), 3.95 (s, 3H), 3.87 (d, *J* = 13.1 Hz, 1H), 3.71 (dd, *J* = 10.5, 4.4 Hz, 1H), 3.68 (d, *J* = 13.1 Hz, 1H), 3.50 (dd, *J* = 10.5, 6.8 Hz, 1H), 3.40 (q, *J* = 6.9 Hz, 1H), 3.26 (dd, *J* = 6.8, 4.4 Hz, 1H), 3.15 (s, 3H), 1.67 (d, *J* = 6.9 Hz, 3H), 1.44 (s, 9H). The signals for the exchangeable protons were not observed. LCMS (ESI, high pH) *t*_R = 0.92 min, *m/z* 441 [M+H]⁺.

***Isopropyl* (((*R*)-1,3-dimethyl-5-(5-methyl-1-((2-(trimethylsilyl)ethoxy)methyl)-1*H*-pyrazol-3-yl)-2-oxo-2,3-dihydro-1*H*-benzo[*d*]azepin-7-yl)methyl)-*L*-serinate, as the main regioisomer [7.69]**

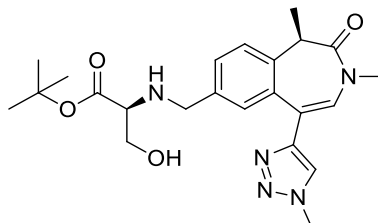


Reductive amination general procedure A2 with aldehyde [7.47] (mixture of SEM-regioisomers) (82.6 mg, 0.18 mmol) and *isopropyl L-serinate*, tosic acid salt [7.08] (88.0 mg, 0.28 mmol). The crude material obtained after the work-up showed mainly the aldehyde starting material so the general procedure A2 was repeated. The crude product obtained was then purified silica column chromatography eluted with a gradient of 0-100% EtOAc in cyclohexane. The relevant fractions were concentrated under reduced pressure and further purified by MDAP (high pH, extended method B). The relevant fractions were concentrated under reduced pressure to give the mixture of SEM-regioisomers [7.69] as a colourless oil (30.0 mg, 23% yield). The mixture of products was used without further purification in the next step.

¹H NMR (400 MHz, CDCl₃) δ 7.40 (dd, *J* = 8.1, 1.2 Hz, 1H), 7.34 (d, *J* = 8.1 Hz, 1H), 6.95 (d, *J* = 1.2 Hz, 1H), 6.73 (s, 1H), 6.15 (s, 1H), 5.15 (d, *J* = 10.9 Hz, 1H), 5.04 (spt, *J* = 6.1 Hz, 1H), 4.93 (d, *J* = 10.9 Hz, 1H), 3.81 (d, *J* = 13.1 Hz, 1H), 3.69 (dd, *J* = 10.8, 4.4 Hz, 1H), 3.61 (d, *J* = 13.1 Hz, 1H), 3.53 (dd, *J* = 10.8, 6.6 Hz, 1H), 3.47 (td, *J* = 10.9, 8.3 Hz, 2H), 3.43 (q, *J* = 6.9 Hz, 1H), 3.27 (dd, *J* = 6.6, 4.4 Hz, 1H), 3.15 (s, 3H), 2.32 (s, 3H), 1.70 (d, *J* = 6.9 Hz, 3H), 1.23 (d, *J* = 6.1 Hz, 3H), 1.22 (d, *J* = 6.1 Hz, 3H), 0.78 (t, *J* = 8.3 Hz, 2H), -0.05 (s, 9H). The signals for the exchangeable protons were not observed. Several signals showed shoulders for the SEM regioisomers; the regioisomer ratio showed presence of 11% of the minor regioisomers determined at the signals major regioisomer 6.95 (d, *J* = 1.2 Hz, 1H), minor

regioisomer 6.93 (d, $J = 1.2$ Hz, 1H). LCMS (ESI, high pH) $t_R = 1.29$ min, m/z 557 [M+H]⁺.

***Tert*-butyl (((*R*)-1,3-dimethyl-5-(1-methyl-1*H*-1,2,3-triazol-4-yl)-2-oxo-2,3-dihydro-1*H*-benzo[*d*]azepin-7-yl)methyl)-*L*-serinate [7.70]**

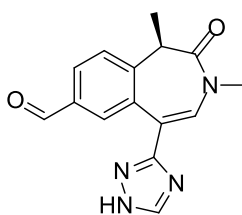


Reductive amination general procedure A1 with aldehyde [7.49] (25 mg, 0.07 mmol) and *tert*-butyl *L*-serinate, hydrochloride [7.11] (21.3 mg, 0.11 mmol). The crude was purified by silica column chromatography, eluted with a gradient of 0-100% EtOAc in cyclohexane, followed by a gradient of 0-25% EtOH in EtOAc. The relevant fractions were concentrated under reduced pressure and the product was further purified by HPLC (Chiralpak AD-H column, 30% EtOH (containing 0.2% *i*PrNH₂) in heptane (containing 0.2% *i*PrNH₂)). The relevant fractions were concentrated under reduced pressure to give the title product [7.70] as a colourless oil (11 mg, 35% yield).

¹H NMR (400 MHz, MeOD) δ 7.93 (s, 1H), 7.47 (dd, $J = 8.1, 1.7$ Hz, 1H), 7.37 (d, $J = 8.1$ Hz, 1H), 7.37 (d, $J = 1.7$ Hz, 1H), 7.21 (s, 1H), 4.13 (s, 3H), 3.82 (d, $J = 13.2$ Hz, 1H), 3.70 (d, $J = 13.2$ Hz, 1H), 3.68 (dd, $J = 12.0, 5.4$ Hz, 1H), 3.62 (dd, $J = 12.0, 5.4$ Hz, 1H), 3.43 (q, $J = 6.9$ Hz, 1H), 3.19 (t, $J = 5.4$ Hz, 1H), 3.14 (s, 3H), 1.63 (d, $J = 6.9$ Hz, 3H), 1.42 (s, 9H). The two exchangeable protons were not observed. ¹³C NMR (101 MHz, CDCl₃) δ 172.1 (C=O), 170.3 (C=O), 146.7 (C_{iv}), 137.7 (C_{iv}), 136.9 (C_{iv}), 134.4 (C_{iv}), 129.6 (CH), 129.0 (CH), 126.4 (CH), 124.4 (CH), 123.3 (CH), 119.1 (C_{iv}), 82.1 (C_{iv}), 62.6 (CH), 62.2 (CH₂), 51.7 (CH₂), 41.1 (CH), 36.7 (CH₃), 35.4 (CH₃), 28.1 (CH₃), 12.8 (CH₃). LCMS (ESI, high pH) $t_R = 0.87$ min, m/z 442 [M+H]⁺. HRMS

(ESI) calculated for $C_{23}H_{32}N_5O_4$ $[M+H]^+$ 442.2455, found 442.2458 (2.03 min). ν_{max} (solution in chloroform, cm^{-1}): 3442 (OH), 3326 (NH), 2978 (CH alkene), 2938 (CH alkane), 1725 (C=O ester), 1663 (C=O amide). $[\alpha_D]^{21.4 \text{ } ^\circ C}_{589 \text{ nm}}$ (c 0.500, MeOH): +118.7°.

(R)-1,3-Dimethyl-2-oxo-5-(1H-1,2,4-triazol-3-yl)-2,3-dihydro-1H-benzo[d]azepine-7-carbaldehyde [7.71], (Table 31, entry 3, p.161)

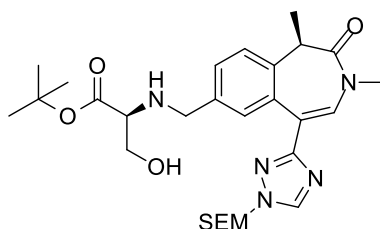


(R)-1,3-Dimethyl-2-oxo-5-(1-((2-(trimethylsilyl)ethoxy)methyl)-1H-1,2,4-triazol-3-yl)-2,3-dihydro-1H-benzo[d]azepine-7-carbaldehyde **[7.50]** (448.8 mg, 0.93 mmol) was dissolved in 1,4-dioxane (5 mL). A 4 M solution of hydrochloric acid in 1,4-dioxane (10 mL, 40.0 mmol) was added and the reaction mixture was stirred at 40 °C for 3 h. The reaction mixture was concentrated under reduced pressure to give a yellow solid. The crude product was purified by reverse phase column chromatography on C18 column, eluted with a gradient of 0-20% MeCN in a 10 mM aqueous solution of ammonium carbonate. The relevant fractions were concentrated under reduced pressure to give the title product **[7.71]** as a white solid (267.5 mg, 97% yield).

1H NMR (400 MHz, DMSO- d_6) δ 14.04 (br. s, 1H), 10.00 (s, 1H), 8.51 (br. s, 1H), 8.14 (br. s, 1H), 7.99 (dd, $J = 8.0, 1.5$ Hz, 1H), 7.58 (d, $J = 8.0$ Hz, 1H), 7.57 (br. s,

1H), 3.46 (q, $J = 6.9$ Hz, 1H), 3.12 (s, 3H), 1.59 (d, $J = 6.9$ Hz, 3H). LCMS (ESI, high pH) $t_R = 0.60$ min, m/z 283 $[M+H]^+$.

***Tert*-butyl (((*R*)-1,3-dimethyl-2-oxo-5-(1-((2-(trimethylsilyl)ethoxy)methyl)-1*H*-1,2,4-triazol-3-yl)-2,3-dihydro-1*H*-benzo[*d*]azepin-7-yl)methyl)-*L*-serinate [7.72]**

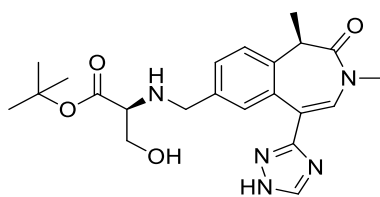


Reductive amination general procedure B with aldehyde [7.50] (195 mg, 0.38 mmol) and *tert*-butyl *L*-serinate, hydrochloride [7.11] (112 mg, 0.57 mmol). The reaction mixture was quenched with methanol and concentrated under reduced pressure to give a yellow oil. The oil was dissolved in EtOAc and washed twice with water. The organic layer was dried through a phase separator and concentrated under reduced pressure to give a yellow oil. The crude product was purified by silica column chromatography eluted with a gradient of 0-100% EtOAc in cyclohexane, followed by a gradient of 0-25% EtOH in EtOAc. The relevant fractions were concentrated under reduced pressure to give the title product [7.72] as a colourless oil (204.8 mg, 70% purity, 68% yield).

¹H NMR (400 MHz, CDCl₃) δ 8.27 (s, 1H), 7.67 (br. s, 1H), 7.46 (s, 1H), 7.44 (br. d., $J = 8.2$ Hz, 1H), 7.31 (d, $J = 8.2$ Hz, 1H), 5.49 (s, 2H), 4.88 (br. s, 1H), 4.05 (d, $J = 13.2$ Hz, 1H), 3.90 (d, $J = 13.2$ Hz, 1H), 3.85 (t, $J = 8.2$ Hz, 2H), 3.62 (d, $J = 7.5$ Hz,

2H), 3.40-3.34 (m, 1H), 3.37 (q, $J = 6.7$ Hz, 1H), 3.15 (s, 3H), 1.62 (d, $J = 6.7$ Hz, 3H), 1.40 (s, 9H), 0.92 (t, $J = 8.2$ Hz, 2H), -0.03 (s, 9H). One of the two exchangeable protons was not observed. LCMS (ESI, high pH) $t_R = 1.25$ min, m/z 558 $[M+H]^+$.

***Tert*-butyl (((*R*)-1,3-dimethyl-2-oxo-5-(1*H*-1,2,4-triazol-3-yl)-2,3-dihydro-1*H*-benzo[*d*]azepin-7-yl)methyl)-*L*-serinate [7.73]**



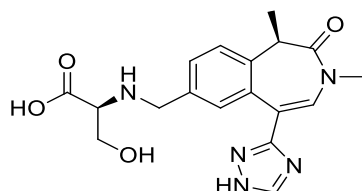
Tert-butyl (((*R*)-1,3-dimethyl-2-oxo-5-(1-((2-(trimethylsilyl)ethoxy)methyl)-1*H*-1,2,4-triazol-3-yl)-2,3-dihydro-1*H*-benzo[*d*]azepin-7-yl)methyl)-*L*-serinate [7.72]

(204 mg, 0.26 mmol) was dissolved in DCM (5 mL) under nitrogen at -78 °C. A 1 M solution of boron tribromide in DCM (0.5 mL, 0.5 mmol) was added and the reaction mixture was stirred 5 min at -78 °C and 15 min at rt. A 1 M solution of boron tribromide in DCM (0.5 mL, 0.5 mmol) was added at -78 °C and stirred for 10 min at this temperature. Then, the reaction mixture was stirred 15 min at rt. The reaction mixture was quenched with a saturated aqueous solution of sodium bicarbonate. The layers were separated and the aqueous layer was extracted with EtOAc. The organic layers were combined, dried through a phase separator and concentrated under reduced pressure to give the crude product [7.73]. The crude product was purified by two MDAP (high pH, extended method A, followed by high pH, extended method B). The relevant fraction was concentrated under reduced pressure to give the title product [7.73] as a colourless oil (5.8 mg, 5% yield).

¹H NMR (400 MHz, MeOD) δ 8.35 (br. s, 1H), 7.51 (dd, *J* = 8.3, 1.7 Hz, 1H), 7.39 (d, *J* = 8.3 Hz, 1H), 7.38 (s, 1H), 7.37 (br. s, 1H), 3.86 (d, *J* = 13.0 Hz, 1H), 3.73 (d, *J* = 13.0 Hz, 1H), 3.71 (dd, *J* = 11.0, 5.1 Hz, 1H), 3.66 (dd, *J* = 11.0, 5.1 Hz, 1H), 3.44 (q, *J* = 6.9 Hz, 1H), 3.24 (t, *J* = 5.1 Hz, 1H), 3.18 (s, 3H), 1.65 (d, *J* = 6.9 Hz, 3H), 1.42 (s, 9H). The exchangeable protons were not observed. LCMS (ESI, high pH) *t*_R = 0.76 min, *m/z* 428 [M+H]⁺.

Isolation and characterisation of the carboxylic acid by-product:

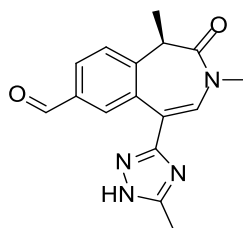
((*R*)-1,3-Dimethyl-2-oxo-5-(1*H*-1,2,4-triazol-3-yl)-2,3-dihydro-1*H*-benzo[*d*]azepin-7-yl)methyl)-*L*-serine



The aqueous layer was concentrated under reduced pressure to give a white solid. The solid was suspended in methanol and the solid was filtered. The filtrate was concentrated under reduced pressure to give a white solid, which was purified by MDAP (high pH, extended method A). The fractions were concentrated under reduced pressure to give the acid product as a white solid (18.5 mg, 18% yield).

¹H NMR (400 MHz, MeOD) δ 8.37 (s, 1H), 7.61 (dd, *J* = 8.3, 1.6 Hz, 1H), 7.55 (d, *J* = 1.6 Hz, 1H), 7.44 (s, 1H), 7.43 (d, *J* = 8.3 Hz, 1H), 4.15 (d, *J* = 13.0 Hz, 1H), 4.10 (d, *J* = 13.0 Hz, 1H), 3.92 (dd, *J* = 11.7, 4.2 Hz, 1H), 3.83 (dd, *J* = 11.7, 6.1 Hz, 1H), 3.48 (dd, *J* = 6.1, 4.2 Hz, 1H), 3.43 (q, *J* = 6.9 Hz, 1H), 3.15 (s, 3H), 1.62 (d, *J* = 6.9 Hz, 3H). The signals for the exchangeable protons were not observed. LCMS (ESI, high pH) *t*_R = 0.44 min, *m/z* 372 [M+H]⁺.

(R)-1,3-Dimethyl-5-(5-methyl-1H-1,2,4-triazol-3-yl)-2-oxo-2,3-dihydro-1H-benzo[d]azepine-7-carbaldehyde [7.74]

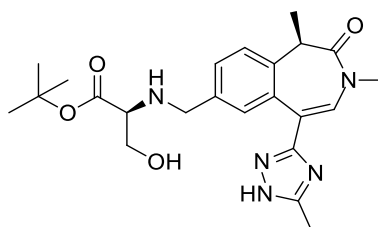


(R)-1,3-Dimethyl-5-(5-methyl-1-((2-(trimethylsilyl)ethoxy)methyl)-1H-1,2,4-triazol-3-yl)-2-oxo-2,3-dihydro-1H-benzo[d]azepine-7-carbaldehyde [7.52] (430 mg, 1.0 mmol) was dissolved in a 4 M solution of HCl in 1,4-dioxane (5 mL, 20.0 mmol) and heated at 40 °C for 3 h. The reaction mixture was concentrated under reduced pressure and dissolved in DMSO. The inorganics were filtered and half of the filtrate was purified by MDAP (formic, method A). The relevant fractions were concentrated under reduced pressure to give a yellow oil. The other half was purified by reverse phase column chromatography on C18 column, eluted with a gradient of 0-30% MeCN in a 10 mM aqueous solution of ammonium carbonate. The relevant fractions were concentrated under reduced pressure. The two purified products were combined to give the title product [7.74] as a yellow oil (169.6 mg, 46% yield).

¹H NMR (400 MHz, CDCl₃) δ 9.93 (s, 1H), 8.09 (d, *J* = 1.7 Hz, 1H), 7.89 (dd, *J* = 8.2, 1.7 Hz, 1H), 7.47 (d, *J* = 8.2 Hz, 1H), 7.44 (s, 1H), 3.43 (q, *J* = 6.9 Hz, 1H), 3.15 (s, 3H), 2.43 (s, 3H), 1.64 (d, *J* = 6.9 Hz, 3H). The exchangeable proton was not observed.

LCMS (ESI, high pH) *t*_R = 0.67 min, *m/z* 297 [M+H]⁺.

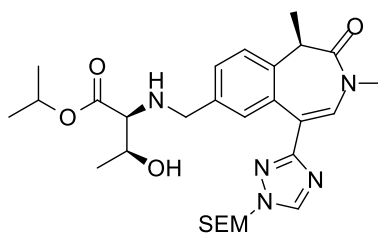
Tert-butyl (((R)-1,3-dimethyl-5-(5-methyl-1H-1,2,4-triazol-3-yl)-2-oxo-2,3-dihydro-1H-benzo[d]azepin-7-yl)methyl)-L-serinate [7.75]



Reductive amination general procedure B with aldehyde **[7.74]** (35 mg, 0.12 mmol) and *tert*-butyl *L*-serinate, hydrochloride **[7.11]** (35 mg, 0.18 mmol). The reaction mixture was quenched with methanol and concentrated under reduced pressure. The residue was partitioned between EtOAc and water. The organic layer was dried through a phase separator and concentrated under reduced pressure. The crude product was purified by MDAP (high pH, extended method B), the relevant fractions were concentrated under reduced pressure to give the title product **[7.75]** as a colourless oil (2.1 mg, 4% yield).

¹H NMR (400 MHz, MeOD) δ 7.50 (dd, $J = 8.3, 1.8$ Hz, 1H), 7.39 (br. s, 1H), 7.38 (d, $J = 8.3$ Hz 1H), 7.32 (s, 1H), 3.85 (d, $J = 13.1$ Hz, 1H), 3.70 (d, $J = 13.1$ Hz, 1H), 3.99 (dd, $J = 10.8, 5.1$ Hz, 1H), 3.65 (dd, $J = 10.8, 5.1$ Hz, 1H), 3.44 (q, $J = 6.9$ Hz, 1H), 3.21 (t, $J = 5.1$ Hz, 1H), 3.18 (s, 3H), 2.48 (s, 3H), 1.66 (d, $J = 6.9$ Hz, 3H), 1.44 (s, 9H). The three exchangeable protons were not observed. LCMS (ESI, high pH) $t_R = 0.78$ min, m/z 442 [M+H]⁺.

Isopropyl (((R)-1,3-dimethyl-2-oxo-5-(1-((2-(trimethylsilyloxy)methyl)-1H-1,2,4-triazol-3-yl)-2,3-dihydro-1H-benzo[d]azepin-7-yl)methyl)-L-allo-threoninate [7.78]

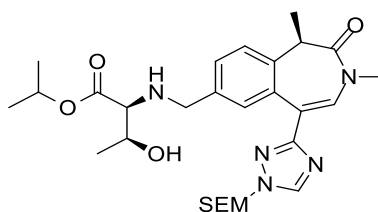


Reductive amination general procedure A2 with aldehyde [7.50] (262 mg, 0.64 mmol) and isopropyl *L-allo*-threoninate, hydrochloride [7.07] (188 mg, 0.95 mmol). The crude product was purified by silica column chromatography eluted with a gradient of 0-100% EtOAc in cyclohexane. The relevant fractions were concentrated under reduced pressure to give the title product [7.78] as a colourless oil (100.4 mg, 23% yield).

¹H NMR (400 MHz, CDCl₃) δ 8.23 (s, 1H), 7.68 (br. s, 1H), 7.48 (s, 1H), 7.36 (dd, *J* = 8.1, 1.2 Hz, 1H), 7.30 (d, *J* = 8.1 Hz, 1H), 5.50 (s, 2H), 5.06 (spt, *J* = 6.1 Hz, 1H), 3.96 (qd, *J* = 6.4, 4.4 Hz, 1H), 3.94 (d, *J* = 13.4 Hz, 1H), 3.66 (t, *J* = 7.9 Hz, 1H), 3.65 (t, *J* = 7.9 Hz, 1H), 3.62 (d, *J* = 13.4 Hz, 1H), 3.39 (q, *J* = 6.9 Hz, 1H), 3.31 (d, *J* = 4.4 Hz, 1H), 3.18 (s, 3H), 2.48 (br. s, 1H), 1.64 (d, *J* = 6.9 Hz, 3H), 1.24 (d, *J* = 6.1 Hz, 3H), 1.23 (d, *J* = 6.1 Hz, 3H), 1.05 (d, *J* = 6.4 Hz, 3H), 0.94 (t, *J* = 7.9 Hz, 2H), -0.01 (s, 9H). Presence of 13% of a diastereomer was calculated at signals 7.68 ppm (main product) and 7.60 ppm (diastereomer). One of the two exchangeable protons was not observed. LCMS (ESI, high pH) *t*_R = 1.25 min, *m/z* 558 [M+H]⁺.

Stereoselective synthesis of molecule [7.78]:

***Isopropyl* (((*R*)-1,3-dimethyl-2-oxo-5-(1-((2-(trimethylsilyl)ethoxy)methyl)-1*H*-1,2,4-triazol-3-yl)-2,3-dihydro-1*H*-benzo[*d*]azepin-7-yl)methyl)-*L-allo*-threoninate [7.78]**



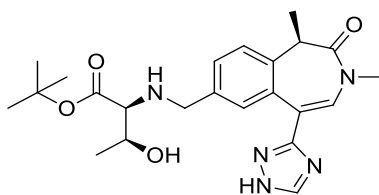
Isopropyl (((*R*)-5-bromo-1,3-dimethyl-2-oxo-2,3-dihydro-1*H*-benzo[*d*]azepin-7-yl)methyl)-*L*-allo-threoninate [**8.03**] (0.90 g, 2.06 mmol) was dissolved in 1,4-dioxane (6.9 mL). 4,4,4',4',5,5,5',5'-Octamethyl-2,2'-bi(1,3,2-dioxaborolane) (1.05 g, 4.12 mmol), dry KOAc (0.61 g, 6.17 mmol) and PdCl₂(dppf) (0.08 g, 0.10 mmol) were added and the reaction mixture was placed under nitrogen atmosphere by three cycles of vacuum-nitrogen. The reaction mixture was stirred at 80 °C for 2 h. The reaction mixture was filtered through celite and rinsed with acetone (10 mL). The filtrate was concentrated under reduced pressure to give the intermediate [**8.05**] as a crude black oil (2.59 g, 38% purity). LCMS (ESI, high pH) *t_R* = 1.22 min, *m/z* 487 [M+H]⁺. The LCMS also showed presence of molecule [**8.06**] (*t_R* = 0.94 min, *m/z* 361[M+H]⁺).

The crude intermediate isopropyl (((*R*)-1,3-dimethyl-2-oxo-5-(4,4,5,5-tetramethyl-1,3,2-dioxaborolan-2-yl)-2,3-dihydro-1*H*-benzo[*d*]azepin-7-yl)methyl)-*L*-allo-threoninate [**8.05**] (1.93 g, 38% purity, 1.51 mmol), 3-bromo-1-((2-(trimethylsilyl)ethoxy)methyl)-1*H*-1,2,4-triazole (0.84 g, 3.0 mmol), Pd Xphos G2 (0.12 g, 0.15 mmol), Xphos (0.14 g, 0.30 mmol), a 2 M aqueous solution of K₃PO₄ (2.3 mL, 4.52 mmol) were suspended in *i*PrOH (20 mL) and water (4 mL). The reaction mixture was placed under nitrogen atmosphere by three cycles of vacuum-nitrogen. The mixture was stirred at 90 °C for 1 h. The reaction mixture was cooled to rt and concentrated under reduced pressure to give a black oil. The residue was partitioned between DCM and water. The aqueous layer was extracted with DCM. The organic layers were combined, dried through a phase separator and concentrated under reduced pressure to give a brown oil. A 120 g silica column was conditioned with 3% NEt₃ in cyclohexane. The product, dissolved in DCM, was loaded onto the column and eluted with a gradient of 0-100% EtOAc in cyclohexane (containing 3% NEt₃). The relevant

fractions were concentrated under reduced pressure to give a yellow oil. A 120 g silica column was conditioned with 3% NEt₃ in cyclohexane. The product, dissolved in DCM, was loaded on the column and eluted with a gradient of 0-100% of solvent A (25% EtOH in EtOAc) in solvent B (cyclohexane containing 3% NEt₃). The relevant fractions were concentrated under reduced pressure to give the desired product **[7.78]** as a colourless oil (582.5 mg, 80% purity, 55% yield).

¹H NMR (400 MHz, MeOD) δ 8.64 (s, 1H), 7.48 (dd, *J* = 8.1, 1.6 Hz, 1H), 7.45 (d, *J* = 1.6 Hz, 1H), 7.42 (s, 1H), 7.35 (d, *J* = 8.1 Hz, 1H), 5.55 (s, 2H), 5.00 (spt, *J* = 6.4 Hz, 1H), 3.89 (qd, *J* = 6.4, 5.4 Hz, 1H), 3.83 (d, *J* = 13.1 Hz, 1H), 3.71 (t, *J* = 7.8 Hz, 2H), 3.62 (d, *J* = 13.1 Hz, 1H), 3.42 (q, *J* = 6.9 Hz, 1H), 3.17 (s, 3H), 3.10 (d, *J* = 5.4 Hz, 1H), 1.64 (d, *J* = 6.9 Hz, 3H), 1.22 (d, *J* = 6.4 Hz, 3H), 1.19 (d, *J* = 6.4 Hz, 3H), 1.16 (d, *J* = 6.4 Hz, 3H), 0.94 (t, *J* = 7.8 Hz, 1H), 0.93 (t, *J* = 7.8 Hz, 1H), -0.01 (s, 9H). The two exchangeable protons were not observed. LCMS (ESI, high pH) t_R = 1.23 min, *m/z* 558 [M+H]⁺.

Tert*-butyl (((*R*)-1,3-dimethyl-2-oxo-5-(1*H*-1,2,4-triazol-3-yl)-2,3-dihydro-1*H*-benzo[*d*]azepin-7-yl)methyl)-*L*-allo-threoninate **[7.79]*

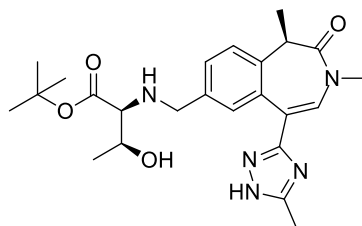


Reductive amination general procedure B with aldehyde **[7.71]** (120.4 mg, 0.34 mmol) and *tert*-butyl *L*-allo-threoninate, hydrochloride **[7.10]** (108 mg, 0.51 mmol) in a 20:1 *i*PrOH: AcOH ratio. The reaction mixture was quenched with methanol and concentrated under reduced pressure to give a yellow oil. The crude product was purified by MDAP (high pH, extended method B). The relevant fractions were

combined and concentrated under reduced pressure to give the title product as a colourless oil [7.79] (15.5 mg, 10% yield).

¹H NMR (400 MHz, MeOD) δ 8.36 (s, 1H), 7.50 (dd, J = 8.1, 1.2 Hz, 1H), 7.39 (d, J = 8.1 Hz, 1H), 7.37 (br. s, 2H), 3.91 (qd, J = 6.6, 4.9 Hz, 1H), 3.87 (d, J = 13.2 Hz, 1H), 3.71 (d, J = 13.2 Hz, 1H), 3.44 (q, J = 6.9 Hz, 1H), 3.18 (s, 3H), 3.14 (d, J = 4.9 Hz, 1H), 1.65 (d, J = 6.9 Hz, 3H), 1.42 (s, 9H), 1.16 (d, J = 6.6 Hz, 3H). The signals for the exchangeable protons were not observed. **¹³C NMR** (101 MHz, CDCl₃) δ 172.0 (C=O), 170.4 (C=O), 137.8 (C_{iv}), 137.0 (C_{iv}), 133.0 (C_{iv}), 132.4 (CH), 130.2 (CH), 127.4 (CH), 124.5 (CH), 117.1 (C_{iv}), 82.2 (CH), 67.3 (CH), 65.3 (CH), 52.1 (CH₂), 41.3 (CH), 35.7 (CH₃), 28.1 (CH₃), 18.4 (CH₃), 12.7 (CH₃). The signals for one methine and one C_{iv} were not observed. **LCMS** (ESI, high pH) t_R = 0.80 min, m/z 442 [M+H]⁺. **HRMS** (ESI) calculated for C₂₃H₃₂N₅O₄ [M+H]⁺ 442.2459, found 442.2454 (2.00 min). ν_{max} (solution in chloroform, cm⁻¹): 3460 (OH), 3129 (NH), 2976 (CH alkene), 2934 (CH alkane), 1727 (C=O ester), 1671 (C=O amide), 1629 (C=C). $[\alpha_D]^{24.6}$ °C_{589 nm} (c 0.500, MeOH): +136.9°.

***Tert*-butyl (((*R*)-1,3-dimethyl-5-(5-methyl-1*H*-1,2,4-triazol-3-yl)-2-oxo-2,3-dihydro-1*H*-benzo[*d*]azepin-7-yl)methyl)-*L*-allo-threoninate [7.80]**



Reductive amination general procedure B with aldehyde [7.74] (35 mg, 0.12 mmol) and *tert*-butyl *L*-allo-threoninate, hydrochloride [7.10] (37.5 mg, 0.18 mmol). Additional *tert*-butyl *L*-allo-threoninate, hydrochloride [7.10] (37.5 mg, 0.18 mmol) was added to the reaction mixture. The reaction mixture was quenched with methanol

and concentrated under reduced pressure to give a white residue. The residue was suspended in DMSO and methanol and filtered through a phase separator. The volatile solvent was removed under reduced pressure to give a solution of the crude product in DMSO. The crude product was purified by MDAP (high pH, extended method B), the relevant fractions were concentrated under reduced pressure to give the title product **[7.80]** as a white solid (2.7 mg, 5% yield).

¹H NMR (400 MHz, MeOD) δ 7.48 (dd, $J = 8.1, 1.7$ Hz, 1H), 7.37 (d, $J = 1.7$ Hz, 1H), 7.36 (d, $J = 8.1$ Hz, 1H), 7.30 (s, 1H), 3.86 (qd, $J = 6.4, 5.4$ Hz, 1H), 3.82 (d, $J = 13.1$ Hz, 1H), 3.64 (d, $J = 13.1$ Hz, 1H), 3.42 (q, $J = 7.0$ Hz, 1H), 3.17 (s, 3H), 3.04 (d, $J = 5.4$ Hz, 1H), 2.47 (s, 3H), 1.65 (d, $J = 7.0$ Hz, 3H), 1.42 (s, 9H), 1.15 (d, $J = 6.4$ Hz, 3H). The three exchangeable protons were not observed. **LCMS** (ESI, high pH) $t_R = 0.82$ min, m/z 456 $[M+H]^+$.

Impact of the nature of the acid counter ion and impact of the pH on the reductive amination yield and chiral centre racemisation (*cf.* Table 28 in section 8.2)

General procedure for entries 1-5:

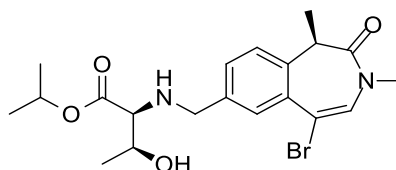
(*R*)-1,3-Dimethyl-2-oxo-5-(1-((2-(trimethylsilyl)ethoxy)methyl)-1*H*-1,2,4-triazol-3-yl)-2,3-dihydro-1*H*-benzo[*d*]azepine-7-carbaldehyde **[7.50]** (1 eq.), the amino ester (1.5 eq.), triethylamine (3 eq.) and the chosen acid (1 eq.) were suspended in THF (10 mL). 4 Å activated molecular sieves were added and the mixture was stirred at 50 °C. The reaction mixture was cooled to rt, sodium triacetoxyborohydride was added and the reaction mixture was stirred at rt. Additional sodium triacetoxyborohydride was added when necessary to complete the reduction of the imine. The reaction mixture was quenched with methanol, concentrated under reduced pressure and a 4 M solution

of HCl in 1,4-dioxane (10 mL, 40 mmol) was added to the residue. The reaction mixture was stirred until the deprotection was complete. The reaction mixture was concentrated under reduced pressure and purified. For entries 1, 3 and 4, the reverse phase column chromatographies were eluted with a gradient of 5-40% MeCN in a 10 mM aqueous solution of ammonium carbonate. NB: The d.e. was determined by ^1H NMR at the benzylic CH_2 doublet at 3.62 ppm (major diastereomer) and 3.64 ppm (minor diastereomer).

Entry	1	2	3	4	5
Parameter					
Aldehyde 7.50	50 mg 0.12 mmol	181 mg 0.44 mmol	181 mg 0.44 mmol	50 mg 0.12 mmol	50 mg 0.12 mmol
Isopropyl L- allo-threonine 7.07	29.3 mg 0.18 mmol	106 mg 0.66 mmol	as HCl salt 130 mg 0.66 mmol	29.3 mg 0.18 mmol	29.3 mg 0.18 mmol
Acid	PPTS 30.5 mg 0.12 mmol	AcOH 25 μ L 0.44 mmol	-	PTSA 23.1 mg 0.12 mmol	TFA 9 μ L 0.12 mmol
NEt₃	51 μ L 0.36 mmol	183 μ L 1.32 mmol	183 μ L 1.32 mmol	51 μ L 0.36 mmol	51 μ L 0.36 mmol
Measured pH	8.4	7.9	7.6	7.2	6.6
Imine formation	50 $^{\circ}$ C 19 h	50 $^{\circ}$ C 19 h	50 $^{\circ}$ C 24 h	50 $^{\circ}$ C 19 h	50 $^{\circ}$ C 19 h
NaBH(OAc)₃	200 mg 0.94 mmol	279 mg 1.32 mmol	279 mg 1.32 mmol	154 mg 0.73 mmol	200 mg 0.94 mmol
Reduction conditions	rt 5 h	rt 2 h	rt 2 h	rt 5 h	rt 5 h
Deprotection conditions	40 $^{\circ}$ C 1 h, rt, 17 h	40 $^{\circ}$ C 3 h, rt, 18 h	rt, 2 h, 40 $^{\circ}$ C 2 h	40 $^{\circ}$ C 1 h, rt, 17 h	40 $^{\circ}$ C 3 h, rt, 18 h
Purification	C18 column chromatog raphy	MDAP high pH extended method B	C18 column chromatog raphy, MDAP method B high pH	C18 column chromatog raphy	MDAP high pH extended method B
Yield d.e. (% determined by ¹H NMR)	33% 80%	24% with d.e. 80% + 8% of a different diastereom eric mixture with a d.e. 80%	15% in two batches 80%	41% 80%	49% in two batches 80%

Stereoselective preparation of:

Isopropyl (((R)-5-bromo-1,3-dimethyl-2-oxo-2,3-dihydro-1H-benzo[d]azepin-7-yl)methyl)-L-allo-threoninate [8.03]



(*R*)-5-Bromo-1,3-dimethyl-2-oxo-2,3-dihydro-1*H*-benzo[*d*]azepine-7-carbaldehyde [6.06] (1 g, 3.40 mmol) and *isopropyl L-allo*-threonine [7.07] (0.82 g, 5.10 mmol) were dissolved in THF (10 mL) and activated 4 Å molecular sieves were added. To the solution were added trifluoroacetic acid (0.025 mL, 0.32 mmol) and four drops of triethylamine. The pH was measured at 5.8 with a pH meter and the reaction mixture was stirred at 50 °C for 18 h. The reaction mixture was cooled to rt and sodium triacetoxyborohydride (2.16 g, 10.20 mmol) was added portion-wise. The reaction mixture was stirred under nitrogen at rt for 4 h. The reaction mixture was quenched with MeOH and concentrated under reduced pressure. The resulting residue was partitioned between EtOAc and water. The aqueous layer was extracted with twice with EtOAc. The organic layers were combined, dried through a hydrophobic frit and concentrated under reduced pressure to give a yellow oil. The crude product was purified by silica column chromatography, eluted with a gradient of 0-100% EtOAc in cyclohexane. The relevant fractions were combined and concentrated under reduced pressure to give the title product [8.03] as a pale yellow oil (1.33 g, 85% yield).

¹H NMR (400 MHz, MeOD) δ 7.71 (d, *J* = 1.3 Hz, 1H), 7.48 (dd, *J* = 8.1, 1.3 Hz, 1H), 7.29 (d, *J* = 8.1 Hz, 1H), 7.04 (s, 1H), 5.03 (spt, *J* = 6.4 Hz, 1H), 3.90 (td, *J* = 6.4, 5.7 Hz, 1H), 3.87 (d, *J* = 13.2 Hz, 1H), 3.70 (d, *J* = 13.2 Hz, 1H), 3.39 (q, *J* = 6.9 Hz, 1H), 3.11 (d, *J* = 5.7 Hz, 1H), 3.05 (s, 3H), 1.61 (d, *J* = 6.9 Hz, 3H), 1.25 (d, *J* = 6.4 Hz,

3H), 1.24 (d, $J = 6.4$ Hz, 3H), 1.21 (d, $J = 6.4$ Hz, 3H). The two exchangeable protons were not observed. ^{13}C NMR (101 MHz, MeOD) δ 174.4 (C=O), 172.1 (C=O), 140.0 (C_{iv}), 137.5 (C_{iv}), 135.8 (C_{iv}), 132.7 (CH), 132.1 (CH), 129.5 (CH), 125.1 (CH), 113.3 (C_{iv}), 69.9 (CH), 69.8 (CH), 67.9 (CH), 52.6 (CH_2), 42.2 (CH), 35.4 (CH_3), 22.4 (CH_3), 22.3 (CH_3), 20.3 (CH_3), 13.2 (CH_3). LCMS (ESI, formic) $t_{\text{R}} = 0.61$ min, m/z 439/441 $[\text{M}+\text{H}]^+$. Analytical chiral HPLC (Chiralpak AD-H column, 25 cm, rt, 15% EtOH in heptane containing 0.1% $i\text{PrNH}_2$, injection volume 3 μL) $t_{\text{R}} = 12.43$ min, 100% e.e. (N.B. epimer at the α -position is at $t_{\text{R}} = 13.99$ min under these conditions). HRMS (ESI) calculated for $\text{C}_{20}\text{H}_{28}\text{BrN}_2\text{O}_4$ $[\text{M}+\text{H}]^+$ 439.1229, found 439.1236 (2.65 min). ν_{max} (solution in chloroform, cm^{-1}): 3449 (OH), 3328 (NH), 2979 (CH alkene), 2934 (CH alkane), 1723 (C=O ester), 1667 (C=O amide), 1622 (C=C). $[\alpha]_{\text{D}}^{23.6}$ $^{\circ}\text{C}$ $_{589\text{ nm}}$ (c 0.500, MeOH): +8.9 $^{\circ}$.

Optimisation of the reaction conditions to obtain [8.04] by reductive amination with isopropyl serine performed on the aldehyde [6.06] (cf. Table 29 in section

8.2)

General procedure for entries 1-3:

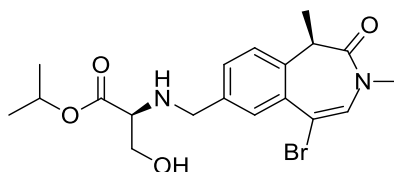
(*R*)-1,3-Dimethyl-2-oxo-5-(1-((2-(trimethylsilyl)ethoxy)methyl)-1*H*-1,2,4-triazol-3-yl)-2,3-dihydro-1*H*-benzo[*d*]azepine-7-carbaldehyde [7.50], the amino ester [7.08], triethylamine and the chosen acid were suspended in THF. 4 Å molecular sieves were added and the mixture was stirred at the chosen temperature. The reaction mixture was cooled to rt (for entries 1 and 2), sodium triacetoxyborohydride was added and the reaction mixture was stirred at rt. The reaction mixture was quenched with methanol and filtered through celite to remove the molecular sieves. The filtrate was concentrated under reduced pressure and partitioned between EtOAc and water (with

addition of a 1 M aqueous solution of LiCl to help phase separation if required). The aqueous layer was extracted with EtOAc. The organic layers were combined, dried through a hydrophobic frit, concentrated under reduced pressure and purified.

Entry Parameter	1	2	3
Aldehyde 6.06	50 mg 0.17 mmol	50 mg 0.17 mmol	60 mg 0.20 mmol
Amino ester	<i>L</i> -serine 40.0 mg 0.27 mmol	<i>D</i> -serine 37.5 mg 0.26 mmol	<i>L</i> -serine.TsOH 81 mg 0.25 mmol
TFA	13 μ L 0.17 mmol	13 μ L 0.17 mmol	Until the desired pH
NEt₃	71 μ L 0.51 mmol	71 μ L 0.51 mmol	Until the desired pH
Measured pH	5.9	6.1	6.5
Imine formation	50 °C 17 h	50 °C 2.5 h	rt 20 h
NaBH(OAc)₃	144 mg 0.68 mmol	162 mg 0.77 mmol	260 mg 1.2 mmol
Reduction conditions	rt 4.25 h	rt 18.7 h	rt 3 h
Purification	MDAP (high pH extended method C)	MDAP (high pH extended method C)	MDAP (high pH extended method C)
Yield d.e. (% determined by chiral HPLC)	66% (53 mg) 58%	57% (46 mg) 82%	51% (46 mg) 98%
Physical form	Colourless oil	White solid	Pale yellow oil

Stereoselective preparation of molecule [8.04]

Isopropyl (((*R*)-5-bromo-1,3-dimethyl-2-oxo-2,3-dihydro-1*H*-benzo[*d*]azepin-7-yl)methyl)-*L*-serinate [8.04] (Table 29 in section 8.2, entry 4)



(*R*)-5-Bromo-1,3-dimethyl-2-oxo-2,3-dihydro-1*H*-benzo[*d*]azepine-7-carbaldehyde [6.06] (754 mg, 2.56 mmol) and isopropyl *L*-serinate, 4-methylbenzenesulfonic acid salt [7.08] (1.23 g, 3.85 mmol) were dissolved in THF (10 mL). Activated 4 Å molecular sieves were added to the reaction mixture and the pH was measured at 2.0. NEt₃ was added dropwise to the reaction mixture until reaching pH 5.9. The reaction mixture was left to stir at rt for 24 h. Sodium triacetoxyborohydride (1.63 g, 7.69 mmol) was added portion-wise and the reaction mixture was stirred under nitrogen at rt for 30 min. The reaction mixture was quenched with MeOH and filtered through celite. The filtrate was concentrated under reduced pressure to give a pale yellow oil. The crude product was partitioned between EtOAc and water. The aqueous layer was extracted with EtOAc twice. The organic layers were combined, dried through a hydrophobic frit and concentrated under reduced pressure to give a yellow oil. The crude product was purified by silica column chromatography, eluted with a gradient of 0-100% EtOAc in cyclohexane. The relevant fractions were concentrated under reduced pressure to give a pale yellow oil. The oil was suspended in diethyl ether and a white solid precipitated. The solid was filtered and the filtrate was concentrated under reduced pressure to give a yellow oil. This oil was purified by silica column chromatography, eluted with a gradient of 0-100% EtOAc in cyclohexane. The

relevant fractions were concentrated under reduced pressure to give the title product **[8.04]** as a colourless oil (825.6 mg, 72% yield).

¹H NMR (400 MHz, MeOD) δ 7.72 (d, $J = 1.7$ Hz, 1H), 7.50 (dd, $J = 8.1, 1.7$ Hz, 1H), 7.30 (d, $J = 8.1$ Hz, 1H), 7.05 (s, 1H), 5.02 (spt, $J = 6.4$ Hz, 1H), 3.89 (d, $J = 13.0$ Hz, 1H), 3.76 (d, $J = 13.0$ Hz, 1H), 3.75 (dd, $J = 10.8, 5.1$ Hz, 1H), 3.71 (dd, $J = 10.8, 5.1$ Hz, 1H), 3.40 (q, $J = 6.9$ Hz, 1H), 3.29 (d, $J = 5.1$ Hz, 1H), 3.05 (s, 3H), 1.61 (d, $J = 6.9$ Hz, 3H), 1.25 (d, $J = 6.4$ Hz, 6H). The two exchangeable protons were not observed. No traces of diastereomeric impurities were observed by ¹H NMR or separated from the column chromatography. **¹³C NMR** (101 MHz, MeOD) δ 174.1 (C=O), 172.1 (C=O), 139.9 (C_{iv}), 137.6 (C_{iv}), 135.9 (C_{iv}), 132.7 (CH), 132.1 (CH), 129.6 (CH), 125.2 (CH), 113.2 (C_{iv}), 70.1 (CH), 64.1 (CH), 63.7 (CH₂), 52.4 (CH₂), 42.2 (CH), 35.4 (CH₃), 22.3 (CH₃), 22.2 (CH₃), 13.2 (CH₃). **LCMS** (ESI, high pH) $t_R = 1.01$ min, m/z 425/427 [M+H]⁺. **HRMS** (ESI) calculated for C₁₉H₂₆BrN₂O₄ [M+H]⁺ 425.1079, found 425.1078 (2.48 min). ν_{max} (solution in chloroform, cm⁻¹): 3454 (OH), 3333 (NH), 2980 (CH alkene), 2934 (CH alkane), 1725 (C=O ester), 1664 (C=O amide), 1626 (C=C). $[\alpha_D]^{23.9}_{589\text{ nm}}$ (c 0.500, MeOH): +16.8°.

Trial Suzuki cross-coupling reactions – Table 30, section 8.3, p.159

The pinacol boronic ester **[8.05]** was prepared following the procedure described p.296. The analysis of intermediate **[7.78]** and molecule **[7.38]** were reported respectively p.294-297 and p.257-259.

Procedure for entries 1-2:

Isopropyl (((*R*)-1,3-dimethyl-2-oxo-5-(4,4,5,5-tetramethyl-1,3,2-dioxaborolan-2-yl)-2,3-dihydro-1*H*-benzo[*d*]azepin-7-yl)methyl)-*L*-allo-threoninate **[8.05]** (88 mg, 0.18 mmol), 3-bromo-1-((2-(trimethylsilyl)ethoxy)methyl)-1*H*-1,2,4-triazole **[7.59]** (135

mg, 0.49 mmol), Pd Xphos G2 (18 mg, 0.02 mmol), Xphos (5.5 mg, 0.01 mmol), a 2 M aqueous solution of K₃PO₄ (0.44 mL, 0.88 mmol) were suspended in 1,4-dioxane (4 mL) and water (1 mL). The reaction mixture was placed under nitrogen atmosphere by three cycles of vacuum-nitrogen. The reaction mixture was stirred at the temperature and for the time indicated below. The reaction mixture was concentrated under reduced pressure to give a black residue. The residue was partitioned between EtOAc and water. The aqueous layer was extracted with EtOAc. The organic layers were combined, dried through a phase separator and concentrated under reduced pressure to give a brown oil. The oil was purified by MDAP (TFA, extended method B). The relevant fractions were concentrated under reduced pressure to give *isopropyl* (((*R*)-1,3-dimethyl-2-oxo-5-(1-((2-(trimethylsilyl)ethoxy)methyl)-1*H*-1,2,4-triazol-3-yl)-2,3-dihydro-1*H*-benzo[*d*]azepin-7-yl)methyl)-*L*-allo-threoninate [7.78] as a pale yellow oil. The product was stirred in a 4 M HCl solution in 1,4-dioxane (5 mL) overnight at rt. The reaction mixture was concentrated under reduced pressure to give a yellow oil. The crude product was purified by MDAP (high pH, extended method B). The relevant fractions were concentrated under reduced pressure to give *isopropyl* (((*R*)-1,3-dimethyl-2-oxo-5-(1*H*-1,2,4-triazol-3-yl)-2,3-dihydro-1*H*-benzo[*d*]azepin-7-yl)methyl)-*L*-allo-threoninate [7.38] as a colourless oil.

Entry 1: Reaction: at room temperature, reaction time 30 h. Intermediate [7.78] (35.5 mg, 30% yield). Product [7.38] (19.6 mg, 24% yield).

Entry 2: 2 M aqueous solution of K₃PO₄ (0.27 mL, 0.54 mmol) were used in the reaction mixture. Temperature: 70 °C, reaction time: 24 h. Intermediate [7.78] (41.5 mg, 35% yield). Product [7.38] (14.1 mg, 16% yield).

Entry 3: Reaction at 120 °C, reaction time 3.5 h.

Isopropyl (((*R*)-1,3-dimethyl-2-oxo-5-(4,4,5,5-tetramethyl-1,3,2-dioxaborolan-2-yl)-2,3-dihydro-1*H*-benzo[*d*]azepin-7-yl)methyl)-*L*-allo-threoninate [8.05] (88 mg, 0.18 mmol), 3-bromo-1-((2-(trimethylsilyl)ethoxy)methyl)-1*H*-1,2,4-triazole [7.59] (135 mg, 0.49 mmol), Pd Xphos G2 (18 mg, 0.02 mmol), Xphos (5.5 mg, 0.01 mmol), a 2 M aqueous solution of K₃PO₄ (0.44 mL, 0.88 mmol) were suspended in 1,4-dioxane (4 mL) and water (1 mL). The reaction mixture was placed under nitrogen atmosphere by three cycles of vacuum-nitrogen. The reaction mixture was stirred at 120 °C for 3.5 h. The reaction mixture was concentrated under reduced pressure to give a black residue. The residue was partitioned between EtOAc and water. The aqueous layer was extracted with EtOAc. The organic layers were combined, dried through a phase separator and concentrated under reduced pressure to give isopropyl (((*R*)-1,3-dimethyl-2-oxo-5-(1-((2-(trimethylsilyl)ethoxy)methyl)-1*H*-1,2,4-triazol-3-yl)-2,3-dihydro-1*H*-benzo[*d*]azepin-7-yl)methyl)-*L*-allo-threoninate [7.78] as a crude brown oil. The oil was loaded on a silica column, eluted with a gradient of 0-100% EtOAc in cyclohexane, followed by a gradient of 0-25% EtOH in EtOAc. The product did not elute.

Entry 4 is the stereoselective synthesis of molecule [7.38] p.259.

Trial deprotection reactions – Table 31, section 8.3, p.161

Entry 1 was reported p.257 (as part of the synthesis of molecule [7.38]).

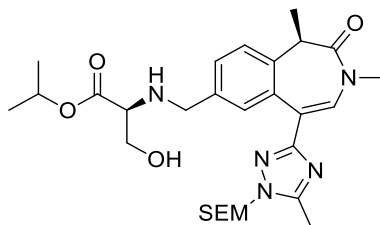
Entry 2 was reported p.257 (synthesis of molecule [7.38]).

Entry 3 was reported p.289 (synthesis of molecule [7.71]).

Entry 4 was reported p.259 (as part of the stereoselective synthesis of molecule [7.38]).

Stereoselective synthesis of molecule [8.07]:

Isopropyl (((*R*)-1,3-dimethyl-5-(5-methyl-1-((2-(trimethylsilyl)ethoxy)methyl)-1*H*-1,2,4-triazol-3-yl)-2-oxo-2,3-dihydro-1*H*-benzo[*d*]azepin-7-yl)methyl)-*L*-serinate [8.07]



Isopropyl (((*R*)-5-bromo-1,3-dimethyl-2-oxo-2,3-dihydro-1*H*-benzo[*d*]azepin-7-yl)methyl)-*L*-serinate [8.04] (90 mg, 0.21 mmol) was dissolved in 1,4-dioxane (45 mL). B₂Pin₂ (107 mg, 0.42 mmol), dry KOAc (62.3 mg, 0.64 mmol) and PdCl₂(dppf) (7.7 mg, 10.6 μmol) were added and the reaction mixture was placed under nitrogen atmosphere by three cycles of vacuum-nitrogen. The reaction mixture was stirred at 80 °C for 2 h. The reaction mixture was filtered through celite and rinsed with acetone (10 mL). The filtrate was concentrated under reduced pressure to give isopropyl (((*R*)-1,3-dimethyl-2-oxo-5-(4,4,5,5-tetramethyl-1,3,2-dioxaborolan-2-yl)-2,3-dihydro-1*H*-benzo[*d*]azepin-7-yl)methyl)-*L*-serinate [8.08] as a crude black oil (100 mg). LCMS (ESI, high pH) t_R = 1.15 min, m/z 473 [M+H]⁺.

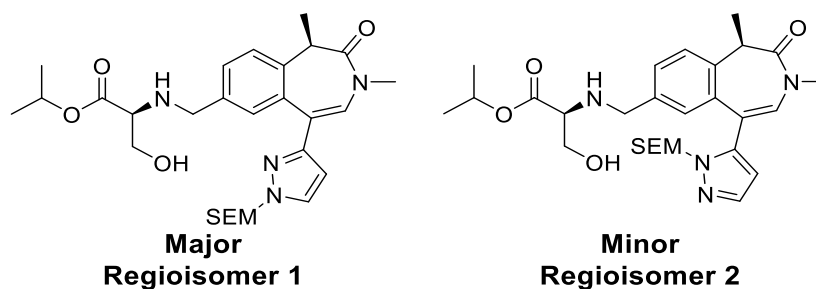
The crude material isopropyl (((*R*)-1,3-dimethyl-2-oxo-5-(4,4,5,5-tetramethyl-1,3,2-dioxaborolan-2-yl)-2,3-dihydro-1*H*-benzo[*d*]azepin-7-yl)methyl)-*L*-serinate [8.08] (100 mg, 0.21 mmol), 3-bromo-5-methyl-1-((2-(trimethylsilyl)ethoxy)methyl)-1*H*-1,2,4-triazole [7.60] (124 mg, 0.42 mmol) Pd Xphos G2 (16.7 mg, 0.02 mmol), Xphos (20.2 mg, 0.04 mmol), a 2 M aqueous solution of K₃PO₄ (0.32 mL, 0.64 mmol) were suspended in *i*PrOH (40 mL) and water (8 mL). The reaction mixture was placed under nitrogen atmosphere by three cycles vacuum-nitrogen. The mixture was stirred at 90

°C for 1.5 h. The reaction mixture was cooled to rt and concentrated under reduced pressure to give a black oil. The residue was partitioned between DCM and water. The aqueous layer was extracted with DCM. The organic layers were combined, dried through a phase separator and concentrated under reduced pressure to give a brown oil. The crude product was split in two fractions. Batch 1 was purified by MDAP (formic extended method B). The relevant fraction was concentrated under reduced pressure to give the title product [**8.07**] as a colourless oil (24.8 mg, 17% yield). Batch 2 was purified by MDAP (high pH, extended method C). The relevant fraction was concentrated under reduced pressure to give the title product [**8.07**] as a pale brown oil (18 mg, 65% pure, 10% yield).

¹H NMR (400 MHz, MeOD) δ 8.24 (s, 2H), 7.58 (d, $J = 8.1$ Hz, 1H), 7.47 (d, $J = 8.1$ Hz, 1H), 7.16 (s, 1H), 7.10 (s, 1H), 5.30 (d, $J = 11.3$ Hz, 1H), 5.09 (d, $J = 11.3$ Hz, 1H), 5.04 (spt, $J = 6.4$ Hz, 1H), 4.02 (d, $J = 13.2$ Hz, 1H), 3.95 (d, $J = 13.2$ Hz, 1H), 3.83 (d, $J = 4.4$ Hz, 1H), 3.82 (d, $J = 4.4$ Hz, 1H), 3.60 (t, $J = 4.4$ Hz, 1H), 3.55 (q, $J = 6.9$ Hz, 1H), 3.53 (t, $J = 7.7$ Hz, 2H), 3.19 (s, 3H), 2.41 (s, 3H), 1.69 (d, $J = 6.9$ Hz, 3H), 1.25 (d, $J = 6.4$ Hz, 3H), 1.23 (d, $J = 6.4$ Hz, 3H), 0.81 (t, $J = 7.7$ Hz, 2H), -0.04 (m, 9H). NMR showed presence of 15% of a SEM regioisomer, determined at the methyl signal at 3.19 ppm (major regioisomer) and 3.16 ppm (minor regioisomer).
LCMS (ESI, high pH) $t_R = 1.18$ min, m/z 558 [M+H]⁺.

Stereoselective synthesis of molecule [8.09]:

Isopropyl (((R)-1,3-dimethyl-2-oxo-5-(1-((2-(trimethylsilyl)ethoxy)methyl)-1H-pyrazol-3-yl)-2,3-dihydro-1H-benzo[d]azepin-7-yl)methyl)-L-serinate
and *isopropyl (((R)-1,3-dimethyl-2-oxo-5-(1-((2-(trimethylsilyl)ethoxy)methyl)-1H-pyrazol-5-yl)-2,3-dihydro-1H-benzo[d]azepin-7-yl)methyl)-L-serinate* [8.09]



The procedure to synthesize *isopropyl (((R)-1,3-dimethyl-2-oxo-5-(4,4,5,5-tetramethyl-1,3,2-dioxaborolan-2-yl)-2,3-dihydro-1H-benzo[d]azepin-7-yl)methyl)-L-serinate* [8.08], was described as part of the stereoselective synthesis of molecule [8.07], p.309.

Isopropyl (((R)-1,3-dimethyl-2-oxo-5-(4,4,5,5-tetramethyl-1,3,2-dioxaborolan-2-yl)-2,3-dihydro-1H-benzo[d]azepin-7-yl)methyl)-L-serinate [8.08] (227.5 mg, 0.48 mmol), the mixture of regioisomers [7.55] (267 mg, 0.96 mmol), Pd Xphos G2 (37.9 mg, 0.05 mmol), Xphos (45.9 mg, 0.1 mmol), a 2 M aqueous solution of K_3PO_4 (0.72 mL, 1.45 mmol) were suspended in *i*PrOH (8 mL) and water (2.0 mL). The reaction mixture was placed under nitrogen atmosphere by 3 cycle vacuum-nitrogen. The mixture was stirred at 90 °C for 2 h. The reaction mixture was cooled to rt and concentrated under reduced pressure to give a brown oil. The residue was partitioned between EtOAc and water. The aqueous layer was extracted with EtOAc. The organic layers were combined, dried through a phase separator and concentrated under reduced pressure to give a brown oil. The crude product was purified on silica column

chromatography, preconditioned with cyclohexane (containing 3% NEt₃), eluted with a gradient of 0-100% EtOAc in cyclohexane (containing 3% NEt₃). The relevant fractions were concentrated under reduced pressure to give the title product [**8.09**] as a colourless oil (47.7 mg, 16% yield), as a mixture of regioisomers in a 57:43 ratio. This ratio was determined from the signals of the methyl in α -position of the amide carbonyl functionality. A second fraction of the desired product was also obtained and was further purified by MDAP (formic, extended method B) to separate the regioisomers. The relevant fractions of the MDAP were concentrated under reduced pressure to give two colourless oils: regioisomer 1 (12.6 mg, 5% yield) and regioisomer 2 (11.4 mg, 3% yield).

Regioisomer 1: ¹H NMR (400 MHz, MeOD) δ 7.81 (d, J = 2.5 Hz, 1H), 7.48 (dd, J = 8.2, 1.7 Hz, 1H), 7.36 (d, J = 8.2 Hz, 1H), 7.32 (d, J = 1.7 Hz, 1H), 7.06 (s, 1H), 6.43 (d, J = 2.5 Hz, 1H), 5.45 (s, 2H), 4.99 (spt, J = 6.4 Hz, 1H), 3.83 (d, J = 13.2 Hz, 1H), 3.69 (dd, J = 5.1, 2.7 Hz, 2H), 3.68 (d, J = 13.2 Hz, 1H), 3.65 (d, J = 8.3 Hz, 1H), 3.63 (d, J = 8.3 Hz, 1H), 3.43 (q, J = 6.9 Hz, 1H), 3.27 (t, J = 5.1 Hz, 1H), 3.14 (s, 3H), 1.64 (d, J = 6.9 Hz, 3H), 1.21 (d, J = 6.4 Hz, 3H), 1.20 (d, J = 6.4 Hz, 3H), 0.93 (d, J = 8.3 Hz, 1H), 0.92 (d, J = 8.3 Hz, 1H), 0.00 (s, 9H). The signals for the exchangeable protons were not observed. ¹³C NMR (101 MHz, MeOD) δ 173.8 (C=O), 172.6 (C=O), 153.0 (C_{iv}), 138.5 (C_{iv}), 138.1 (C_{iv}), 135.9 (C_{iv}), 133.2 (CH), 131.0 (CH), 130.4 (CH), 129.6 (CH), 125.0 (CH), 124.6 (C_{iv}), 107.8 (CH), 81.2 (CH₂), 70.1 (CH), 67.8 (CH₂), 63.9 (CH₂), 63.4 (CH), 52.4 (CH₂), 42.3 (CH), 35.7 (CH₃), 22.3 (CH₃), 22.2 (CH₃), 18.8 (CH₂), 13.2 (CH₃), -1.1 (CH₃). LCMS (ESI, high pH) t_R = 1.27 min, m/z 543 [M+H]⁺. HRMS (ESI) calculated for C₂₈H₄₃N₄O₅Si [M+H]⁺ 543.2999, found 543.2997 (3.92 min). ν_{max} (solution in chloroform, cm⁻¹): 3349 (OH), 3333 (NH), 2976

(CH alkene), 2938 (CH alkane), 1727 (C=O ester), 1663 (C=O amide), 1626 (C=C).
[α D]^{24.6 °C}_{589 nm} (c 0.500, MeOH): +97.9°. **Regioisomer 2:** ¹H NMR (400 MHz, MeOD)
 δ 7.62 (d, J = 1.8 Hz, 1H), 7.56 (dd, J = 8.3, 1.5 Hz, 1H), 7.44 (d, J = 8.3 Hz, 1H), 7.05
(d, J = 1.5 Hz, 1H), 6.92 (s, 1H), 6.57 (d, J = 1.8 Hz, 1H), 5.21 (d, J = 11.1 Hz, 1H),
5.02 (qd, J = 6.4, 6.1 Hz, 1H), 4.96 (d, J = 11.1 Hz, 1H), 3.97 (d, J = 13.2 Hz, 2H),
3.92 (d, J = 13.2 Hz, 1H), 3.86 (d, J = 5.6 Hz, 1H), 3.79 (d, J = 4.4 Hz, 1H), 3.56 (q, J
= 7.0 Hz, 1H), 3.54 (td, J = 5.6, 4.4 Hz, 1H), 3.41 (d, J = 8.0 Hz, 1H), 3.37 (d, J = 8.0
Hz, 1H), 3.15 (s, 3H), 1.68 (d, J = 7.0 Hz, 3H), 1.24 (d, J = 6.4 Hz, 3H), 1.22 (d, J =
6.1 Hz, 3H), 0.73 (t, J = 8.0 Hz, 2H), -0.07 (s, 9H). **LCMS** (ESI, high pH) t_R = 1.26
min, m/z 543 [M+H]⁺.

References

- 1 Chaudhari, K.; Rizvi, S.; Syed, B. A. *Nat. Rev. Drug Discov.* **2016**, *15*, 305–306.
- 2 McInnes, I. B.; Schett, G. N. *Engl. J. Med.* **2011**, *365*, 2205–2219.
- 3 Wada, T. T.; Araki, Y.; Sato, K.; Aizaki, Y.; Yokota, K.; Kim, Y. T.; Oda, H.; Kurokawa, R.; Mimura, T. *Biochem. Biophys. Res. Commun.* **2014**, *444*, 682–686.
- 4 Haringman, J. J.; Gerlag, D. M.; Zwinderman, A. H.; Smeets, T. J. M.; Kraan, M. C.; Baeten, D.; McInnes, I. B.; Bresnihan, B.; Tak, P. P. *Ann. Rheum. Dis.* **2005**, *64*, 834–838.
- 5 Fujiwara, N.; Kobayashi, K. *Curr. Drug Targets: Inflammation Allergy* **2005**, *4*, 281–286.
- 6 Qiao, Y.; Ivashkiv, L. B. *Inflammation Cell Signaling*, **2015**, *1*, 1–5.
- 7 Meng, S.; Zhang, L.; Tang, Y.; Tu, Q.; Zheng, L.; Yu, L.; Murray, D.; Cheng, J.; Kim, S. H.; Zhou, X.; Chen, J. *J. Dent. Res.* **2014**, *93*, 657–662.
- 8 Tough, D. F.; Tak, P. P.; Tarakhovsky, A.; Prinjha, R. K. *Nat. Rev. Drug Discov.* **2016**, *15*, 835–853.
- 9 Keating, S. T.; Plutzky, J.; El-Osta, A. *Circ. Res.* **2016**, *118*, 1706–1722.
- 10 Miller, T. C.; Simon, B.; Rybin, V.; Grötsch, H.; Curtet, S.; Khochbin, S.; Carlomagno, T.; Müller, C. W. *Nat. Commun.* **2016**, *7*, 1–13.
- 11 Verdin, E.; Ott, M. *Nat. Rev. Mol. Cell Biol.* **2015**, *16*, 258–264.
- 12 Padmanabhan, B.; Mathur, S.; Manjula, R.; Tripathi, S. *J. Biosci.* **2016**, *41*, 295–311.
- 13 Bamborough, P.; Chung, C. *Med. Chem. Commun.* **2015**, *6*, 1587–1604.
- 14 Filippakopoulos, P.; Picaud, S.; Mangos, M.; Keates, T.; Lambert, J.; Barsyte-lovejoy, D.; Felletar, I.; Volkmer, R.; Mu, S.; Pawson, T.; Gingras, A.; Arrowsmith, C. H.; Knapp, S. *Cell*, **2012**, *149*, 214–231.
- 15 Doroshow, D. B.; Eder, J. P.; LoRusso, P. M. *Ann. Oncol.* **2017**, *28*, 1776–1787.
- 16 Wadhwa, E.; Nicolaidis, T. *Cureus*, **2016**, *8*, e620.

-
- 17** Lee, D. U.; Katavolos, P.; Palanisamy, G.; Katewa, A.; Sioson, C.; Corpuz, J.; Pang, J.; DeMent, K.; Choo, E.; Ghilardi, N.; Diaz, D.; Danilenko, D. M. *Toxicol. Appl. Pharmacol.* **2016**, *300*, 47–54.
- 18** Wang, Q.; Li, Y.; Xu, J.; Wang, Y.; Leung, E. L. H.; Liu, L.; Yao, X. *Sci. Rep.* **2017**, *7*, 1–11.
- 19** Nicholls, S. J.; Puri, R.; Wolski, K.; Ballantyne, C. M.; Barter, P. J.; Brewer, H. B.; Kastelein, J. J. P.; Hu, B.; Uno, K.; Kataoka, Y.; Herrman, J. P. R.; Merkely, B.; Borgman, M.; Nissen, S. E. *Am. J. Cardiovasc. Drugs*, **2016**, *16*, 55–65.
- 20** Needham, L.; Davidson, A. H.; Bawden, L. J.; Belfield, A.; Bone, E.; Brotherton, D. H.; Bryant, S.; Charlton, M. H.; Clark, V. L.; Davies, S. J.; Donald, A.; Day, F.; Krige, D.; Legris, V.; McDermott, J.; McGovern, Y.; Owen, J.; Patel, S. R.; Pintat, S.; Testar, R. J.; Wells, G. M.; Moffat, D.; Drummond, A. H. *J. Pharmacol. Exp. Ther.* **2011**, *339*, 132–142.
- 21** Mander, P.; Brown, J.; Boardely, R.; Chung, C. W.; Ramirez-Molina, C.; Beaumont, D.; Lewis, H.; Brant, C.; Molnar, J.; Kendrick, S.; Skouteris, G.; Fowler, G. Unpublished results, GSK, **2016**.
- 22** Waring, M. J.; Arrowsmith, J.; Leach, A. R.; Leeson, P. D.; Mandrell, S.; Owen, R. M.; Pairedeau, G.; Pennie, W. D.; Pickett, S. D.; Wang, J.; Wallace, O.; Weir, A. *Nat. Rev. Drug Discov.* **2015**, *14*, 475–486.
- 23** Wang, S.; Ran, X.; Zhao, Y.; Yang, C.; Liu, L.; Bai, L.; Mceachern, D.; Stuckey, J.; Meagher, J. L.; Sun, D.; Li, X.; Zhou, B.; Karatas, H.; Lou, R.; Chinnaiyan, A.; Asangani, I. WO/2014/164596, **2014**.
- 24** Sekirnik, A. R.; Hewings, D. S.; Theodoulou, N. H.; Jursins, L.; Lewendon, K. R.; Jennings, L. E.; Rooney, T. P. C.; Heightman, T. D.; Conway, S. J. *Angew. Chem. Int. Ed.* **2016**, *55*, 8353–8357.
- 25** Demont, E. H.; Gosmini, R.; Luc, M. Tetrahydroquinolines derivatives as bromodomain inhibitors. WO2011054848, **2011**.
- 26** White, G.; Hirst, D.; Tape, D.; Theodoulou, N.; Gray, M.; Alder, C. Unpublished results, GSK, **2015**.

-
- 27 Egan, W. J.; Merz, K. M.; Baldwin, J. J. *J. Med. Chem.* **2000**, *43*, 3867–3877.
- 28 Young, R. J.; Green, D. V. S.; Luscombe, C. N.; Hill, A. P. *Drug Discov. Today* **2011**, *16*, 822–830.
- 29 Leeson, P. D.; Springthorpe, B. *Nat. Rev. Drug Discov.* **2007**, *6*, 881–890.
- 30 Bayliss, M. K.; Butler, J.; Feldman, P. L.; Green, D. V. S.; Leeson, P. D.; Palovich, M. R.; Taylor, A. J. *Drug Discov. Today* **2016**, *21*, 1719–1727.
- 31 Schultes, S.; de Graaf, C.; Haaksma, E. E. J.; de Esch, I. J. P.; Leurs, R.; Krämer, O. *Drug Discov. Today Technol.* **2010**, *7*, e157–e162.
- 32 Hopkins, A. L.; Groom, C. R.; Alex, A. *Drug Discov. Today* **2004**, *9*, 430–431.
- 33 Mortenson, P. N.; Murray, C. W. Assessing *J. Comput. Aided. Mol. Des.* **2011**, *25*, 663–667.
- 34 Shilliday, F.; Chung, C. Unpublished results, GSK. **2015**.
- 35 Galdeano, C.; Ciulli, A. *Future Med. Chem.* **2016**, *8*, 1655–1680.
- 36 Seal, G. Unpublished results, GSK, **2016**.
- 37 Ritchie, T. J.; Ertl, P.; Lewis, R. *Drug Discov. Today* **2011**, *16*, 65–72.
- 38 Veber, D. F.; Johnson, S. R.; Cheng, H.; Smith, B. R.; Ward, K. W.; Kopple, K. D. *J. Med. Chem.* **2002**, *45*, 2615–2623.
- 39 Chiba, M.; Ishii, Y.; Sugiyama, Y. *AAPS J.* **2009**, *11*, 262–276.
- 40 *In vitro* clearance assays were run at Cyprotex Ltd. Physico-chemical parameters were measured by the new chemical entity-medicinal chemistry analytical discovery group (GSK). hWB pIC₅₀ and Brd4 BD1 pIC₅₀ assays were run by the screening, profiling & mechanistic biology group (GSK). Liver blood flow percentages were estimated by the quantitative pharmacology group (GSK) using the well-stirred model reported in: Rowland, M.; Benet, L. Z.; Graham, G. G. *J. Pharmacokinet. Biopharm.* **1973**, *1*, 123–136. Wilkinson, G. R.; Shand D. G. *Clin. Pharmacol. Ther.* **1975**, *18*, 377–390.
- 41 Fleming, C. D.; Bencharit, S.; Edwards, C. C.; Hyatt, J. L.; Tsurkan, L.; Bai, F.; Fraga, C.; Morton, C. L.; Howard-Williams, E. L.; Potter, P. M.; Redinbo, M. R. *J. Mol. Biol.* **2005**, *352*, 165–177.
- 42 Hatfield, M. J.; Potter, P. M. *Expert Opin. Ther. Pat.* **2011**, *21*, 1159–1171.

-
- 43** Zou, L.; Jin, Q.; Wang, D.; Qian, Q.; Ge, G.; Yang, L. *Curr. Med. Chem.* **2018**, *1*, 1627–1649.
- 44** Wadkins, R. M.; Hyatt, J. L.; Wei, X.; Yoon, K. J. P.; Wierdl, M.; Edwards, C. C.; Morton, C. L.; Obenauer, J. C.; Damodaran, K.; Beroza, P.; Danks, M. K.; Potter, P. M. *J. Med. Chem.* **2005**, *48*, 2906–2915.
- 45** Gregory, R. Unpublished results, GSK, **2016**.
- 46** Charlton, M. H.; Brotherton, D. H.; Owen, J.; Clark, V. L.; Testar, R. J.; Davies, S. J.; Moffat, D. F. C. *Med. Chem. Commun.* **2012**, *3*, 1070–1076.
- 47** Imai, T.; Taketani, M.; Shii, M.; Hosokawa, M.; Chiba, K. *Drug Metab. Dispos.* **2006**, *34*, 1734–1741.
- 48** Williams, E. T.; Bacon, J. A.; Bender, D. M.; Lowinger, J. J.; Guo, W.; Ehsani, M. E.; Wang, X.; Wang, H.; Qian, Y.; Ruterbories, K. J.; Wrighton, S. A.; Perkins, E. J. *Drug Metab. Dispos.* **2011**, *39*, 2305–2313.
- 49** Hosokawa, M. *Molecules*, **2008**, *13*, 412–431.
- 50** White, G. Unpublished results, GSK. **2015**.
- 51** Prashad, M.; Kim, H.-Y.; Har, D.; Repic, O.; Blacklock, T. J. *Tetrahedron Lett.* **1998**, *39*, 9369–9372.
- 52** Dunetz, J. R.; Xiang, Y.; Baldwin, A.; Ringling, J. *Org. Lett.* **2011**, *5*, 2009–2012.
- 53** Evans, D. A.; Bartroli, J.; Shih, T. L. *J. Am. Chem. Soc.* **1981**, *103*, 2127–2129.
- 54** Edge, C. Unpublished results, GSK, **2019**.
- 55** Becke, A. D. *J. Chem. Phys.* **1993**, *98*, 5648–5652.
- 56** Franc, M. M.; Pietro, W. J.; Hehre, W. J.; Binkley, J. S.; DeFrees, D. J.; Pople, J. A.; Gordon, M. S. *J. Chem. Phys.* **1982**, *77*, 3654–3665.
- 57** Bull, S. D.; Davies, S. G.; Garner, A. C.; Kruchinin, D.; Key, M.-S.; Roberts, P. M.; Savory, E. D.; Smith, A. D.; Thomson, J. E. *Org. Biomol. Chem.* **2006**, *4*, 2945–2964.
- 58** Collado, I. G.; Massanet, M.; Alonso, M. S. *Tetrahedron*, **1994**, *50*, 6433–6440.
- 59** Jacques, J.; Marquet, A. *Org. Synth.* **1973**, *53*, 111.
- 60** Baccolini, G.; Dalpozzo, R.; Todesco, P. E. *Heteroat. Chem.* **1992**, *3*, 345–349.
- 61** Kumar, A.; Rao, M. S.; Mehta, V. *Indian J. Chem.* **2011**, *50*, 1123–1127.
- 62** Saikia, I.; Borah, A. J.; Phukan, P. *Chem. Rev.* **2016**, *116*, 6837–7042.
- 63** Dey, M.; Dhar, S. S. *Green Chem. Lett. Rev.* **2012**, *5*, 639–642.

-
- 64 Brown, D. G.; Boström, J. *J. Med. Chem.* **2016**, *59*, 4443–4458.
- 65 Miyaura, N.; Yamada, K.; Suzuki, A. *Tetrahedron Lett.* **1979**, *20*, 3437–3440.
- 66 Miyaura, N.; Suzuki, A. *Chem. Commun.* **1979**, *19*, 866–867.
- 67 Lu, Z.; Wilsily, A.; Fu, G. C. *J. Am. Chem. Soc.* **2011**, *133*, 8154–8157.
- 68 Lennox, A. J. J.; Lloyd-Jones, G. C. *Chem. Soc. Rev.* **2014**, *43*, 412–443.
- 69 Dillon, E.; Dame, O. F. N. *J. Am. Chem. Soc.* **1942**, *64*, 1128–1129.
- 70 Kosak, T. M.; Conrad, H. A.; Korich, A. L.; Lord, R. L. *Eur. J. Org. Chem.* **2015**, *34*, 7460–7467.
- 71 Cherng, Y. *Tetrahedron* **2002**, *58*, 887–890.
- 72 Xia, Y.; Cao, K.; Zhou, Y.; Alley, M. R. K.; Rock, F.; Mohan, M.; Meewan, M.; Baker, S. J.; Lux, S.; Ding, C. Z.; Jia, G.; Kully, M.; Plattner, J. J. *Bioorg. Med. Chem. Lett.* **2011**, *21*, 2533–2536.
- 73 Woodhead, A. J.; Chessari, G.; Besong, G. E.; Carr, M. G.; Hiscock, S. D.; O'Brien, M. A.; Rees, D. C.; Saalau-Bethell, S. M.; Willems, H. M. G.; Thompson, N. T. PCT. WO 2013/064538 A1, **2013**.
- 74 Boechat, N.; da Costa, J. C. S.; Mendonça, J. D. S.; Paes, K. C.; Fernandes, E. L.; de Oliveira, P. S. M.; Vasconcelos, T. R. A.; de Souza, M. V. N. *Synth. Commun.* **2005**, *35*, 3187–3190.
- 75 Periasamy, M.; Thirumalaikumar, M. *J. Organomet. Chem.* **2000**, *609*, 137–151.
- 76 Bit, R.; Brown, J.; Humphreys, P.; Jones, K. L. WO 2016/146738, **2016**.
- 77 Mitsunobu, O.; Yamada, M. *Bull. Chem. Soc. Jpn.* **1967**, *40*, 2380–2382.
- 78 Buonomo, J. A.; Aldrich, C. C. *Angew. Chem. Int. Ed.* **2015**, *54*, 13041–13044.
- 79 Huang, H.; Kang, J. Y. *J. Org. Chem.* **2017**, *82*, 6604–6614.
- 80 Cheng, C. Y.; Wu, S. C.; Hsin, L. W.; Tam, S. W. *J. Med. Chem.* **1992**, *35*, 2243–2247.
- 81 Tsunoda, T.; Ozaki, F. *Tetrahedron Lett.* **1994**, *35*, 5081–5082.
- 82 Tsunoda, T.; Nagaku, M.; Nagino, C.; Kawamura, Y.; Ozaki, F.; Hioki, H.; Itô, S. *Tetrahedron Lett.* **1995**, *36*, 2531–2534.
- 83 Guram, A. S.; Rennels, R. A.; Buchwald, S. L. *Angew. Chem. Int. Ed.* **1995**, *34*, 1348–1350.
- 84 Louie, J.; Hartwig, J. F. *Tetrahedron Lett.* **1995**, *36*, 3609–3612.
- 85 Buitrago-Santanilla, A.; Colandrea, V. Unpublished results, GSK, **2016**.

-
- 86 King, S. M.; Buchwald, S. L. *Org. Lett.* **2016**, *18*, 4128–4131.
- 87 Sunesson, Y.; Lime, E.; Lill, S. O. N.; Meadows, R. E.; Norrby, P. *J. Org. Chem.* **2014**, *79*, 11961–11969.
- 88 Mitchell, D. Unpublished results, GSK, **2016**.
- 89 Seal, G.; Gregory, R.; Harada, I. Unpublished results, GSK, **2017**.
- 90 Brown, J.; Bit, R.; Jones, K.; Seal, G.; Shipley, T.; Humpreys, P. Unpublished results, GSK, **2017**.
- 91 Patrick, G. L. *An Introduction to Medicinal Chemistry*; Oxford University Press, 2017; p 402–404.
- 92 Shipley, T. Unpublished results, GSK, **2017**.
- 93 Ishiyama, T.; Murata, M.; Miyaura, N. *J. Org. Chem.* **1995**, *60*, 7508–7510.
- 94 Molander, G. A.; Trice, S. L. J.; Kennedy, S. M.; Dreher, S. D.; Tudge, M. T. *J. Am. Chem. Soc.* **2013**, *134*, 11667–11673.
- 95 Cox, P. A.; Reid, M.; Leach, A. G.; Campbell, A. D.; King, E. J.; Lloyd-Jones, G. *C. J. Am. Chem. Soc.* **2017**, *139* (37), 13156–13165.
- 96 Potter, P. M.; Wadkins, R. M. *Curr. Med. Chem.* **2006**, *13*, 1045–1054.
- 97 Seal, G. Unpublished results, GSK, **2018**.
- 98 Kolb, H. C.; Hoffmann, H. M. R. *Tetrahedron: Asymmetry* **1990**, *1*, 237–250.
- 99 Vakalopoulos, A.; Hoffmann, H. M. R. *Org. Lett.* **2000**, *2*, 1447–1450.
- 100 Felix, A. M. *J. Org. Chem.* **1974**, *39*, 1427–1429.
- 101 MetaSite is a commercial software package available from Molecular Discovery Ltd, UK.
- 102 Cruciani, G.; Carosati, E.; De Boeck, B.; Ethirajulu, K.; Mackie, C.; Howe, T.; Vianello, R. *J. Med. Chem.* **2005**, *48* (22), 6970–6979.
- 103 Deeks, N. Unpublished results, GSK, **2017**.
- 104 Jean, D. J. S.; Fotsch, C. *J. Med. Chem.* **2012**, *55*, 6002–6020.
- 105 Dalvie, D. K.; Kalgutkar, A. S.; Khojasteh-Bakht, S. C.; Obach, R. S.; O'Donnell, J. P. *Chem. Res. Toxicol.* **2002**, *15* (3), 269–299.
- 106 Sukhninder, K.; Gupta, M. *Glob. J. Pharm. Sci.* **2017**, *1*, 1–11.
- 107 Meanwell, N. A. *J. Med. Chem.* **2018**, *61*, 5822–5880.
- 108 Zhang, Z.; Tang, W. *Acta Pharm. Sin. B* **2018**, *8*, 721–732.
- 109 Love, J.; Chung, C. Unpublished results, GSK. **2018**.

-
- 110 Thomas, P. Unpublished results, GSK, **2017**.
- 111 Desiraju, G. R. *Chem. Commun.* **2005**, 24, 2995–3001.
- 112 Sarkhel, S.; Desiraju, G. R. *Proteins* **2004**, 54, 247–259.
- 113 Uldry, A. C.; Griffin, J. M.; Yates, J. R.; Pérez-Torralba, M.; Santa María, M. D.; Webber, A. L.; Beaumont, M. L. L.; Samoson, A.; Claramunt, R. M.; Pickard, C. J.; Brown, S. P. *J. Am. Chem. Soc.* **2008**, 130, 945–954.
- 114 Nittinger, E.; Inhester, T.; Bietz, S.; Meyder, A.; Schomburg, K. T.; Lange, G.; Klein, R.; Rarey, M. *J. Med. Chem.* **2017**, 60, 4245–4257.
- 115 Campbell, S.; Davis, A.; Ward, S. *The Handbook of Medicinal Chemistry: Principles and Practice*; Royal Society of Chemistry, 2015; p 99.
- 116 Li, Y. L.; Zhu, W.; Mei, S.; Glenn, J. PCT. WO 2013/14068796 A1, **2013**.
- 117 Marineau, J. J.; Zahler, R.; Ciblat, S.; Winter, D. K.; Kabro, A.; Roy, S.; Schmidt, D.; Chuaqui, C.; Malojcic, G.; Piras, H.; Whitmore, K. M.; Lund, K. I.; Sinko, B.; Sprott, K. PCT. WO 2018/US42017 A1, **2017**.
- 118 Brecibar, A.; Guedat, P.; Mohamed-Arab, C. PCT. WO 2010/EP59917 A1, **2010**.
- 119 Pugliese, A.; Francis, S.; McArthur, D.; Sime, M.; Bower, J.; Belshaw, S. PCT. WO 2018/GB52338 A1, **2018**.
- 120 Sato, S.; Sakamoto, T.; Miyazawa, E.; Kikugawa, Y. *Tetrahedron* **2004**, 60 (36), 7899–7906.
- 121 Böhm, H.-J.; Banner, D.; Bendels, S.; Kansy, M.; Kuhn, B.; Müller, K.; Obst-Sander, U.; Stahl, M. *Chembiochem* **2004**, 5, 637–643.
- 122 Harada, I. Unpublished results, GSK, **2018**.
- 123 Gregory, R.; Harada, I. Unpublished results, GSK, **2018**.
- 124 Palleria, C.; Di Paolo, A.; Giofrè, C.; Caglioti, C.; Leuzzi, G.; Siniscalchi, A.; De Sarro, G.; Gallelli, L. *J. Res. Med. Sci.* **2013**, 18, 601–610.
- 125 Ballard, P.; Brassil, P.; Bui, K. H.; Dolgos, H.; Petersson, C.; Tunek, A.; Webborn, P. J. H. *Drug Metab. Rev.* **2012**, 44 (3), 224–252.
- 126 Food and drug administration website,
www.fda.gov/Drugs/DevelopmentApprovalProcess (Accessed February 2019).
- 127 The compounds were dosed intravenously at 1 mg/kg, and orally at 10mg/kg.
- 128 Nishimuta, H.; Houston, J. B.; Galetin, A. *Drug Metab. Dispos.* **2014**, 42, 1522–1531.

-
- 129** Jackson, S.; Hortense, E. Unpublished results, GSK, **2018**.
- 130** Humphreys, P.; Aylott, H.; Schiltz, P.; Hortense, E.; Jackson, S. Unpublished results, GSK, **2018**.
- 131** Thomas, P. Unpublished results, GSK, **2018**.
- 132** Bochevarov, A. D.; Harder, E.; Hughes, T. F.; Greenwood, J. R.; Braden, D. A.; Philipp, D. M.; Rinaldo, D.; Halls, M. D.; Zhang, J.; Friesner, R. A *Int. J. Quantum Chem.* **2013**, *113* (18), 2110–2142.
- 133** Yamada, S.; Hongo, C.; Yoshioka, R.; Chibata, I. *J. Org. Chem.* **1983**, *48*, 843–846.
- 134** Grigg, R.; Gunaratne H.Q.N. *Tetrahedron Lett.* **1983**, *24*, 4457–4460.
- 135** Barry, L. G.; Pugniere, M.; Castro, B.; Previero, A. *Int. J. Pept. Protein Res.* **1993**, *41*, 323–325.
- 136** Yokoyama, Y.; Hikawa, H.; Murakami, Y. *J. Chem. Soc. Perkin I* **2001**, *12*, 1431–1434.
- 137** Pérez-Faginas, P.; Aranda, M. T.; García-López, M. T.; Infantes, L.; Fernández-Carvajal, A.; González-Ros, J. M.; Ferrer-Montiel, A.; González-Muñiz, R. *PLoS One* **2013**, *8*, 1–9.
- 138** Pérez-Faginas, P.; Teresa-Aranda, M.; Torre-Martínez, R. D. L.; Quirce, S.; Fernández-Carvajal, A.; Ferrer-Montiel, A.; González-Muñiz, R. *RSC Adv.* **2016**, *6*, 6868–6877.
- 139** Clayden, J.; Greeves, N.; Warren, S.; Wothers, P. *Organic chemistry*; Oxford University Press, 2001, 229–239.
- 140** Aylott, H. Unpublished results, GSK, **2018**.
- 141** Dennis, K. Unpublished results, GSK, **2018**.
- 142** Wang, D.; Zou, L.; Jin, Q.; Hou, J.; Ge, G. *Acta Pharm. Sin. B* **2018**, *8*, 699–712.